THE ROLE OF ENDOTHELIAL RICTOR (MTORC2) IN ANGIOGENESIS *IN VIVO* AND *IN VITRO*

Dissertation
zur
Erlangung der naturwissenschaftlichen Doktorwürde
(Dr. sc. nat.)
vorgelegt der
Mathematisch-naturwissenschaftlichen Fakultät
der
Universität Zürich

von

Fabio Aimi
aus
Italien

Promotionskomitee

Prof. Dr. Christian Grimm (Vorsitz)

Prof. Dr. med. vet. Max Gassmann

Prof. Dr. med. Edouard Battegay

Prof. Dr. Gerhard M. Christofori

Dr. Rok Humar (Leitung der Dissertation)

Zürich, 2016

TABLE OF CONTENTS

1. SUMMARY 7
2. ZUSAMMENFASSUNG 11
3. INTRODUCTION 15
3.1. Development of the circulatory system 15
3.1.1. Blood vessels 15
3.1.1.1. Capillary structure 16
3.1.1.1.1. Endothelial cells (ECs) 17
3.1.1.1.2. Mural cells: vascular smooth muscle cells (vSMCs) and pericytes 19
3.1.1.1.3. Vascular basement membrane (vBM) 20
3.2. Blood vessel formation 20
3.2.1. Vasculogenesis 20
3.2.2. Angiogenesis 21
3.2.2.1. Modulators of angiogenesis 22
3.2.2.1.1. Vascular endothelial growth factor (VEGF) 22
3.2.2.1.2. Fibroblast growth factor (FGF) 24
3.2.2.1.3. Hepatocyte growth factor (HGF) 25
3.2.2.1.4. Hypoxia 26
3.2.2.1.5. Nitric oxide (NO) 27
3.2.2.1.6. Thrombospondins (TSPs) 29
3.2.2.2. Sprouting angiogenesis 29
3.2.2.2.1. Notch system: tip/stalk cell differentiation 29
3.2.2.2.2. Lumen formation 30
3.2.2.2.3. ANG-TIE2 interaction: vessel maturation 31
3.2.2.3. Intussusceptive angiogenesis 32
3.3. Pathological angiogenesis 33
3.3.1. Angiogenesis in wet age-related macular degeneration (wARMD) 34
3.3.2. Angiogenesis in rheumatoid arthritis (RA) 35
3.3.3. Angiogenesis in tumors 35
3.3.4. Anti-angiogenic therapies 36
3.4. The mammalian target of rapamycin (mTOR) 37
3.4.1. The mammalian target of rapamycin complex 1 (mTORC1) 38
3.4.1.1. p70 ribosomal S6 kinase 1 (S6K1) 39
3.4.1.2. Eukaryotic initiation factor 4E (eIF4E) 39
3.4.2. The mammalian target of rapamycin complex 2 (mTORC2) 39
3.4.2.1. AKT 40
3.4.2.2. Serum and Glucocorticoid- regulated Kinase 1 (SGK1) 41
3.4.2.3 Protein Kinase C alpha (PKCα) 41
3.4.3. The mammalian target of rapamycin (mTOR) in angiogenesis 42
4. AIM OF THE THESIS 43
5. RESULTS – Part A 44

5.1. Loss of endothelial homozygous *Rictor* results in embryonic lethality around embryonic day (E) 11.5–12.5 ... 45
5.2. Endothelial-specific *Rictor* knockout has no obvious effect on viability and weight gain during adolescence into adulthood ... 49
5.3. *Rictor* knockout in mouse aortic endothelial cells (MAEC) differentially disables the formation of capillary-like endothelial networks. ... 51
5.4. FGF2 amplifies RICTOR protein and RICTOR-dependent phosphorylation of AKT on Serine 473 and PKCα on Serine 657 ... 53
5.5. The structure of the capillary bed of the striated skin muscle is not altered by endothelial-specific *Rictor* knockout ... 56
5.6. Wounding-induced capillary diameter remodeling is not impaired by endothelial-specific *Rictor* knockout ... 58
5.7. Endothelial-specific *Rictor* knockout limits increases in the capillary diameter of existing skin vasculature in response to high doses of FGF2 ... 59
5.8. Endothelial-specific *Rictor* knockout strongly reduces FGF2-induced neovascularization in matrigel plugs and prevents local hemorrhage ... 60
5.9 Supplementary data ... 63
6. RESULTS – Part B ... 68
6.1. Endothelial cell culture system ... 68
6.1.1. Mouse aortic endothelial cells isolated by aortic rings are positive for the EC markers VE-Cadherin and von Willebrand Factor ... 68
6.1.2. Adenoviral transfection of *Rictor* floxed MAECs leads to strong *Rictor* ablation ... 71
6.2. VEGFA as MAECs activator ... 73
6.2.1. *Vegfr1* (*Flt*-1), *2* (*Flk-1/KDR*) are not modulated by *Rictor* knockout ... 73
6.2.2. *Ang2* is up-regulated in starved *Rictor* knockout cells ... 75
6.3. Transcriptomic analysis of mTORC2-deficient MAECs ... 76
6.3.1. Gene array analysis ... 76
6.3.2. Validation of the selected genes ... 79
6.4. mTORC2 ablation leads to a higher *Mcp-1* transcription induction in 24 hours of FGF2 stimulation ... 82
6.5. Secretome-analysis ... 83
6.5.1. mTORC2 knockout doesn't affect the secretion of angiogenic molecules under FGF2 stimulation ... 83
6.5.2. mTORC2 regulates VEGFA-induced HGF secretion ... 84
6.6. mTORC2, eNOS and nitric oxide production in MAECs ... 85
6.7. mTORC2 has no impact on actin cytoskeleton rearrangement ... 86
7. DISCUSSION ... 88
7.1. Embryonal development ... 88
7.2. FGF2-induced capillary remodeling and neo-angiogenesis *in vivo* ... 89
7.3. FGF2 in angiogenesis and osteogenesis ... 89
7.4. FGF2- and VEGFA-induced signaling via mTORC2 downstream targets AKT and PKCα ... 90
7.5. A hypothetical VEGFA-mTORC2-HGF loop? ... 91
7.6. mTORC2 is involved in *Ang2* expression but not in *Vegfrs* mRNA modulation ... 92
7.7. Endothelial RICTOR and inflammatory molecules ... 92
7.8. A potential role for RICTOR in endothelial to mesenchymal transition? ... 93
7.9. Outlook and technical considerations ... 94

7.9.1. Endothelial cells characterization and variability 94
7.9.2. Hypoxia as a natural angiogenic stimulus 95
7.10 Conclusion 96
8. MATERIALS AND METHODS 97
8.1. Animal procedures 97
8.2. Whole mount embryo staining 97
8.3 Alizarin Red and Alcian Blue stainings 97
8.4. Histological analysis 98
8.5. Determination of *Rictor* mRNA expression levels in endothelial cells from thoracic aorta 98
8.6. Isolation of endothelial cells 98
8.7. Endothelial cells characterization 99
8.8. Cell culture and treatments 99
8.9. Generation of *Rictor* KO cells 100
8.10. Endothelial network-formation assay *in vitro* 100
8.11. Fluorescent labeling of wild-type and *Rictor* KO cells 100
8.12. RNA extraction and real-time PCR 101
8.13. Protein extraction and immunoblotting 102
8.14. Proliferation assay 103
8.15. Migration assay (wound healing) 103
8.16. Mouse dorsal skin fold chamber and matrigel sealing 104
8.17. Intravital microscopy 104
8.18. Matrigel plug assay 105
8.19. Whole mount cytoskeleton fluorescence staining 106
8.20. Transcriptome analysis 106
8.21. Angiogenic ligands 106
8.22. Nitrites quantification 106
8.23. Soluble VEGFR1 quantification 107
8.24. Statistical analysis 107
9. REFERENCES 108
10. ABBREVIATIONS 132
11. AKNOWLEDGEMENTS 137
12. *CURRICULUM VITAE* 138

LIST OF FIGURES

Figure 1. Evolution of the circulatory system..... 15
Figure 2. Artery..... 16
Figure 3. Capillary..... 17
Figure 4. Endothelial junctions..... 18
Figure 5. Vasculogenesis in *Danio rerio*[44]..... 21
Figure 6. Sprouting angiogenesis in *Danio rerio*[44]..... 22
Figure 7. VEGF forms and their receptors[107]..... 24
Figure 8. FGF and its receptor[116]..... 25
Figure 9. Hypoxia leads to VEGF expression via HIF system [141]..... 26
Figure 10. VEGF induces NO production and angiogenesis via eNOS activation [185]..... 28
Figure 11. Tip and Stalk cell selection is dependent on the Notch signaling pathway [208]..... 30
Figure 12. Vascular lumen formation models: cell and cord hollowing..... 31
Figure 13. Implication of ANG-TIE2 system in vessel maturation [230]..... 32
Figure 14. Intussusceptive angiogenesis[235]..... 33
Figure 15. Vascularization in wet ARMD..... 34
Figure 16. Angiogenesis in rheumatoid arthritis..... 35
Figure 17. Tumor angiogenesis[251]..... 36
Figure 18. Anti-angiogenic therapies targeting VEGF[270]..... 37
Figure 19. Schematic representation of mTOR signaling pathway [277]..... 38
Figure 20. Constitutive homozygous endothelial *Rictor* knockout during embryonic development is generally lethal..... 46
Figure 21. Lethality and growth retardation of induced endothelial *Rictor* knockout mice peaks around E12..... 48
Figure 22. *Rictor* knockout does not affect weight gain and viability in adolescent mice..... 50
Figure 23. *Rictor* knockout in mouse aortic endothelial cells (MAEC) decreases endothelial network formation..... 52
Figure 24. FGF2 amplifies RICTOR protein and *Rictor*-dependent phosphorylation of AKT on Ser[473] and PKCα on Ser[657]..... 55
Figure 25. *Rictor* knockout disables a sustained increase in skin capillary diameters and restricts extensive capillary remodeling in response to FGF2..... 57
Figure 26. Fibroblast growth factor 2(FGF2)-induced angiogenesis in matrigel plugs is reduced in *Rictor*$^{i\Delta ec}$ mice..... 61
Figure 27. MAECs sprouting from aortic rings..... 68
Figure 28. MAECs monolayer..... 69
Figure 29. Characterization of the isolated MAECs..... 70
Figure 30. SMCs contamination assessment..... 70

Figure 31. GFP expression in transfected MAEC. 71
Figure 32. *Rictor* mRNA levels of 3 different cell isolates. 71
Figure 33. *Cre* recombinase mRNA levels. 72
Figure 34. RICTOR and CRE protein levels in MAECs. 72
Figure 35. *Vegfa* and *Vegfrs* mRNA levels. 74
Figure 36. Soluble VEGFR1 protein levels. 75
Figure 37. *Jagged1* and *Ang2* mRNA levels. 75
Figure 38. Venn diagram. 77
Figure 39. Volcano plots. 77
Figure 40. Validation of the angiogenesis-related modulated genes (1-6 hours). 80
Figure 41. Validation of the angiogenesis-related modulated genes (24 hours). 81
Figure 42. *Mcp1*, *Icam-1* and *Vcam-1* mRNA expression. 82
Figure 43. Angiogenic ligand protein array. 83
Figure 44. Angiogenic ligands secreted in the culture supernatants. 84
Figure 45. Nitrites amount in the MAECs supernatant, measured by Griess reaction. 86
Figure 46. Immunofluorescent stain of MAEC actin cytoskeleton. 87

SUPPLEMENTARY FIGURES

Figure S1. *Rictor*$^{i\Delta ec}$ embryos display a delay in ossification. 63
Figure S2. Histological analysis of *Rictor*$^{i\Delta ec}$ embryos with Tx-injections starting at E 8.5 and E14.5 in comparison to control embryos. 64
Figure S3. Endothelial *Rictor* knockout does not modulate hematological profile. 65
Figure S4. Characterization of endothelial cells. 65
Figure S5. Endothelial *Rictor* KO decreases VEGFA-induced MAEC proliferation. 66
Figure S6. Modification of the dorsal skinfold chamber. 66
Figure S7. Fluorescent intravital staining for *ricinus communis* agglutinin I (RCA I). 67
Figure S8. Dose response of FGF2-matrigel plugs in control mice 67

LIST OF TABLES

Table 1. List of genes modulated in *Rictor* knockout MAECs (Transcriptome Analysis) 78
Table 2. Primers list 101
Table 3. Antibodies list 103

1. SUMMARY

The mammalian target of rapamycin (mTOR) is a Serine/Threonine kinase involved in many cellular processes. In the last decades mTOR has been described to assemble into two different complexes: mTORC1 and mTORC2.

The mTOR complex 1 is constituted, beside the kinase mTOR, by four other proteins (mLST8, PRAS40, DEPTOR and RAPTOR) and senses the micro-environmental levels of nutrients, amino acids, energy, oxygen and growth factors. This complex regulates protein and lipid synthesis, autophagy, glucose metabolism, cell proliferation and growth. Its activity can strongly and specifically be inhibited by rapamycin which can induce conformational changes in the kinase and affect the integrity of the complex.

The other complex containing the kinase TOR, mTORC2, is constituted beside the kinase mTOR by five regulatory binding proteins (mLST8, DEPTOR, SIN1, PROTOR and RICTOR). The presence of these associated proteins and in particular of RICTOR and SIN1 was shown to be basic for mTORC2 stability and function. The information regarding functions and activation mechanisms of mTORC2 are still scarce compared to the well-studied and firstly described mTORC1.

In the last years many groups thus have been investigating the role of the mTOR complex 2 and they discovered that its activity is influenced by growth factors stimulation. It has been also demonstrated that mTORC2 can regulate the actin cytoskeleton, cell migration and growth, mainly acting via its major downstream targets AKT, PKCα (Protein Kinase Cα) and SGK1 (Serum and Glucocorticoid- regulated Kinase 1). Differently from its brother mTORC1, mTORC2 is sensitive to rapamycin only in some cell types, such as in endothelial cells, but only after prolonged exposure at higher concentrations.

The endothelial cells are the principal constituents of the blood vessels and are directly involved in angiogenesis, a morphogenetic event that consists in the creation of new blood vessels starting from pre-existing ones. This process is particularly important during development, when new blood vessel supply growth and functionality of the body tissues but, it can also take place in pathological situations such as during inflammation and tumor vascularization.

In the angiogenic process, the endothelial cells are induced to proliferate, migrate and differentiate in response of external stimuli such as growth factors or hypoxia. The tumor cells secrete high doses of growth factors such as VEGF (Vascular Endothelial Growth Factor) and FGF (Fibroblast Growth Factor) that stimulates the abnormal vascular growth within the tumor mass. In many tumor cells, the mTOR pathway was also found

particularly active; therefore a first approach to block tumor growth was to use drugs targeting the mTOR kinase.

Despite the interesting results obtained in terms of decreased angiogenesis within the tumor and consequent inhibition of the tumor growth, it was not clear whether both of the two mTOR complexes are involved in angiogenesis and whether endothelial mTORC2 plays a role in this process.

In order to understand whether mTORC2 is involved in angiogenesis we used a mouse model in which the *Rictor* gene was disrupted in the endothelium as consequence of CRE-mediated genome recombination.

During these *in vivo* experiments we could show that the constitutive ablation of endothelial *Rictor* is generally lethal during midgestation (embryonic day 11.5-12.5) and the few surviving embryos displayed vascular defects and a delayed ossification in fingers, toes and vertebrae.

Therefore, to assess the role of mTORC2 in angiogenesis, we decided to induce the knockout in adult animals via Tamoxifen injection.

In these mice, we monitored the alteration of the skin muscle capillary architecture stimulated by the FGF2-rich matrigel, on a daily basis using intravital microscopy. Furthermore, we assessed *de novo* angiogenesis into FGF2-loaded matrigel plugs implanted under the mouse skin.

Our *in vivo* data clearly demonstrated that the absence of mTORC2 in endothelial cells leads to a limited FGF2-induced angiogenic remodeling of the capillary vasculature by preventing the heterogeneous increase of the capillary diameter. Furthermore, *Rictor* knockout strongly reduced the formation of aberrant capillaries into matrigel plugs. Thus, our data suggested a crucial function of endothelial mTORC2/RICTOR in extensive angiogenesis.

In the wake of these findings, I proceeded to analyze cellular and molecular mechanisms to explain the phenotypes observed *in vivo*. To achieve this goal, it was used an *in vitro* system constituted by aortic endothelial cells derived from of mice (MAECs) with a floxed *Rictor* gene.

Within these cells, mTORC2 functionality was disrupted as consequence of *Rictor* exons excision induced by CRE-recombinase produced in the MAECs after adenoviral transfection.

To mimic an angiogenic environment, the endothelial cells were activated using the two most important pro-angiogenic molecules FGF2 and VEGFA.

From a cellular point of view, I could demonstrate that mTORC2 was not involved in FGF2-induced MAECs proliferation, migration and cytoskeleton rearrangement. However, we clearly observed that FGF2-driven endothelial network formation required RICTOR.

On the other hand, we observed that VEGFA-induced MAECs proliferation involved mTORC2 signaling, while VEGFA didn't act via mTORC2 to induce MAEC-network formation and -cytoskeleton rearrangement.

On a molecular level, I could demonstrate that in primary MAECs, phosphorylation of PKCα on Ser^{657} residue was increased in response to FGF2 and absent after *Rictor* knockout. Interestingly, the levels of PKCα total protein were strongly dependent on mTORC2 function, whereas PKCα transcription was not affected by *Rictor* knockout.

AKT levels were not affected by mTORC2 ablation, but its phosphorylation on the residue Ser^{473} in response to FGF2 required mTORC2.

I could furthermore observe that in quiescent wild-type endothelial monolayers RICTOR protein levels were very low. After FGF2 stimulation, however, intracellular RICTOR protein levels increased in a dose-dependent manner in control cells.

Moreover, either under VEGFA or FGF2 stimulation, the presence of mTORC2 did not influence the transcription of some of the most important growth factors receptors (VEGFRs) involved in sprouting angiogenesis and endothelial cells differentiation.

To obtain then, information on a large scale about mTORC2-regulated genes and proteins in response to FGF2 and VEGFA, I compared the transcriptome and the secretome of *Rictor* knockout versus control MAECs. From the comparisons I could not substantiate the existence of any gene cluster or secreted protein involved in angiogenesis that might support with a molecular explanation the phenotypes observed *in vivo*. However, I could observe that in MAECs, the absence of mTORC2 can regulate the production of growth factors involved in angiogenesis: indeed, in response to VEGFA, *Rictor* ablation decreases the secretion of HGF, a growth factor which was shown to increase endothelial cells growth and motility and to be particularly expressed in some types of tumors, such as breast cancer.

Furthermore, I saw that, in starved cells, the loss of *Rictor* increased the transcription of *Ang2*, a gene involved in vascular remodeling that can either lead to capillary maturation or, in absence of pro-angiogenic stimuli, even to vessel regression.

Interestingly, I could register that the transcription of the pro-inflammatory molecule *Mcp*-1 remained at higher levels in MAECs lacking *Rictor* in response to FGF2, indicating a possible mild inflammatory phenotype in mTORC2 deficient endothelial cells.

Finally, I also observed that MAECs produced nitrites in an mTORC2-dependent manner in response to acetylcholine, suggesting a possible role of mTORC2 in vasodilation.

In conclusion, based on our results, we can state that endothelial mTORC2 is crucial for embryonic development and its absence leads to lethality, distinct vascular defects, growth retardation and delayed ossification. Moreover, we showed that in adult mice

mTORC2 is involved in FGF2-driven angiogenesis: under FGF2 stimulation, mTORC2 absence impairs the heterogeneous increase of the capillary diameter in dorsal skin fold muscle and compromises the formation of aberrant capillaries in matrigel plugs. Mechanistically, these *in vivo* and *in vitro* phenotypes might be explained with a reduced activity of AKT whose phosphorylation on the residue Ser ^{473} was strongly decreased in *Rictor* knockout cells. Another mechanism that may explain the importance of mTORC2 in angiogenesis might be supply by PKCα whose presence was shown to be strongly dependent on mTORC2 integrity.

These findings can have an important clinic impact, since we could demonstrate that mTORC2 is involved in angiogenesis. New therapies targeting specifically this multimeric complex can be designed in order to prevent aberrant angiogenesis in tumors or in other diseases displaying an abnormal vascular growth.

2. ZUSAMMENFASSUNG

Die Serin/Threonin-Kinase Mammalian Target of Rapamycin (mTOR) ist an vielen zellulären Prozessen beteiligt. In den letzten Jahrzehnten ist mTOR, in zwei verschiedenen Komplexen, mTORC1 und mTORC2, gezeigt worden.

Der mTOR-Komplex 1 besteht neben der Kinase mTOR aus vier weiteren Proteinen (mLST8, PRAS40, DEPTOR und RAPTOR) und erfasst die Mikro-Umwelt Mengen an Nährstoffen, Aminosäuren, Energie, Sauerstoff und Wachstumsfaktoren. Dieser Komplex reguliert Protein- und Lipidsynthese, Autophagie, Glukosestoffwechsel, Zellproliferation und das Wachstum. Seine Aktivität wird stark und spezifisch von Rapamycin gehemmt, welches Konformationsänderungen in der Kinase induziert.

Der zweite Komplex mTORC2, besteht, neben der Kinase-TOR, aus fünf weiteren regulatorischen Bindungsproteine: mLST8, DEPTOR, SIN1, PROTOR und RICTOR. Das Vorhandensein dieser assoziierten Proteine, insbesondere RICTOR und SIN1, ist essentiell für mTORC2 Stabilität und Funktion. Die Informationen bezüglich Funktionen und Aktivierungsmechanismen von mTORC2 sind verglichen mit dem gut untersuchten und zuerst beschriebenen mTORC1 noch immer gering.

In den letzten Jahren haben viele Forschungsgruppen die haben Rolle des mTOR-Komplex 2 untersucht: Sie haben gezeigt, dass die Aktivität von mTORC2 durch Wachstumsfaktor-Stimulation beeinflusst wird. Daneben wurde auch gezeigt, dass mTORC2 das Aktin-Zytoskelett, Zellmigration und Wachstum regulieren kann. Dies geschieht vor allem über seine wichtigsten nachgelagerten Moleküle in der Signalkette: AKT, PKCα (Protein Kinase Cα) und SGK1 (Serum and Glucocorticoid-regulated Kinase 1). mTORC2 nur in einigen Zelltypen wie zum Beispiel in Endothelzellen sensitiv auf Rapamycin und dies auch nur nach längerer Exposition und bei höheren Konzentrationen.

Die Endothelzellen sind ein Hauptbestandteile der Blutgefäße und sind direkt in der Angiogenese beteiligt. Angiogenese ist ein morphogenetischer Prozess, bei dem neuen Blutgefäßen aus-bereits existierenden geschaffen werden. Dieser Prozess ist besonders wichtig bei der Entwicklung, wenn neue Blutgefäßversorgung, Wachstum und Funktion der Körpergewebe gebildet werden. Angiogenese kann auch in pathologischen Situationen, wie bei Entzündungen und Tumorvaskularisierung stattfinden.

Im angiogenen Prozess werden die Endothelzellen induziert, um Proliferation, Migration und Differenzierung in Abhängigkeit von externen Stimuli, wie Wachstumsfaktoren oder Hypoxie zu vermitteln.

Tumore sezernieren hohe Dosen an Wachstumsfaktoren wie VEGF (Vascular Endothelial Growth Factor) und FGF (Fibroblast Growth Factor), die das abnormale Gefässwachstum

innerhalb der Tumormasse stimuliert. In vielen Tumorzellen wurde der mTOR-Signalweg als besonders aktiv gezeigt. Medikamente gegen die mTOR-Kinase zu verwenden ist daher ein therapeutischer Ansatz, um das Tumorwachstum zu blockieren.

Trotz diesen interessanten Ergebnissen im Sinne von verminderter Angiogenese im Tumor und damit einhergehender Hemmung des Tumorwachstums, war es nicht klar, ob beide mTOR-Komplexe an der Angiogenese beteiligt sind, und ob mTORC2 in den Endothelzellen eine Rolle in diesem Prozess spielt. Um zu verstehen, ob mTORC2 an der Angiogenese beteiligt ist, verwendeten wir ein Mausmodell, in dem das *Rictor* Gen im Endothel als Folge einer Cre-vermittelten Rekombination des Genoms konstitutiv oder durch Tamoxifen-induziert deletiert wurde.

Die konstitutive Ablation von endothelialem *Rictor in vivo* war in der Regel letal nach der Hälfte der Schwangerschaft (embryonale Tage 11.5 bis 12.5) und die wenigen überlebenden Embryonen zeigten Gefässdefekte und eine verzögerte Verknöcherung in Fingern, Zehen und Wirbeln.

Bei adulten Mäusen beobachteten wir mit Intravitalmikroskopie die Veränderung der Haut- Muskel- Kapillar-Architektur, welche durch FGF2-angereichertes Matrigel stimuliert wurde. Ferner beurteilten wir die *de novo* Angiogenese in FGF2- beladenen Matrigel Plugs, die unter der Haut von Mäusen implantiert wurden. Unsere *in vivo*-Daten zeigten deutlich, dass die Abwesenheit von *Rictor* im Endothel zu einer stark begrenzten FGF2-induzierten Angiogenese führt und das extensive Remodeling von Kapillaren verhindert wurde indem die Kapillardurchmesser-Vergrösserung begrenzt wurde. Außerdem zeigen endotheliale *Rictor* knockout Tiere keine aberrante Kapillarneubildung im Matrigel Plug im Vergleich zu Kontrollen. Wir demonstrieren also eine entscheidende Funktion von mTORC2/RICTOR in extensiver Angiogenese hin.

Basierend auf diesen Ergebnissen habe ich zelluläre und molekulare Mechanismen analysiert, um den in vivo beobachteten Phänotyp auf molekulare Ebene zu erklären. Hierzu wurde ein *in-vitro*-System bestehend aus murinen Endothelzellen (mouse aortic endothelial cells, MAECs) verwendet, die aus Mausaorten mit einem gefloxten *Rictor* Gen isoliert wurden. In diesen Zellen wurde die mTORC2 Funktion als Folge von *Rictor* Exon Exzision mittels der CRE-Rekombinase nach adenoviraler Transfektion eliminiert. Um ein angiogenes Umfeld in vitro zu imitieren, wurden die Endothelzellen mit den beiden wichtigsten pro-angiogenen Molekülen FGF2 und VEGFA stimuliert.

Auf der zellulären Ebene konnte ich zeigen, dass FGF2 getriebene endotheliale Netzwerkbildung RICTOR-abhängig ist. An FGF2-induzierter MAEC Proliferation, -Migration oder Zytoskelett Reorganisation war mTORC2 nicht beteiligt. Weiterhin beobachteten wir, dass VEGFA induzierte MAEC Proliferation mTORC2 abhängig war.

VEGFA-vermittelte Bildung von kapillarähnliche Netzwerken *in vitro* wurde jedoch nur leicht durch *Rictor* knockout vermindert.

Auf der molekularen Ebene konnte ich zeigen, dass die FGF2-vermittelte Phosphorylierung von PKCα an der Position Ser^{657} nach *Rictor* knockout eliminiert wurde. Interessanterweise wurde das PKCα Gesamtprotein nach *Rictor* knockout abgebaut, während PKCα Transkription stabil blieb. Der AKT Proteinspiegel wurden nicht von mTORC2 Ablation reduziert, jedoch die FGF2 vermittelte Phosphorylierung von AKT an der Position Ser^{473}.

Ich konnte weiterhin beobachten, dass der RICTOR Proteinspiegel im nicht-stimulierten Monolayer von wildtyp Endothelzellen sehr niedrig war. Nach FGF2 Stimulation jedoch erhöhte sich der RICTOR Proteinspiegel stark und in einer Dosis-abhängigen Weise in Kontrollzellen.

mTORC2 hatte keinen Einfluss auf die VEGFA oder FGF2 stimulierte Transkription von einigen der wichtigsten Wachstumsfaktor-Rezeptoren (VEGFRs), welche in der "sprossenden" Endothelzell Phänotyp-Änderung und Differenzierung beteiligt sind.

Um weitreichendere Informationen zu mTORC2-regulierten Gene und Proteine zu erhalten, verglich ich das Transkriptom und das Sekretom von *Rictor* Knockout versus Kontroll-MAECs nach Stimulation mit FGF2 und VEGFA. Aus diesen Vergleichen konnte ich nicht belegen, dass spezifische mTORC2-abhängige Gen-Cluster oder an der Angiogenese beteiligte sekretierte Protein, welche die *in vivo* beobachteten Phänotypen erklären könnten, offensichtlich sind. Allerdings konnte ich beobachten, dass durch VEGFA-induzierte Sekretion von HGF durch *Rictor* knockout deutlich gehemmt war. HGF erhöht Endothelzell-Wachstum und Motilität insbesondere in einigen Tumortypen, so z.B. bei Brustkrebs.

Ferner beobachtete ich, dass in nicht stimulierten Zellen *Rictor* Ablation zu erhöhter *Ang2* Transkription führt. ANG*2* ist im vaskulären Remodelling beteiligt, und führt entweder zur Kapillar-Reifung, oder, in Abwesenheit von proangiogener Stimuli, zur Gefäss-Regression. Weitere Resultate deuten auf einen möglicherweise leicht entzündlichen Phänotyp in mTORC2 defizienten Endothelzellen: Die FGF2-induzierte Transkription des pro-inflammatorischen Moleküls MCP-1 blieb auf signifikant höheren Ebenen in *Rictor* knockout MAECs. Schließlich habe ich auch beobachtet, dass Nitrite in MAECs in einer mTORC2- abhängigen Weise in Reaktion auf Acetylcholin hergestellt wurden, was auf eine mögliche Rolle von mTORC2 in Vasodilatation hinweist.

Zusammenfassend konnten wir zeigen, dass endotheliales mTORC2 entscheidend für die embryonale Entwicklung ist und seine Abwesenheit zu Letalität, verschiedenen Gefäßdefekten, Wachstumsstörungen und zur verzögerten Knochenbildung führt. Wir haben gezeigt, dass bei erwachsenen Mäusen mTORC2 in FGF2 vermittelter Angiogenese

beteiligt ist: Nach FGF2 Stimulation limitiert mTORC2 Defizienz die heterogene Erhöhung der Kapillardurchmesser in den Kapillaren der dorsalen Hautfaltenmuskel. mTORC2 Defizienz verhindert auch die Bildung von aberranten Kapillaren in Matrigelplugs. Mechanistisch konnten wir diese *in vivo* und *in vitro*-Phänotypen mit einer verringerten Aktivität von AKT in Sinne von stark reduzierter Phosphorylierung an Position Ser ^{473} in *Rictor* Knockout-Zellen assoziieren. Ein weiterer Mechanismus, der die Bedeutung der mTORC2 in der Angiogenese erklären könnte, sind die Expressionslevel von PKCα, die stark von mTORC2 Integrität abhängig waren.

Die Erkenntnis, dass endotheliales mTORC2 an der extensiven Angiogenese zentral beteiligt ist, könnte für zukünftige klinische Anwendungen wichtig sein. Insbesondere könnten neue Therapieansätze, die speziell diesen multimeren Komplex ins Visier nehmen, aberrante Angiogenese verhindern. Anwendungsgebiete könnten Tumore oder andere Krankheiten wie diabetische Arthritis oder altersbedingte Makuladegeneration sein, bei welchen ein abnormales Gefässwachstum beteiligt ist.

3. INTRODUCTION

3.1. Development of the circulatory system

During evolution, animals developed several strategies to provide all the needed substances to cells and tissues constituting their organism and, at the same time, to remove metabolic waste and toxic products (e.g. lactate and oxidized molecules) generated[1]. These functions by creating internal circulatory systems firstly developed in triploblasts[1]. The blood vascular system is an example of a circulatory system characterized by the presence of vessels and pumping organs that can be found during evolution already in *annellidae*[1] (Figure 1A). *Vertebrata*, however, were the first to line up the blood vessels with an endothelial layer[1]. The complexity of the blood vascular system increased with the development of the heart (cardiovascular system) which in *pisces* is constituted by one atrium and one ventricle in series. In warm blooded animals, i.e., *aves* and *mammalia*, the cardiovascular system is composed of four distinct chambers that contribute in creating a double circulatory system which divides the oxygenated from the deoxygenated blood[1]. In these animals, the heart pushes the blood all over the body through sophisticated structures: the blood vessels (Figure 1B).

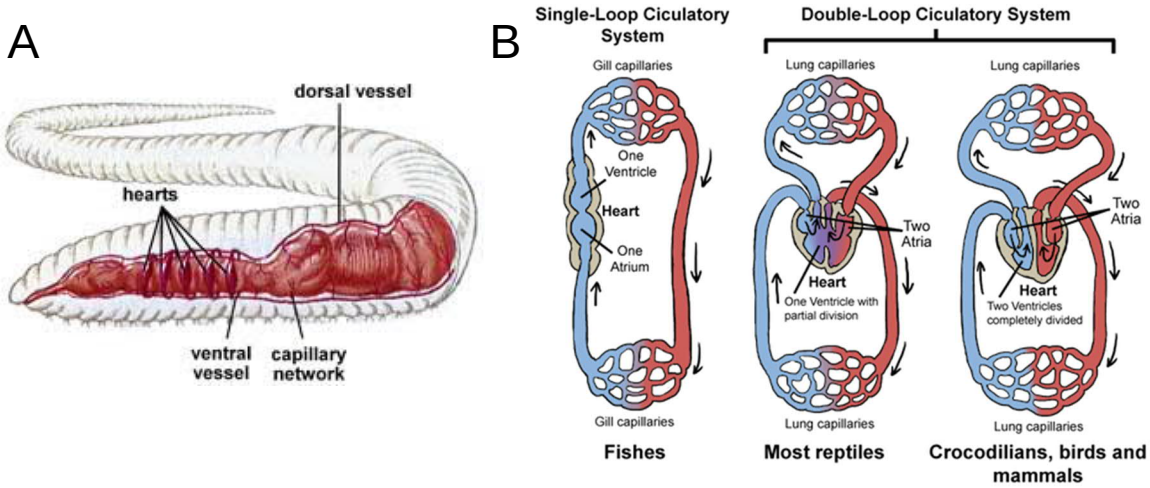

Figure 1. Evolution of the circulatory system.
Circulatory system in *anellidae* (A)[2] and in *vertebrata* (B)[3].

3.1.1. Blood vessels

In *mammalia*, the blood vessels can be divided in three different groups, each of them with different structures and proprieties: arteries, veins and capillaries [4].

The arteries, for example, transport the blood from the heart to the periphery and are constituted by a tight layer of mural cells, able to resist to the high blood pressure generated by the contraction of the heart [4].

The veins, on the other hand, transport the blood from the periphery back to the heart and are characterized by the presence of valves within the vessel lumen to prevent backflow of blood that is not anymore under direct pressure by the heart [4].

The last class of blood vessels is constituted by the capillaries: very small vessels, with a diameter of 5-10 µm, located in the periphery that connect the small arteries to the small veins, and allow the fluid transfer through the vessel wall and the surrounding environment[4].

The large vessels, corresponding to arteries and veins are characterized by three different layers: *tunica intima, tunica media, tunica adventitia* (or *externa*)[5].

The internal layer, *tunica intima*, is constituted by endothelial cells (EC) which create a continuous monolayer that prevent blood leakage [5]. Surrounding the endothelium, *tunica media*, composed by vascular smooth muscle cells (vSMCs), nerve cells and extracellular matrix (elastin, collagen, proteoglycans), enables the vessel contraction, whereas, the fibroblast and the collagen fibers present in the external layer, *tunica adventitia*, provide a structural support for the vessel [5] (Figure 2).

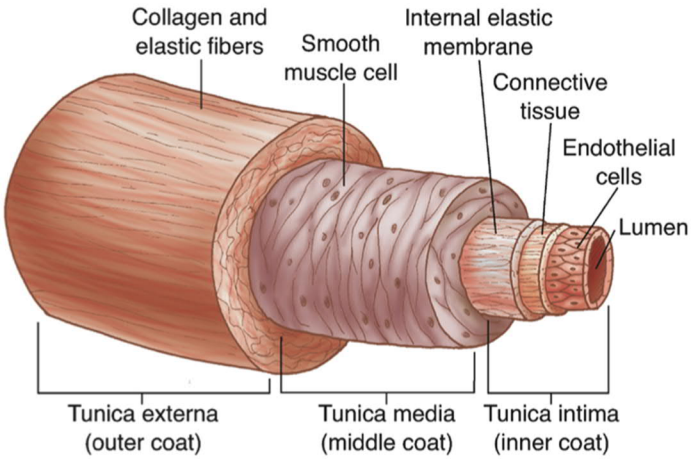

Figure 2. Artery[6].

The artery wall layers: *tunica intima*, with ECs and connective tissue; *tunica media*, mostly characterized by vSMCs and the *tunica externa* or *adventitia* composed by collagen and elastic fibers.

3.1.1.1. Capillary structure

The small blood vessels, the capillaries, generally are constituted by an endothelial cell monolayer surrounded by pericytes and basement membrane that help the maintenance of capillary structure and physiology [7] (Figure 3A).

The endothelial cell monolayer must fulfill different functions and therefore has various morphologies: it can be continuous, fenestrated or sinusoidal [8, 9].

The continuous monolayer of endothelial cells is uninterrupted and allows the passage of small molecules (H_2O, gasses, ions) or lipids[8, 9]. The capillaries characterized by a continuous monolayer are mostly localized in skeletal muscles and in the skin [8, 9].

The fenestrated endothelium, instead, is mostly present in the intestines and in the kidney glomeruli, because it can allow the passage of bigger molecules through endothelium *fenestrae* (diameter 60-80 nm) which is required for the kidneys' filtration and the intestinal uptake[8-10].

The sinusoidal endothelium presents an interrupted endothelial cell layer, with openings that allow even the passage of circulating cells (30-40 µm in diameter) and is located mostly in the bone marrow, in the lymph nodes and in the liver [8, 9, 11] (Figure 3B).

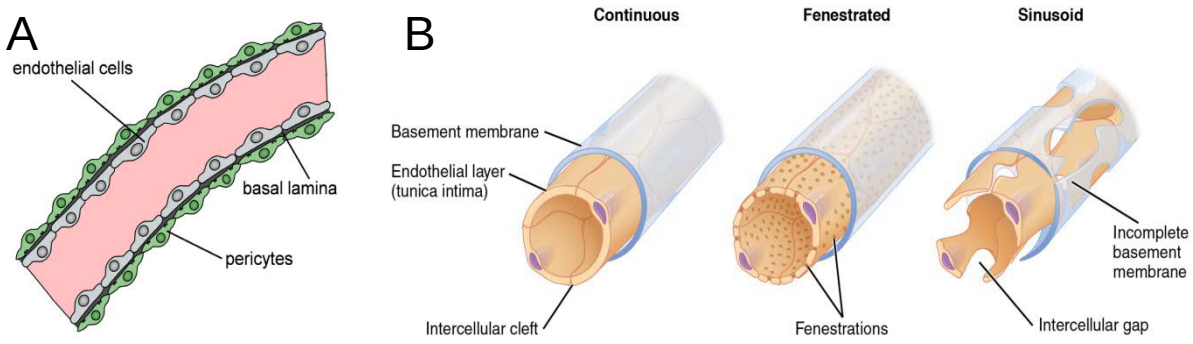

Figure 3. Capillary.

Simplified capillary composition: the endothelial layer is surrounded by the basal lamina (or vascular basement membrane, vBM) and pericytes (A)[12]. Representation of the three types of endothelium: continuous, fenestrated and sinusoidal (B)[13].

3.1.1.1.1. Endothelial cells (ECs)

Endothelial cells (ECs) represent the bricks constituting the internal blood vessel layer. They are organized in a cobblestone monolayer[14] and show heterogenic characteristics within the same organism but even within the same vascular bed [8]. From a structural point of view, for example, in rat blood vessels, the aortic ECs are longer and narrower (55 x 10 µm) compared to the pulmonary artery ECs that are broad and short (30 x 14 µm). In the pulmonary vein, ECs are large and round whereas in the inferior vena cava ECs are long, narrow and rectangular[15]. ECs can show heterogeneity also from a functional point of view. In the activated endothelium for example, the presence of the pro-inflammatory molecule E-selectin is restricted to the venular side of the capillaries and to the venules [16]. The generation of the endothelial cell-heterogeneity might be due to the local microenvironment or to epigenetic regulation which can modulate the gene expression and therefore the endothelial cell phenotype [17].

Despite the different characteristics within the organism, endothelial cells play important roles in several processes. First of all, they constitute a semipermeable layer that selectively allows the passage of molecules and cells: small molecules, H_2O and gasses can diffuse by passing between the endothelial cells whereas bigger molecules cross the cells using *caveolae*. The immune cells cross the endothelium layer either in a transcellular way or as consequence of endothelial cell junctions opening [18, 19]. These junctions that seal the endothelial cells to each other can be divided in two important groups. The first one is represented by the adherens junctions (AJ), which are located in the basal position of the endothelial cells and are characterized by the presence of the VE-Cadherin molecule, an established EC marker (expressed also in cytotrophoblasts [20]). The second group included the tight junctions (TJ) which are located in the apical part of the ECs and are mostly constituted by the proteins claudin, occludin and JAM [21, 22] (Figure 4). The opening of the junctional complexes is mediated by the cytoskeleton for example in presence of cytokines (e.g. vascular endothelial growth factor, VEGF [22, 23]) or inflammatory molecules (e.g. interleukins [19] or tumor necrosis factor α [24]).

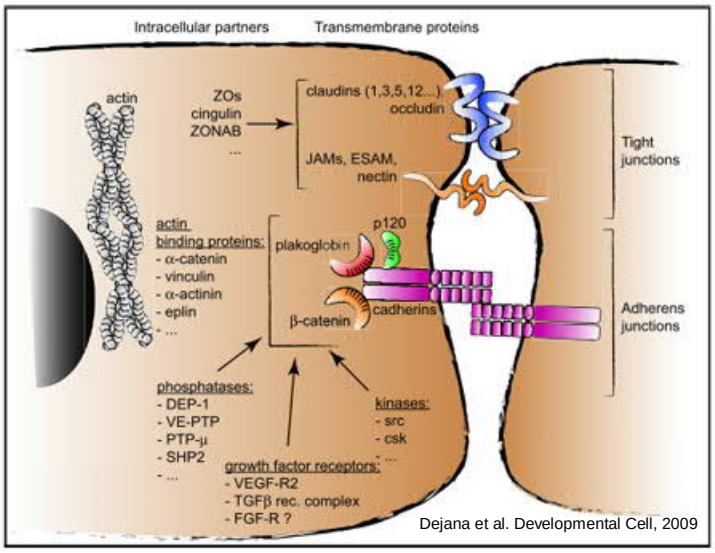

Figure 4. Endothelial junctions.

Tight and adherens junctions connect adjacent endothelial cells contributing to the creation of a semipermeable cellular layer.

Endothelial cells are also an important orchestrator of angiogenesis: they sense the presence of pro-angiogenic molecules (growth factors, nitric oxide, cytokines, chemokines, hormones) or oxygen and initiate the angiogenic process [25]. In presence of pro-angiogenic factors, the endothelial cells initiate the degradation of the basal membrane and get rid of the mural cells in order to be free to migrate, proliferate and establish a network with other endothelial cells [25].

The inflammation process also requires the activation of endothelial cells [19, 22]. In presence of pro-inflammatory molecules, the endothelial cells, in post-capillary venules, start expressing E-selectin and P-selectin which facilitate rolling of leukocytes on the endothelium[19]. Consecutively, the adhesion molecules intercellular adhesion molecule-1 (ICAM-1) and vascular cell adhesion molecule-1 (VCAM-1) are expressed, facilitating immune cells to adhere to the endothelium [19]. The leukocytes extravasation process is also mediate by CD31 (or PECAM1), a transmembrane protein that can associate to the endothelial junctions, considered a marker for ECs (also expressed in leukocytes and platelets)[26].

Endothelial cells can also regulate the coagulation process and try to maintain an anti-thrombotic surface[27]. However, in presence of cytokines, such as interleukins (e.g. IL-6, IL-8) or tumor necrosis factor α (TNFα), ECs up-regulate tissue factor (TF) expression , that can lead to the formation of *thrombi*[28] in pathological situations.

3.1.1.1.2. Mural cells: vascular smooth muscle cells (vSMCs) and pericytes

The vascular smooth muscle cells (vSMCs) are components of the bigger vessels (arteries and veins) wall[29] and characterized, for example, by the expression of the molecular marker SM22α[30]. These cells are involved in maintaining the vessel shape and integrity. In response to vasoactive stimuli (e.g. nitric oxide), vSMCs induce vessel contraction and relaxation leading to alteration of the luminal diameter with consequent modulation of the blood pressure[31]. It was also observed that vSMCs can also contribute to vessel remodeling during pregnancy, exercise and after vascular injury [32]. When an injury occurs or during development, the smooth muscle cells, beside proliferate and migrate, synthesize extracellular matrix proteins. SMCs also show heterogeneity [33] within the same vessel: they can be contractile with elongated and spindled shapes or synthetic with an epithelioid phenotype which are characterized by either a cobblestone morphology or rhomboid shapes with higher proliferative and migratory capacity [34]. Pericytes are other mural cells surrounding the endothelium in venules and capillaries [29] and characterized, for example, by the marker neuron glial 2 (NG2). Pericytes are embedded in the basement membrane and are involved in the angiogenic process [35] interacting with the endothelium via paracrine signaling or by direct physical contact [36]. They can regulate endothelial cell-proliferation[37], -differentiation and growth arrest [35]. The loss of pericytes can lead to aneurysm[37], suggesting their involvement in maintaining the vascular structure and functionality. Pericytes play also a role in regulating the capillary diameter and therefore in regulating the blood flow[38].

3.1.1.1.3. Vascular basement membrane (vBM)

The vascular basement membrane (vBM) is a layer of specialized extracellular matrix (50 – 100 nm) that surrounds the endothelium separating it from the connective tissue and constituting another barrier to the cell extravasation [39].

The vBM is formed by several proteins, most abundant are: type IV collagen, laminin, nidogen/entactin and perlecan[40]. After the interaction with the cell surface these proteins can self-assemble in a complex network which confers structural support during the tissue development[39]. ECs can regulate extracellular matrix dynamics by controlling the matrix components synthesis, secretion or enzymatic degradation[41]. During sprouting angiogenesis, for example, the endothelial cells secrete matrix metalloproteases (MMPs) which degrade the vascular membrane allowing the endothelial cell migration with consequent capillary formation[42]. The vBM can also guide endothelial cells differentiation[43], migration[44] and proliferation[45].

Endothelial cells can interact with the matrix proteins for example via integrins[46], which connect the extracellular environment to the cytoskeleton[47], influence the cell migration[48], proliferation, differentiation and survival.

3.2. Blood vessel formation

In *vertebrata*, the blood vessels are generated in two different ways: vasculogenesis or angiogenesis. In both of the processes ECs, EC precursors and growth factors play a basic role[49].

3.2.1. Vasculogenesis

The process of blood vessel generation occurring by a *de novo* production of endothelial cells is called vasculogenesis[49]. During this process, which was well described in *Danio rerio* (Zebrafish)[49], the blood vessels are created in tissues where they are not yet present. During *Danio rerio* embryonic development, mesoderm-derived endothelial cell precursors (angioblasts) migrate towards a vascular endothelial growth factor (VEGF) gradient to the embryonic midline. At this location, the assembly of several angioblasts forms the dorsal aorta (DA) and the posterior cardinal vein (PCV)[50-52] (Figure 5). Endothelial cells split into an arterial or a venous phenotype after the assembly of the DA and the PCV, when the DA-associated ECs start expressing their marker EphB2, whereas the PCV-associated ECs express the marker EphB4 (EphB2 receptor) [53, 54].

In adults, vasculogenesis occurs in pathologic situations when circulating endothelial cells progenitors (derivatives of stem cells) give rise to new blood vessels after growth factors

stimulation (e.g. in tumor development[55], in revascularization of ischemic tissues[56] and in endometriosis[57]).

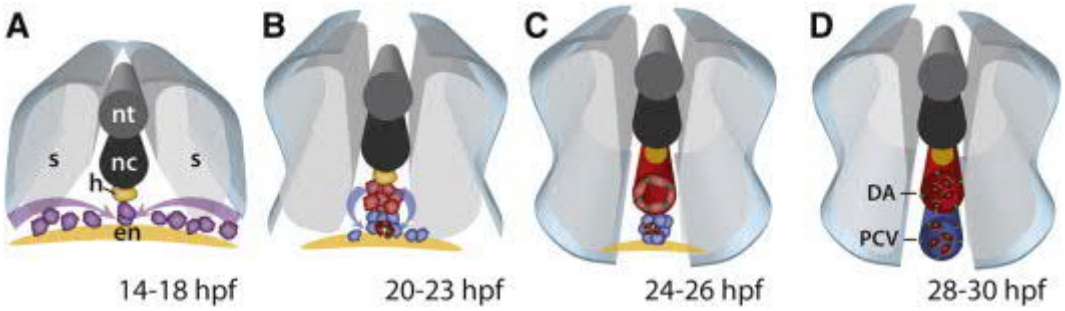

Figure 5. Vasculogenesis in *Danio rerio*[49].

The formation of the DA and PVC occurs within 30 hours after fertilization. The sequence represents the different stages of the two big vessels formation, starting from the angioblasts migration toward the middle line until the hypochord (h). The lumen formation takes place next, first in the DA and then in the PCV.

3.2.2. Angiogenesis

Angiogenesis is a process where new blood vessels are generated from pre-existing ones [49]. Two different ways of physiological angiogenesis are described in the literature: sprouting angiogenesis[58] and intussusceptive angiogenesis (also known as splitting angiogenesis) [59]. Angiogenesis takes place mostly during development and was well described in *Danio rerio* during the formation of the intersegmental vessels (ISVs) and the dorsal longitudinal anastomotic vessels (DLAV)[50]. After the DA and PCV formation, new angiogenic buds sprout from the DA and sense chemotactically the vascular endothelial growth factor (VEGF) gradient generated by the somites using filopodia-like structures. These ECs migrate to the dorsal-lateral surface of the neural tube, branch and then interconnect to form the DLAV[50]. The new vessels then mature and the blood starts flowing (Figure 6).

In adults, angiogenesis can be induced by inflammation. Leukocytes can be recruited by an activated endothelium expressing the adhesion molecules ICAM-1 or VCAM-1 [8]. These cells can then extravasate by increasing endothelial permeability through the secretion of VEGF[60, 61], a growth factor not only responsible for the endothelial permeability but also for the activation of the endothelium. The stimulated ECs can then start proliferating, migrating and remodeling the capillary structure [62, 63].

Angiogenesis in adults can be observed also during the ovarian cycle [64], wound healing[65] or in pathological situation (such as solid tumor growth [66], rheumatoid arthritis[67], atherosclerosis[68], cutaneous psoriasis[69], eye disease[70, 71]).

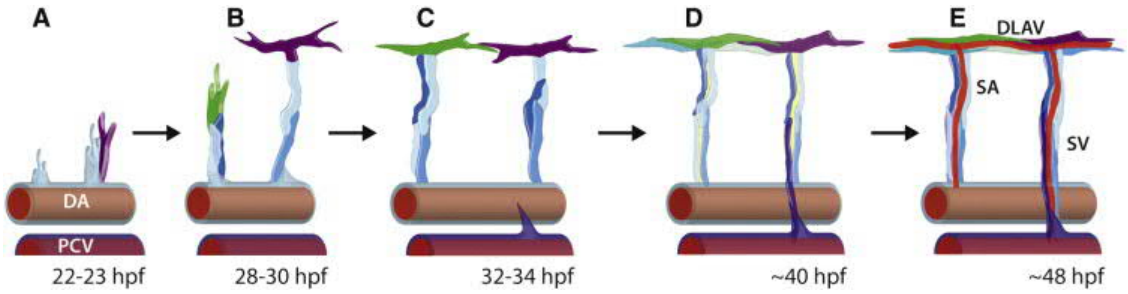

Figure 6. Sprouting angiogenesis in *Danio rerio*[49].

The formation of the intersegmental vessels (ISVs) and of the dorsal longitudinal anastomotic vessel (DLAV) occurs within two days after fertilization. The ISVs are originated from buds sprouting out from the DA. The following connection between these endothelial cells generates the DLAV.

3.2.2.1. Modulators of angiogenesis

In adults, in physiological situation, endothelial cells are maintained in a quiescent state by a balance of pro-angiogenic and anti-angiogenic molecules. When this equilibrium is broken and the ECs are stimulated by a higher amount of pro-angiogenic factors occurs the "angiogenic switch" and angiogenesis starts[72]. The most important growth factors able to stimulate angiogenesis by enhancing ECs growth, differentiation, migration and proliferation are vascular endothelial growth factor (VEGF)[73] and fibroblast growth factor (FGF)[74]. However, many other growth factors can have important effects on the blood vessels and modulate angiogenesis such as platelet derived growth factor (PDGF)[75], hepatocyte growth factor (HGF)[76] or transforming growth factor (TGF)[77]. Also the concentration of particular gasses modulates angiogenesis: nitric oxide (NO)[78] and oxygen deprivation (hypoxia)[79, 80] were demonstrated to be pro-angiogenic. The thrombospondins (TSPs), on the other hand, are well known anti-angiogenic factors which can counter balance pro-angiogenic stimulation to maintain the vasculature quiescent[81]. Other molecules, such as the semaphorins can act either as angiogenic inducers or repressors by stimulating respective receptor-mediated intracellular signaling[82].

3.2.2.1.1. Vascular endothelial growth factor (VEGF)

Vascular endothelial growth factor (VEGF) is the most studied pro-angiogenic molecule. Historically, it is also known as vascular permeability factor (VPF) because of its ability to increase endothelial permeability[18, 83].

This protein is produced and secreted by several cell types (endothelial cells[84], immune cells[85], tumor cells[86], astrocytes[87], neurons[88], SMCs[89]) and stimulates angiogenesis and vasculogenesis[73]. During angiogenesis, it can induce EC-sprouting[90], -migration[62], -proliferation[91] and -survival[92]. VEGF plays also an important role in blood vessel

maturation during the processes of lumen formation[93] and of establishing the EC polarity[94].

VEGF is also involved in inflammation by promoting the expression of V/ICAM-1 and E-Selectin on ECs[95], increasing the adhesion of immune cells to the endothelium[96].

The most known member of the VEGF family is VEGFA. In endothelial cells, it can be induced in response to hypoxia via hypoxia inducible factor (HIF)[84] and as consequence of FGF2 stimulation[97].

Different VEGFA isoforms can be generated by alternative splicing, which can remove one or two domains responsible for the interaction with the extracellular matrix (ECM) and lead to a different affinity for the ECM proteins: $VEGF_{188}$ (high affinity for the matrix), $VEGF_{164}$ (middle diffusible) and $VEGF_{120}$ (lower affinity for the matrix and more diffusible)[98, 99].

VEGFA has two main membrane receptors: VEGFR1 and VEGFR2. Their expression is restricted to endothelial cells, with few exceptions (e.g. melanocytes[100], monocytes[101], neurons[102], hematopoietic cells[103], trophoblasts[104]). In presence of their ligand, these receptor tyrosine kinases can homo or hetero- dimerize and lead to auto or trans-phosphorylation causing initiation of intracellular signals that activate the endothelial cells[105]. Different intracellular pathways can be modulated upon VEGFR2 activation. The most important are the PI3K/AKT-S6K, which stimulates cell proliferation and survival; the SRC, that regulates cell permeability and survival and the PLCγ1/DAG-IP3/PKC, that mediates tubulogenesis[105]. VEGF treatment of ECs leads also to MAPK pathway activation[106] and eNOS induction[107]. Afterwards, the VEGFA-VEGFR2 complex can be internalized in endosomes and degraded by lysosomes[108].

VEGFR1, though having a stronger affinity for VEGFA, mainly acts as negative modulator of VEGFA effects due to its weak kinase activity and its intracellular signaling remains poorly understood[105].

As consequence of alternative splicing, VEGFR1 and VEGFR2 can also be lacking of the transmembrane domains (sVEGFR1 and sVEGFR2). These molecules are secreted in the perivascular space and act as VEGFA scavengers preventing VEGF binding to the membrane receptors[109]. The presence of these soluble forms in the matrix leads to a VEGFA gradient that helps directed endothelial sprout growth, but also mediates vessel maturation via mural cells recruitment[109]

Other members of the VEGF family are VEGFB and PlGF (Placental Growth Factor). They bind the VEGFR1 and, while the first is involved in embryonic angiogenesis and in heart EC fatty acid uptake, the second one plays an important role during development, ischemia, skin wound healing, inflammation and in tumors[110].

VEGFC and VEGFD are the other two members of the VEGF family which are mainly involved in lymphangiogenesis and in the development of the lymphatic tissue. Differently from the other VEGF forms, they can bind, beside VEGFR2, the VEGFR3, strongly expressed on the lymphatic endothelial cells[111] (Figure 7).

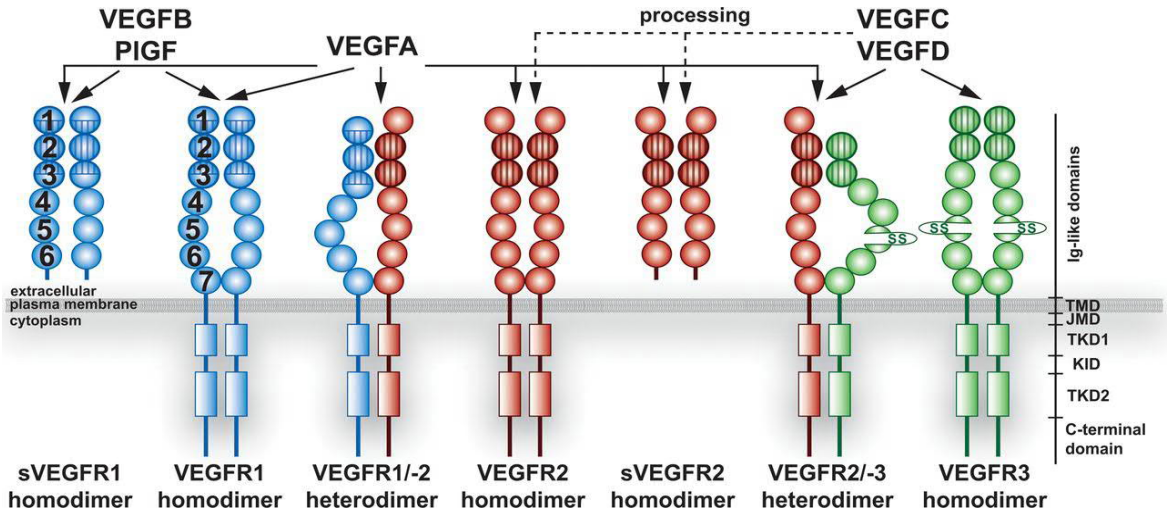

Figure 7. VEGF forms and their receptors[112].

3.2.2.1.2. Fibroblast growth factor (FGF)

The FGF family of growth factors is constituted by at least 20 different proteins which can stimulate angiogenesis and endothelial cell assembly during vasculogenesis[113]. Basic fibroblast growth factor (bFGF or FGF2) was the first pro-angiogenic molecule to be identified[74] and it is considered a more potent angiogenic molecule then VEGF[114]. FGF2 and acid fibroblast growth factor (aFGF or FGF1) can stimulate endothelial cell proliferation[115], migration[116] and capillary-like network formation[117].

The secretion mechanism of FGF1 and FGF2 is still unclear but it is postulated to be independent from the endoplasmic reticulum-Golgi pathway[118].

FGF has a high affinity for heparan sulfates proteoglycans (HSPGs) and can therefore be stored in the vascular basement membrane[119]. HSPGs and heparin can help the dimerization of the FGFRs after FGF binding and influence FGF effects[120].

There are 4 different FGF receptors on the endothelial cell membrane called: FGFR1, FGFR2, FGFR3, and FGFR4. More variants of FGFRs can furthermore be generated through alternative splicing[121]. The kinase activity of FGFRs can lead to auto-phosphorylation of different tyrosine residues. For example, phosphorylation on Tyr[463] residue induces EC proliferation via mitogen- activated protein kinases (MAPK) cascade[115] whereas Tyr[766]

phosphorylation stimulates EC cytoskeletal rearrangement and cellular shape change via phospholipase C γ (PLC-γ) [122] (Figure 8).

It was demonstrated that FGF and VEGF can crosstalk to enhance the angiogenic activity: FGF2 up-regulates VEGF expression in ECs [97], stimulates hypoxia-induced VEGF release via phosphoinositide 3-kinase (PI3K) or hypoxia-inducible factor 1 (HIF1) [123] and increases VEGF uptake by up-regulating the Nrp-1 expression in vSMCs [124]. In rat embryos, it was also observed that VEGF driven vessel assembly was compromised if FGF2 was scavenged[125].

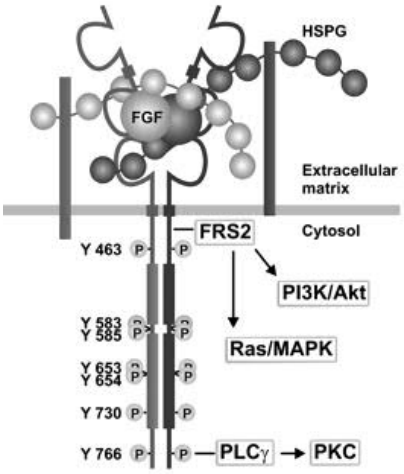

Figure 8. FGF and its receptor [121].

The bound of FGF to its receptor leads to the phosphorylation of several residues in the cytoplasmic domains of the receptors with the consequent activation of different pathways.

3.2.2.1.3. Hepatocyte growth factor (HGF)

The hepatocyte growth factor (HGF), also known as scatter factor (SF), is a protein secreted by mesenchymal [126] and vascular [127, 128] cells that can influence the behavior of endothelial, epithelial and hematopoietic progenitor cells. This protein modulates morphogenesis, cell growth [76], cell migration [76] and cell proliferation [129] and therefore is considered a potent pro-angiogenic factor [76]. In embryos, it has importance for organ development [130], particularly in myogenesis [131]; whereas in adults it is involved in tissue regeneration and wound healing [132]. In pathological situation, HGF can stimulate tumor growth. In breast cancer, for example, HGF promotes capillary-like tubes formation [133]. Its receptor, HGFR (c-Met), is a membrane tyrosine kinase [134], which can activate MAPK cascade to induce endothelial cell migration and growth [135]. The anti-apoptotic effect of HGF is mediated in EC through bcl-2 up-regulation [136], whereas EC proliferation can be stimulated by the activation of the PI3K-AKT pathway [137]. The PI3K-AKT pathway activated

in EC after HGF treatment leads also to cytoskeleton rearrangement, lamellipodia formation and consequent migration induction [138].

3.2.2.1.4. Hypoxia

The presence of oxygen (O_2) within tissues is basic for metabolic cellular activities. The correct oxygen supply is provided by erythrocytes which carry hemoglobin-bound oxygen from the lungs throughout the body using blood vessels as transport path [139]. A hypoxic condition is generated when a tissue doesn't receive the correct amount of oxygen. In this status, vascular remodeling and angiogenesis are induced such as it happens during development (e.g. in retina vascularization [80, 140]), wound healing [65] and in pathological situations (e.g. in tumors [79], atherosclerotic plaques [68], retinopathies [70, 71] or rheumatoid arthritis [67]).

On a cellular level, hypoxia has been shown to stimulate endothelial cell migration [141] and network formation [142], whereas contradictory data are published about hypoxia-driven EC proliferation [141, 143].

Hypoxia induces angiogenesis generally by up-regulating VEGF [84]. Endothelial cells can sense the presence of oxygen by molecules called hypoxia inducible factors (HIFs) [144] whose family is constituted by several members. The most studied components of this family are the αβ heterodimeric proteins HIF-1 and HIF-2. The subunit HIF-1β (also named ARNT) is constitutively expressed and can bind HIFα in hypoxic conditions. In normoxia, the HIF functionality is primarily regulated by prolyl hydroxylases (PHDs) which promote the binding of the von Hippel-Lindau protein (VHL) to HIFα with consequent ubiquitination and proteolytic degradation of the subunit [145] (Figure 9).

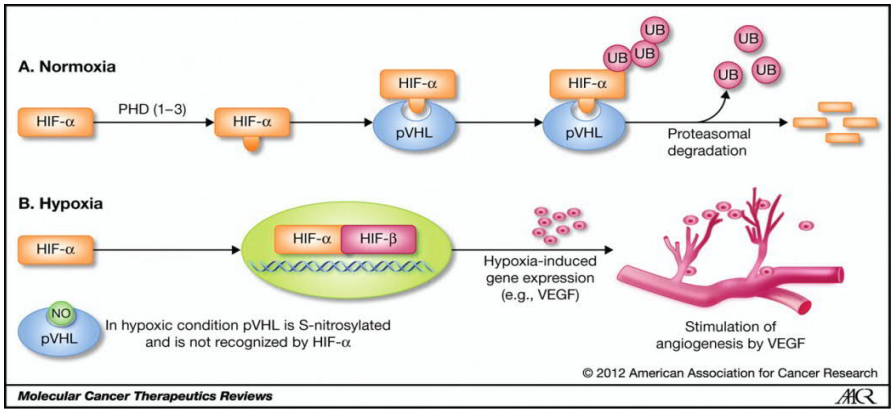

Figure 9. Hypoxia leads to VEGF expression via HIF system [146].

In normoxia, due to the VHL protein mediation, HIFα is degraded by the proteasome. In oxygen absence, VHL protein doesn't mediate the HIFα degradation and the HIF complex is formed leading to gene transcription. One of the genes induced by the activation of the HIF system is VEGF which leads ECs proliferation with consequent tissue vascularization.

The erythropoietin (EPO) gene, one of the first genes identified to be up-regulated in hypoxic condition, is transcribed by the stabilized HIF complex [147]. Several other genes involved in angiogenesis can also be modulated in endothelial cells in hypoxic conditions: *Vegf*[84], *Ang2*[148], *Pdgf-b*[149], *Mmp2*[150], *Vegfr1-2*[151], *soluble Vegfr1*[152], *inducible Nitric oxide synthase (iNOS)* [153].

On the post transcriptional level, hypoxia was shown to regulate VEGFR2 [154] activity and stabilize *Vegf* mRNA translation in 293T cells[155], enhancing its pro-angiogenic effects.

3.2.2.1.5. Nitric oxide (NO)

Nitric oxide (NO), or nitrogen monoxide, is a reactive inorganic gas with an unpaired electron that confers it free radical properties. It has biological half-life of few seconds and it is rapidly oxidized to nitrites (NO_2^-) and nitrates (NO_3^-) in blood and tissues (Figure 10). The amount of nitrites can be assessed by colorimetric Griess reaction [156].

Many cell types, such as endothelial cells[157], macrophages[158], monocytes[159], neutrophils[160] and neurons[161] can synthesize NO, in presence of calmodulin, from the substrates: L-arginine, O_2 and nicotinamide adenine dinucleotide phosphate (NADPH) by using the nitric oxide synthase (NOS) enzymes[162, 163].

$$\text{L-arginine} + \frac{3}{2}\,\text{NADPH} + \text{H}^+ + 2\,\text{O}_2 \rightleftarrows \text{citrulline} + \text{NO} + \frac{3}{2}\,\text{NADP}^+$$

Mammals possess three different NOS types: neuronal (nNOS or NOS1), inducible (iNOS or NOS2) and endothelial (eNOS or NOS3). The nNOS, particularly expressed in neurons [161] and type II skeletal muscles[164], is mostly involved in cell communication[165] whereas iNOS, present in immune cells[158-160], and induced by cytokines, contributes to the response against pathogens[166, 167]. Differently from the other two NOSs, eNOS is a membrane-associated protein present in endothelial cells[168], whose activation, with consequent NO production, leads to SMCs relaxation and consequently to vasodilation [169, 170]. It was observed that also the wound healing process [171] and the VEGF-induced endothelial permeability[78] are facilitated by eNOS.

Nitric oxide can be considered a pro-angiogenic molecule for several reasons, for example, on the cellular level it can stimulate EC migration [172], proliferation[171, 173] and survival[174, 175]. Molecularly, nitric oxide and eNOS are involved in angiogenesis on two different stages: either they mediate the effect of angiogenic factors or they stimulate the expression of these molecules.

In endothelial cells, NO mediates VEGF mitogenic effects [176] and, at the same time, its production via eNOS is stimulated by VEGF [107]. In literature, however, in parallel to the

works on endothelial cells presenting VEGFA as a molecule that up-regulates *eNOS* mRNA or eNOS activity[107, 177] there are some studies demonstrating that VEGFA has no effects on eNOS regulation[178] (Figure 10).

Despite that, the idea that NO and eNOS can stimulate angiogenesis is sustained by the studies showing that FGF2 can up-regulate eNOS and, at the same time, in endothelial cells, NO can induce FGF2 expression[173].

The effect of hypoxia, a condition that, as shown before, leads to angiogenesis, on eNOS is also still not clear: while hypoxia is reported to be an *eNOS* transcriptional repressor[179, 180], there are some other publications demonstrate the opposite effect[181].

NO can fulfill its pro-angiogenic effects not only on endothelial cells but also on vSMCs, where it is shown to induce a strong VEGF expression[182].

Despite the physiological activity of NO, this molecule can be involved in different vascular pathologies: an impaired NO production is a characteristic of diseases such as atherosclerosis[183] or hypertension[184]. Nitric oxide has also important anti-inflammatory proprieties, but when it is overproduced (e.g. in rheumatoid arthritis), it can induce inflammation[185]. Despite that, the pro-inflammatory cytokine TNFα was shown to be responsible for eNOS down-regulation in endothelial cells[186, 187], even if it was observed that TNFα treatment of endocardial ECs increased nitrite levels[188].

Another interesting feature of nitric oxide is its anti-thrombogenic propriety, which inhibits platelet aggregation by increasing their cyclic adenosine monophosphate (cAMP) concentration[189].

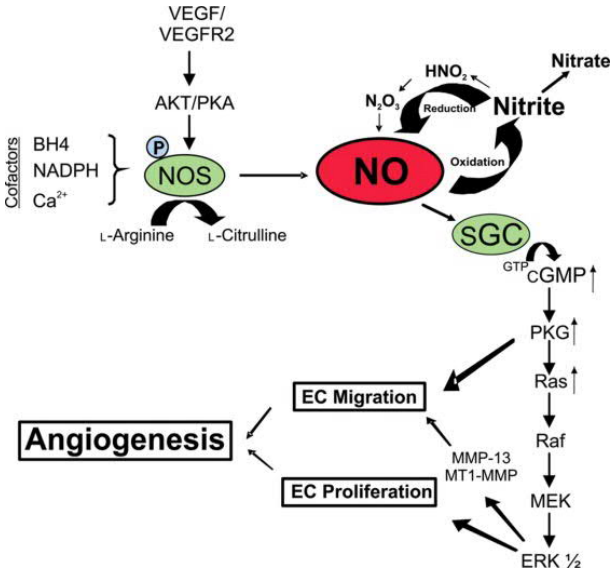

Figure 10. VEGF induces NO production and angiogenesis via eNOS activation[190].

As consequence of VEGF stimulation, nitric oxygen synthase is activated. The nitric oxide produced leads to the activation of a cascade of intracellular events causing endothelial cell migration, proliferation and angiogenesis. Nitric oxide is unstable and it is rapidly oxidized to nitrites and nitrates.

3.2.2.1.6. Thrombospondins (TSPs)

Thrombospondins (TSPs) are proteins mostly secreted by platelets [191] or endothelial cells[192] leading to several anti-angiogenic effects [81]. The most studied member of this family is TSP1. TSP1 inhibits EC proliferation [193] and growth[194]. By binding the CD36 antigen on the EC membrane[195, 196], TSPs can also impair EC migration [194] and apoptosis[197] .

On a molecular level, it is shown that TSP1 can inhibit tumor angiogenesis by blocking VEGF release from the vBM and by inhibiting the activation of the matrix metalloprotease 9 (MMP9)[198]. Moreover, the TSPs can fulfill their anti-angiogenic action by scavenging VEGF[199], FGF[200] and HGF[201] or, even inhibiting NO signaling after binding to the cellular antigen CD47[202].

Due to all these anti-angiogenic proprieties, therapies administering exogenous TSPs or proteins stimulating TSPs secretion are considered or used in the first clinical trials in order to block tumor vascularization and growth [203, 204].

3.2.2.2. Sprouting angiogenesis

Sprouting angiogenesis is a specific form of angiogenesis that is composed of several stages regulated by growth factors and coordinated by an intense intra and inter-cellular signaling. These molecules initiate a cascade of processes that lead to: activation of the ECs, local degradation of the basal membrane (vBM) by matrix metalloproteases (MMPs), loss of pericytes and SMCs, EC migration, proliferation, network formation, lumen creation, recruitment of new pericytes and SMCs, deposition of new vBM molecules and finally blood flow[58].

3.2.2.2.1. Notch system: tip/stalk cell differentiation

One of the basic pathways involved in sprouting angiogenesis is represented by the Notch/Dll4/Jagged signaling pathway. In angiogenic conditions, small differences in VEGF concentrations might selectively activate some ECs in the quiescent endothelium [205]. When the interaction between VEGF and VEGFR2 activates the EC, the cell acquires an endothelial tip-cell phenotype, which is characterized by an increased mobility and a higher number of filopodia[90]. On a molecular level, the tip cell down-regulates VEGFR1/sVEGFR1[206] and starts expressing more VEGFR2[206], VEGFR3[207] and the membrane protein delta like ligand 4 (DLL4) [208].

The tip cell communicates to the neighboring ECs by the interaction between DLL4 and its receptor Notch present on the ECs. When the Notch pathway is activated, a cascade of intracellular signals leads to the repression in the ECs of the potential tip phenotype and

stimulate the differentiation in stalk cells[208]. These cells are characterized by a lower migration but higher proliferation rate and by well-established intercellular junctions [90]. Molecularly, the stalk cells display a high Notch signaling which leads to a weaker activation of the cell, characterized by VEGFR2 down-regulation [209] and VEGFR1/sVEGFR1 expression increase[210].

The stalk cells communicate back to the tip cells via the membrane ligand Jagged1, which binds Notch expressed on the tip cells and contributes to inhibit its signaling in tip cells [211] (Figure 11). These interactions facilitate the generation of the angiogenic sprouts led by a tip cell with high migratory ability, sensing and following the VEGF gradient. The tip of the sprout is followed by proliferating stalk cells responsible for the tube elongation by proliferation and consecutive lumen formation [90]. A new capillary is generated when tip cells belonging to different sprouts contact each other: only after, the vessel starts being perfused by blood. In case of shear stress absence, the sprout regresses [212].

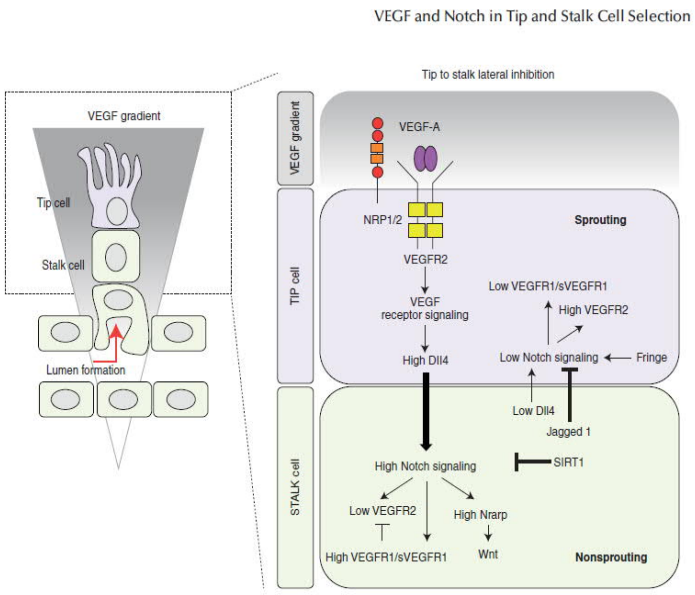

Figure 11. Tip and Stalk cell selection is dependent on the Notch signaling pathway [213].
The VEGF gradient drives sprout formation. Within the sprout the cells communicate to each other: the tip cells that migrate sensing the VEGF gradient are followed by the proliferating stalk cells. The two species of endothelial cells express different VEGFRs due to the Notch signaling between tip and stalk cells. Tip cells express high levels of VEGFR2 and low amount of VEGFR1 and sVEGFR1. Through DLL4 the tip cell represses the VEGFR2 and increases VEGFR1 and sVEGFR1 expression in the following stalk cells.

3.2.2.2.2. Lumen formation

Two models that can explain the vascular lumen formation process during sprouting angiogenesis are cell or cord hollowing. During cell hollowing, pinocytic vesicles, fusing to each other within the EC, create large and empty vacuoles. Neighboring ECs can merge

their vacuoles by exocytosis generating an elongated and continuous vacuole along the endothelial sprout. These empty vacuoles fuse then to the lumen of the perfused capillary[214, 215]. Since the vesicles merging in vacuoles carry endothelial surface markers, the polarity of the endothelial cell is established during the lumen formation process [215].

However, the most common mechanism explaining the vascular lumen formation is cord hollowing. Cord hollowing process starts from a double EC layer and it requires a repolarization of the ECs[216]. The opposing ECs move all the pinocytic vesicles, carrying the apical markers (e.g. CD34 sialomucin) to the interphase where they fuse together to form a narrow lumen within the EC double layer[217] (Figure 12). The CD34-sialomucin negative charges, the cytoskeleton (F-actin fibers and microtubules) rearrangement and the VE-Cadherin redistribution, separates then the apical sides of the two opposing ECs and increases the luminal diameter[216, 217].

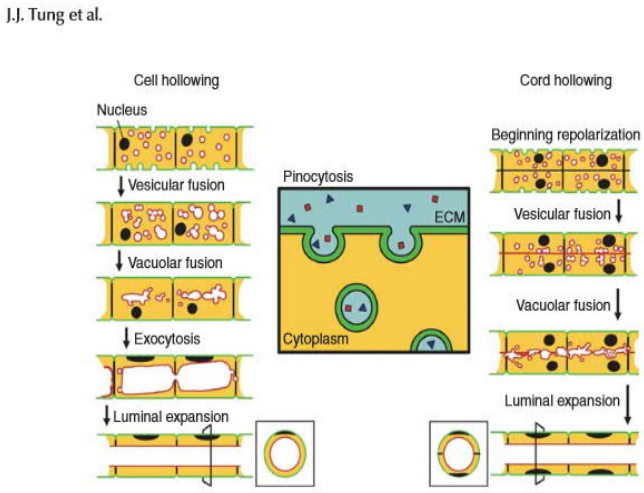

Figure 12. Vascular lumen formation models: cell and cord hollowing [218].
In hollowing models, the lumen is created by merging the vacuoles of different cells. The main difference between the two models is that while in cell hollowing is required a line of endothelial cells, the cord hollowing need an endothelial cells double layer.

3.2.2.2.3. ANG-TIE2 interaction: vessel maturation

In order to become functional, the sprouting capillary needs to recruit pericytes and to re-establish the vBM. At the site of active angiogenesis, ECs can recruit pericytes by releasing platelet derived growth factor (PDGF)[219]. The pericytes sense and move towards the PDGF gradient by the receptor PDGFR and contribute to the capillary stabilization by enwrapping it[220]. The interaction between endothelial cells and pericytes becomes stronger with the ANG-TIE2 cross-talk. The TIE receptors (TIE1 and TIE2) are transmembrane proteins with a tyrosine kinase activity[221]. TIE2, in particular, is considered an EC marker[222] because of its characteristic expression in the endothelium,

although it can also be found on monocytes/macrophages [223] and hematopoietic cells [224]. Angiopoietin 1 and 2 (ANG1 and ANG2) are multimeric ligands mostly secreted by platelets [225] pericytes [226] and endothelial cells [227] that compete for the TIE2 receptor [228, 229]. ANG1 promotes vessel stability and maturation by mediating pericytes interaction with the ECs [230]. ANG2, instead, is expressed at the sites of remodeling endothelium and destabilizes the vessel architecture: ANG2 intravitreal inoculation leads to pericytes loss [231]. ANG2 expression is highly regulated: in quiescent endothelium it is low, whereas it increases in hypoxic condition [148, 232] and under VEGF [148] or tumor necrosis factor α (TNFα) [233] stimulation. The presence of VEGF associated to the ANG2 signaling on the endothelium is crucial to decide the future of the remodeling vessel: VEGF and ANG2 co-presence leads to vessel growth, whereas the absence of VEGF during ANG2 stimulation leads to vessel regression by EC apoptosis [234] (Figure 13).

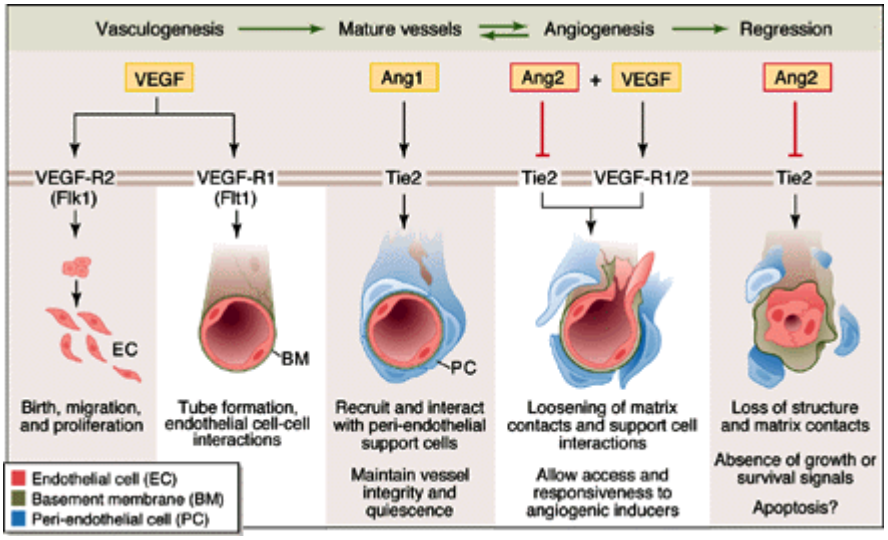

Figure 13. Implication of ANG-TIE2 system in vessel maturation [235].
Due to the ANG1 presence, a sprout can mature and stimulate the interaction with the pericytes. On the other hand, when ANG2 is released, the pericytes detach from the endothelial monolayer and the vessel is destabilized. In this condition, the presence of VEGF induces angiogenesis, whereas its absence leads to vessel regression.

3.2.2.3. Intussusceptive angiogenesis

Intussusceptive angiogenesis is another mechanism of angiogenesis, described for the first time during the postnatal growth of rat lung capillaries [236, 237]. This type of vessel formation consists in the splitting of an existing blood vessel in two different ones, due to a protrusion of the vessel wall into the capillary lumen. The first step of the intussusception process requires an increase of the existing vessel size followed by the direct contact of the endothelial cells present on the opposite side of the capillary wall. After that, the endothelial layer and the basal membrane are cut and a pillar is formed. The final step

consists in the pericytes and fibroblasts invasion of the pillar, with consequent matrix formation, and maturation of the new blood vessels[238, 239] (Figure 14). This angiogenic mechanism contributes to expand the vascularized surface. Compared to sprouting angiogenesis this process is much faster and morpho-energetically more efficient since it doesn't require endothelial cell migration and proliferation, base membrane degradation and invasion of the surrounding tissue[59, 238, 239].

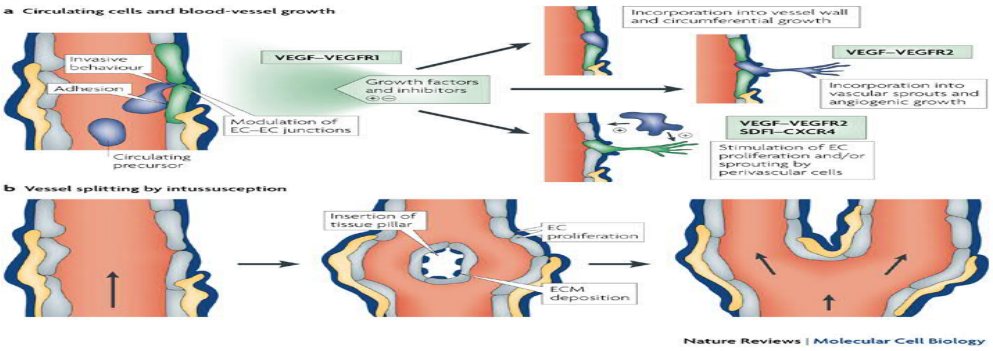

Figure 14. Intussusceptive angiogenesis[240].
A single blood vessel, as consequence of pillar formation is split in two increasing the vascularized area.

3.3. Pathological angiogenesis

Angiogenesis is a highly regulated process that takes place mostly during development in physiological condition. In adulthood, anti-angiogenic molecules counterbalance the signaling coming from pro-angiogenic ligands and maintain the endothelium in a quiescent state. When this equilibrium is broken angiogenesis restarts[72]. However, when the presence of pro-angiogenic signals is strong and sustained, an uncontrolled angiogenesis begins, leading to the development of an un-functional, immature and aberrant vasculature that can drive malignancy and pathologies. Two of the major conditions that unbalance the equilibrium are hypoxia and inflammation. A hypoxic environment, as previously described, leads to the induction of VEGF, the most studied pro-angiogenic factor[84, 87]. Similarly the immune cells, recruited by the endothelium through pro-adhesive molecules during the inflammation process, secrete VEGF[8]. This inflammatory reaction increases endothelial permeability[8] and, at the same time, can also stimulate angiogenesis[60, 61]. Age related macular degeneration, rheumatoid arthritis and tumor development are three examples of pathologies characterized by aberrant angiogenesis.

3.3.1. Angiogenesis in wet age-related macular degeneration (wARMD)

The retina is a highly organized tissue characterized by the presence of photoreceptors, cells which have an elevated metabolic demand with high oxygen consumption. With aging, cell waste and immune system-related molecules can accumulate under the retinal pigment epithelium (RPE) and generate small glycolipids and protein deposits called "drusen"[241-243]. Immune cells, such as macrophages, converge with the drusen and try to eliminate the deposits[244]. In this area, the immune cells and a hypoxic environment lead to an increase in VEGF concentration[243, 245]. The presence of high amount of VEGF stimulates aberrant angiogenesis: an uncontrolled growth of the choroidal vasculature through the Bruch's membrane. The invasion of the subretinal space causes the disruption of the photoreceptor architecture, leading to vision impairment[243]. Moreover, in the late stages, the continuous VEGF stimulation contributes in making the new vessels in the subretinal space extremely permeable and prone to breakage[243]. Local hemorrhages are markers of wARMD which aggravates the pathology of vision loss[243] (Figure 15).

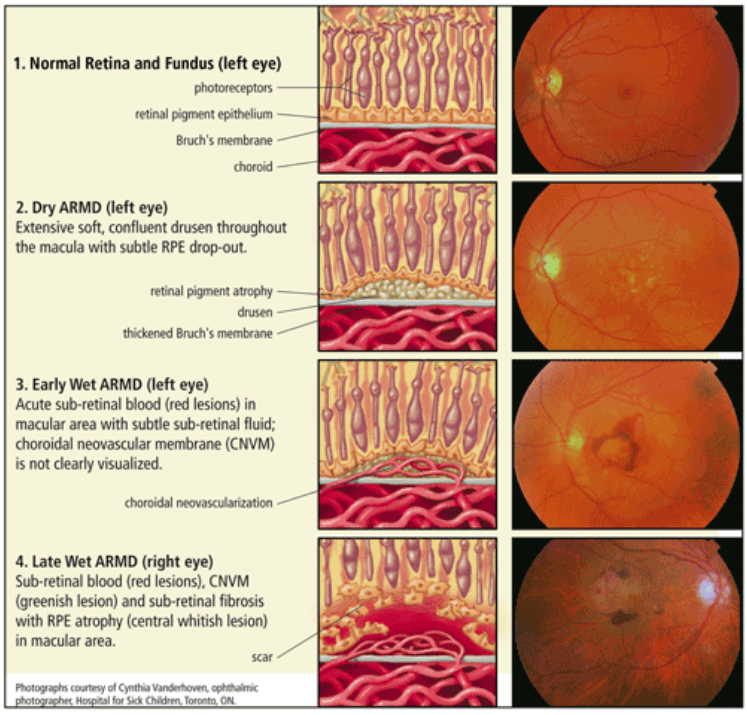

Figure 15. Vascularization in wet ARMD.

The photoreceptors layer architecture is disrupted as consequence of the vascularization of an area between the retinal pigment epithelium and the Bruch's membrane. The vessels generated are weak and prone to breakage, generating hemorrhages. This situation leads to vision impairment and in the worst cases even to blindness.

3.3.2. Angiogenesis in rheumatoid arthritis (RA)

Rheumatoid arthritis (RA) is a chronic inflammatory disease leading to stiffness in multiple joints and, in the worst cases, to cartilage and bone damage [246, 247]. During RA, the synovium is infiltrated by a high number of cells involved in inflammation [246] whose levels correlates to the increasing levels of VEGF [49] and TNFα [248]. The high proliferative and metabolic cellular activity within the synovium creates a hypoxic environment which boosts VEGF release [247, 249, 250]. The presence of VEGF activates the endothelial cells that start proliferating leading to angiogenesis [247]. The induced vascularization of the synovium can provide nutrients and oxygen to the active cells in the synovium responsible to the damages in the joint (Figure 16).

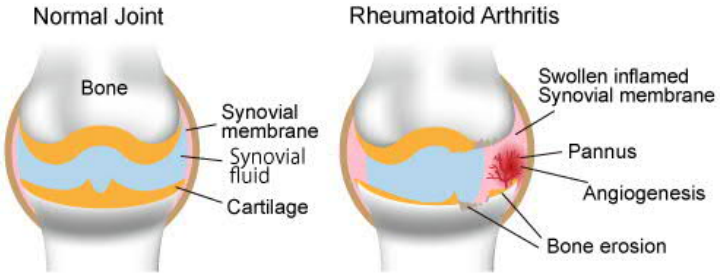

Figure 16. Angiogenesis in rheumatoid arthritis [251].

3.3.3. Angiogenesis in tumors

The high metabolic activity of tumor cells requires a supply of a large amount of nutrients (e.g. glucose) and other metabolites [252]. In order to obtain all the needed molecules, the tumor cells stimulate angiogenesis by secreting a large variety of growth factors [66, 253]. Moreover, due to the high metabolic activity of the tumor cells a hypoxic environment is generated and that additionally stimulates the secretion of VEGF [254]. Immune cells, such as tumor associated macrophages (TAMs) and TIE2-expressing monocytes (TEMs) are frequently present in tumors. These cells contribute to angiogenesis and tumor growth by secreting pro-angiogenic factors such as VEGF and matrix metalloprotease 9 (MMP9) [255, 256]. The continuous growth factors stimulation leads to aberrant angiogenesis, characterized by the generation of tortuous, dilated, leaky and immature capillaries that are poorly stabilized by pericytes [257] (Figure 17). These characteristics lead to high interstitial pressure, hypoperfusion and heterogeneity in blood flow and oxygenation within the tumor which remains in large part hypoxic [257]. Tumor vascularization, however, can also follow other mechanisms: vasculogenesis induced by circulating EC progenitors,

vascular co-option and vascular mimicry were observed during solid tumor development[258].

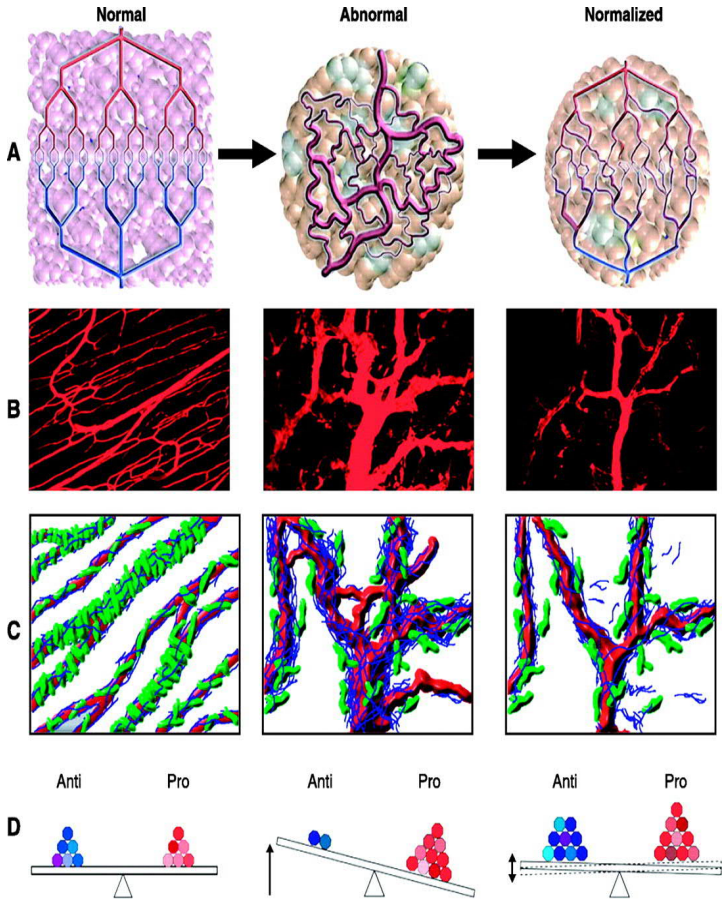

Figure 17. Tumor angiogenesis[257].

Due to extreme and sustained growth factors stimulation, the endothelial cells create an aberrant vasculature in tumors. The capillaries (in red) are dilated, tortuous and lacking of pericytes growth (in green).

3.3.4. Anti-angiogenic therapies

In the last decades, several anti-angiogenic therapies were designed in order to rescue patients from pathologies such as tumors, eye diseases, atherosclerosis, cutaneous psoriasis and rheumatoid arthritis[259, 260]. At the base of these strategies lays the idea that inhibiting vascular growth or normalizing its characteristics can attenuate the disease symptoms or can even contribute to defeat the pathology. Several molecules were designed to target specific pro-angiogenic factors, such as VEGF. These molecules can act on the growth factor-pathway at different levels by blocking VEGF/VEGFRs synthesis (e.g. ribozymes)[261, 262], scavenging VEGF (e.g. anti-VEGF antibodies[263], their fragments[264], aptamers[265], traps[266] or sVEGFR1[267]), competing for VEGFRs[268] or inhibiting the VEGFRs signaling[269] (Figure 18). Some of these molecules are used in clinics since less than 10 years, obtaining interesting therapeutic results[263, 264]. The use of antiangiogenic drugs is

very effective in neo vascular ARMD patients: the association of the vetreporfin photodynamic therapy (PDT) with the intravitreal injection of anti-VEGF antibody fragment led to a better result in terms of visual acuity in one year [270]. In vascularized carcinomas, the use of the anti-VEGF antibody can increase the radiotherapy efficacy by normalizing the tumor vasculature leading to a better tissue oxygenation [257, 271]. However, tumors were shown to be able to develop resistance against anti-VEGF therapies, probably by inducing other growth factors pathways, such as FGF/FGFR: therefore a synergistic inhibition of both VEGF and FGF signaling pathways might lead to a better and stable therapeutic strategy [272-274]. Other methodologies oriented to reduce pathological angiogenesis are based on the use of anti-inflammatory agents, such as non-steroidal anti-inflammatory drugs (NSAIDs). The NSAIDs inhibit the pro-inflammatory cyclooxygenase 2 (COX2). COX2 leads to prostaglandins production that correlates with VEGF expression making the NSAIDs interesting molecules to indirectly block tumor angiogenesis and growth [275].

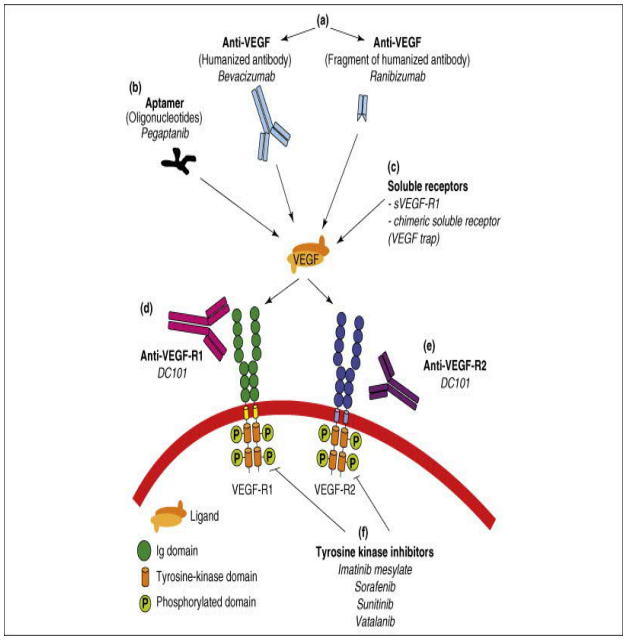

Figure 18. Anti-angiogenic therapies targeting VEGF [276].

Several drugs are designed in order to block angiogenesis acting of VEGF. These molecules can act: directly targeting VEGF (a, b, c), binding VEGF membrane receptors (d, e) or blocking VEGFRs intracellular signaling (f).

3.4. The mammalian target of rapamycin (mTOR)

In the 1975, an antifungal metabolite secreted from the bacterium *Streptomyces hygroscopicus* was discovered on the island of Rapa Nui [277]. This macrolide was named rapamycin and exhibited strong anti-proliferative proprieties. In 1991, targets of

rapamycin (TOR1, TOR2 and FKBP12) were characterized in *Saccharomyces cerevisiae*: mutations in these genes confer rapamycin resistance to yeast [278]. In 1994, a TOR ortholog (mTOR) was found in mammals [279, 280]. The mammalian TOR is a serine/threonine protein kinase, downstream to phosphatidylinositol 3-kinase (PI3K), present in two distinct complexes called mTORC1 and mTORC2 which are composed by unique and common proteins and have different functions, targets and sensitivity to rapamycin [281, 282] (Figure 19).

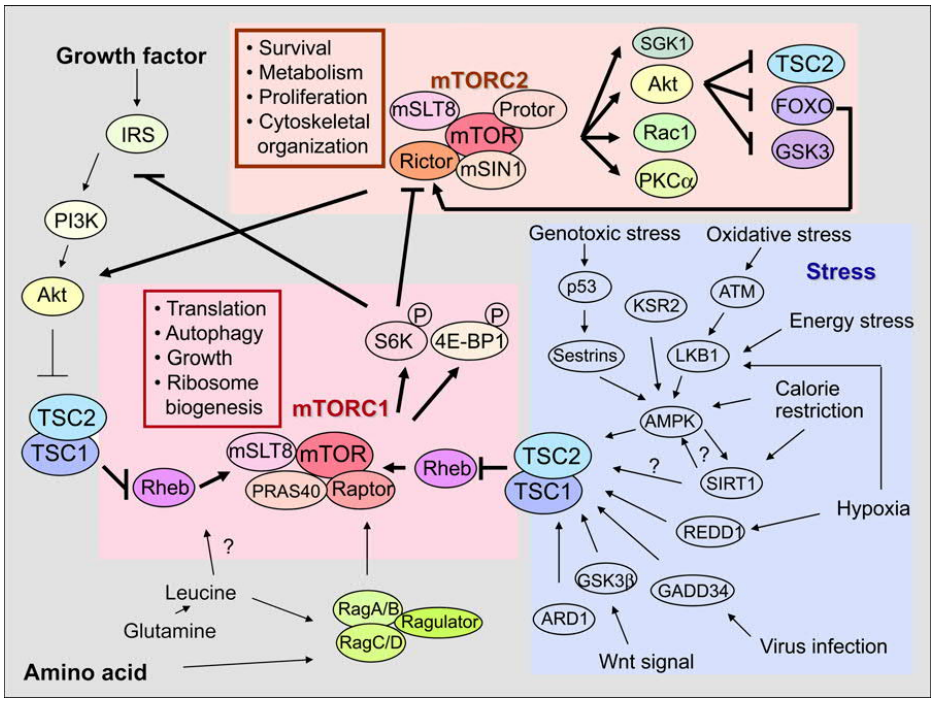

Figure 19. Schematic representation of mTOR signaling pathway [283].

3.4.1. The mammalian target of rapamycin complex 1 (mTORC1)

The mammalian target of rapamycin complex 1 (mTORC1) is constituted by the core protein kinase mTOR and by four other regulatory binding proteins: mLST8, PRAS40, DEPTOR and RAPTOR [281, 284].

Rapamycin by binding the intracellular receptor FKBP12 generates a complex that targets the FKBP12-Rapamycin Binding (FRB) domain which blocks mTORC1 activity either by changing the kinase conformation or affecting the complex integrity [279, 281, 285, 286].

The mTOR complex 1 senses nutrients and energy levels and its activity is controlled by growth factors, amino acids, oxygen and oxidative stress [281, 284, 286, 287].

One of the main function of mTORC1 is to control the protein *de novo* synthesis but it is also involved in autophagy inhibition [288, 289], control glucose homeostasis control [290, 291] and lipid synthesis regulation [292, 293].

It is activated by the GTP-Rheb protein which is maintained inactive by the tuberous sclerosis complex (TSC1/2)[294, 295]. Growth factor stimulation induces the PI3K/Ras pathway that leads to AKT and MAPK–dependent TSC2 phosphorylation. When this phosphorylation occurs, the TSC1/2 complex falls apart and consequently mTORC1 is activatied[295]. Cytokines, such as TNFα, instead, activate mTORC1 by phosphorylating TSC1 through IKKβ[296].

When adenosine triphosphate (ATP) concentration decreases, 5' adenosine monophosphate activated protein kinase (AMPK) can block mTORC1 activity either via TSC2 or by directly phosphorylating RAPTOR[287, 297]. HIF1α, stabilized in hypoxic conditions, induces REDD1 transcription which protects TSC1/2 complex integrity leading to the consequent mTORC1 hypophosphorylation and inhibition [298].

The two major downstream targets of mTORC1 are involved in the protein synthesis: p70 ribosomal S6 kinase 1 (S6K1) and the eukaryotic initiation factor 4E (eIF4E) binding protein 1 (4EBP1)[281, 299].

3.4.1.1. p70 ribosomal S6 kinase 1 (S6K1)

S6K1 induces the protein synthesis by activating the ribosomal protein S6 (S6RP) and the eukaryotic translation initiation factor 4B (eIF4B) [299-301].

S6K1 function is induced by mTORC1 mostly by phosphorylation on Ser [371] and Thr[389], which allows further phosphorylation by PDK1 [299, 302, 303].

However, through a negative feedback loop, activated S6K1 can also decrease mTORC1 activity by inhibiting the sensitivity to insulin of its receptor, inducing insulin resistance in diabetes mellitus[304]. This negative feedback loop involving mTORC1, GSK3 and IRS is activated also in cells lacking of mTORC1 inhibitor complex TSC1/2 [305, 306].

3.4.1.2. Eukaryotic initiation factor 4E (eIF4E)

Active mTOR complex 1 induces the protein synthesis also by phosphorylating the translation inhibitor 4EBP1. When this regulation occurs, it provokes 4EBP1 withdrawal from the eukaryotic translation initiation factor 4E (eIF4E) which is then free to bind eIF4G and recruit eIF4A and eIF4B. This newly formed complex binds the 5'-CAP of the mRNA and start the translation process [299, 307].

3.4.2. The mammalian target of rapamycin complex 2 (mTORC2)

The mammalian target of rapamycin complex 2 (mTORC2) is a multimeric complex that similarly to mTORC1, contains the proteins mTOR, mLST8 and DEPTOR, but, differently

from it, is characterized by the regulatory proteins SIN1, PROTOR and rapamycin-insensitive companion of TOR (RICTOR)[308]. RICTOR or SIN1 are critical for mTORC2 stability and their ablation leads to the disruption of the complex.

Differently from mTORC1, mTORC2 is inhibited by rapamycin only in some cell types (e.g. ECs, vSMCs) and only after long exposure[309]. Treatment with rapamycin leads to a decreased mTORC2 signaling, probably due to a diminished availability of the free mTOR kinase[309].

Growth factor stimulation can influence mTORC2 activity[310]. Phosphatidylinositol 3, 4, 5 - triphosphate (PIP_3), produced by the phosphoinositide 3-kinases (PI3K) is one upstream regulator of mTORC2[311]. Recently, it was demonstrated that even TSC1/2 is required for mTORC2 activity[294].

Differently from mTORC1, mTORC2 functions are only beginning to be explored; it is however known that mTORC2 specifically can regulate the actin cytoskeleton [308, 312, 313], the cell growth[313] and migration mostly by modulating the activity of its major downstream targets: AKT[309], PKCα[308, 313] and SGK1[314].

3.4.2.1. AKT

AKT (or protein kinase B, PKB) regulates the activity of a myriad of substrates that are involved in many cellular processes, such as proliferation [315, 316], survival[92, 316, 317] and migration[62, 316, 318]. AKT plays a central role also during angiogenesis since, in endothelial cells, it is activated in response to VEGF[23] and it also mediates VEGF production in hypoxic conditions[319].

The role of AKT signaling in angiogenesis was studied in physiological situations (e.g. during development) and in pathologies, such as during tumor vascularization [316, 320-323]. In melanoma, for example, it was shown that AKT ablation leads to an increased vessel density which are however immature and leaky[323].

As mentioned before, AKT has many downstream targets, one of the most studied is the tuberous sclerosis protein 2 (TSC2) whose phosphorylation leads to mTORC1 activation[324]. Another AKT substrate is eNOS which is phosphorylated on Ser^{1179} residue and whose activity generates nitric oxide[325]. The activity of GSK3, a protein involved in cellular processes such as control of glycogen and protein synthesis, is also controlled by AKT[326, 327]. The gene transcription regulated by the forkhead box protein O1/3 (FoxO1/3) can be modulated by mTORC2 via AKT[328, 329].

Two AKT residues must be phosphorylated to induce the full kinase activation in response to growth factors (e.g. insulin-like growth factor, IGF): Thr^{308} in the activation loop (A-loop) and Ser^{473} in the hydrophobic motif (HM)[330]. The kinase responsible for the

modification on Thr[308] is the phosphoinositide-dependent protein kinase 1 (PDK1) [331, 332], whereas on Ser[473] is PDK2 (later identified as mTORC2) [333-335]. However, other kinases can perform PDK2 activities such as Integrin-linked kinase (ILK) [336-338]. AKT can also be activated as consequence of PI3K-independent phosphorylation of its Tyr [176] residue[339].

AKT is phosphorylated by mTORC2 on two different sites: in the HM on Ser [473] residue and in the turn motif (TM) on Thr[450] residue[333-335]. The phosphorylation in the TM is stable and takes place during AKT synthesis, when the polypeptide is still in the ribosome [340] and it is essential for the protein stability[334]. However, despite different data published, AKT levels seem to be only slightly affected by mTORC2 ablation probably by the protective action of the chaperon protein named heat shock protein 90 (Hsp90) [333, 334].

3.4.2.2. Serum and Glucocorticoid- regulated Kinase 1 (SGK1)

The Serum and Glucocorticoid-regulated Kinase 1 (SGK1) is a molecule whose activity regulates many proteins[341] mostly involved in cell proliferation[341, 342], survival[343], inflammation[344, 345], sodium and other ions transport[346].

It is activated in response to growth factors or insulin and it is up-regulated by osmotic stress[341, 347]. SGK1 is phosphorylated by mTORC2 on Ser[422] in the hydrophobic motif (HM)[314], whereas less clear is the mTORC2-specific site in the turn motif (TM), probably Thr[368]. Deletion of mTORC2 doesn't lead to SGK1 degradation but can contribute to its dysregulation leading to an aberrant forkhead box protein O1/3 (FoxO1/3) phosphorylation[314]. Phosphoinositide-dependent kinase 1 (PDK1) is also involved in SGK1 activation: by phosphorylation of the Thr [256] residue it leads to maximal SGK1 activity[341, 347].

3.4.2.3 Protein Kinase C alpha (PKC**α**)

Protein kinase C alpha (PKCα) belongs to the PKC family of serine/threonine protein kinases and leads to the phosphorylation of several targets involved in different pathways[348]: for example, it is responsible for actin cytoskeleton rearrangement [313, 349, 350], cell permeability[351] and migration[352, 353]. Moreover, in endothelial cells, PKCα is able to directly phosphorylate AKT on Ser[473] and to induce eNOS activity by phosphorylating Ser[1179] residue[336, 354].

PKCα activity can be regulated by the interaction with the cell membrane that increases calcium and diacylglycerol (DAG)[332, 355]. The full PKCα activation also requires the phosphorylation of its activation loop (A-loop) which is catalyzed by the phosphoinositide-dependent kinase 1 (PDK1) [356].

PKCα phosphorylation in the turn motif (TM) on Thr 638 and in the hydrophobic motif (HM) on Ser657 instead requires mTORC2[333, 334]. These posttranslational modifications are strongly decreased or even abolished in RICTOR absence and are important for PKCα maturation, stability and signaling[313, 333, 334]. The heat shock protein 90 (Hsp90) can prevent proteasome-mediated PKCα degradation in RICTOR absence, that takes place particularly when the TM is not phosphorylated[333, 334].

3.4.3. The mammalian target of rapamycin (mTOR) in angiogenesis

In many tumor cells the axis PI3K/AKT/mTOR is particularly active[315]. The dysregulation of the proteins involved in this network can lead to uncontrolled cell proliferation, migration, survival and metabolism, as it happens in tumor cells[313, 315, 321, 357]. These cells are also able to produce and secrete large amounts of growth factors (e.g. in hypoxic conditions VEGF) which stimulate aberrant angiogenesis, leading to the tumor vascularization[321]. Therefore, many treatments for tumors and clinical trials were based either on blocking the action of these growth factors on endothelial cells[263, 268, 269] or by targeting components of the PI3K/AKT/mTOR axis[358, 359]. In particular, it was observed that treatments with rapamycin or rapamycin-based drugs could limit the tumor growth by inhibiting cell proliferation and angiogenesis[360, 361]. In parallel to decreased angiogenesis, the pharmacological inhibition of the PI3K/mTOR pathway, led to a type of "normalization" of the tumor vasculature with vessels characterized by a more physiological shape, structure and proprieties[362]. This normalization enabled better anti-tumor treatment by chemo- and radiotherapy.

Interestingly, the use of drugs targeting both mTOR complexes induces a greater inhibition of the tumor growth and angiogenesis[363]. From these *in vivo* data, the idea that mTORC2 might have a specific impact on angiogenesis arose. This hypothesis was supported also by *in vitro* data generated in our group: in 2002, we discovered that rapamycin could block the sprouts formation in aortic rings and the proliferation of ECs and vSMCs induced by growth factors (FGF2 and PDGF) in hypoxic conditions[364]. In 2007, we showed that mTOR complexes mediate the effect of hypoxia on endothelial cells proliferation, mostly via AKT signaling[365]. Based on all of these observations, it is evident that mTOR is needed to induce angiogenesis *in vivo* and *in vitro*. However, since rapamycin and mTOR-inhibiting drugs target both mTOR complexes, it is not yet clear whether individual roles for the two complexes exist in angiogenesis.

4. AIM OF THE THESIS

In the last decade, the number of studies focusing on mTOR increased considerably, due to the importance of this kinase in several cellular pathways, frequently involved in diseases. Previous results of our group and others clearly showed an important role of mTOR in angiogenesis, a physiological phenomenon which can also lead to the development of several diseases such as cancer [361-365].

This kinase, however, is part of two different complexes (mTORC1 and mTORC2) which have different functions and substrate specificities. While the role of mTORC1 has been intensively studied, the implication of mTORC2 in cellular and physiological processes remains to be elucidated in detail. Therefore, many research groups dedicated their efforts in understanding the role of mTORC2 in different tissues and organs. Our group is particularly interested to determine which function(s) is attributed to mTORC2 in angiogenesis, specifically in the endothelium.

In the studies included in this thesis, we tried to understand:

1. *In vivo*: the role of endothelial mTORC2 in angiogenesis, using a tissue-specific inducible knockout mouse system and different models of angiogenesis

2. *In vitro*: cellular and molecular mechanisms that might explain a possible role of endothelial mTORC2 in angiogenesis using mouse aortic endothelial cells (MAECs) isolated from *Rictor*-floxed mice.

The mTORC2 deficiency was induced by disruption of the *Rictor* gene, an essential mTORC2 component, mediated by genome recombination

5. RESULTS – Part A

Endothelial *Rictor* is crucial for midgestational development and sustained and extensive FGF2-induced neovascularization in the adult

Fabio Aimi[1+], Stavroula Georgiopoulou[1+], Ina Kalus[1], Fabienne Lehner[1], Alica Hegglin[2], Përparim Limani[4], Vinicius Gomez de Lima[1], Markus Rüegg[3], Michael N. Hall[3], Nicole Lindenblatt[2,5], Elvira Haas[1], Edouard J. Battegay[1,5,6], Rok Humar[1,5 *]

[1] Department of Internal Medicine, University Hospital, CH-8091 Zürich, Switzerland

[2] Division of Plastic and Reconstructive Surgery, University Hospital, CH-8091 Zürich, Switzerland

[3] Biozentrum, University of Basel, CH-4057 Basel, Switzerland

[4] Division of Visceral and Transplant Surgery, University Hospital, CH-8091 Zürich, Switzerland

[5] Zürich Center for Integrative Human Physiology, University of Zürich, Switzerland

[6] Center of Competence Multimorbidity and University Research Priority Program "Dynamics of Healthy Aging", University of Zurich, Switzerland

[+]These authors contributed equally to this manuscript

Contributions to the work

R.H. and E.J.B. produced the original idea, designed experiments and wrote the manuscript. F.A. isolated the endothelial cells, induced the knockout, performed the cellular and molecular biology experiments and contributed writing the manuscript. R.H. performed the vWF and VEGFR1 stainings and the VEGFA-induced proliferation. R.H., F.A. and V.G.L. performed matrigel plug experiments. S.G., I.K., N.L. and A.K. performed dorsal skinfold experiments and intravital microscopy. S.G. analyzed intravital videos and contributed writing the manuscript. I.K. assessed embryonic development and contributed writing the manuscript. F.L. and R.H. performed endothelial network-formation assays. M.N.H. and M.R. generated *Rictor*$^{flox/flox}$ mice. E.H. detected *Rictor* knockout in aortic samples and revised the manuscript. All authors have reviewed, discussed and approved the results and conclusions of this manuscript.

5.1. Loss of endothelial homozygous *Rictor* results in embryonic lethality around embryonic day (E) 11.5–12.5

Whole-body mTORC2 knockout mice are embryonically lethal. Guertin and colleagues suggested vascular defects as a potential reason for early embryonic death[310, 328]. We further investigated the loss of *Rictor* in endothelial cells during embryogenesis by using a constitutive VE-Cadherin promoter-driven *Cre* and LacZ reporter containing *Rictor* knockout[366]. The analysis of 101 pups revealed two homozygous *Rictor* knockout mice, indicating predominant embryonic lethality. Heterozygous *Rictor* knockout and wild-type mice were born at expected Mendelian ratios (Figure 20A). Interestingly, the two surviving *Rictor*$^{\Delta ec}$ mice were females, fertile, and phenotypically normal. When further used for breeding, these two *Rictor*$^{\Delta ec}$ mice gave birth only to heterozygous and wild-type *Rictor* pups. On E10.5, LacZ reporter-positive *Rictor*$^{\Delta ec}$ and wild-type embryos displayed endothelial cell-specific CRE recombination, as visualized by β-galactosidase staining in intersegmental vessels, intracranial arteries, and the dorsal aorta. LacZ activity in the dorsal longitudinal anastomotic vessel was clearly visible in wild-type embryos but was less prominent in *Rictor*$^{\Delta ec}$ embryos, indicating reduced or delayed angiogenesis into the periphery from intersegmental vessels (Figure 20B). However, *Rictor*$^{\Delta ec}$ embryos generally appeared normal and were viable at this time point. We found noticeable distinct vascular features in few selected but not all *Rictor*$^{\Delta ec}$ embryos compared to controls: vascular remodeling around the vitelline artery that usually occurs at this or earlier time-points[367] was characterized by the presence of numerous, thin parallel anastomosing vessels which are not observed in wild-type mouse embryos. Furthermore we found dilated intracranial vessels in *Rictor*$^{\Delta ec}$ but not in controls (Figure 20B).

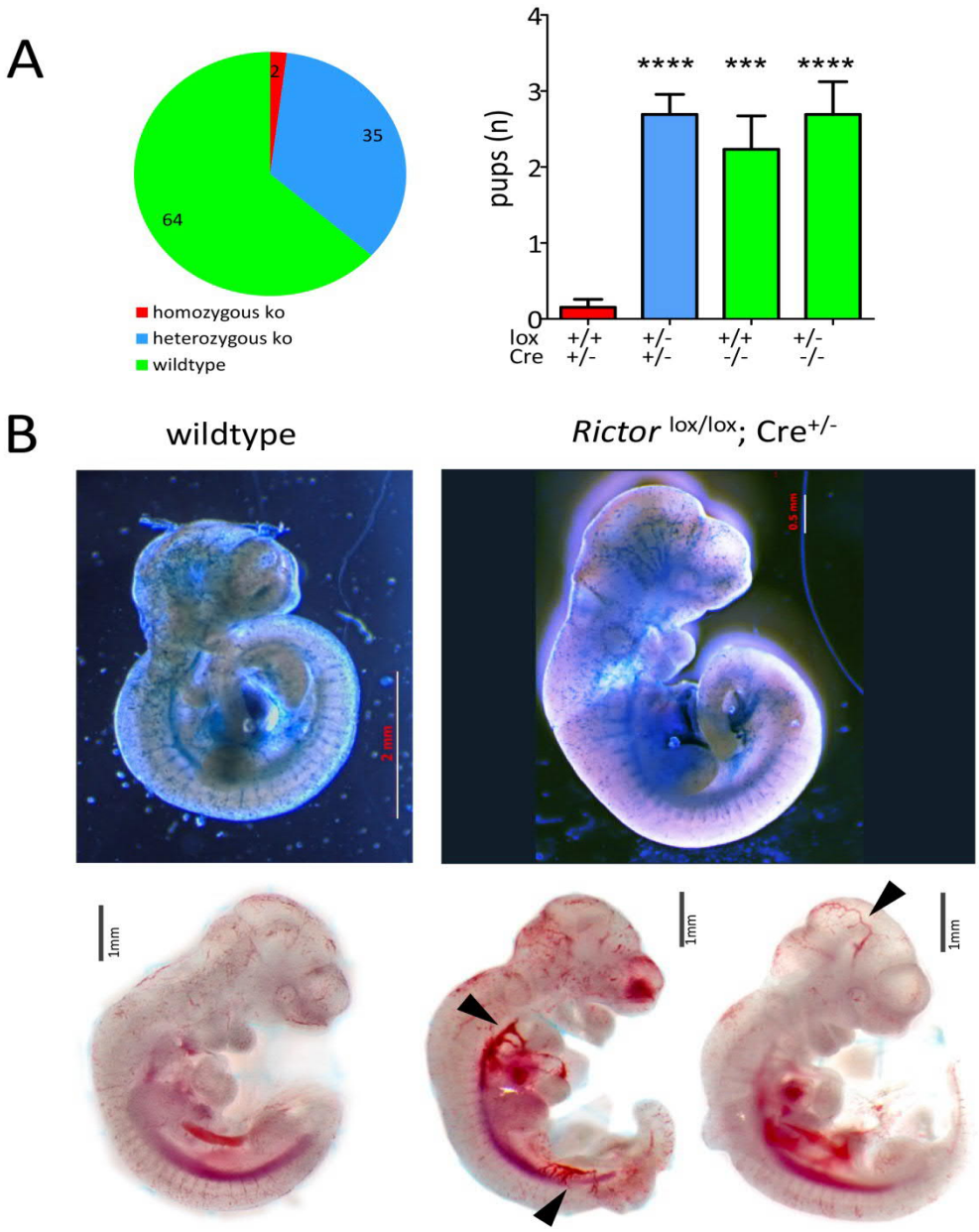

Figure 1

Figure 20. Constitutive homozygous endothelial *Rictor* knockout during embryonic development is generally lethal.

Rictor$^{flox/flox}$ females were mated with *Rictor*$^{flox/-}$; *VE-Cadherin-Cre*$^{+/-}$; *LacZ reporter* $^{+/+}$ males to generate homozygous deletion of *Rictor* in the endothelium. Litter genotypes were determined by qPCR and are displayed as total distribution and average number of pups per genotype ($n_{total\ pups}$=102, ****P<0.0001, ***P<0.001, 1-way ANOVA with Bonferroni multiple comparison) (A). The abovementioned breeding scheme was used to isolate embryonic day (E) 10.5 wild-type and endothelial *Rictor* knockout embryos. Representative β-galactosidase staining (blue) of E10.5 embryos (upper panels) shows the active sites of *VE-Cadherin-Cre* recombination. Images show E10.5 representative embryos before staining. Arrows on the right indicate distinct vascular remodeling or dilation in *Rictor* knockout embryos (B).

This feature has also been observed in *Rictor* whole body knockout embryos in the study by Guertin et al.[328]. Thus, erythropoiesis and vasculogenesis of the primitive vascular plexus, which is completed on E10.5[368], was not modulated by endothelial mTORC2. To precisely determine the time point of lethality, overlapping tamoxifen-injection schemes in pregnant mice with homozygous loxed *Rictor* gene and inducible VE-Cadherin CreER^{T2} recombinase were used (Figure 21A). Injecting tamoxifen three times in pregnant mice, starting at E7.5, produced marked and significant reductions in litter size (Figure 21B). However, injecting tamoxifen twice at E7.5 did not result in any differences in litter size (Figure 21B). Knockdown of *Rictor* by 60% is achieved with two injections of tamoxifen, whereas nearly homozygous (92%) knockout is achieved with three injections of tamoxifen every second day[369]. Thus, with three injections starting on E7.5, knockout of *Rictor* was likely to be maximal starting from E11.5–E12.5. On E17.5, one third of the embryos were growth-retarded, and the remaining embryos were absorbed (Figure 21C). In addition, more than 90% of analyzed embryos were growth-retarded after tamoxifen injections began on E6.5 and E8.5 (Figure 21C). Interestingly, tamoxifen injections that began on E12.5 and E14.5 had no influence on viability and growth (Figure 21C).

Embryos that were injected with tamoxifen on E8.5 had a body length of approximately 14 mm, whereas embryos that were injected on E14.5 had a body length of 19.5 mm. Wild-type embryos at embryonic day 17.5 displayed a body length of 18–22 mm (Figure 21D). Furthermore, growth-retarded embryos did not display wrinkled skin; instead, the skin was rather thin, and subcutaneous veins were visible (Figure 21E). To investigate whether endothelial-specific *Rictor* knockout causes a delay in vascularization, embryos received three injections of tamoxifen that started on E7.5, after which they were sacrificed at E12.5. The majority of endomucin-stained vascular plexi were present in both *Rictor*$^{i\Delta ec}$ and control embryos. Again, we detected a few distinct vascular features, such as reduced sprouting angiogenesis in subdermal vessels in the ventral region of *Rictor*$^{i\Delta ec}$ embryos (Figure 21F). Also, the temporary hyaloid vessels in the eye had formed incompletely (Figure 21F). In growth-retarded *Rictor*$^{i\Delta ec}$ mice that were first injected with tamoxifen on E.6.5 and E8.5, ossification centers in the fingers were strongly reduced or missing when analyzed on E17.5 as compared to embryos that were first injected on E14.5 (Figure 21G, alizarin red (bone) and alcian blue (cartilage) staining and quantification of ossification centers below). Embryos that were first injected on E14.5 displayed an ossification progress comparable to wild-type mice as demonstrated earlier by Gollner et al.[370]. Similarly, the progress of ossification in the vertebrae was clearly delayed in embryos that were first injected with tamoxifen on E8.5, and the long bones of the upper and lower limbs were significantly shorter in embryos that received their first tamoxifen

injections on E6.5 and E8.5 (Figure S1). Furthermore, CD31 staining from skin, brain, skeletal muscle, lung, and colon sections of growth-retarded *Rictor*$^{i\Delta ec}$ mice were morphologically indistinguishable from sections of wild-type control mice (Figure S2).

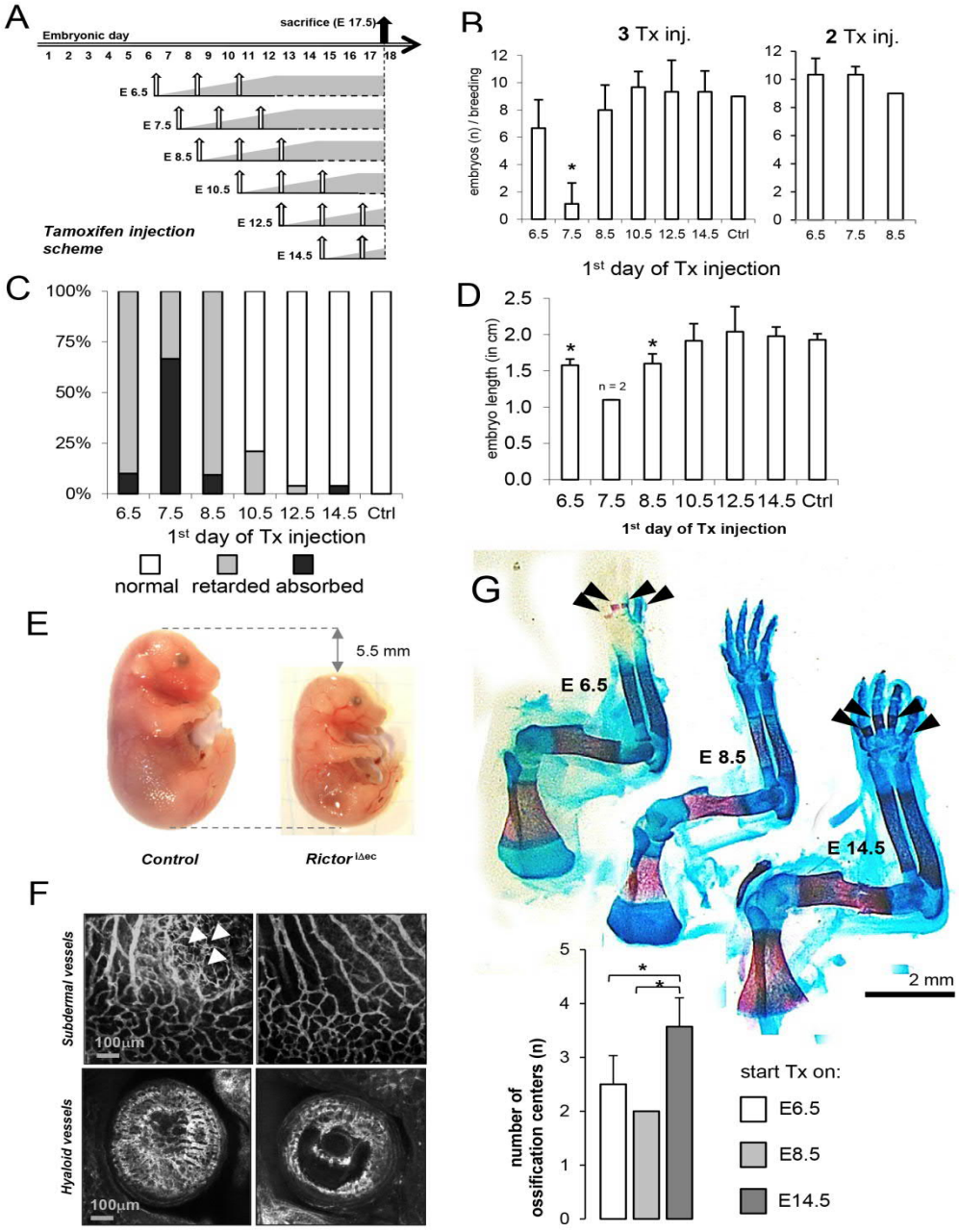

Figure 2

Figure 21. Lethality and growth retardation of induced endothelial *Rictor* knockout mice peaks around E12.

Tamoxifen (Tx) injection scheme: Three doses of Tx (1 mg, intraperitoneally) were administered to pregnant females every 48 hours, beginning on E6.5, E7.5, E8.5, E10.5, E12.5, and E14.5. Pregnant females were sacrificed, and embryos were harvested on E17.5 for further histological analysis. Grey area symbolically

depicts stepwise *Rictor* knockout. Control females were injected with corn oil (A). *Rictor*$^{i\Delta ec}$ mice exhibit decreased litter size. Statistical analysis of the litter size of individual breedings (n_{Eday}) after three and two Tx injections at different time points ($n_{E6.5}$ =3, $n_{E7.5}$ =3, $n_{E8.5}$ =4, $n_{E10.5}$ =3, $n_{E12.4}$ =4, $n_{E14.5}$ =4,) compared to controls (n=7). *P<0.05. Student's t-test (B). Growth retardation and embryonic lethality around midgestation in *Rictor*$^{i\Delta ec}$ embryos. Statistical analysis of normal, growth retarded, and absorbed embryos per breeding after Tx-injection at different time points. Total litter size for breeding at each time point was set to 100%, $n_{breedings}$=3 (C). *Rictor*$^{i\Delta ec}$ embryos display reduced body length on E17.5. Statistical analysis of the length of surviving embryos per litter at different starting time points of Tx injections. n=4 (embryos per time point, length was measured in both extremities), *P<0.01 compared to controls. Student's t-test (D). Representative picture of a E17.5 *Rictor*$^{i\Delta ec}$ embryo that was induced by Tx on E8.5 in comparison to a wild-type embryo (E). *Rictor*$^{i\Delta ec}$ embryos display distinct vascular deficits. Pregnant females were injected with three Tx injections starting on E7.5. Embryos were then harvested at E12.5 and stained with the vessel-specific antibody, endomucin. Scale bar=100 µm. Arrows indicate angiogenic sprouts (F). *Rictor*$^{i\Delta ec}$ embryos display a delay in ossification. Representative pictures of the upper limbs of embryos stained with alizarin red (bone) and alcian blue (cartilage). Arrows: ossification centers. Below quantification with number of ossification centers in fingers upon knock down of *Rictor* at indicated starting time points of Tx injections. *P < 0.05, **P < 0.01, compared to E14.5; n=4, Mann-Whitney Rank Sum Test (G).

In summary, endothelial *Rictor* knockout resulted in lethality, which peaked around E12 based on analysis of lethality and growth retardation induced by overlapping Tx-injection regimens. Although *Rictor* knockout did not affect vascular plexus formation, distinct abnormal vascular features, such as delayed angiogenesis into the periphery, were detected, and growth retardation was accompanied by delayed bone ossification in fingers, toes and vertebrae.

5.2. Endothelial-specific *Rictor* knockout has no obvious effect on viability and weight gain during adolescence into adulthood

We proceeded to analyze the general requirement of endothelial mTORC2/RICTOR using the inducible VE-Cadherin-driven CreER^{T2} variant (*Rictor*$^{i\Delta ec}$) during adolescence from the age of 4 weeks (at the time of tamoxifen-induced *Rictor* knockout) to adulthood, up to an age of 28 weeks. No statistically significant differences in weight gain were observed between genotypes and genders (Figure 22A). Furthermore, all groups displayed normal health and viability. At the end of the weight study, the aorta from male control and *Rictor*$^{i\Delta ec}$ mice were removed, the endothelium was scraped and *Rictor* mRNA levels were determined by quantitative polymerase chain reaction (qPCR) to show stable, efficient, and significant knockdown of *Rictor* (Figure 22B). Adolescent double transgenic mice (*Cre*$^{+/+}$; *Rictor*$^{lox/lox}$) also displayed specific CRE expression in capillaries from the mouse dermal skin muscle, as shown by estrogen receptor-specific staining in tissues that were used for intravital experiments (Figure 22C). Although VE-Cadherin promoter-driven CRE

recombination may also affect hematopoietic development[369], we found similar hematological profiles in 8-week-old control and *Rictor*$^{i\Delta ec}$ mice. These profiles were comparable to those of healthy C57/Bl6 mice (Figure S3).

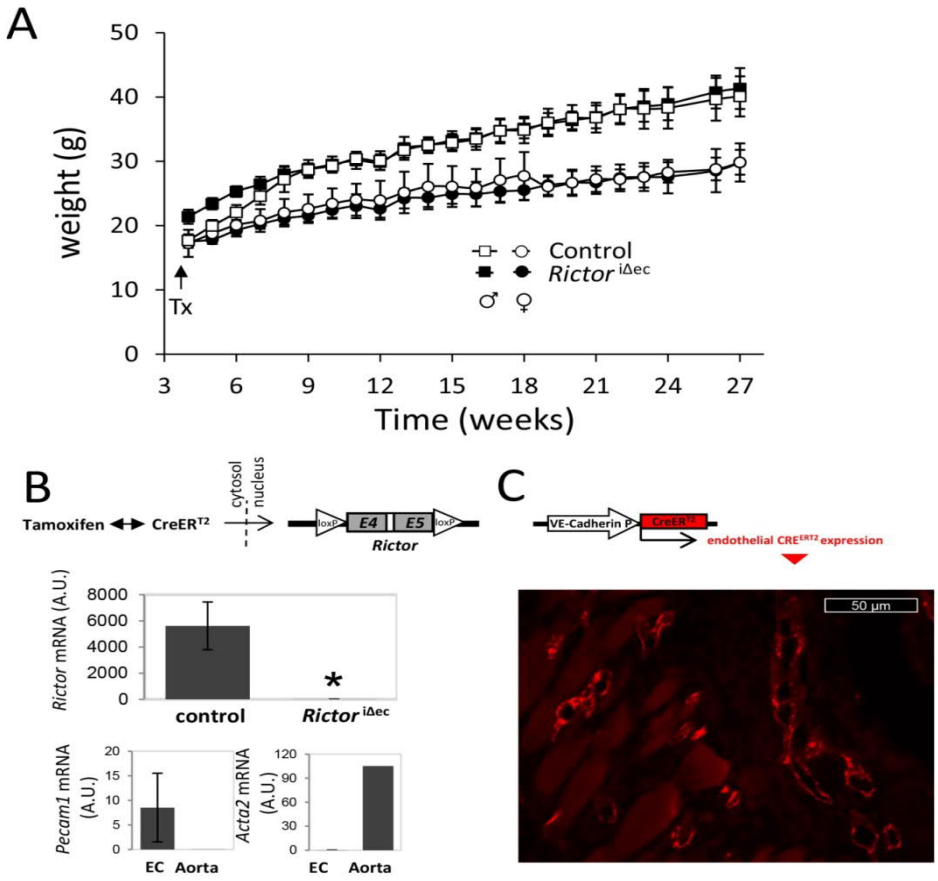

Figure 3

Figure 22. *Rictor* knockout does not affect weight gain and viability in adolescent mice.
Body weights were followed in male and female mice over a period of 27 weeks after induction of knockout or control on week 4. No significant differences were detected in male or female *Rictor*$^{i\Delta ec}$ mice compared to control mice. n=10 per genotype and gender, 2-way ANOVA with group-wise comparison. All mice displayed normal health, behavior, and viability (A). After 27 weeks, the aortae of a subset of male mice were excised and isolated. The endothelial layer was scraped, and RNA was extracted for quantitative polymerase chain reaction (qRT-PCR) analysis to test for efficient excision of *Rictor* (n=3/2, *P<0.05. 2-tailed T-test), and qualitatively for purity of endothelial tissue (endothelial marker *Pecam1*, smooth muscle marker *αSma*). Total aorta mRNA was used as comparative control (B). Representative immunostainings for estrogen receptor 2 (red fluorescence) in histological sections of the skinfold from 10-week-old *Rictor*$^{i\Delta ec}$ mice demonstrates specific expression of CreER^{T2} recombinase associated with capillaries (C).

These experiments demonstrate that the stable ablation of endothelial mTORC2 in adolescent mice, which persisted until late adulthood, did not cause obvious general health problems, as supported by normal hematological profiles, weight gain, and viability.

5.3. *Rictor* knockout in mouse aortic endothelial cells (MAEC) differentially disables the formation of capillary-like endothelial networks.

Our results so far suggested, that knockout of *Rictor* in endothelial cells has no obvious effects on the development during adolescence in mice and therefore may not affect basic physiologic parameters of the endothelial cell such as survival and homeostatic functions in the existing and developing vasculature. Before continuing investigations about the role of mTORC2 in activated endothelium *in vivo*, we used an *in vitro* assay to determine the angiogenic response of control and *Rictor* knockout mouse aortic endothelial cells to the two major angiogenic molecules FGF and VEGF (Figure S4). After plating on a basement membrane (BM) matrix gel, endothelial cells build capillary-like tubes with a lumen within a short time. Cells initially attach to the matrix and then migrate towards each other, after which they align and form tubes[371]. We found that control MAEC formed connected master segments in the presence of the diluent (1% fetal calf serum [FCS]), FGF2 and VEGFA (Figure 23A). The ability of *Rictor* knockout MAEC (*Rictor* KO MAEC) to build stable contacts and connecting tubes was substantially disabled: *Rictor* knockout prevented MAEC from forming capillary-like tubes in unstimulated conditions. Upon FGF2 stimulation, *Rictor* KO MAEC arranged into star-like shapes, with sprouts extending from cell clusters, but did not establish contacts to other cell clusters and formed significantly less master segments compared to control (Figure 23A). A stable CRE-induced *Rictor* knockout with blunted AKT phosphorylation on Ser^{473} was detected during these experiments (Figure 23A). In contrast to the study by Wang et al.[372], VEGFA stimulation partially rescued endothelial network formation in *Rictor* KO MAEC. *Rictor* KO MAECs were able to form some substantial networks and organized tubes, albeit in in numbers that were small and similar to those of control MAECs (Figure 23A). To further evaluate differences in mTORC2/RICTOR requirement for FGF2- and VEGFA-induced tube formation *in vitro*, we performed co-culture experiments. Control and *Rictor* KO MAEC were mixed at a 1:1 ratio. VEGFA-stimulated *Rictor* KO MAECs established master segments autonomously without adhering to control MAECs (Figure 23B; on the right: arrows indicating individual *Rictor* KO master segments). FGF2-stimulated *Rictor* KO MAECs were always found as part of master segments that were formed by control MAECs. Thus, FGF2-induced cell clusters projected sprouts but were unable to form mature capillary-like networks in *Rictor* KO MAEC cells (Figure 23B; on the left: arrows indicating unconnected *Rictor* KO sprouts).

As we found that the angiogenic response to FGF2 was significantly more affected by *Rictor* knockout than that to VEGFA, we further focused on FGF2-mediated responses in endothelial cells and angiogenesis assays *in vivo* in this study.

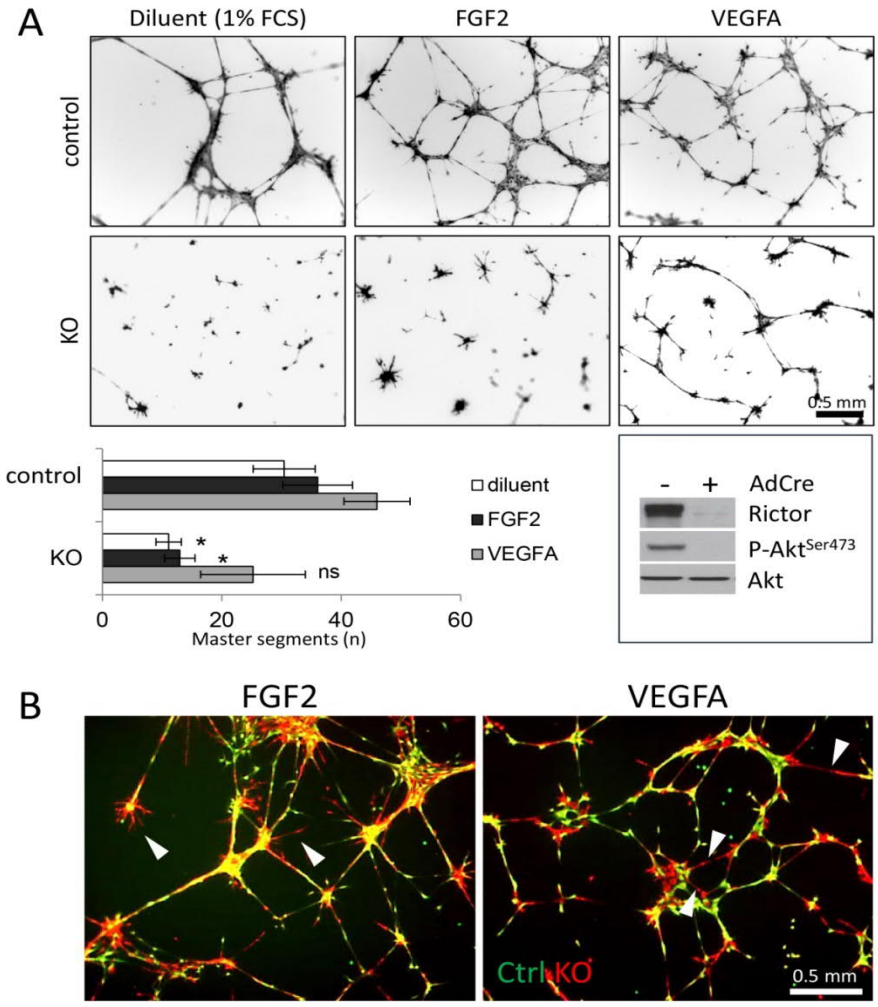

Figure 4

Figure 23. *Rictor* knockout in mouse aortic endothelial cells (MAEC) decreases endothelial network formation.

Control and *Rictor* knockout MAEC (*Rictor* KO MAEC) were seeded on growth factor-reduced matrigel and stimulated with diluent (1% fetal calf serum [FCS]), FGF2 (25 ng/ml), and vascular endothelial growth factor (VEGFA; 25 ng/ml). Representative micrographs show endothelial network formation after 18 hours. Quantification (total number of master segments that connect to at least two other segments) of endothelial tube formation from three experiments is shown below. (Bars; mean and SEM, $n_{exp}=3$, *P<0.05 versus control. Paired T-Test). Western blot lower right showing RICTOR, Phospho-AKT Ser ^{473}, and total AKT expression from control (AdCre^{-}) and *Rictor* KO (AdCre^{+}) MAECs (A). Endothelial network formation of *Rictor* KO MAEC after co-culture with control MAEC. Control and *Rictor* KO MAEC were labeled with green and red tracking dyes, respectively, mixed at a 1:1 ratio, and seeded on growth factor-reduced matrigel. Tube formations of endothelial cultures after 18-hours stimulation with FGF2 or VEGFA were photographed on a fluorescence microscope (4× magnification). Arrows mark endothelial segments composed of *Rictor* KO MAEC only in VEGFA-treated cultures, whereas *Rictor* KO MAEC could only participate in segment formation through

association with control cells in FGF2-treated cultures. FGF2-treated *Rictor* KO MAEC typically formed star-shaped centers with omni-directional sprouting and no connection to neighboring centers (B).

5.4. FGF2 amplifies RICTOR protein and RICTOR-dependent phosphorylation of AKT on Serine 473 and PKCα on Serine 657

Interestingly, we found a consistently low expression of RICTOR in starved, unstimulated and subconfluent MAEC isolate, whereas FGF2 amplified RICTOR protein levels. Quantification demonstrated a significant increase in RICTOR protein at 5 ng/ml of FGF2 peaking at an 8-fold expression compared to diluent at 50 ng/ml of FGF2. (Figure 24A, upper left panels). We assessed how FGF2-induced signaling is altered in mTORC2-deficient endothelial cells and focused on one of the main mTORC2 downstream targets, PKCα and AKT[333]. In control MAEC, FGF2 induced the dose-dependent phosphorylation of the hydrophobic motif (HM) of PKCα on Ser[657]. Interestingly, deletion of *Rictor* strongly decreased PKCα protein levels and accordingly blunted the phosphorylation of the HM of PKCα in response to FGF2, FCS, and insulin (Figure 24A). PKCα signaling was strongly disabled in *Rictor* KO MAEC, and this was most likely a result of total PKCα protein destabilization and degradation due to absent phosphorylation[333]. We then assessed the impact of *Rictor* deletion in MAEC on mTORC downstream target protein kinase AKT (also known as PKB). The phosphorylation of the activation loop (A-loop) on Thr[308] by phosphoinositide-dependent kinase 1 (PDK1) and of the HM at Ser[473] of AKT by mTORC2 results in AKT activation[335,373]. In control MAEC, FGF2 induced a marked and dose-dependent phosphorylation of AKT on Ser[473] that peaked at 25 ng/ml of FGF2. *Rictor* knockout efficiently and significantly blunted FGF2-, FCS-, and insulin-induced AKT phosphorylation (Figure 24A, quantification to the right). The disruption of mTORC2 has been shown to decrease the A-loop phosphorylation of AKT in some cancer cell lines [335]. In control MAEC, A-loop phosphorylation was robustly induced by FGF2, FCS, and insulin. After *Rictor* knockout, we did not detect a significant reduction in the A-loop phosphorylation of AKT (Figure 24A). These results are consistent with reports in cells or tissues that were derived from mice with genetic deletions of mTORC2 components. In these mice, A-loop phosphorylation was not disrupted in the absence of HM phosphorylation[328,329,333].

The depletion of AKT phosphorylation by *Rictor* knockout may influence mTORC1 signaling. AKT phosphorylates and inhibits tuberous sclerosis 2 (also known as tuberin), thus resulting in the activation of mTORC1-S6 kinase 1 (S6K1) [324]. We found that FGF2 dose-dependently promoted S6K1 phosphorylation in control MAEC. After *Rictor* knockout, a minor but insignificant reduction in FGF2-induced S6K1 phosphorylation was detected (Figure 24A). No differences in the phosphorylation of extracellular signal-

regulated kinase 1 and 2 (Erk1/2) by the FGF2 gradient were observed in control MAEC and *Rictor* KO MAEC (Figure 24A)[374].

A close cross-talk exists among FGF2 and the different members of the VEGF family during angiogenesis and several studies have suggested that FGF2 induces neovascularization indirectly by activation of the VEGF/VEGFR system[375]. We confirmed that *Vegfa* mRNA substantially increased after FGF2 stimulation, yet *Rictor* knockout did not affect this induction. To investigate whether endothelial mTORC2 might modulate *in vitro* angiogenesis in response to FGF2 by regulation of VEGF receptors, we measured the mRNA-levels of the two main VEGF-receptors *Flt1* (VEGFR1), which is characteristic for stalk cells and quiescent endothelium, and *Kdr* (VEGFR2), upregulated in tip cells[376]. Interestingly we found a strong FGF2-induced upregulation of the membrane form of *Flt1* (*mFlt1*) and an even stronger induction of *soluble Flt1 receptor* (*sFlt1*) mRNA (Figure 24B). *Kdr* message was present and decreased after FGF-stimulation (Figure 24B). However, *Rictor* knockout cells induced *mFlt1* and *sFlt1* and reduced *Kdr* message congruent to control cells after FGF2 stimulation, which argues against endothelial tip-stalk-cell modulation by mTORC2. FGF2 also stimulates VEGFA in endothelial cells of forming capillaries and cultured aortic endothelial cells[97]. Similarly, *FGF receptor 1* (*Fgfr1*) message equally increased in control and *Rictor* KO MAEC. The decrease in PKCα protein after *Rictor* knockout was due to posttranscriptional mechanisms as PKCα gene expression was equal in control and *Rictor* KO MAEC (Figure 24B).

Furthermore, we did not observe any significant differences in endothelial proliferation over a period of 72 hours in the dose response to FGF2 (Figure 24C) or FGF2-induced-migration in a wound assay (Figure 24D). However, a weak but significant ($P<0.05$, $n_{exp}=4$) reduction in proliferation was detected in the presence of FCS (Figure 24C). Similarly, we found a significant reduction in VEGFA-induced proliferation by *Rictor* knockout (Figure S5).

In conclusion, FGF2 amplified RICTOR protein in control MAEC and *Rictor* deletion in FGF2-stimulated MAEC strongly blunted PKCα signaling and reduced AKT activity by depleting Ser^{473} phosphorylation. *Rictor* deletion had no effects on mTORC1 signaling and FGF2-induced proliferation, migration nor did it interfere with FGF2-induced modulation of *Flt1*, *Kdr* and *Vegfa* expression levels.

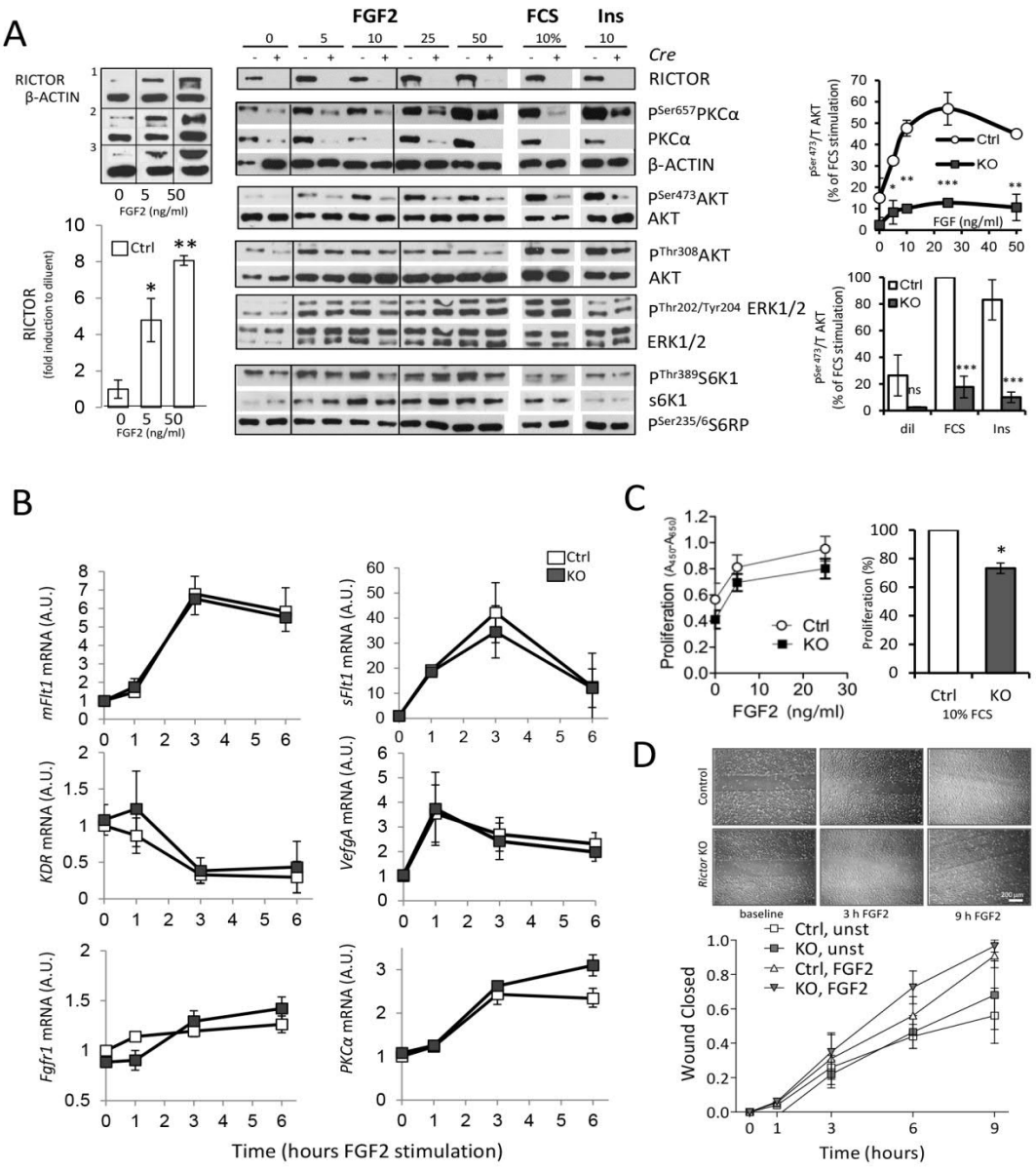

Figure 5

Figure 24. FGF2 amplifies RICTOR protein and *Rictor*-dependent phosphorylation of AKT on Ser^{473} and PKC**α** on Ser^{657}.

Subconfluent and starved control and *Rictor* KO MAEC were stimulated for 15 min with increasing doses (5–50ng/ml) of FGF2. As controls, MAEC were treated with 10% FCS or 1 µg/ml insulin (Ins). Western blots show the expression of RICTOR and downstream and targets of mTORC2. Low expression of RICTOR is detected in starved, unstimulated and confluent control MAEC, whereas FGF2 increased RICTOR protein levels. Quantification demonstrated a significant increase in RICTOR protein at 5 ng/ml of FGF2 peaking at an 8-fold expression compared to diluent at 50 ng/ml of FGF2 in 3 repeated experiments in a MAEC isolate. (control=white bars, n_{exp}=3, *P<0.05, **P<0.001, 1-way ANOVA with Bonferroni multiple comparison, upper left panels). Furthermore, PKCα protein was nearly absent in *Rictor* KO MAEC compared to control (middle panels). Densitometric quantification shows dose-dependent AKT phosphorylation on Ser^{473} in response to FGF2 in control MAEC with significant blunting in *Rictor* KO MAEC and similar reductions in response to FCS and Ins (right panels, n_{exp}=3, *P<0.05, **P<0.01, ***P<0.001, repeated measures ANOVA). Lower middle blots show no changes in S6K1 phosphorylation on Thr^{389} compared to total S6K1 and phosphorylation of p42/44

MAPK on Thr^{202}/Tyr^{204} compared to total p42/44 MAPK after *Rictor* knockout (A). Three individual confluent and starved control and *Rictor* KO MAEC isolates were stimulated for 1–6 hours with 25 ng/ml FGF2. mRNA expression for membrane-bound and *soluble VEGF receptor 1* (*mFLT1, sFlt1*), *VEGF receptor 2* (*Kdr*), *Vegfa* (*Vegfa*), FGF receptor 1 (*Fgfr1*) and protein kinase Cα (*PKCα*) were detected by quantitative real-time PCR (n=3, ns knockout versus control, repeated measures ANOVA) (B). Control and *Rictor* KO MAEC were seeded subconfluently, cultured for 25 hours in growth medium with 1% FCS, and then stimulated with FGF2 or 10% FCS for 3 days. Cell proliferation was measured by WST-1 reagent. Absolute proliferation values (Absorption=A_{450nm}-A_{650nm}) in FGF2-stimulated control (open circles) or *Rictor* KO (filled squares) MAEC are presented. No significant differences were observed for FGF2-stimulated proliferation after *Rictor* knockout (n=3, repeated measures ANOVA). In response to 10% FCS (right), proliferation of *Rictor* KO MAEC was significantly lower compared to that of control MAEC (n_{exp}=3, two-tailed T-test) (C). Control and *Rictor* KO MAECs were grown to confluency, cultured for 25 hours in growth medium with 0.5% FCS, and a uniform scratch applied to the monolayer. Migration of MAECs was measured after FGF2 (25ng/ml) or diluent administration for 1, 3, 6 and 9 hours (wound completely closed=1, n=3, no differences between groups by repeated measures ANOVA) (D).

5.5. The structure of the capillary bed of the striated skin muscle is not altered by endothelial-specific *Rictor* knockout

In preparation to study mTORC2-dependent vascular changes in response to wounding and FGF2 *in vivo*, we first recorded the capillary morphology in the existing striated skin muscle (*Panniculus carnosus*) vascular bed as baseline. To do so we surgically mounted a dorsal skinfold chamber[377, 378] to 8-week-old control and *Rictor*$^{i\Delta ec}$ mice. We observed that the baseline capillary bed, which was recorded 3 days post-chamber surgery, appeared very similar in 8-week-old control and *Rictor*$^{i\Delta ec}$ mice (Figure 25A). Analysis of all capillary diameters measured at baseline did not reveal significant differences (Figure 25A). In both experimental groups, the vascular bed consisting of the *panniculus carnosus* with its capillary structures was organized in the typical parallel orientation, and the subcutaneous layer with draining arterioles and venules exhibited the typical perfusion pattern of the dorsal skinfold chamber capillaries, as observed in previous studies[377]. Thus, ablation of endothelial *Rictor* did not interfere with the development or directly observable functionality of the intact, unstimulated dermal microvasculature in adolescent mice, which is in line our observation of normal growth, viability and weight gain of adolescent mice lacking endothelial *Rictor*.

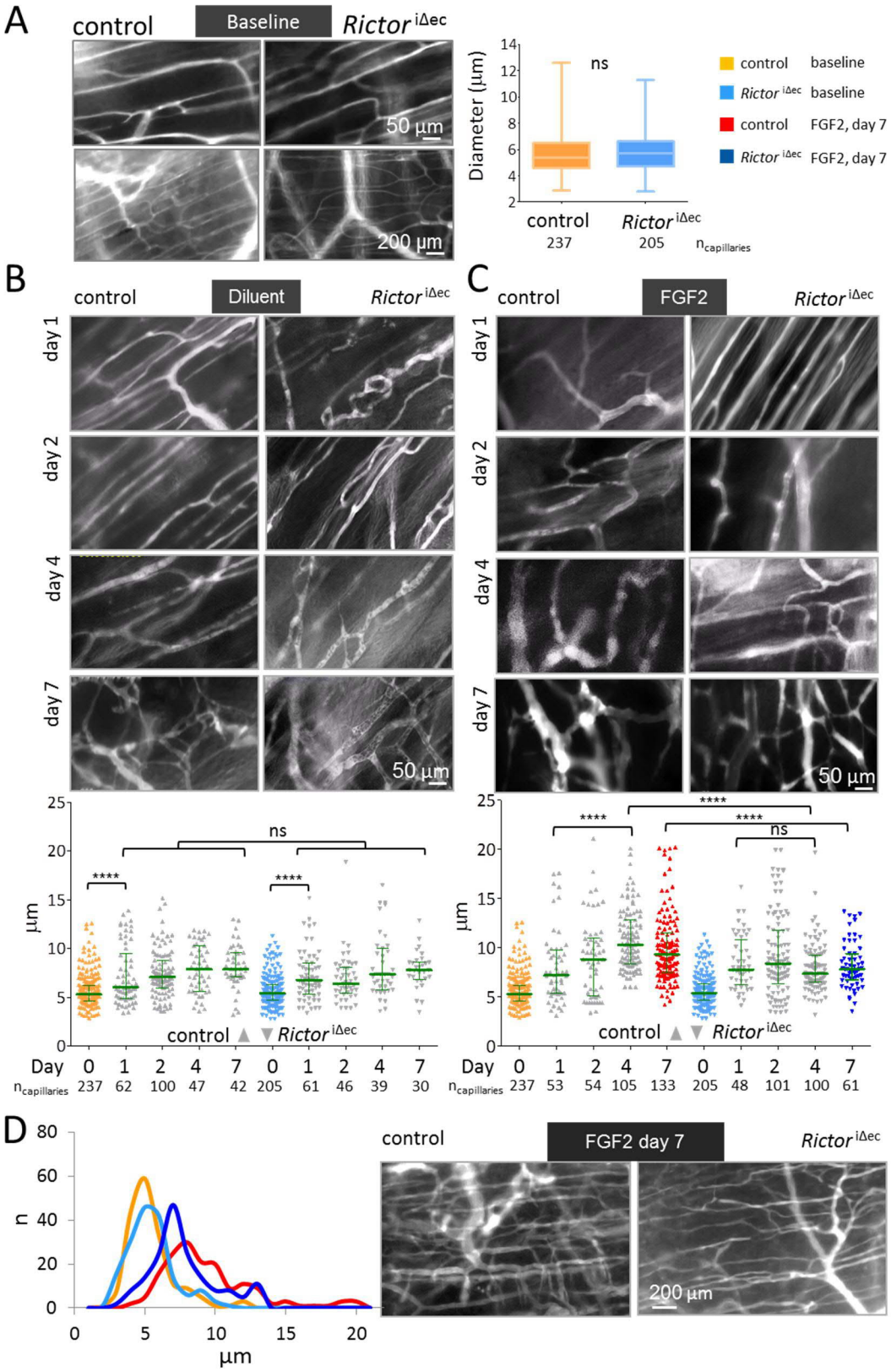

Figure 25. *Rictor* knockout disables a sustained increase in skin capillary diameters and restricts extensive capillary remodeling in response to FGF2.

Stacked frames of representative videos of the capillary vasculature were recorded through the dorsal skinfold chamber by intravital fluorescence microscopy. Baseline capillary bed of the skin muscle was assessed in 10-week-old mice (6 weeks after knockout induction) by intravital microscopy through the unmodified dorsal

skinfold chamber. Upper (20× magnification) and lower micrographs (10×) display representative skin capillary beds of control (left) and *Rictor*$^{i\Delta ec}$ (right) mice. Capillary diameters from 10 control and *Rictor*$^{i\Delta ec}$ mice were quantified and pooled for statistical analysis (n=253/206, no differences between groups , 2-tailed T-test and Whisker plot, indicating median, 25% percentile and total range to the right). Color scheme applies for whole figure 6 and is displayed in upper right corner (A). Wound response of the capillary bed. Skin muscle capillary structure from day 1, 2, 4 and day 7 in control (left) and *Rictor*$^{i\Delta ec}$ mice (right) after wound sealing with heparin-containing matrigel (20× magnification). Capillary diameters from 4 control and *Rictor*$^{i\Delta ec}$ mice were quantified and pooled for statistical analysis by 1-way ANOVA followed by Bonferroni multiple comparison (Scatter plot with medians on the below; number of capillaries ($n_{capillaries}$) are indicated below the X-axis, ****P<0.0001) (B). Heterogeneous capillary diameter increases in the FGF2-stimulated capillary bed. Skin muscle capillary structure from day 1, 2, 4 and day 7 in control (left) and *Rictor*$^{i\Delta ec}$ mice (right) after wound sealing with FGF2 (1.5 µg/ml; heparin-containing matrigel, 20× magnification). Capillary diameters from 7 control and *Rictor*$^{i\Delta ec}$ mice were quantified and pooled for statistical analysis by 1-way ANOVA followed by Bonferroni multiple comparison (Scatter plot and medians below; number of capillaries are indicated below the X-axis, ****P<0.0001) (C). Capillary remodeling in the FGF2-stimulated capillary bed. The line graph displays the normalized distribution of capillaries (n_{max}=100) resolved in a 1-µm range after FGF2 stimulation for 7 days and illustrates differences in remodeling between groups. Micrograph to the right shows 10x magnification of the vascular bed of control and *Rictor*$^{i\Delta ec}$ mice after 7 days of FGF2 exposure (D).

5.6. Wounding-induced capillary diameter remodeling is not impaired by endothelial-specific *Rictor* knockout

We then modified this chamber by additionally removing cutis and subcutis on the opposite side of the observation window. This defect was sealed by growth factor-reduced matrigel (Figure S6). In the first set of experiments, we included diluent (heparin) in matrigel to assess baseline alterations as a response to wound healing processes without exogenous growth factor stimulation. Capillaries were observed and recorded on a daily basis by intravital microscopy up to 7 days after matrigel sealing (Figure 25B). Vascular morphological parameters were quantified in vessels where perfusion was observable. The vessels encompassed diameters ranging from 4 to 20 µm, thus capillaries and some small arterioles or venules. Capillary diameters significantly increased from day 1, 2, 4 and 7 compared to the baseline by about 2 µm in average for both control and *Rictor*$^{i\Delta ec}$ capillary diameters (Figure 25B). Importantly, the microvasculature of the *panniculus carnosus* responded similarly to wounding and matrigel sealing in control and *Rictor*$^{i\Delta ec}$ mice as we did not detect significant differences compared to controls at days 1, 2, 3, and 7 (Figure 25B).

5.7. Endothelial-specific *Rictor* knockout limits increases in the capillary diameter of existing skin vasculature in response to high doses of FGF2.

To assess remodeling in terms of individual increases in capillary diameters in response to strong angiogenic stimulation, we exposed the existing capillary bed to a high dose of FGF2 (1.5 µg/ml). We focused on FGF2, since we found that *Rictor* deletion specifically disabled FGF2- but not VEGFA-dependent angiogenesis *in vitro* as shown earlier in this manuscript. Furthermore, FGF2 also promotes maturation of larger vessels such as arterioles[379]. Intravital recordings through the dorsal skinfold chamber in control and *Rictor*$^{i\Delta ec}$ revealed that diameters increased at day 1 and day 2 after FGF2 exposure (Figure 25C, day 1 and 2). In both groups, diameters had increased for about 3.5 µm and we found no statistical difference between groups after testing by Bonferroni multiple comparisons (Figure 25C). At days 4 and 7, capillary diameters further increased in the control group ($P<0.0001$ when comparing diameters at day 1 to diameters at day 4 of the control group). In addition, tortuous and bulbous vascular structures developed, which were observed in capillaries and small draining arterioles and venules (Figure 25C, day 4 and 7). In *Rictor*$^{i\Delta ec}$ mice, however, FGF2-induced capillary enlargement stopped and rather regressed after day 2. Statistically, capillary diameters at days 4 were not different from those measured at day 1. Diameters measured on day 4 and 7 in *Rictor*$^{i\Delta ec}$ were significantly smaller compared to the control group on those days (Figure 25C). We observed, that at the end of the recording the vascular bed in *Rictor*$^{i\Delta ec}$ mice underwent a far more restrained and different mode of remodeling. Thin-connecting anastomoses emerged between capillaries and draining arterioles in *Rictor*$^{i\Delta ec}$ mice, and the orientation of capillaries remained largely parallel (Figure 25C and D, day 7). The dilated and tortuous capillary structures that developed in control mice after longer (4 and 7 days) exposure to FGF2 are also found in vascularized tumors, which in addition exhibit hyperpermeability[380]. We assessed vessel leakage of the FGF2-stimulated skin vascular bed on day 7 by intravenously injecting fluorescently labeled *ricinus communis* agglutinin I (RCA-I)[381]. Preliminary data could however not support an obvious decrease in permeability by endothelial *Rictor* deletion as plasma leakage points were present in capillary structures from both control and *Rictor*$^{i\Delta ec}$ mice to a similar extent (Figure S7).

Taken together, loss of endothelial *Rictor* normalized vascular structure after 4 days of exposure to FGF2 and prevented the formation of a heterogeneous, irregular microvascular bed as seen in controls (Figure 25D). This suggests that endothelial mTORC2 is central to the FGF2-mediated remodeling response that creates larger and heterogeneously sized capillaries and small arterioles in the existing skin capillary bed beyond day 4.

5.8. Endothelial-specific *Rictor* knockout strongly reduces FGF2-induced neovascularization in matrigel plugs and prevents local hemorrhage

As technical limitations disabled us to monitor sprouting angiogenesis in the dorsal skinfold chamber, we used the matrigel plug angiogenesis assay to assess whether endothelial mTORC2 deficiency may alter *de novo* vascularization in adult mice *in vivo* in response to strong stimulation by FGF2 (1.5 µg/ml). Concentrations of FGF2 in this range have been used previously to achieve maximal neovascularization after 7 days [382] and to achieve macroscopically a hemorrhagic appearance (Figure S8). Knockout of *Rictor* in the endothelium was induced during adolescence in *Rictor*$^{i\Delta ec}$ mice. At 7 days after implantation, blood-containing microvessels and signs of hemorrhage were macroscopically evident in FGF2-containing plugs from control mice. In contrast, FGF2-containing plugs from *Rictor*$^{i\Delta ec}$ mice displayed homogenous, unobtrusive vascularization. An estimation of blood content by optical densitometry demonstrated a significant decrease after *Rictor* knockout in FGF2 containing plugs compared to control plugs (Figure 26A, 1st row). FGF2-induced vessels protruded to about 800 µm from the surface of the plug into the center in plugs from control mice, whereas microvessels protruded significantly less to only about 300 µm in plugs from *Rictor*$^{i\Delta ec}$ mice. FGF2-induced microvessel protrusion into the plugs from *Rictor*$^{i\Delta ec}$ mice was not completely abolished as we calculated a significant difference to diluent containing plugs (Figure 26A, 2nd row). The presence of leaked erythrocytes in the FGF2-containing plugs from control mice demonstrated local hemorrhage (Figure 26B, left micrographs). In contrast, the microvasculature in FGF2-containing plugs from *Rictor*$^{i\Delta ec}$ mice was composed of homogenously small capillaries with no evidence of hemorrhage (Figure 26B, right micrographs). During the 7 days of FGF2 administration, the matrigel plug was encapsulated by a thin layer of stromal tissue that also contained arterioles and venules. We found similar vessel densities in plugs from both experimental groups (data not shown), whereas the luminal diameter was significantly smaller in vessels of the stromal capsule from *Rictor*$^{i\Delta ec}$ mice compared with control mice. No stromal vessels were found in diluent containing plugs from both groups (Figure 26A, 3rd row). Angiogenesis occurring during postnatal development is usually connected with inflammation [383]. Macrophages were demonstrated to promote angiogenesis via FGFs and placental growth factor signaling[383] or by the release of pro-angiogenic molecules [383, 85]. We therefore investigated by CD68 immunostaining whether the stromal halo around the plugs may contain varying amounts of macrophages that could influence *de novo* angiogenesis in our experimental setting. However, we found no significant differences in the ratio between CD68$^+$ cells to total cell nuclei in the peripheral stroma when comparing diluent and FGF2-containing plugs from both groups (Figure 26A, last row). The total amount of CD68$^+$ cells per field

counted was also not significantly modulated, however we noticed a trend towards higher macrophage count in stromal halos around FGF2-containing matrigel plugs from *Rictor*$^{i\Delta ec}$ mice (Figure 26A, last row).

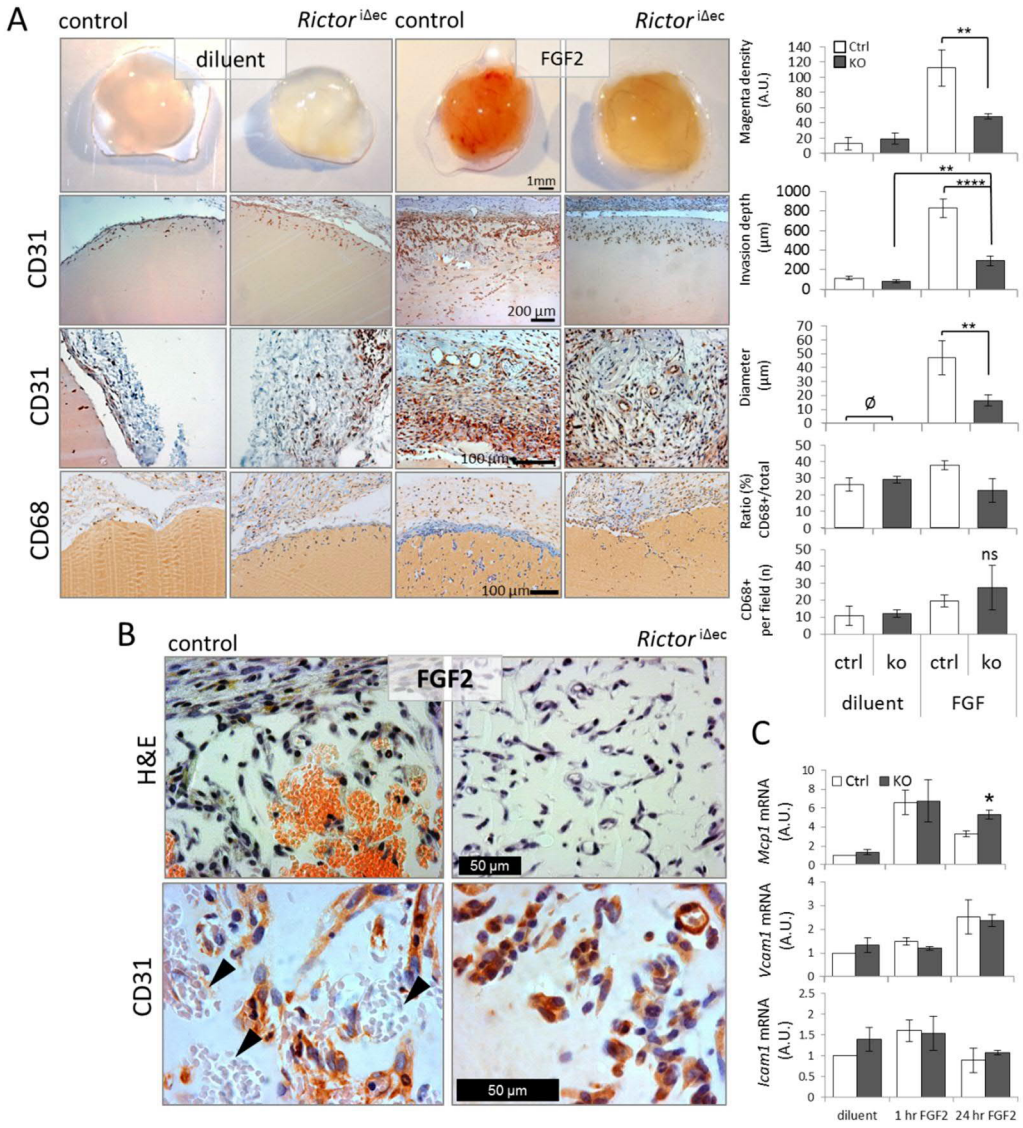

Figure 26. Fibroblast growth factor 2(FGF2)-induced angiogenesis in matrigel plugs is reduced in *Rictor*$^{i\Delta ec}$ mice.

Matrigel containing heparin (diluent) or 1.5 µg/ml FGF2 with heparin (FGF2) was injected subcutaneously into the ventral flank of 8-week-old male control and *Rictor*$^{i\Delta ec}$ mice. The plugs were removed 7 days later and analyzed. Representative macro-photographs (scale bar=1mm) of matrigel plugs from control (left) and *Rictor*$^{i\Delta ec}$ mice (right) are displayed. Estimation of blood content by optical densitometry is shown on the right (n_{plugs}=4; **P<0.01; 1-way ANOVA with Bonferroni multiple comparison) (A, 1st row). Paraffin-embedded, diluent and FGF2-containing plugs were sectioned horizontally and immunostained for CD31 (brown) and haematoxylin (blue/nuclei). Representative micrographs show 10× magnification and display the depth of newly in grown microvessels from the surface towards the center of the diluent and FGF2 containing matrigel plug. Quantification to the right displays the significant reduction in the ingrowth (µm) of neo-vessels into plugs from *Rictor*$^{i\Delta ec}$ mice compared to control mice (n_{plugs} =4/7; **P<0.01, ****P<0.0001; 1-way ANOVA with

Bonferroni multiple comparison test) (A, 2nd row). Representative micrographs of peripheral stroma covering diluent and FGF2-containing matrigel plugs from control and *Rictor*$^{i\Delta ec}$ mice. The area and the number of identifiable inner microvessel diameters were measured. No vessels were found in peripheral stroma covering diluent-containing plugs. A significant reduction in the inner luminal diameter in stromal vessels from FGF2-containing matrigel plugs from *Rictor*$^{i\Delta ec}$ mice was detected compared with those from control mice. (graph to the right; n_{plugs} =3; *P<0.05;2-tailed T-test) (A, 3rd row). Representative micrographs of macrophage marker CD68-immunostainings of peripheral stroma and matrigel. Graphs to the right show ratio of CD68$^+$/total cell nuclei in the stroma, and average of CD68$^+$cells per field counted in the stroma (n_{plugs} =4, no significant differences found after 1-way ANOVA/Bonferroni multiple comparison test) (A, 4th row). Representative micrographs displaying haematoxylin and eosin stained (H&E) matrigel areas showing local leakage and hemorrhagic areas in FGF2 containing plugs from control mice compared to plugs from *Rictor*$^{i\Delta ec}$ mice (upper micrographs). Lower micrographs show higher magnification of CD31-stained matrigel areas. Arrowheads point to local spots of leaked erythrocytes in FGF2-containg control plugs (B). Confluent and starved control and *Rictor* KO MAECs were stimulated for 1 and 24 hours with 25 ng/ml FGF2 or diluent. mRNA expression of *monocyte-attracting protein 1* (*Mcp1*), *vascular* and *inducible cell adhesion molecules 1* (*Vcam1, Icam1*) was detected by quantitative real-time PCR (n=3; *P<0.05; 1-way ANOVA with Bonferroni multiple comparison test) (C).

To further investigate the possibility of a mild FGF2-dependent pro-inflammatory state after endothelial *Rictor* knockout we measured the mRNA levels of *monocyte-attracting protein 1* (*Mcp1*) and *vascular*- and *inducible cell adhesion molecules* (*Vcam1, Icam1*) in MAECs. FGF2 increased *Vcam1* mRNA after 24 hours similarly in both control and *Rictor* knockout MAECs. A slight and insignificant increase for *Icam1* mRNA was observed. FGF2 robustly (ca. 6.6 fold) induced *Mcp1* mRNA in control and *Rictor* knockout MAECs. Interestingly, *Mcp1* mRNA remained at high levels (ca. 5.3 fold induction) after 24h of FGF2 stimulation and was significantly higher compared to controls (3.3 fold) at this time-point (Figure 26C). Thus, it is unlikely, that the strong reduction of FGF2-induced angiogenesis into matrigel plugs along with 'normalized' microvessel features by deletion of endothelial *Rictor in vivo* is caused by an altered inflammatory response.

Taken together, we observe a dense, heterogeneous neo-vasculature with several patches of hemorrhage indicating disrupted or leaky capillaries that formed after 7 days of FGF2-exposure in control mice. In contrast endothelial *Rictor* knockout strongly and significantly reduced neo-vessel ingrowth in response to FGF2 with capillaries remaining homogenously small, with no evidence of hemorrhagic spots.

5.9 Supplementary data

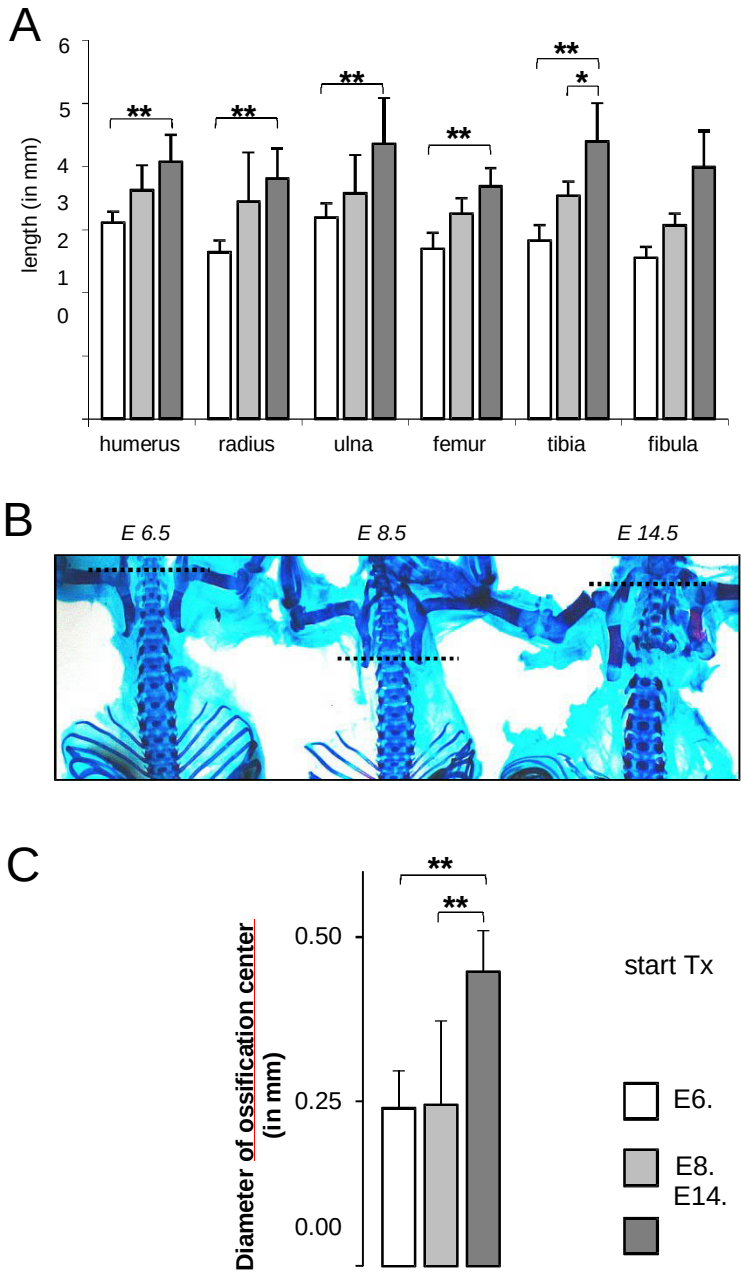

Figure S1. *Rictor*$^{i\Delta ec}$ embryos display a delay in ossification.

Quantification of length of long bones of the upper limb (humerus, radius und ulna) and lower limb (femur, tibia and fibula) of endothelial specific *Rictor* deficient embryos injected with Tx at E6.5 (white bars), E8.5 (grey bars) and E14.5 (dark bars) as starting time point. n=4, Students t-test ** p <0 .01 * p < 0.05 compared to E14.5 (A). Representative pictures of the lower spine of embryos stained with alizarin red (bone) and alcian blue (cartilage) for skeletal analysis indicated starting time points for Tx injections. Dotted line: border ossificated vertebrae (B). Statistical analysis of diameter of ossification centers in lumbar vertebrae upon knock out of *Rictor* at indicated starting time points compared to E14.5. n=4, Mann-Whitney Rank Sum Test ** p < 0.01 (C).

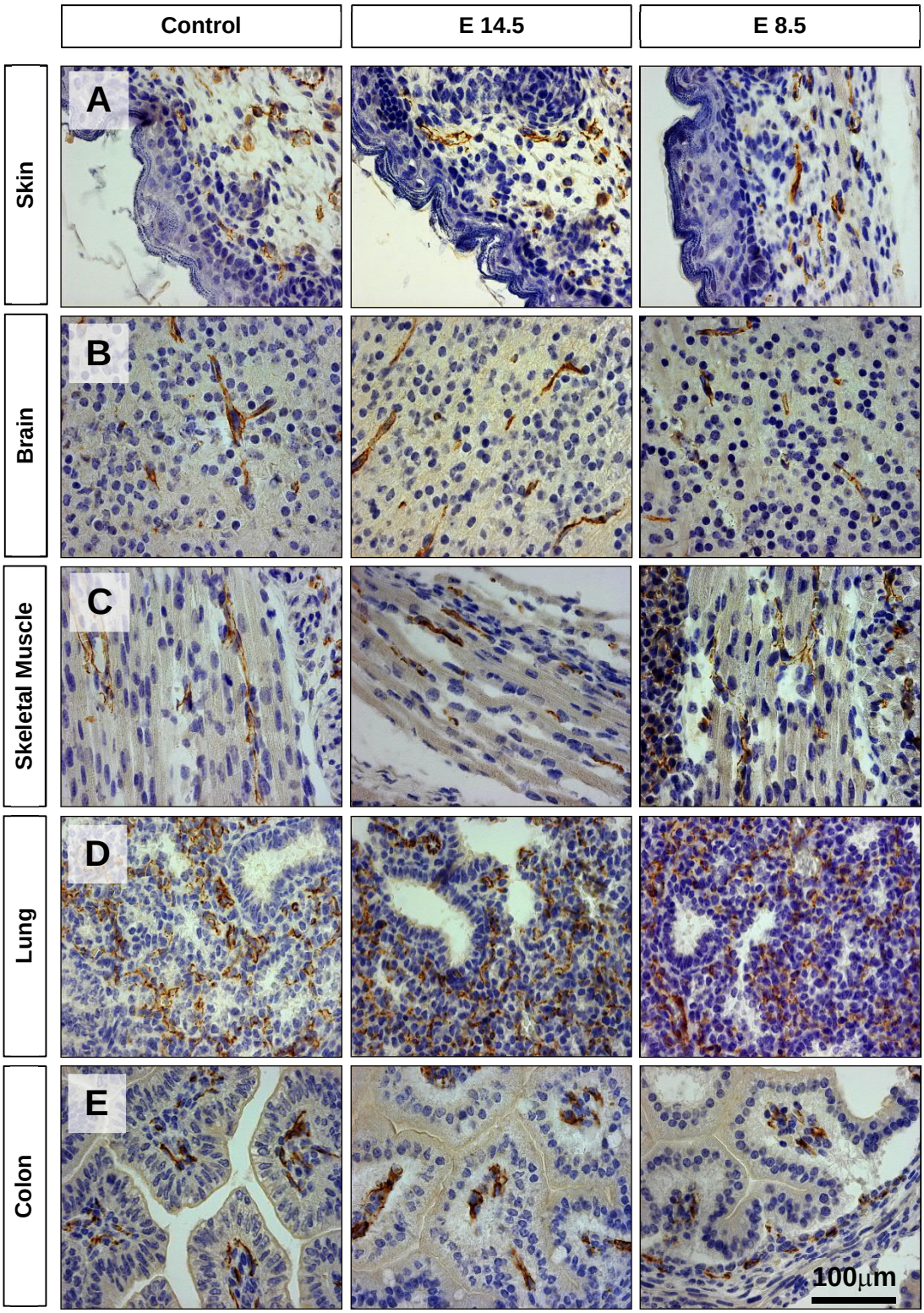

Figure S2. Histological analysis of *Rictor*$^{i\Delta ec}$ embryos with Tx-injections starting at E8.5 and E14.5 in comparison to control embryos.

Embryos were harvested at E17.5, fixed, embedded in paraffin and longitudinally sections were immunohistologically stained with anti CD31 antibody to detect endothelium. A: skin, B: brain, C: skeletal muscle, D: lung and E: colon. CD31, brown; nuclear counterstain, blue. Scale bar = 100 mm.

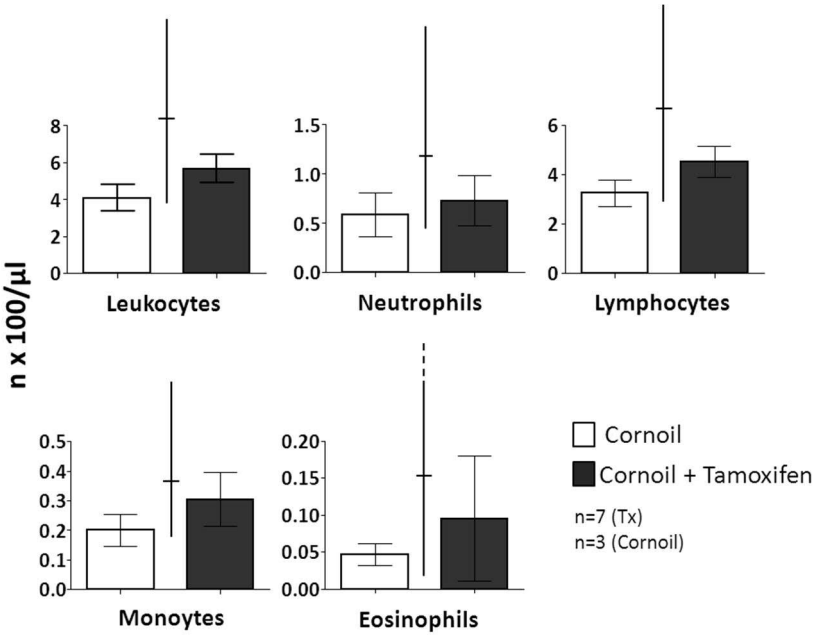

Figure S3. Endothelial *Rictor* knockout does not modulate hematological profile.

Hematological profile (Count of leukocytes, neutrophils, lymphocytes, monocytes and eosinophils) was assessed from 10 weeks old Cornoil and Tamoxifen/Cornoil-injected male $Cre^{+/+}$; $Rictor^{lox/lox}$ mice. Line between bars indicates normal range of parameters for C57/Bl6 mice

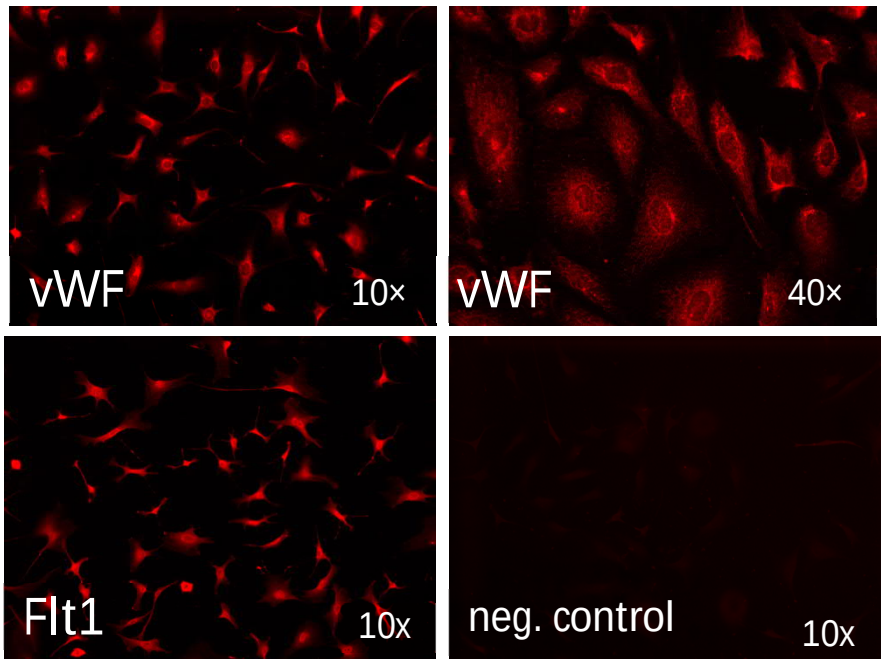

Figure S4. Characterization of endothelial cells.

Fluorescent Immune-staining (red) of a representative endothelial cell isolate for endothelial cell markers von Willebrand Factor (vWF) and VEGF receptor 1 (Flt1). The 40x magnification of vWF-staining shows a vWF-typical granular pattern. As negative control, a staining without primary antibody is shown.

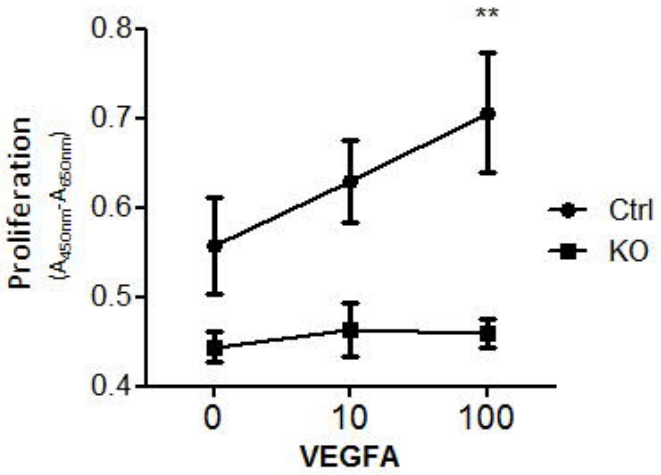

Figure S5. Endothelial *Rictor* KO decreases VEGFA-induced MAEC proliferation.

Control and *Rictor* KO MAEC were seeded subconfluently, cultured for 25 hours in growth medium with 1% FCS and then stimulated with diluent, 10 ng/ml and 100 ng/ml of VEGFA. Cell proliferation was measured by WST-1 reagent. Points (±SE) represent absolute proliferation values (Absorption=A450nm-A650nm) in FGF2 stimulated wild-type (circles) or *Rictor* KO (squares) MAEC. Proliferation was significantly ($P<0.001$, $n_{exp}=3$) decreased in *Rictor* KO MAEC compared to controls at 100 ng/ml VEGFA stimulation.

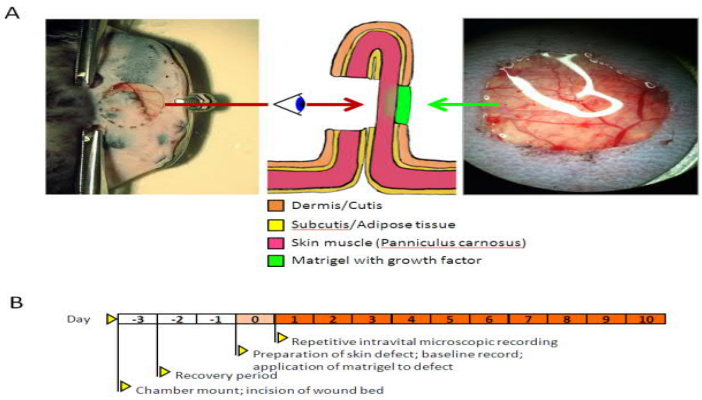

Figure S6. Modification of the dorsal skinfold chamber.

Skin was detached from the underlying muscle and removed in a circular area of 7 mm in diameter from the side opposite to the observation window of the chamber. This defect on the back of the chamber was sealed with 20 µl growth factor-reduced matrigel containing heparin (5 IU) with or without FGF2 (1.5 µg/ml). Afterwards, it was covered with a glass cover slip incorporated into the titanium frame.

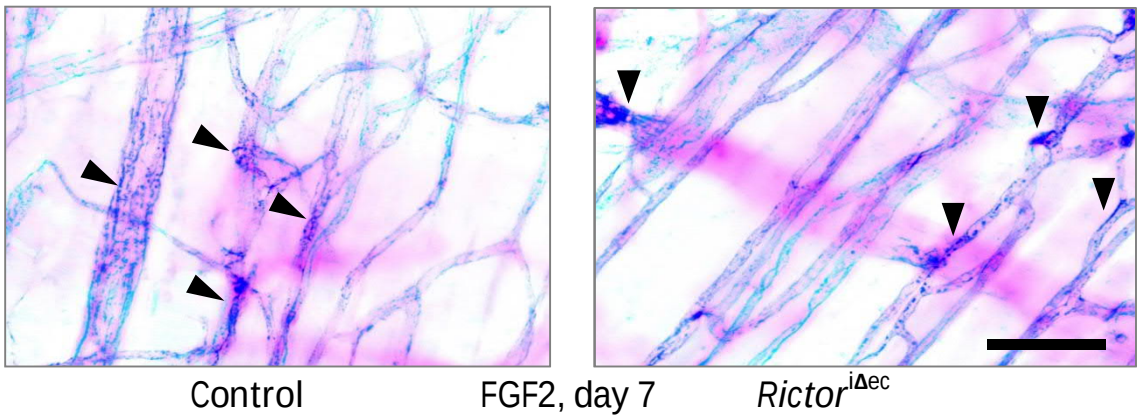

Figure S7. Fluorescent intravital staining for *ricinus communis* agglutinin I (RCA-I).

RCA-I is a galactose-binding lectin from castor beans, that binds to endothelial cells at sites of plasma leakage. Methods: 50 µl (1 µg/µl) of TRITC-RCA-I (Vector labs) in PBS was injected via tail vein in anesthetized mice carrying a dorsal skinfold chamber for 30 min. Then, mice were euthanized and skin muscle dissected from the skinfold chamber observation window, and mounted on coverslips. Fluorescence was recorded by optical-grid sectioning of ca. 10×3 µm sections (Zeiss, Apotome 2, 25x magnification). Inverted image of orthogonal projections of are shown below (blue=leakage points, arrowheads mark regions with increased positive staining). Pilot experiment (n=2).

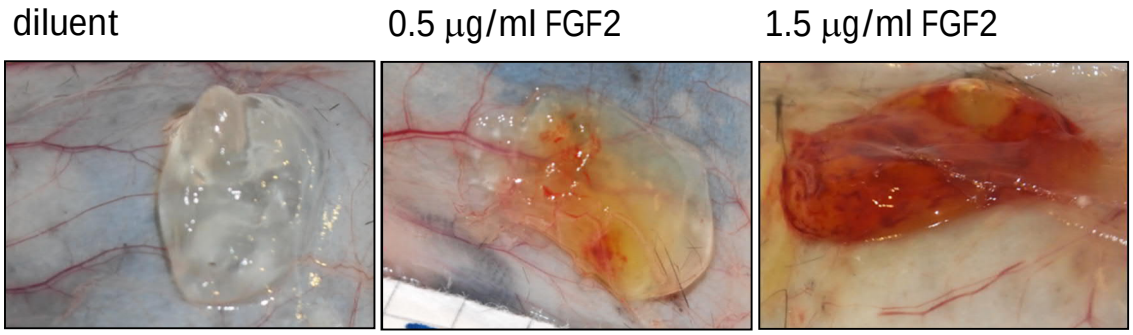

Figure S8. Dose response of FGF2-matrigel plugs in control mice.

Diluent, 0.5 µg/ml and 1.5 µg/ml FGF2 containing matrigel plugs were implanted in each flank of each mouse. For experiments, plugs were removed 7 days post implantation and analyzed.

6. RESULTS – Part B

6.1. Endothelial cell culture system

6.1.1. Mouse aortic endothelial cells isolated by aortic rings are positive for the EC markers VE-Cadherin and von Willebrand Factor

The three different mouse aortic endothelial cell (MAEC) isolates used during this PhD-study were obtained from the aortae of three 8 weeks old male mice (MAEC ISO1-ISO2-ISO3). The aortic endothelial cells sprouted from aortic rings that were embedded into a fibrin gel, proliferated and migrated into the three-dimensional surrounding after endothelial growth factor-stimulation (Figure 27). After subculture and up to two months of continuous growth, a sufficient amount of cells with passage numbers between 6 and 8 were isolated and characterized.

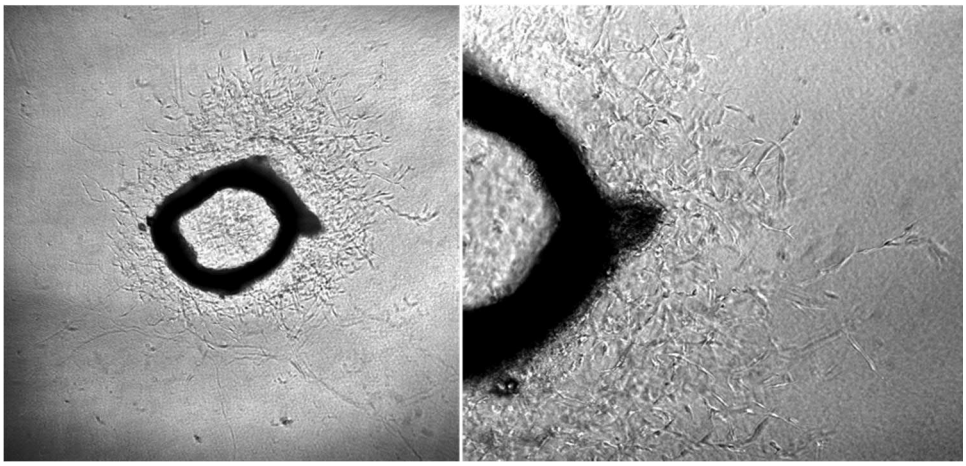

Figure 27. MAECs sprouting from aortic rings.
Micrographs of aortic ring embedded in Fibrin gel with cells sprouting out of the ring seven days after explant (4x and 10x magnification).

Endothelial morphology was a first feature considered in order to characterize the isolated cells: the isolated cells formed cobblestone-like monolayers which is a typical feature of cell-contact mediated growth arrest in endothelial cells (Figure 28)[21].

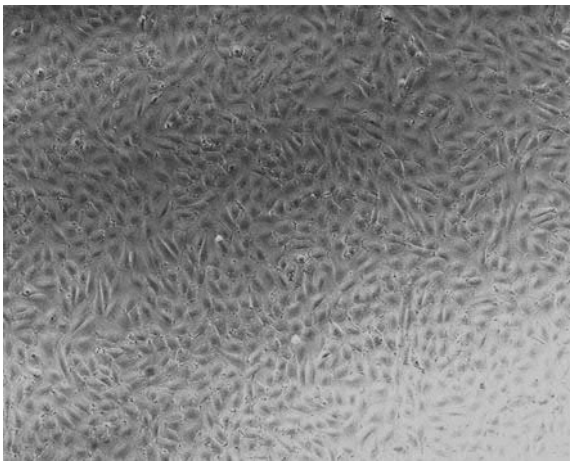

Figure 28. MAECs monolayer.
Cobblestone monolayer formed by the isolated cells growing in full medium, passage number 8 (magnification 4×).

Cell isolates displaying cobblestone-morphology were further characterized by the presence of endothelial cell markers. Molecules frequently used to identify endothelial cells are VE-Cadherin[384], TIE2[385], CD31 and CD34[386]. We assessed their expression on the transcriptional level by real-time PCR. The cells (ISO1, ISO2 control, ISO2 knockout and ISO3) were then grown in full medium until confluence. RNA was extracted and the real-time PCR performed. As a negative control the RNA extracted from adipocytes was used. As a positive control RNA extracted from the aortic arch (AArch), which contains endothelial cells, smooth muscle cells, fibroblasts and perivascular cells, was used. Furthermore RNA from commercially available MAECs isolated by magnetic sorting with the same passage number was also used as positive control. All cell isolates were strongly positive for the important endothelial cell marker *VE-Cadherin*. *Cd34*, an antigen expressed in EC and endothelial progenitor cells[386], was detected at low levels (Figure 29). We did not detect gene expression of the typical endothelial cell marker *Cd31* (also known as *Pecam1*) including splice variants in our cells. Similarly expression of the angiopoietin receptor *Tie2* was not detected.

After endothelial cells are extracted from an *in vivo* environment and cultured *in vitro* as monoculture, down-regulation of many genes has been reported. Human tonsils endothelial cells lost specialized characteristics, such as the marker DARC or other ECs markers such as VEGFR3, SelE or vWF already 2 days after isolation[387]. ECs might down regulate the expression of these genes through epigenetic modulation during the process of *in vitro* cultivation due to the absence of the natural vascular bed[388].

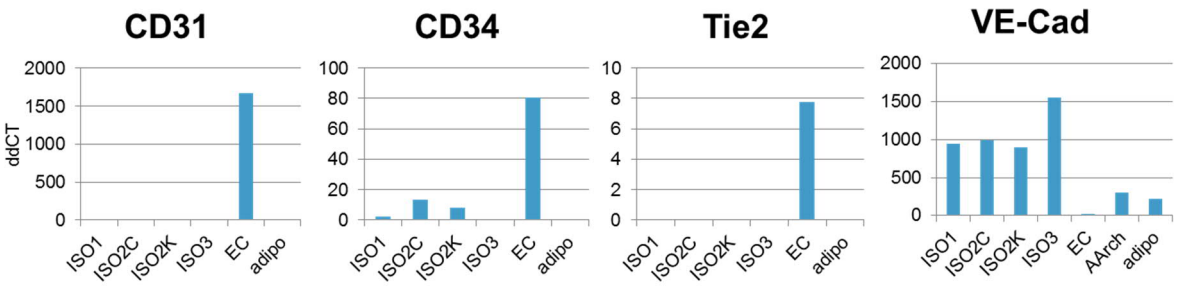

Figure 29. Characterization of the isolated MAECs.

Real-time PCR of *Cd31*, *Cd34*, *Tie2* and *VE-Cadherin* expression in the three cell isolates (ISO1, ISO2 presented as variant Control and *Rictor* knockout, ISO3), adipocytes, aortic arch and EC (isolated by MACS).

Low levels of *Sm22α*, a marker for SMCs, were detected in the cultured cell isolates, when compared to the levels observed in the aortic arch or in the ECs-SMCs co-culture (shortly named SMC), suggesting that in isolated cells some SMCs are present (Figure 30).

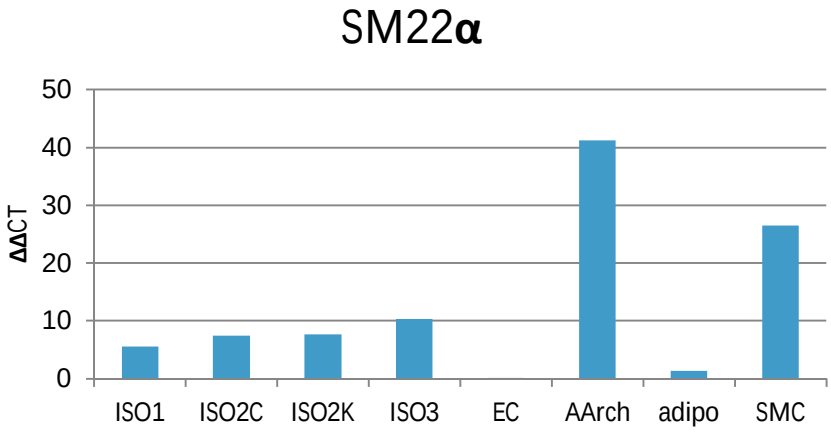

Figure 30. SMCs contamination assessment.

Real-time PCR for *Sm22α* mRNA levels in the three cell isolates (ISO1, ISO2C, ISO2K, ISO3) compared to aortic arch, adipocytes, SMCs-ECs co-culture and ECs (isolated by magnetic sorting).

On the protein level, MAEC isolates were positive for a further EC marker, von Willebrand Factor (vWF)[386] as seen by immune fluorescence staining (data produced by Dr. Humar, Figure S4).

Thus, the isolated MAECs were positive for the EC markers VE-Cadherin and vWF and could form confluent monolayer with the typical EC cobblestone shape.

Taken together, all these data suggest that the cells isolated from aortic rings are endothelial cells with some SMCs contamination.

6.1.2. Adenoviral transfection of *Rictor* floxed MAECs leads to strong *Rictor* ablation

In order to generate endothelial cells lacking mTORC2 activity, MAECs were isolated from mice that have the 4th and 5th *Rictor* exons flanked by loxP sequences[292]. RICTOR is an essential component of the multi-complex that forms mTORC2 [308]. The excision of this gene could then be performed by infecting sub-confluent MAECs by adenovirus containing a vector constitutively expressing the CRE-recombinase and green fluorescent protein (GFP). Green fluorescence, indicating a successful transfection was checked the day after transfection and both the cell groups (control with GFP alone and knockout with GFP and CRE-recombinase) resulted to be efficiently transfected, with a strong GFP expression (Figure 31).

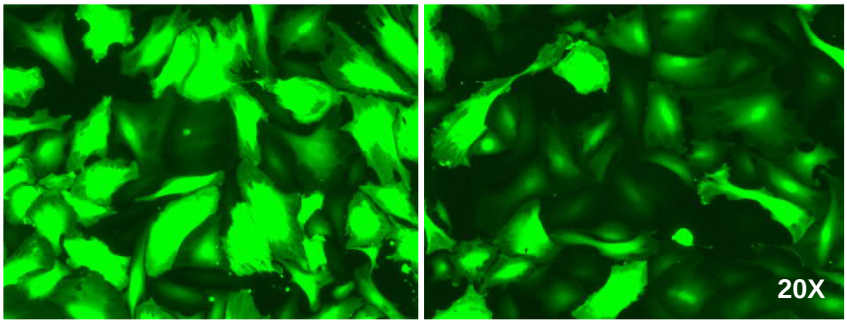

Figure 31. GFP expression in transfected MAEC.
Control cells on the left and knockout on the right. Pictures taken one day after transfection.

To verify whether *Rictor* was ablated in the transfected cells, *Rictor* mRNA was quantified by real-time PCR at different time points after transfection. In Figure 32, the chart indicates the *Rictor* mRNA levels in 3 different cell isolates three weeks after transfection. The amount of *Rictor* mRNA in the Ad-CRE-GFP treated cells resulted in being strongly reduced compared to the control cells.

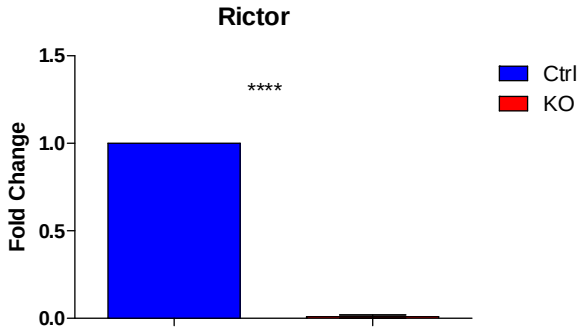

Figure 32. *Rictor* mRNA levels of 3 different cell isolates.

Rictor mRNA levels detected three weeks after adenoviral transfection by real-time PCR and normalized on the amount of *Rictor* mRNA present in the control cells of each cell isolate. The difference in *Rictor* expression was statistically significant (P value < 0.0001).

Also the *Cre* recombinase mRNA level was evaluated through real-time PCR quantification, in order to exclude any possible interference of this protein on the cell system, and therefore being able to distinguish between the CRE-mediated and the RICTOR-mediated effects[389]. *Cre* recombinase message was intense three days after Ad-CRE-GFP transfection, but it decreased strongly three weeks after transfection (Figure 33).

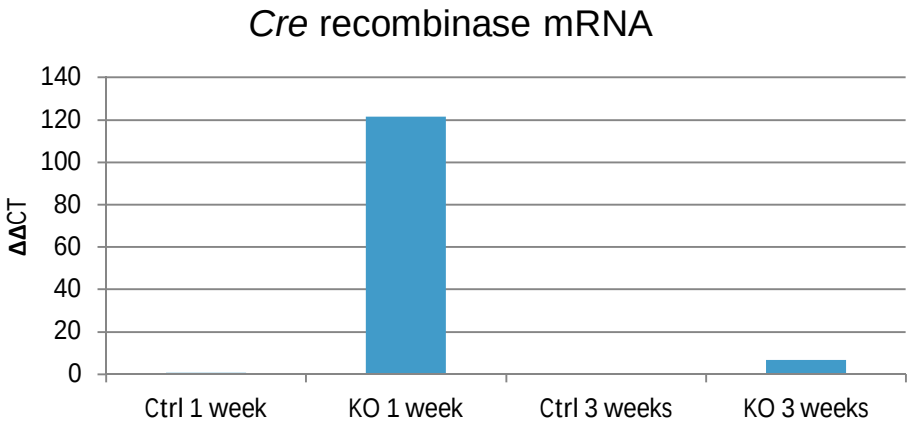

Figure 33. *Cre* recombinase mRNA levels.
Cre mRNA levels in *Rictor* control and knockout cells, were measured by real-time PCR 1 and 3 weeks after adenoviral transfection.

Finally, *Rictor* knockout induction in MAECs five days after transfecting the cells with two doses of Ad-CRE-GFP virus was proven on the protein level, by western blotting and detection of RICTOR and CRE protein. CRE was strongly expressed only in the MAECs transfected with Ade-CRE-GFP adenovirus (both with a low and with a high dose of adenovirus), where RICTOR levels where ablated (Figure 34).

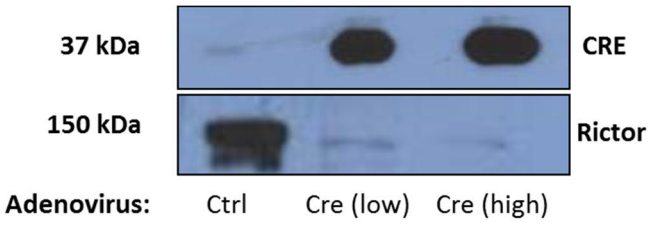

Figure 34. RICTOR and CRE protein levels in MAECs.
Immunoblots of cell lysates isolated five days after adenoviral transfection. Two different volume of Ad-CRE-GFP virus were used, obtaining the similar result in terms of RICTOR ablation.

The adenoviral transfection then revealed itself to be a good method to generate, three weeks after transfection, MAECs lacking of RICTOR displaying only a slight presence of the CRE recombinase.

6.2. VEGFA as MAECs activator

We detected a strong reduction of neovascularization in response to the potent angiogenic molecule Fibroblast Growth Factor 2 (FGF2) in mice that lack endothelial RICTOR *in vivo* (see section "Results – Part A"). Angiogenesis is a highly regulated process in which endothelial cells are activated by pro-angiogenic molecules such as Vascular Endothelial Growth Factor A (VEGFA)[390]. Other groups demonstrated that FGF2 can induce VEGF or modulate VEGF-elicited responses[375]. We also showed by qRT-PCR that as consequence of FGF2 stimulation there is an induction of *Vegfa* transcription (Figure 24B).

As FGF2 induced VEGFA in our endothelial cells, we included VEGFA besides FGF2 as angiogenic stimulus to further assess potential mTORC2 dependent effectors of the angiogenic response in our endothelial cell isolates.

6.2.1. *Vegfr1* (*Flt*-1), *2* (*Flk-1/KDR*) are not modulated by *Rictor* knockout

The VEGFRs induce and are regulated by the Notch signaling pathway. This is particularly important during sprouting angiogenesis when the differentiation of the endothelial cells into stalk and tip occurs[391]. The expression of different VEGFRs in the endothelium during sprouting angiogenesis confers to the different endothelial characteristics: whereas the tip cells, expressing mostly VEGFR2, have a higher migratory ability and filopodia formation, the stalk cells, expressing mostly VEGFR1, can only follow the tip cells and proliferate [90, 213].

We hypothesized that mTORC2 deficiency might lead to modulation of key angiogenic RTKs or angiogenic receptors and thereby might halt the angiogenic response in the endothelium. We focused on the receptors of the potent angiogenic molecule VEGFA.

The modulation of these growth factors receptors was studied by real-time PCR in a confluent monolayer of starved cells stimulated with 25 ng/ml of FGF2 or VEGFA for 1, 3 or 6 hours.

In addition to the results in the section "Results – Part A" showing that the induction of *Vegfa*, *Vegfr1*, *sVegfr1* and *Vegfr2* mRNA is not affected by mTORC2 ablation under FGF2 stimulation (Figure 24B), we observed the same outcome using the pro-angiogenic molecule VEGFA (

Figure 35).

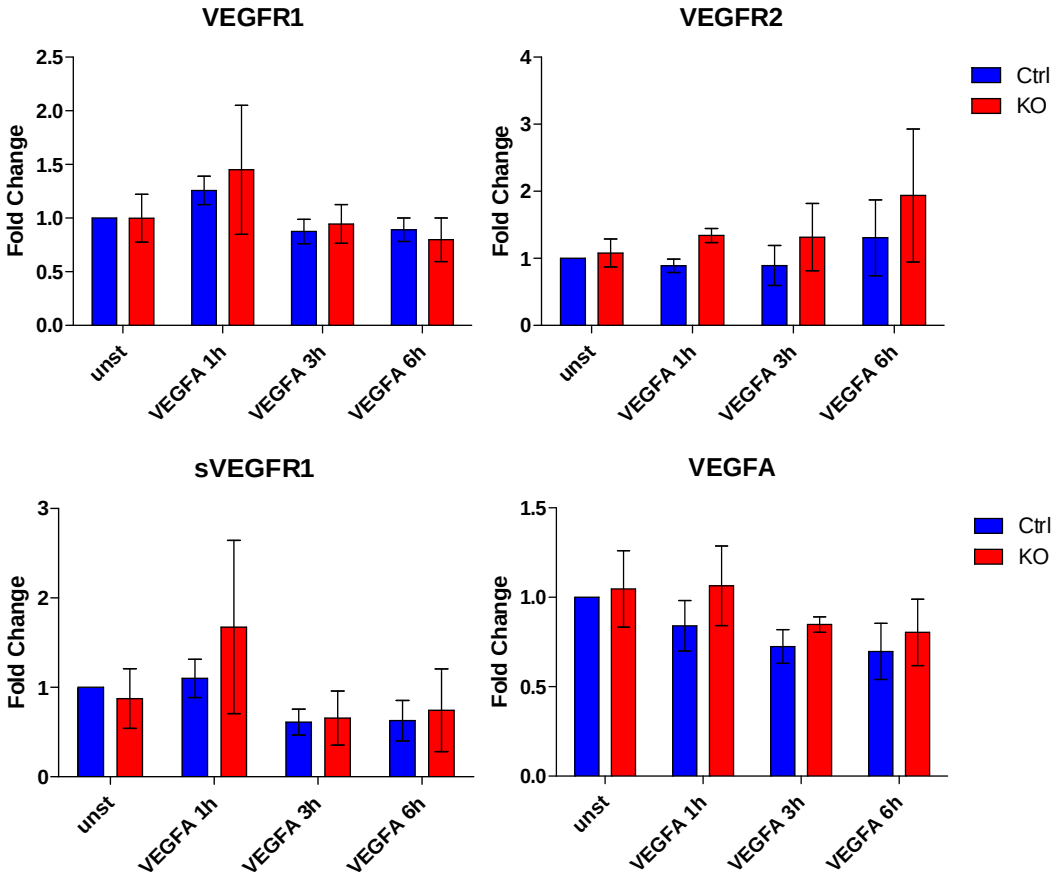

Figure 35. *Vegfa* and *Vegfrs* mRNA levels.

Time course (1-6 hours) after FGF2 or VEGFA stimulation. Real-time PCR data, values normalized on the control unstimulated.

Preliminary data indicated, after *Rictor* knockout, an increased expression of *sVegfr1*, whose codified protein, lacking of the transmembrane domain [392], is secreted and acts as VEGF scavenger [105], fulfilling an anti-angiogenic function.

However, since the induction of the *sVegfr1* message was variable in the three cell isolates, we assessed sVEGFR1 protein levels in all control and *Rictor* knockout cells to better understand whether mTORC2 can influence sVEGFR1 secretion,

To do so, the supernatant from confluent MAECs stimulated for 24 hours with 25 ng/ml of FGF2 or VEGFA was collected and analyzed by ELISA. The results showed that sVEGFR1 protein levels in the supernatant were up-regulated after VEGFA and particularly FGF2 stimulation however, its secretion was unaltered in mTORC2 knockout cells (Figure 36).

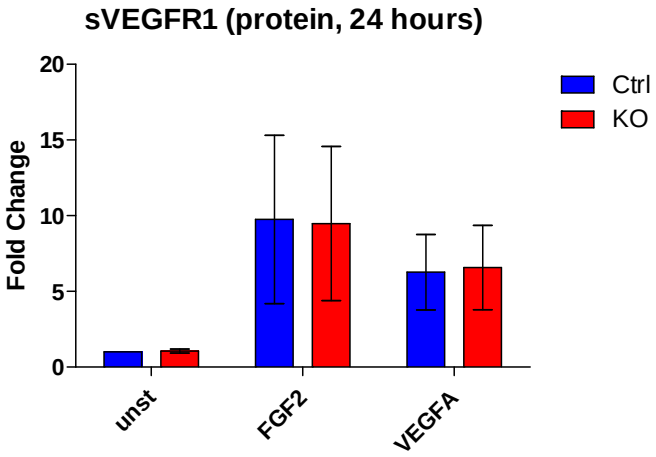

Figure 36. Soluble VEGFR1 protein levels.

24 hours of incubation with FGF2 or VEGFA. ELISA data, values normalized on the control unstimulated.

6.2.2. *Ang2* is up-regulated in starved *Rictor* knockout cells

To assess whether the deficiency of mTORC2 might lead to endothelial cells with different tip/stalk cell characteristics the induction of other genes involved in the Notch pathway was investigated. In parallel, we also considered the genes of the ANG-TIE axis which are involved in vessel stability and remodeling.

The modulation of these genes was studied by real-time PCR in a confluent monolayer of starved cells stimulated with 25 ng/ml of FGF2 or VEGFA for 1, 3 or 6 hours. We found that *Jagged1* and *Ang2* gene expression was down-regulated in response to FGF2 stimulation whereas VEGFA had no effect on their message. *Rictor* knockout did not further modulate *Jagged1* expression. However *Ang2* mRNA was significantly up-regulated in the knockout cells when left unstimulated in the starving medium (Figure 37). The expression of the gene transcripts *Notch1*, *Dll4*, *Ang1* and *Frizzled* was not detectable at the described conditions.

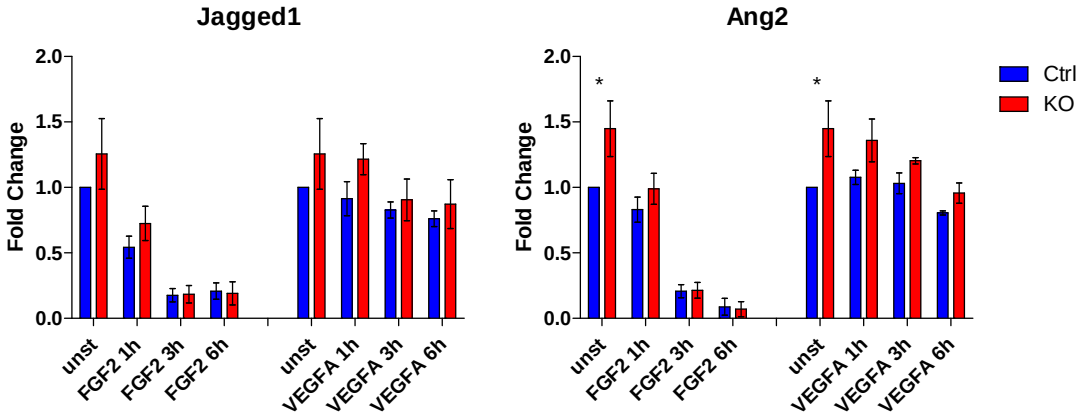

Figure 37. *Jagged1* and *Ang2* mRNA levels.

Time course (1-6 hours) after FGF2 or VEGFA stimulation. Real-time PCR data, values normalized on the control unstimulated (P value < 0.05).

6.3. Transcriptomic analysis of mTORC2-deficient MAECs

6.3.1. Gene array analysis

As we did not detect significant or wide-spread mTORC2-dependet modulation of genes associated with angiogenesis by an 'intelligent guess' approach, we broadened our investigations by analyzing the MAECs transcriptome by gene arrays. The MAECs, derived from three different animals, were seeded and grown until confluence. When the monolayer was formed, the cells, starved for 24 hours, were stimulated with FGF2 or VEGFA at the concentration of 25 ng/ml. The genes transcription was investigated 3 and 24 hours after stimulation to cover an acute and a chronic response to the growth factors after mTORC2 disruption. After incubating the cell culture with the GF, the RNA was extracted, purified and its integrity was analyzed with the Bioanalyzer. The analysis of randomly selected samples showed RNA in an excellent quality, described by RIN (RNA Integrity Number) factor between 9.8-10/10 and therefore suitable to perform the chip hybridization. A part of the RNA extracted was converted in cDNA and the presence of *Rictor* and *Cre* in the transcriptome was assessed by real-time PCR. These samples, with confirmed *Rictor* ablation and low *Cre* expression, were then further processed by the Functional Genomics Center Zurich (FGCZ) where the Affymetrix work-flow was performed. The data generated in the FGCZ were then analyzed in detail in our laboratory with the help of Dr. Christian Schaer by using the software JMP Genomics 7.0 (© SAS Institute Inc.). The samples were analyzed comparing the genes modulated in the knockout cells to the ones modulated in the controls, in absence of stimuli or after FGF2 or VEGFA incubation for 3 hours and 24 hours. Our analysis demonstrated that the biological variability between the cell isolates from three different animals played a stronger role than the stimuli-induced changes used during the experiment. However, FGF2 was able to significantly induce or repress the transcription of several genes, both in 3 and in 24 hours (Figure 39). On the other hand, modulation of gene expression in MAECs stimulated with VEGFA was weak and did not display statistical significant compared to the unstimulated cells in starving conditions. We therefore proceeded to assess whether the FGF2-induced transcriptome was modulated by mTORC2 deletion. We found that a rather small set of genes was differentially modulated by *Rictor* deletion in response to a 3 and 24 hour stimulation by FGF2 when compared to control cells. Interestingly the overlap between the 3 hour set and the 24 hour set of genes was small, thus indicating that FGF-induced gene expression changes over time (Figure 38).

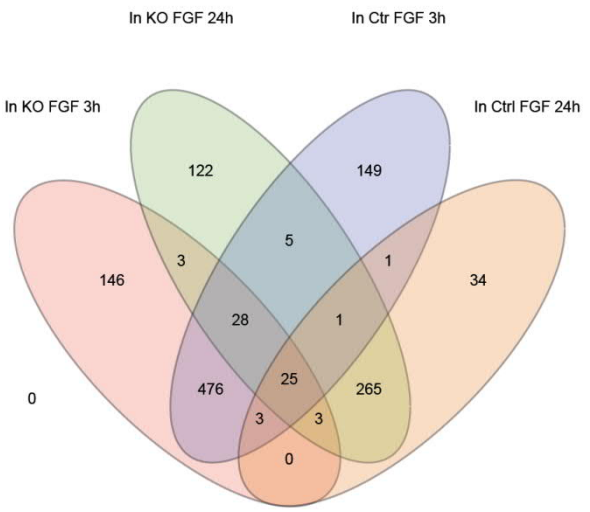

Figure 38. Venn diagram.

Chart summarizing differentially regulated genes in *Rictor* control and knockout MAECs in response to 3 and 24 hour of stimulation by FGF2.

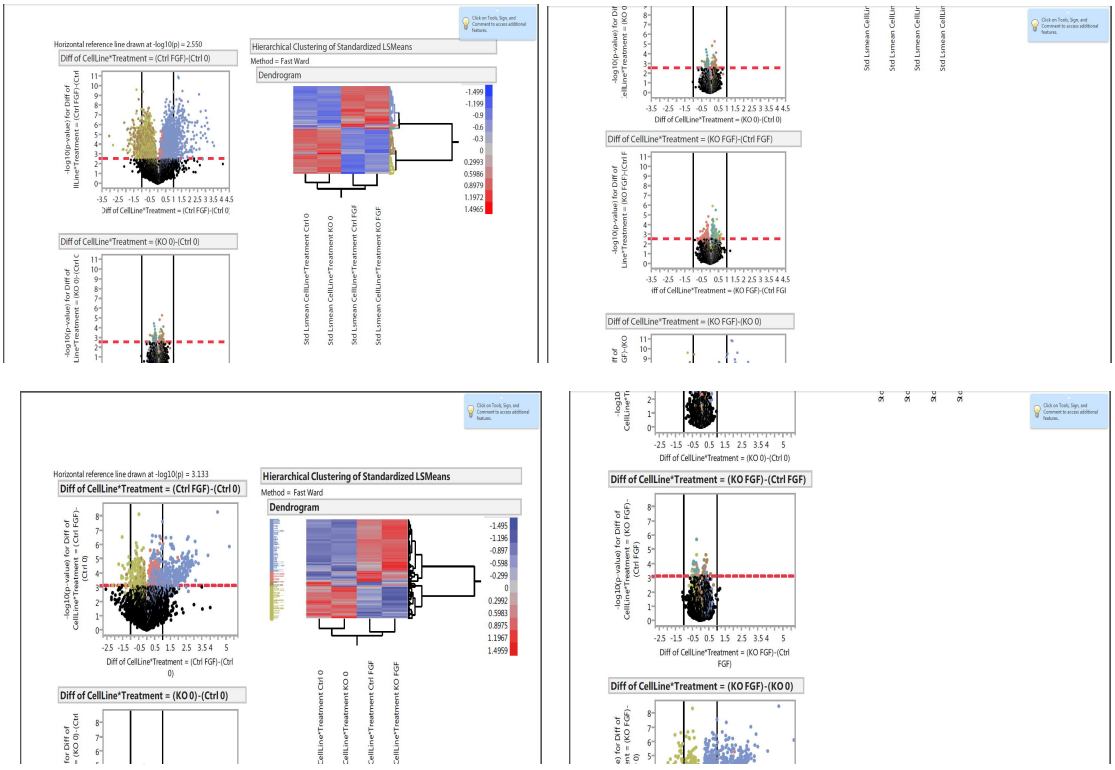

Figure 39. Volcano plots.

These charts visualize changes between FGF2 and untreated control and *Rictor* knockout MAEC-derived transcripts. On the top the charts corresponding to the 3 hours incubation, on the bottom the charts of the 24 hours stimulated samples. On the left, diagram of FGF2 modulated genes (up-regulated on the right and down-regulated on the left) in control cells. On the right, diagram of the genes modulated in *Rictor* knockout cells in comparison to the control cells in the same conditions. The red line represents the threshold of false detection rate (FDR < 0.05). The vertical lines represent the border of the strongly modulated genes which are outside of the area generated by the lines.

A pool of 28 genes involved in angiogenesis and differently expressed in knockout cells under FGF2 stimulation was identified (Table 1). These genes resulted in being weakly regulated as consequence of mTORC2 ablation but, however, this difference was statistically significant (FDR < 0.05)

Table 1. List of genes modulated in *Rictor* knockout MAECs (Transcriptome Analysis)

downregulated (not upregulated in FGF2 KO in 3 hours)	
Affymetrix Identifier	*Gene name*
17280310	ID2
17548973	Pten
17490628	FLT3l
17343299	Notch3
17400813	Notch2
17486967	Calmodulin (Calm3)
17287848	Smad5
17301502	α1B adrenergic receptor (Adra1a)

upregulated (not downregulated in FGF2 KO in 3 hours)	
Affymetrix Identifier	*Gene name*
17396240	MURF2 (Trim55)
17374488	Thrombospondin1 (Thbs1)
17221014	CD34
17396240	MURF2 (Trim55)
17234647	Integrin beta2 (Itgb2)
17356897	CALDAG-GEF1 (Rasgrp2)

downregulated (not upregulated in FGF2 KO in 24 hours)	
Affymetrix Identifier	*Gene name*
17379037	Plcg1
17343299	Notch3
17233347	Gja1 (Connexin34)
17392151	Jagged1 (Jag1)
17323909	Dvl3 (Disheveled)
17370977	Pkp4 (Plakophilin 4)
17368714	Hamartin (Tsc1)
17224211	Tensin1 (Tns1)
17228825	Klhl20 (kelch-like 20)
17366750	microRNA467a1
	microRNA467a2
	microRNA467a4

upregulated (not downregulated in FGF2 KO in 24 hours)	
Affymetrix Identifier	*Gene name*
17548559	Emp1 (epithelial membrane protein 1)

17213213	Casp8 (Caspase 8)
17353923	Pcdh1 (Protocadherin 1)

6.3.2. Validation of the selected genes

To confirm the differences in gene expression elicited by *Rictor* deletion observed in the gene array analysis (Table 1), we proceeded to validate the results in time-course experiments. Control and *Rictor* knockout MAECs were stimulated with FGF2 or VEGFA for 1, 3, 6 and 24 hours, RNA extracted, and qRT-PCR performed to detect the genes identified to be modulated in the gene array analysis. 16 genes out of 28 with CT value lower than 34 were detectable in MAECs-derived cDNA. The real-time analysis showed that the induction of *Flt3L*, *Id2* and *Notch3* was decreased after the treatment with FGF2 in a time frame of 6 hours. The same stimulus up-regulated *Thbs1* expression. Similarly; VEGFA could reduce the transcription of *Id2* within 6 hours from the addition of the GF. However, none of these transcripts were differentially modulated by *Rictor* knockout at the time points and by the stimuli investigated (Figure 41 and Figure 41), suggesting that in these conditions, on the transcription level, mTORC2 has no detectable impact on gene expression associated with angiogenesis in MAECs.

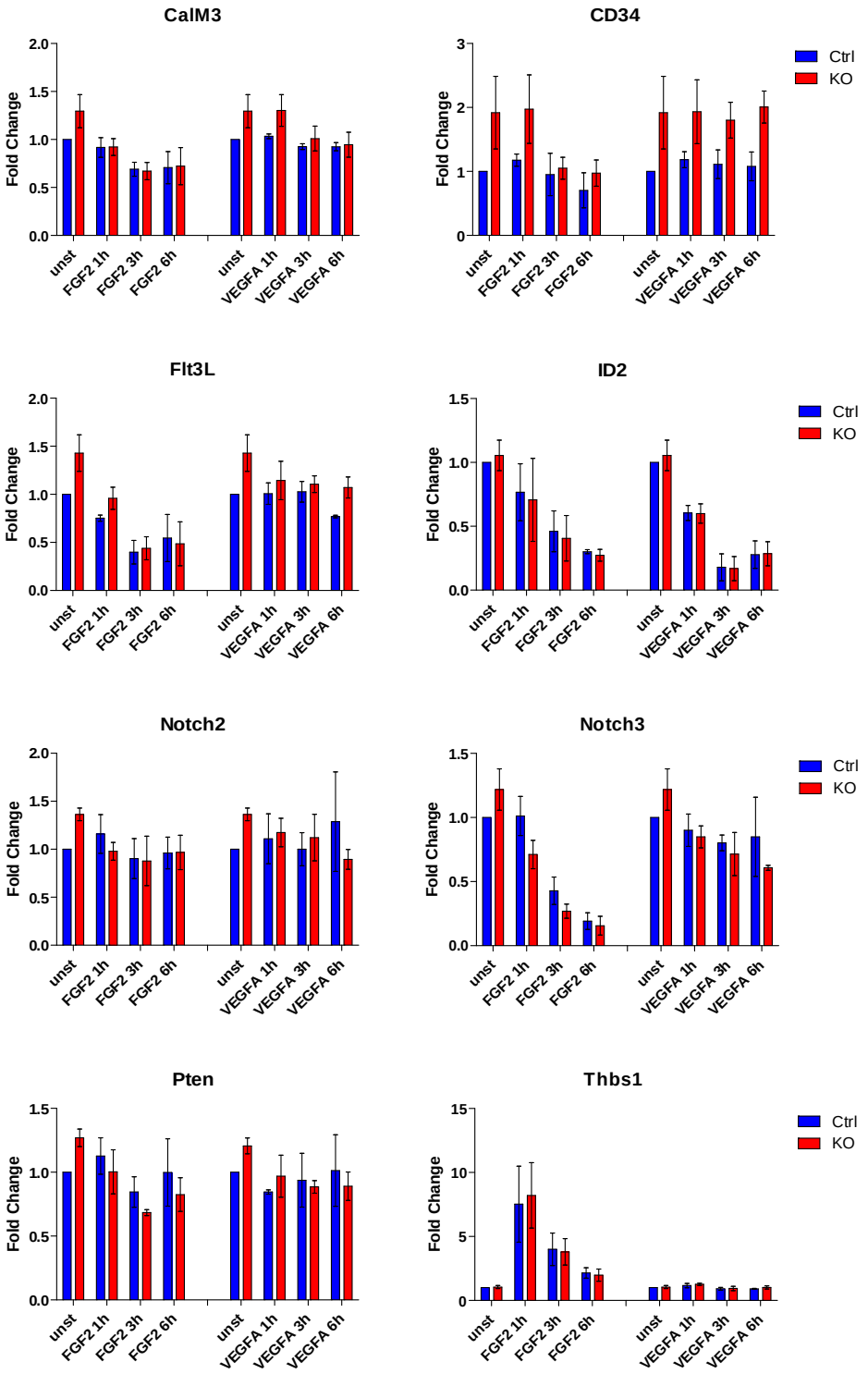

Figure 40. Validation of the angiogenesis-related modulated genes (1-6 hours).
Treatments with FGF2 or VEGFA were performed on a starved confluent MAEC monolayer of three different cell isolates. Real-time PCR data, values normalized on the control unstimulated.

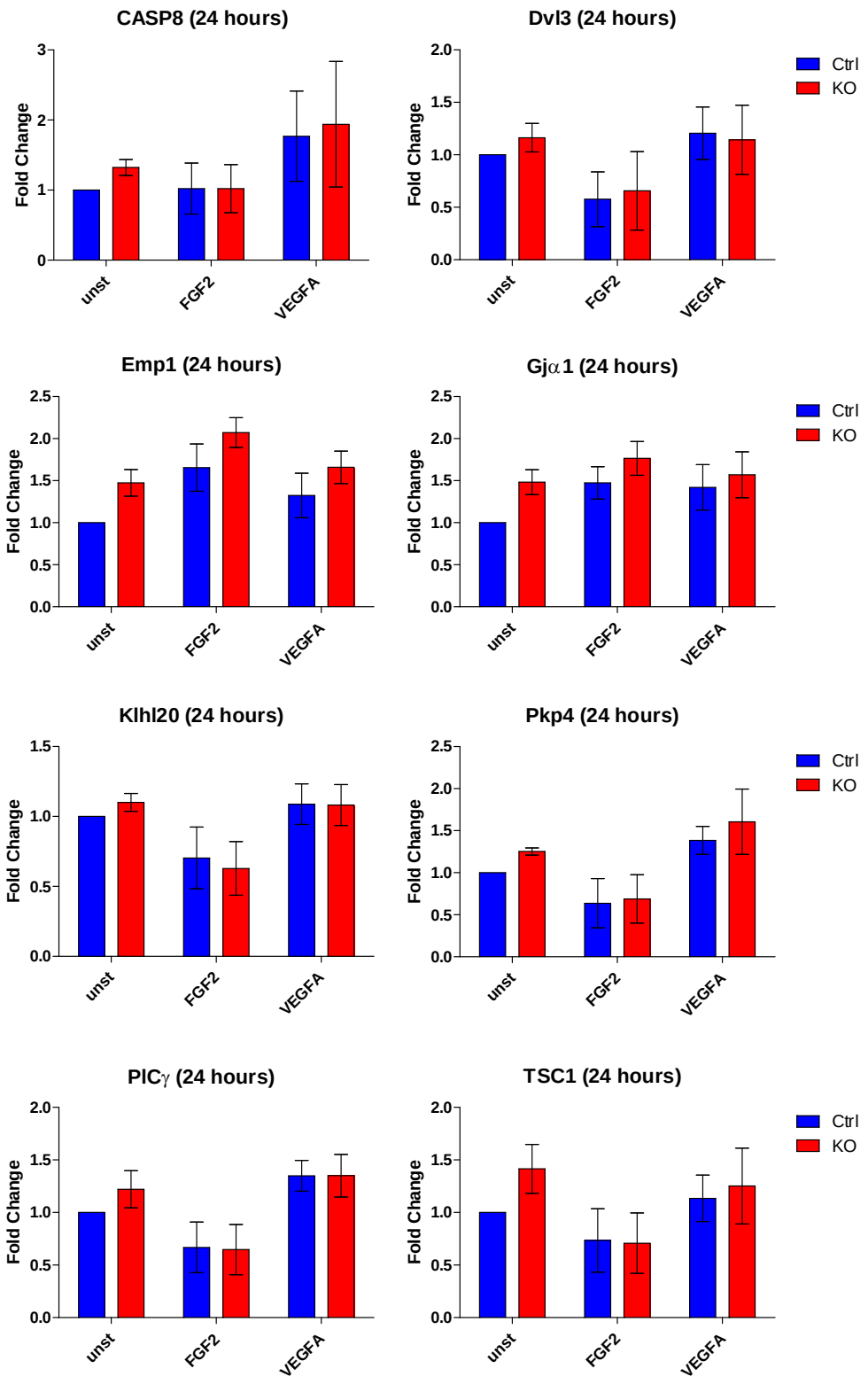

Figure 41. Validation of the angiogenesis-related modulated genes (24 hours).
Treatments with FGF2 or VEGFA were performed on a starved confluent MAEC monolayer of three different cell isolates. Real-time PCR data, values normalized on the control unstimulated.

6.4. mTORC2 ablation leads to a higher *Mcp-1* transcription induction in 24 hours of FGF2 stimulation

In adulthood, angiogenesis can occur during wound healing[393] and in the female reproductive system[394], but also in pathological situations such as in tumor development [66] or in inflammation[60]. Immune cells can secrete cytokines and GFs[395, 396] that stimulate angiogenesis. These cells can be recruited by the secretion of chemokines, such as MCP-1[397], and adhere to the endothelium binding VCAM-1 and ICAM-1[398]. To understand whether the deficiency of mTORC2 in endothelial cells might influence the inflammatory response, the expression of the inflammatory molecules *Vcam-1*, *Icam-1* and *Mcp-1* was analyzed in three different starved cell isolates. These confluent cells were stimulated for 1, 3, 6 or 24 hours with 25 ng/ml of FGF2 or VEGFA. The RNA levels were measured by real-time PCR and the ΔΔCT values were normalized on unstimulated control. The results showed that FGF2 increased *Vcam-1* and *Mcp-1* transcription in 6 hours. VEGFA did not induce the expression of the inflammatory molecules investigated. No differences, however, were noticed in the expression FGF2-induced *Vcam-1* and *Mcp-1* after 6 hours of stimulation in knockout compared to control cells. Interestingly, within 24 hours, when *Mcp-1* induction decreased, cells stimulated with FGF2 and lacking mTORC2, showed a 60% higher induction of this gene (Figure 42). This result might point to a possible role of mTORC2 in repressing chronic inflammation via *Mcp-1*.

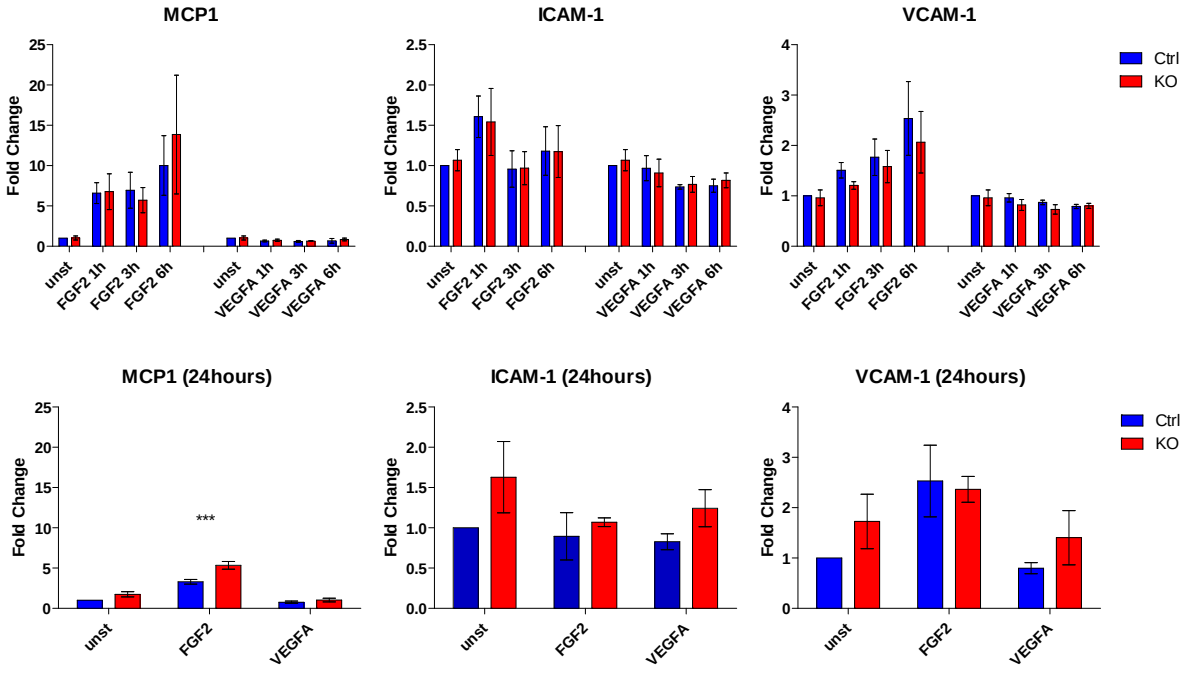

Figure 42. *Mcp1*, *Icam-1* and *Vcam-1* mRNA expression.

The mRNA levels were detected after 1, 3, 6 or 24 hours of FGF2 or VEGFA stimulation. Real time PCR data, values normalized on the control unstimulated. (24 hours of FGF2 stimulation data are also described in Figure 26). (P value < 0.05).

6.5. Secretome-analysis

6.5.1. mTORC2 knockout doesn't affect the secretion of angiogenic molecules under FGF2 stimulation

Our *in vivo* data strongly suggest a role of mTORC2 in FGF2-driven angiogenesis (see section "Results - Part A"). However, since we did not find significant mTORC2-dependent modulation of gene expression on the transcriptional level (Figure 41 and Figure 41), we hypothesized that changes may occur post-transcriptionally and alter protein levels as we documented for PKCα whose transcription was not modulated whereas its protein levels strongly depended on RICTOR presence (Figure 24A and B).

Endothelial cells can up-regulate the expression of angiogenic factors in hypoxic conditions[84] or after growth factor stimulation[97]; moreover, we showed that FGF2 up-regulates the transcription of angiogenic molecules (for example *Vegfa* or *sVegfr1*, Figure 24B). We therefore investigated if angiogenic molecules are differentially secreted after *Rictor* knockout in the supernatant of confluent starved MAECs stimulated for 24 hours with 25 ng/ml of FGF2 or VEGFA.

The supernatants, obtained from the cell culture of three different cell isolates, were incubated on a membrane anchored with antibodies targeting 53 different molecules involved in angiogenesis (see section 8.21). The amount of the proteins under investigation was detected by a chemiluminescent reaction (Figure 43). Densitometric analysis was performed using ImageJ.

Figure 43. Angiogenic ligand protein array.
Each dot doublet represents a secreted molecule which impacts angiogenesis. The two membranes were incubated with the supernatants for 24 hours with VEGFA. Arrows indicate dot blots corresponding to the HGF protein.

9 of the 53 ligands were detectable in the supernatants of all the three cell isolates.

In response to FGF2 or in unstimulated conditions, none of the ligands assessed resulted in being differentially secreted in cells deficient in mTORC2 (Figure 44).

6.5.2. mTORC2 regulates VEGFA-induced HGF secretion

In response to VEGFA, we could identify one protein whose secretion is influenced by the presence of the mTORC2 complex. We found indeed that the Hepatocyte Growth Factor (HGF) protein secreted levels were decreased in *Rictor* knockout cells (Figure 44). This difference corresponding to ca. 50% down-regulation was statistically significant ($P < 0.05$). HGF is a potent mesenchyme-derived cytokine that can stimulate EC proliferation, growth and motility *in vitro*[76] whereas, *in vivo*, it is a potent angiogenic factor[76], involved in wound healing[132] and in organ development[130]. HGF is also found to be overexpressed in invasive human cancers, such as breast cancer[133] where it can promote the formation of capillary-like tubes.

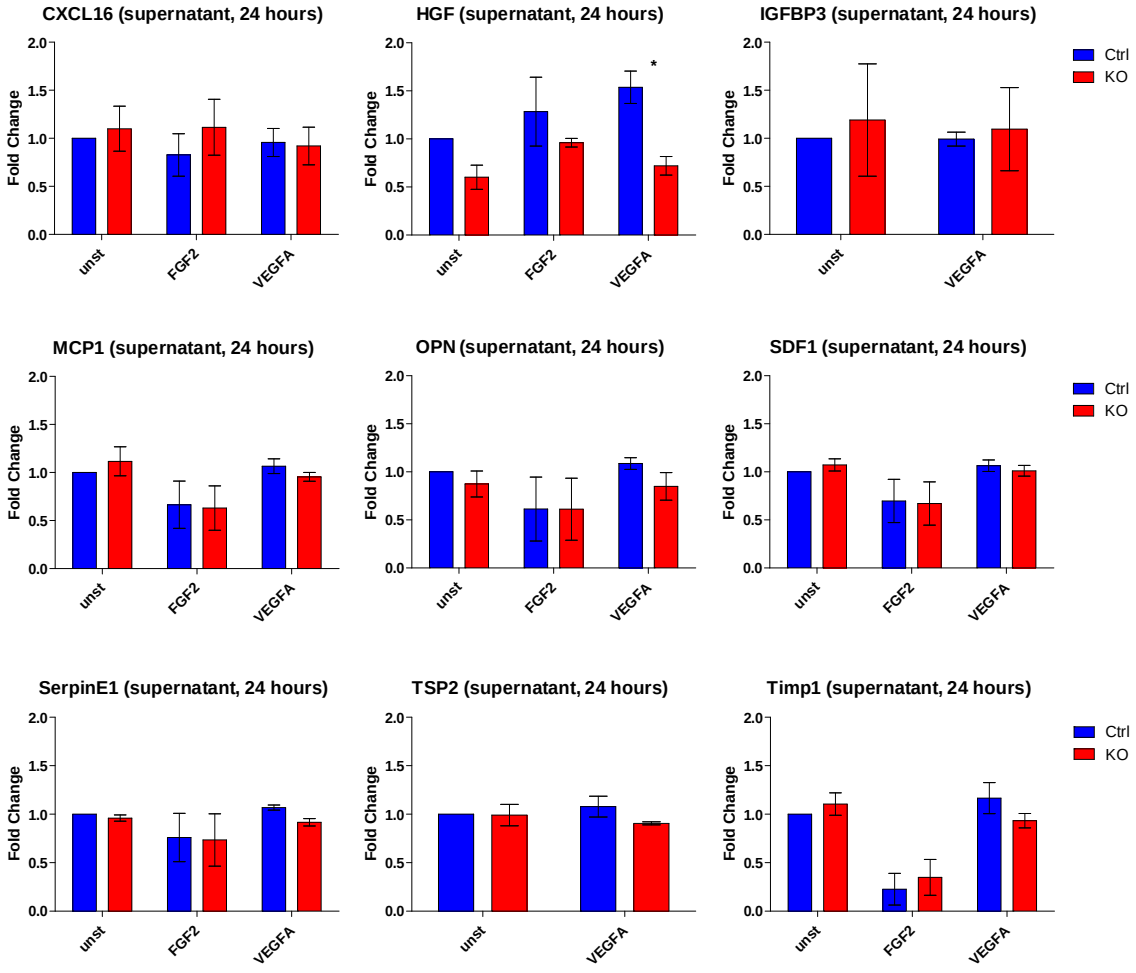

Figure 44. Angiogenic ligands secreted in the culture supernatants.

The secreted proteins from three different cell isolates were collected after 24 hours of stimulation with FGF2 or VEGFA. Values reported as fold change in comparison to the control unstimulated. (P value < 0.05).

6.6. mTORC2, eNOS and nitric oxide production in MAECs

Nitric oxide (NO) is a central molecule to enable angiogenesis. NO stimulates endothelial migration[172], survival[174] and proliferation[173]. VEGF-dependent effects in angiogenesis require NO[176] which is up-regulated, along with endothelial-specific NO synthase (eNOS) [107]. NO also up-regulates FGF2[173] and, in rat SMC, VEGF synthesis[182]. In endothelial cells, PKCα[354] and AKT[325] can activate eNOS by phosphorylating its Ser[1179] residue and consequently lead to NO production. Our previous *in vitro* analysis showed that total PKCα protein levels are strongly reduced as well as the levels of AKT phosphorylated on Ser [473] residue after mTORC2 disruption in primary cultures of MAECs [333] (see also Figure 24A). We therefore aimed at elucidating, whether mTORC2 can influence NO production in endothelial cells. We first attempted to determine the mRNA and protein levels of eNOS by real-time PCR and immunoblots however, they were undetectable in confluent MAECs growing in full medium or in starving conditions. We therefore decided to quantify the nitrites accumulating in our MAECs supernatants (consequence of NO oxidation) as indirect measure of NO production. MAECs were seeded in 6-well plates and grown until confluence. After starvation, the monolayer was stimulated for 20 minutes, 24 or 48 hours with the angiogenic molecules FGF2 (25 ng/ml), VEGFA (25 ng/ml) and with FCS (10%), ACh (10 µM) or TNFα (10 ng/ml), used as controls. The supernatant was then collected and the levels of nitrites measured by spectrophotometry after the Griess reaction (see section 8.22). After 20 minutes, we could observe an induction in nitrite production in MAECs stimulated with FGF2, VEGFA and TNFα (Figure 45). However, though nitrite levels appeared to be lower in supernatants of *Rictor* knockout cells, no statistical difference was computed comparing values from control to *Rictor* knockout cells. After 24 hours of ACh incubation, an induction in nitrite levels was observed in the control cell supernatant whereas knockout cell supernatant displayed a clearly lower and statistically significant ($P<0.05$) amount of nitrites (Figure 45). Based on these results, we may not assume, that FGF2-induced NO production is essentially decreased by mTORC2 deficiency. We have therefore to exclude the possibility for the time being, that FGF2-induced angiogenesis *in vivo* might involve the mTORC2-NO axis. However, the significant decrease in NO production in response to ACh after *Rictor* knockout might point to potential deficiencies in vasorelaxation.

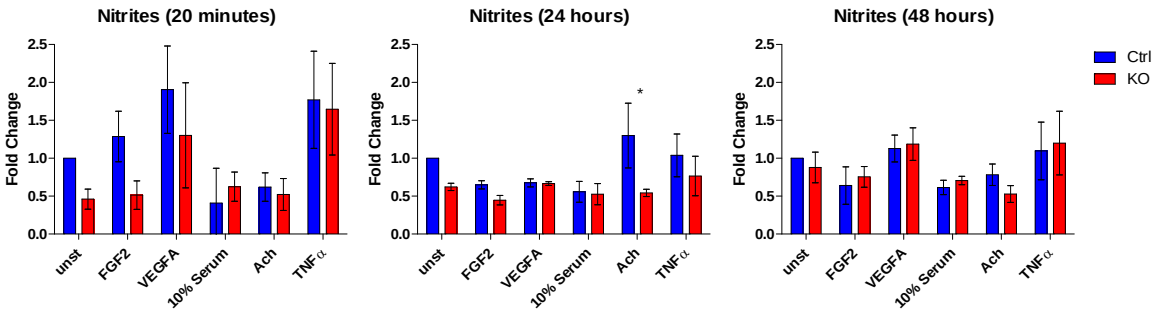

Figure 45. Nitrites amount in the MAECs supernatant, measured by Griess reaction.
The three cell isolates used in the experiments were either unstimulated or treated with FGF2, VEGFA, FCS, Ach or TNFα for 20 minutes, 24 or 48 hours. Values normalized on the control unstimulated. (P value < 0.05).

6.7. mTORC2 has no impact on actin cytoskeleton rearrangement

mTORC2 and PKCα strongly influence the cytoskeletal organization [312, 348]. The cytoskeleton plays an important role in many cellular processes such as cell adhesion and migration[399]. The migratory ability is an essential feature of endothelial cells during angiogenesis[400, 401]. We therefore analyzed whether *Rictor* knockout cells might show a different organization of actin fibers, an important component of the cytoskeleton. In particular, we focused on potential defects in F-actin polymerization and altered cell shape in *Rictor* knockout cells[312, 348, 349]. MAECs were seeded in culture slides, starved and stimulated with FGF2 or VEGFA at the concentration of 25 ng/ml for 1, 3 or 6 hours. The cells were then permeabilized and stained with fluorescent-labeled Phalloidin and photographed under a fluorescent microscope. Unstimulated cells showed a similar actin distribution, without the formation of extensive actin filaments both in knockout and control cells. One hour after FGF2 or VEGFA stimulation, the presence of actin fibers was noticeable both in control and in knockout cells. The distribution and the edge of the actin filaments were comparable in control and *Rictor* knockout cells (Figure 46). Also the cell shape was not affected by the ablation of mTORC2.

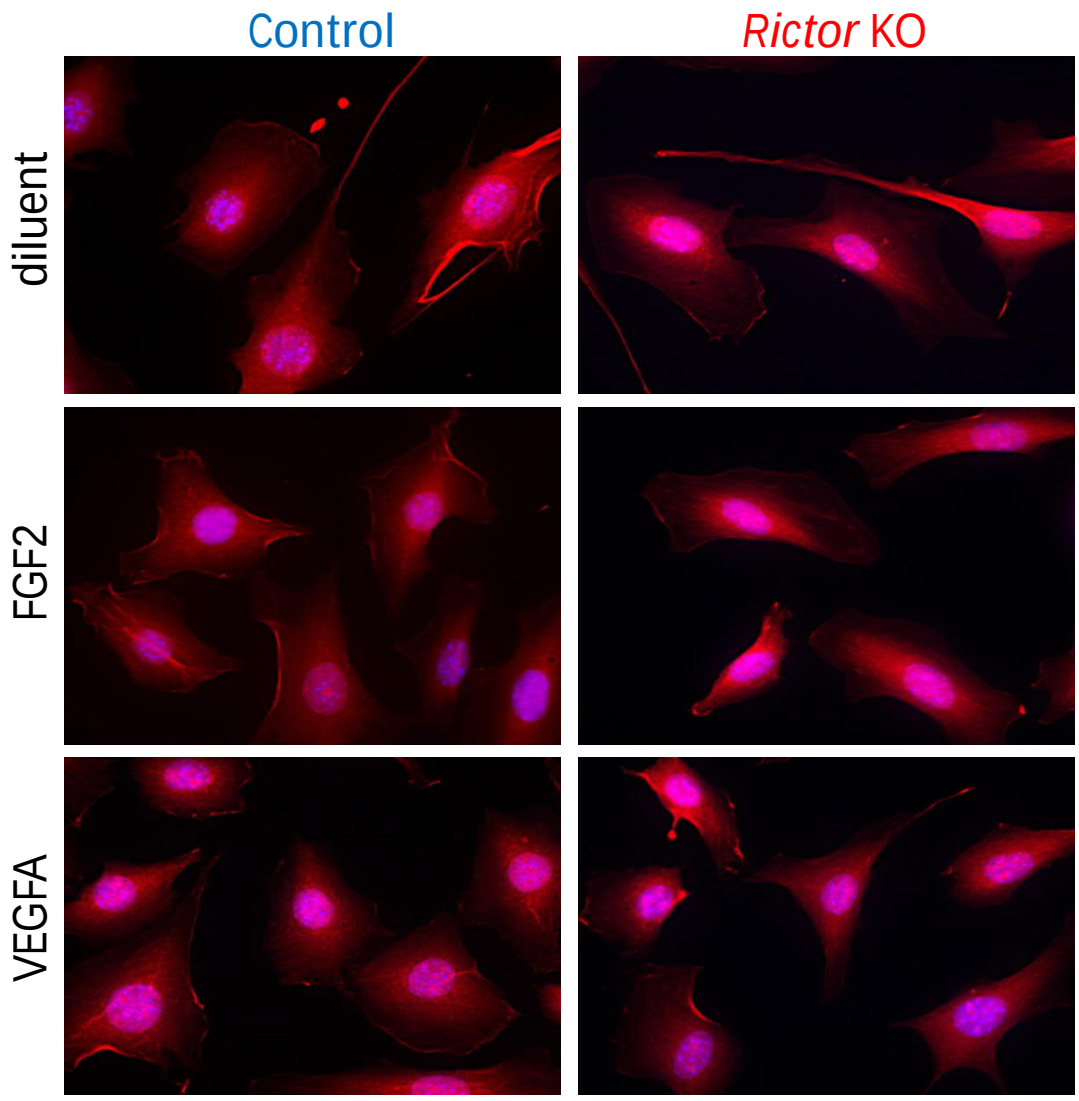

Figure 46. Immunofluorescent stain of MAEC actin cytoskeleton.

MAECs, control and *Rictor* knockout, incubated with FGF2 or VEGFA for one hour and afterwards stained using Phalloidin (orange) binding the acting filaments and DAPI (pink) detecting the nuclei.

7. DISCUSSION

In this study we (A) deleted *Rictor* in the endothelium to study the general requirement of endothelial mTORC2 during embryonic and adolescent development and (B) used *Rictor* knockout in endothelial cells to elucidate potential molecular mechanisms.

7.1. Embryonal development

Our analysis of embryonic development using constitutive and inducible VE-Cadherin-CRE-specific *Rictor* knockout confirmed that homozygous *Rictor* deletion in endothelial cells is almost completely lethal and results in embryonic death around E12. Guertin et al. proposed that vascular defects may contribute to the lethality of whole-body *Rictor* knockout embryos on E10.5[328]. Furthermore, Wang et al. demonstrated that the homozygous and Tie2-CRE-driven *Rictor* knockout is embryonically lethal[372]. However, other than reductions in peripheral vascularization, we did not detect gross abnormalities of the normal vascular plexi on E10.5 (Figure 20 and Figure 21). Surviving embryos around this time frame showed rather distinct deficits in vascularization and were growth-retarded. The vascular embryonic phenotype strongly resembled the one found in total mTORC2-deficient mice lacking *Rictor* or mLST8, which are both essential mTORC2 components[310, 328]. Therefore, we suggest that the critical embryonic function of mTORC2 at midgestation originates in the endothelium. Specifically, we detected a delayed ossification of the vertebrae, toes, and fingers (Figure 21). Delayed ossification may explain growth retardation but may not categorically explain embryonic lethality of *Rictor*$^{i\Delta ec}$ in the confined midgestational timeframe. Thus, other essential functions that are regulated by mTORC2 during this short period in midgestation are probable and may also account for lethality.

Many signaling pathways that are involved in early embryonic development are also recapitulated during tumorigenesis[402]. As we found that endothelial mTORC2 was required during a confined, midgestational timeframe but had no apparent influence on viability before midgestation (E8.5), beyond midgestation (E14.5), physiological vascular development, vascular maintenance and growth from adolescence into adulthood, we hypothesized that endothelial *Rictor* might promote only 'aberrant' endothelial phenotype modulation such as in tumor angiogenesis or during a transition to an invasive mesenchymal phenotype. Guertin et al. demonstrated that *Rictor* has no significant role by itself in maintaining the integrity of a normal prostate epithelium *in vivo* but requires *Rictor* to be transformed into an invasive, malignant phenotype by *Pten* deletion, which

results in strong PI3K activation[403]. Similarly, *Drosophila* embryos lacking mTORC2 activity are viable and display only minor growth defects[404] [403]. However, *PTEN* loss-induced tissue overgrowth in the *Drosophila* eye requires dTORC2[404].

7.2. FGF2-induced capillary remodeling and neo-angiogenesis *in vivo*

We found that particularly FGF2 and not VEGFA depended on the mTORC2 signaling hub to establish a capillary-like endothelial network on matrigel substrate when we tested these PI3K-activating angiogenic molecules *in vitro*. We found that FGF2 elicited a strong and fast increase in the diameter of existing skin capillaries in the dorsal skinfold chamber after two days of stimulation in both control and *Rictor*$^{i\Delta ec}$ mice (Figure 25). Over a period of 7 days, FGF2 induced the progressive and extensive remodeling of vessel structures characterized by heterogeneous and larger diameter sizes that also included larger arterioles and a tortuous vascular bed in control mice. *Rictor*$^{i\Delta ec}$ mice however, could not maintain heterogeneous capillary size remodeling beyond day 2 of FGF2 exposure and returned to 'normalized' vascular features with homogeneously and smaller sized capillary diameters and parallel-oriented capillaries. Tortuous and dilated capillaries are also found in vascularized tumors. Tumor blood vessels furthermore display hyper-permeability, and do not mature into functional vasculature[405, 406]. However, we could not detect fewer leakage points in FGF2-stimulated skin capillaries *Rictor*$^{i\Delta ec}$ in preliminary investigations.

However, the supply of FGF2 to the skin muscle over a period of seven days was limited by the volume of the matrigel carrier (16 µl) and may not have provided saturated FGF2-stimulation at all times. We therefore continued our investigations using the matrigel plug assay carrying pathologically high doses of FGF2 in a volume of 200 µl to induce aberrant, leaky and tumor-like angiogenesis as reported before[382]. Indeed, we observed a dense, heterogeneous neo-vasculature with several patches of hemorrhage that formed after 7 days in control mice (Figure 26). Endothelial *Rictor* knockout strongly and significantly reduced FGF2-mediated neo-vessel ingrowth, and capillaries remained homogenously small with no microscopic signs of leakage. Our study thus demonstrates that endothelial mTORC2 acted as a central signaling hub for FGF2-induced persistent capillary diameter increases and remodeling into heterogeneous capillary structures and formation of a leaky, tumor-like neo-vasculature in the adult mouse.

7.3. FGF2 in angiogenesis and osteogenesis

FGF2, which is not secreted through vesicular pathways, can be exported from cells with unique extrusion pathways or large amounts can be released upon cell death[407,382]. FGF2

has been selectively determined as a crucial tumorigenic cytokine in prostate cancers in which both FGF2 and FGF2 receptor subtypes are co-expressed [408] [409]. In addition many other tumor types express FGF2/FGFRs at high levels [410, 411, 412-414, 382]. On the other hand, fibroblast growth factors are involved in the formation of skeletal elements within the developing limb [415-417]. Several FGFs are expressed in developing endochondral bone. FGF2 was the first FGF ligand to be isolated from growth plate chondrocytes [52]. FGF2 expression has also been observed in periosteal cells and in osteoblasts [51, 418]. Targeted deletion of FGF2 causes a relatively subtle defect in osteoblastogenesis, leading to decreased bone growth and bone density [419, 51].

7.4. FGF2- and VEGFA-induced signaling via mTORC2 downstream targets AKT and PKCα

Many researchers have demonstrated that FGF2 induces AKT phosphorylation on Ser [473] in endothelial cells [420]. In other reports, mTORC2 contributed to AKT stability and activity [333, 334]. Here, we show that mTORC2 is required for AKT phosphorylation on the Ser [473] residue and that this phosphorylation is increased in a FGF2 dose dependent manner (Figure 24A). In our system, we could also observe that mTORC2 is required for PKCα stabilization, as demonstrated previously [313, 333, 334] (Figure 24A). Therefore the impact of mTORC2 on angiogenesis, observed in our experiments *in vivo* may be explained with a different AKT or PKCα activity within the endothelial cells. These two kinases were influence different phenomena implicated in angiogenesis, such as cell proliferation, migration, differentiation or network formation; perhaps by regulating FoxOs activity [328, 329] or other downstream factors [62, 92, 315-318, 352, 353].

Not all of these cellular responses, however, were affected by a different activation or presence of the two kinases AKT and PKCα in our cell culture experiments: FGF2-driven proliferation and migration were not differently regulated in mTORC2 knockout cells (Figure 24B). VEGFA-driven proliferation instead, decreased as consequence of *Rictor* knockout (Figure S5). Also the ability of endothelial cells to establish a capillary-like network *in vitro* under FGF2 stimulation was impaired in *Rictor* knockout cells, but the same effect was not detected during VEGFA stimulation (Figure 23). Thus, the different *in vivo* and *in vitro* phenotypes observed in mTORC2 knockout endothelial cells might be due to a post-transcriptional regulation of AKT and PKCα.

AKT and PKCα can activate eNOS [325, 336, 354]. Since eNOS function consists in producing NO, an instable molecule which is implicated in vasodilation [169, 170] and angiogenesis [78, 171-176], we decided to investigate the levels of NO in our cell culture system and quantify the nitrites, a product originated by the NO oxidation in the cell supernatants [156, 190]. In these

experiments, VEGFA robustly stimulated nitrite production but, however, mTORC2 absence did not alter the nitrite levels (Figure 45). On the other hand, starved or FGF2-stimulated mTORC2 knockout cells produced lower amounts of nitrites then the control cells, but this difference didn't result in being statistically significant (Figure 45). The difference between control and *Rictor* knockout cells in nitrite production after 24 hours of ACh stimulation, however, was statistically significant. Thus, mTORC2 might be involved in vaso-relaxation via ACh-mediated NO/nitrite production (Figure 45). In future, it might be interesting to investigate the role of mTORC2 in vascular function in detail to understand whether AKT and PKCα are directly involved in this phenomenon. Moreover, in order to obtain more precise data regarding nitric oxide production, instruments directly measuring NO, such as chemiluminescence analyzer or amperometric NO sensors, could be used.

7.5. A hypothetical VEGFA-mTORC2-HGF loop?

During the analysis, of the angiogenic factors released in the culture supernatants, a high variability between the isolates was observed: proteins strongly secreted in one isolate resulted to be absent in the other (see section 7.9.1). Despite that, the secretion of the hepatocyte growth factor (HGF) was quantifiable in all the isolates (Figure 44). In the knockout MAEC monolayer, VEGFA-induced secretion of HGF was strongly reduced. HGF is a growth factor expressed in malignancies such as breast cancer [133, 421] that can stimulate angiogenesis by increasing endothelial cell growth and mobility [76, 137]. VEGF is also one of the main pro-angiogenic factors frequently expressed in tumors. A further characterization of the molecular interaction connecting HGF secretion to VEGFA stimulation via mTORC2 might be of clinical interest since, as demonstrated earlier, blocking HGF in mouse xenografts leads to a decreased tumor invasiveness and growth [421]. Therefore, using compounds inhibiting both mTORC2 and HGF might lead to a stronger effect.

Additionally, it was observed that VEGFA and HGF can contribute synergistically to endothelial cell proliferation and migration [137]. This observation is in line with our results of the VEGFA-induced proliferation assay performed (Figure S5) where the control endothelial cells had a higher proliferation rate compared to *Rictor* knockout cells. Further *in vitro* works may confirm the involvement of endothelial mTORC2 in HGF secretion under VEGFA stimulation.

7.6. mTORC2 is involved in *Ang2* expression but not in *Vegfrs* mRNA modulation

The Notch signaling pathway modulates the expression of VEGF receptors in endothelial cells. This pathway is involved in differentiating the endothelial cells into tip and stalk phenotypes that perform individual roles in sprouting angiogenesis [213]. VEGFA was shown to up-regulate *Vegfr1* and *Vegfr2* transcription in endothelial cells [422-424]. In our system we found that VEGFA up-regulated sVEGFR1 secretion (Figure 35 and Figure 36). On the other hand, it is shown that FGF up-regulates *Vegfr2* mRNA expression *in vivo* [425]. Again, we found that FGF2 strongly increased *Vegfr1* and *sVegfr1* transcription whereas it reduced *Vegfr2* ones (Figure 24B). FGF2 was also observed to induce sVEGFR1 secretion (Figure 36). In all of these processes, however, mTORC2 was never involved and therefore we suggest that mTORC2 doesn't contribute in endothelial tip/stalk cell differentiation.

FGF2 and VEGFA increase *Ang2* expression in endothelial cells [426, 427]. In our cell culture system *Ang2* expression strongly decreased after FGF2 stimulation or remained constant after adding VEGFA (Figure 37). Interestingly, *Rictor* knockout cells compared to controls induced higher levels of *Ang2* in unstimulated conditions (Figure 37). ANG2 is particularly expressed in the remodeling endothelium but it was suggested that endothelial cells exposed to this protein in absence of VEGF can undergo in apoptosis [235]. Thus, hypothetically, mTORC2 could be involved in the transition from a quiescent endothelium towards a remodeling one or drive towards apoptosis when survival signals are missing.

7.7. Endothelial RICTOR and inflammatory molecules

Transcripts codifying for the inflammation molecules *Icam-1* and *Vcam-1* were analyzed. The expression of these molecules was not affected by the *Rictor* knockout (Figure 42). However, the expression of *Mcp-1* mRNA remained significantly higher in *Rictor* knockout cells after 24 hours of FGF2 stimulation (Figure 42). MCP-1 was shown to enhance endothelial cell migration during wound repair [428]. During the time course in our wound healing assay, however, we couldn't observe any vantage in motility of the mTORC2 knockout cells stimulated with FGF2 (Figure 24D).

MCP-1 is also involved in monocytes recruitment [397]. Interestingly, we observed a small, though statistically insignificant trend, towards denser packed stromal halo in FGF2-containing matrigel plugs from *Rictor* knockout animals and consecutively higher $CD68^+$ macrophages (Figure 26). Thus, hypothetically, mTORC2 might play a role in chronic inflammation, perhaps by inhibiting the monocytes recruitment to the endothelium. Indeed, related research from our unit demonstrated that ablation of *Rictor* in adipocytes lead to increased expression of inflammatory cytokines [429]. Thus, decreased mTORC2 activity turned on a cascade of inflammatory pathways.

Still, a possible higher *Mcp-1* induction in *Rictor* knockout MAECs is likely unrelated to our main findings of a crucial requirement of the FGF2-RICTOR axis in capillary remodeling and extensive angiogenesis (Figure 25 and Figure 26) since higher amount of MCP-1 released from the endothelium should lead to a higher amount of monocytes recruited, cells which have the ability to secrete growth factors (e.g. VEGF) with pro-angiogenic effects.

The amount of MCP-1 protein was also studied during the secretome analysis, but its presence in the medium was not affected by the absence of mTORC2 after 24 hours of stimulation (Figure 44). Further investigations on MCP-1 protein levels are therefore required in order to understand whether the difference observed on the RNA level is also reproduced on the protein one.

7.8. A potential role for RICTOR in endothelial to mesenchymal transition?

Interestingly we found that quiescent and starved MEAC expressed low levels of RICTOR in control cells. High doses of FGF2 however induced RICTOR protein in correlation with high phosphorylation of AKT on Ser^{473} (Figure 24A). Comparable findings were reported during the epithelial to mesenchymal transition (EMT). Transforming growth factor (TGF-β), a strong inducer of EMT, increased RICTOR protein and thereby formation of mTORC2 in mouse mammary gland epithelial cells[430]. Without RICTOR, the epithelial cells arrested in an intermediate stage between epithelial and mesenchymal without displaying a motile and invasive phenotype[430]. Interestingly, TGF-β1 treatment also induces an interaction between RICTOR and integrin-linked kinase (ILK) and promotes ILK-dependent EMT. This complex was detected in cancer but not in normal cell types[431] and overlaps with mTORC2 in the function as AKT Ser^{473} kinase[432]. Thus, RICTOR could promote EMT by forming different complexes.

In parallel to EMT, endothelial to mesenchymal transition (EndoMT) can be induced by transforming growth factor (TGF-β)[433]. EndoMT is a newly recognized type of cellular trans-differentiation that participates in development, but also in pathological conditions such as cancer and fibrosis[433-435]. New studies have shown that EndoMT represents a dedifferentiation of endothelial cells to a stem cell phenotype, which can re-differentiate into bone or cartilage cells[435, 433, 436]. Thus, hypothetically, endothelial RICTOR may be required during midgestation to promote the transition of endothelial cells to a mesenchymal, osteogenic phenotype to promote FGF2-directed ossification of limbs and vertebrae. During further development through normal adolescence where most vasculature is quiescent, with only 0.01% of endothelial cells undergoing division[437], endothelial *Rictor* knockout may represent the characteristics of an unchallenged

quiescent endothelial monolayer with low RICTOR expression and AKT activity. Recent studies suggest, during angiogenic sprouting, endothelial cells express many of EndoMT-driving genes and break down basement membrane. However, they retain intercellular junctions and migrate as a connected train of cells[434]. This process has been termed a partial EndoMT[434]. The permanently activated phenotype of tumor vasculature may well reflect the chronic activation of the EndoMT process, driven by persistent angiogenic cascades, leading to excessive sprouting and a failure to settle back into the mature, stable phenotype[434]. Thus, hypothetically, endothelial mTORC2, assembled through increased FGF2-increased RICTOR presence may promote neovascularization by a sustained partial EndoMT.

7.9. Outlook and technical considerations

In parallel to our main findings, I kept looking for a potential molecular mechanism in order to explain our *in vivo* phenotypes (section "Results – Part B"). I therefore investigated on the transcription level which genes are modulated after mTORC2 ablation under FGF2 or VEGFA stimulation. I used gene arrays to analyze the general transcriptome in MAECs after *Rictor* knockout and I also investigated on the proteins, involved in angiogenesis, secreted by MAECs after *Rictor* knockout by using antibody arrays.
However, these high-throughput analyses did not reveal any gene or protein regulated upon FGF2 administration in a *Rictor*-dependent way in MAECs. Thus, no further molecular explanation for our *in vivo* phenotype could be elucidated using MAECs *in vitro.*

7.9.1. Endothelial cells characterization and variability

The approach used to isolate the MAECs is a technique already described in literature and frequently used in our group to isolate endothelial cells from murine aortas. During this procedure, under constant stimulation of growth factors (FGF2, VEGFA, ECGS), the endothelial cells sprout out of aortic rings previously cleaned form the perivascular tissue. Three different cell isolates (ISO1-2-3) characterized by the typical endothelial cobblestone cell shape could be obtained. To assess whether these cells were indeed endothelial cells, the most important markers for endothelial cells were analyzed by real-time PCR. *Cd31* mRNA and its smaller spliced variant, both codifying for the membrane protein expressed mainly on the EC surface[26, 386, 438], were not expressed in our endothelial isolates. The same outcome was given by the analysis of the other marker *Tie2* and partially by *Cd34*. However, the three isolates exhibited the typical endothelial cell shape, expressed the endothelial marker *VE-Cadherin* and were positive for endothelial marker vWF. Thus, some classical markers for the endothelium could not be maintained in

cultured cells, whereas others were expressed and the morphology homogeneity exhibited an endothelial phenotype.

The main issue faced by using these cells was the high biological variability displayed by these isolates which perhaps contributed to hide most of the differences generated after knocking out *Rictor* in the high throughput experiments (transcriptome and secretome analysis).

The source of this biological variability might be due to the MAECs isolation procedure, a process that was already documented to alter the normal endothelial cells behavior and gene expression observed *in vivo*, possibly due to the change of the microenvironment or to epigenetic mutations[387, 388]. Moreover, another source of variability might be a possible different doubling time of the cell isolates. The cells sprouting out the aortic rings need differential time for outgrowth. Some rings, also belonging to the same aorta, led to a quick endothelial cells growth, characterized by many sprouts outgrowing from the ring. For other rings, the time required from the endothelial sprouts to reach the well edge, was much longer. During this period, indeed, the cells undergo to a different number of divisions, which may contribute to increase the variability from isolate to isolate.

Another source of variability might be the presence of contaminating cells sprouting out from the aortic rings together with the endothelial cells since not all of the perivascular and mural cells (e.g. SMCs, Figure 30) can be easily removed by hand.

In order to obtain isolates of purer quality, more trials were performed, either placing the aortic rings in hypoxic environment or incubating them with different growth factors and for different time periods, but only co-cultures, mostly constituted by SMCs, could be obtained. We also tried the MACS and FACS-sorting techniques to isolate either aortic or lungs endothelial cells, but the main issues, faced during these strategies, was the low percentage of surviving endothelial cells after 2 or 3 passages in culture. This problem might have been avoided by immortalizing the sorted cells but it would have altered the intracellular molecular pathways. Again, another opportunity to obtain isolates of purer quality might be to use wild-type ECs (not *Rictor* floxed) available in commerce and to induce the knockout of the gene of interest with different strategies (e.g. siRNAs, shRNAs, PNAs or other techniques) whose efficacy may not be as high as in our adenoviral system.

7.9.2. Hypoxia as a natural angiogenic stimulus

Based on the cellular assays which demonstrated in normoxia that the ablation of *Rictor* led to *in vitro* phenotypes in our MAEC (Figure 23 and Figure S5); we investigated on potentially modulated molecular pathways under normoxic conditions. However, since angiogenesis is strongly induced in hypoxic conditions, in future it might be more fruitful

to use hypoxia as primary stimulus for the activation of the endothelial cells; or also to combine it with growth factor stimulation (e.g. FGF2, VEGFA, PDGFB). In this way, the activation of the endothelial cells might be more pronounced and the existence of possible molecular pathways modulated after mTORC2 disruption may emerge.

7.10 Conclusion

In conclusion, our data suggest that the endothelial FGF2-RICTOR axis is not required during endothelial quiescence or moderate capillary remodeling, but it is crucial for midgestational development and sustained and extensive neovascularization in the adult.

Moreover, on the molecular level, we observed that endothelial mTORC2 is involved in the secretion of HGF as consequence of VEGFA stimulation and it also modulates *Ang2* and *Mcp*-1 transcription respectively in starved and in FGF2-stimulated endothelium monolayer. Furthermore, we hypothesize that mTORC2 might also be implicated in vasodilation since its absence in MAECs led to a reduced amount of nitrites produced under ACh stimulation. Again, we could show that RICTOR is required for PKCα stability and AKT activation but, however, in our system, we could not find molecular pathways involved in angiogenesis to be affected by *Rictor* ablation.

Therefore, further studies are needed to uncover the exact and maybe related molecular nature that enables endothelial mTORC2/RICTOR to promote both ossification in the embryo and extensive and aberrant FGF2-dependent angiogenesis in the adult.

Other directions for future investigations might regard the possible role played by endothelial mTORC2 in several different processes: NO-mediated vasorelaxation, VEGFA-promoted HGF secretion, MCP-1-induced inflammation or ANG2-driven vascular remodeling.

8. MATERIALS AND METHODS

8.1. Animal procedures

Mice with floxed *Rictor* exons[292, 439] were crossed with mice that express tamoxifen inducible Cre-ER^{T2} under the control of the endothelium-specific VE-cadherin promoter (VECad-Cre-ER^{T2})[369] (kind gift of Dr. Iruela-Arispe, Department of Molecular, Cell & Developmental Biology, UCLA, USA) both on a congenic C57Bl/6J background. Offspring were genotyped for CRE-recombinase, *Rictor*^{floxed} and *Rictor*^{wt} alleles using qPCR. Briefly, DNA was isolated from ear biopsies and amplified by qPCR with the following primer pairs (5'-3'): Forward: GCG GTC TGG CAG TAA AAA CTA TC; Reverse: GTG AAA CAG CAT TGC TGT CAC TT. The mice were bred, housed and handled according to the local animal ethics committee. All procedures with mice were approved by the Veterinary Office of the Canton of Zürich, Switzerland under licenses 77/2009 and 179/2012.

8.2. Whole mount embryo staining

Embryos were stained with an antibody against endomucin according to Vieira et al.[440]. In brief, embryos were fixed for two hours on ice with PBS containing 4% PFA. After three washing steps with PBS containing 0.1% Triton X-100 and blocking of unspecific binding sites by incubation with PBS containing 10% FCS and 0.1% Triton X-100 for 30 minutes at room temperature, embryos were incubated with rat monoclonal antibody against endomucin (1:100, Santa Cruz Biotechnology) dissolved in PBS over night at 4°C followed by five washing steps with PBS at room temperature. After incubation with secondary antibody anti-rat Alexa Fluor-555 (1:200, Molecular Probes) over night at 4°C and three further washing steps with PBS, embryos were mounted and analyzed by laser scanning confocal microscopy (SP5; Leica, Wetzlar, Germany). Staining of whole embryos for LacZ was as described previously[441].

8.3 Alizarin Red and Alcian Blue stainings

For skeletal staining, embryos were fixed in 95% ethanol for more than four days, after removal of fat and connective tissue, incubated in acetone for one day and stained with 0.15% alcian blue 8GS (Sigma-Aldrich)/ 0.05% alicarin red S (Sigma-Aldrich)/ 5% acetic acid in 70% ethanol at 37°C for two days. After bleaching in 1% KOH for 12 to 48 hours embryos were de-stained with graded washes of glycerin (20% glycerin in 1% KOH, 50%

glycerin in 1% KOH and 80% KOH in 1% glycerin). Embryos were stored in 100% glycerin.

8.4. Histological analysis

Embryos and dissected organs from adult mice were fixed in 4% PFA in PBS, transferred to ethanol and embedded in paraffin. Longitudinally-sectioned paraffin-embedded embryos and organs were stained with haematoxylin and eosin. For CD31 staining paraffin sections were stained as described previously [442]. Sections from dorsal chambers were de-paraffinized and rehydrated in xylene and isopropanol and antigens retrieved by boiling in trisodium citrate. Rabbit polyclonal anti-mouse Estrogen Receptor α antibody (Millipore) was used for detection and visualized by secondary goat anti-rabbit Alexa-Fluor 555 (Invitrogen) using microscopes and cameras from Zeiss and Olympus.

8.5. Determination of *Rictor* mRNA expression levels in endothelial cells from thoracic aorta

Rictor deletion was induced in VECad-CreER^{T2}; *Rictor*$^{floxed/floxed}$ mice at an age of four weeks with five consecutive intraperitoneal tamoxifen (Tx) injections according to the protocol of Monvoisin et al.[369]. (2 mg Tx /ml dissolved in corn oil at a concentration of 80 mg/kg bodyweight, T5648, Sigma-Aldrich). Littermate control mice were injected with corn oil alone. This injection protocol was used for all experiments in this study.

Aortae were excised from 6 month old Tx-injected (*Rictor*$^{i\Delta ec}$) and control mice (Ctrl), cleaned from adhering tissue and opened longitudinally. Endothelial cells were carefully scraped directly in RLT buffer (Qiagen) and RNA was extracted using the RNAeasy micro kit (Qiagen) according to the recommendations of the manufacturer. Equal amounts of RNA were transcribed to cDNA by WT (Whole Transcript)-Ovation™ Pico RNA Amplification System (NuGEN). Quantitative real-time PCR was performed using a SYBR green-based standard protocol. Primer list is shown in section 'Real-time quantitative reverse transcription polymerase chain reaction'. Specificity of the primers was tested by melt curve and agarose gel analysis and sequencing. Relative expression levels were calculated using the comparative ΔCt method [443]

8.6. Isolation of endothelial cells

Mouse aortic endothelial cells (MAECs) were isolated from aortae of 8-10 weeks old *Rictor* floxed (exons 4 and 5) C57BL/6 mice [444, 364]. Briefly, fibrin gels were prepared by mixing 3 mg / ml of fibrinogen with serum-free DMEM complemented with non-essential amino

acids, Sodium Pyruvate, Pen-Strep and thrombin on ice. 24-well plates were coated with the prepared fibrin gel allowed to polymerize at 37°C. The excised aorta was cleaned, cut in small rings and placed on top of the gel and overlaid by fibrin gel. After gel had polymerized pre-warmed growth media (serum-free DMEM that contained 10 % FCS, 200 µg / ml of ECGS, 10 ng/ml of FGF2 and 0.1 IE /ml of heparin) was loaded to the wells. To protect the fibrin gel from degradation, 300 µg / ml of ε-amino caproic acid (Sigma A-7824) diluted in PBS was added to all wells every other day. After 10 days of culturing, capillary-like sprouts were observed under the microscope. The outgrown cells were harvested by pipetting up and down the fibrin gel. The gel-cell mixture was transferred to a six-well plate which had previously been coated with 0.1% gelatin gold, and 1 ml / well of growth media w/o heparin was added. The next day, cells were washed once with warm PBS and new EC growth media was added. Confluent cells were split 1:2 by trypsinization using TrypLETM-Express and characterized.

8.7. Endothelial cells characterization

The characterization of the isolated cells was performed by macroscopic observation of the cell shape, analysis of the transcriptome and staining of surface markers. *Cd31*, *Cd34*, VE-Cadherin and *Sm22α* expression was analyzed in confluent monolayer of cells growing in full medium, using the primers listed in the Table 2. The expression of these genes in the isolated cells was compared to their expression in SMC, adipocytes, fibroblasts, aortic arch, and other MAECs (Cell Biologics, #C57-6052). The presence of the endothelial marker von Willebrand Factor was detected by immune fluorescent stain using von Willebrand Factor antibody (vWF, LabForce AG).

8.8. Cell culture and treatments

For all the experiments using MAECs, cell culture dishes were coated with 0.1% gelatin gold (Carl Roth GmbH, #4274.1) for 20 minutes at 37°C. MAECs were maintained in DMEM (Biochrom, #FG435), complemented with 10%, 1% or 0.5% (complete or starvation mediums) FCS (Biochrom, #S0615), 1% sodium pyruvate (GIBCO, #15140), 1% non-essential amino acids (GIBCO, #11140) and 1% penicillin-streptomycin (GIBCO, #15140). Stimulation with the growth factors FGF2 (R&D Systems, #3139-FB/CF) or VEGFA (R&D Systems, #493-MV/CF) always included coupling with heparin (Braun, #3511014) at a fixed ratio (1 IU heparin per 1.5 µg/ml GF) one hour before at room temperature. Other molecules used in cell treatments were ACh (Sigma, #A6625), TNFα (Sigma, #T7539) and insulin (Sigma, #I0516).

8.9. Generation of *Rictor* KO cells

Rictor knockout was induced by adenoviral transfection of CRE-Recombinase on *Rictor* floxed MAEC. 2.5x10^5 *Rictor* floxed MAECs were seeded on a 6 cm culture dish. The next day, the media was removed and a virus (100 MOI) that contained either Ade-CRE-GFP (Vector Biolabs 1045) or Ade-CMV-GFP (Vector Biolabs 1060) was added in 1 ml of growth media to the cells. After 7 hours, the media was removed, replaced by 4 ml of normal growth media, and incubated at 37°C. Endothelial cells expressed GFP the following day. Down-regulation of *Rictor* and disruption of mTORC2 signaling was assessed by using qRT-PCR and Western blotting. Steps that involved handling viruses or virus-transfected cells were performed in a level-2 biosafety hood (Skan VSB 90) in a certified cell culture laboratory.

8.10. Endothelial network-formation assay *in vitro*

Angiogenesis *in vitro* was assessed on the basis of a tube formation assay. Twenty-four-well culture plates (Costar; Corning) were coated with growth factor-reduced matrigel (BD Biosciences) in a total volume of 150µL and allowed to solidify for 30 min at 37°C. MAEC were trypsinized and re-suspended to a concentration of 10^5/mL in DMEM / 1% FCS. 500µl of the cell suspension were added into each well and complemented with diluent (heparin) and growth factors (FGF2; VEGFA 25ng/ml with heparin). Then the cells were incubated at 37°C for eighteen hours. The appearance of endothelial network was observed under an inverted microscope by fluorescence with a 4x objective (IX70, Olympus) and photographed. Number of master segments was quantified automatically using the Macro 'Angiogenesis Analyzer' by Gilles Carpentier (Gilles Carpentier contribution: Angiogenesis Analyzer, ImageJ News, 5 October 2012) for NIH Image J 1.47v Program.

8.11. Fluorescent labeling of wild-type and *Rictor* KO cells

Wild-type and *Rictor* KO MAEC were plated subconfluently (~10^6 cells) in a 15 cm cell culture dish and incubated overnight. For wild-type cells, tracking dye green (CytoPainter, abcam ab138891) was dissolved in 100 µl DMSO (=stock solution (1000x)). 20µl of stock solution was mixed with 5 ml assay buffer. Cells were washed once with PBS, and 5 ml tracking dye green working solution added to the cells and incubated for 45 min at 37 °C in an CO_2 incubator. For KO cells, 10 µl of tracking dye Red DMSO stock solution (500X, Cytopainter, abcam ab138893) was mixed with 50µl of assay buffer for the working solution. Cells were washed once with PBS, 6 ml of growth medium and 60 µl of the working solution added to the cells and incubated for 45 min at 37 °C in a CO_2 incubator.

Then, wild-type and KO cells were washed three times with PBS and 20 ml of growth medium added to the culture. After 2 hours, efficacy of fluorescent labeling was assessed using an Olympus IX71 microscope using Fluorescein isothiocyanate (FITC) (Ex/Em = 490/520 nm) and Texas Red filter sets (Ex/Em = 570/600 nm) and cells were photographed.

8.12. RNA extraction and real-time PCR

qRT-PCR was performed as described previously[429, 445]. RNA was isolated using RNAeasy Mini kit (Qiagen, Hilden, #74106), followed by a on column DNA digestion (Qiagen, Hilden, Germany). cDNA was transcribed from total RNA using iScript™ Reverse Transcription Supermix for RT-qPCR (BIO-RAD, #170-8841). To control for DNA contamination in the qRT-PCR, for each sample a control reaction missing reverse transcriptase was additionally amplified.

Primers used are listed in the Table 2. Primers were tested by cDNA dilution series to obtain optimal reaction conditions. qRT-PCR was performed using an iCycler iQ Real Time PCR Detection System (Biorad, Reinach, Switzerland) and iQ™ SYBR® Green Supermix (Biorad, #170-8882). Melting curve of each representative reaction was analyzed. The qRT-PCR was quantified using the formula: $2^{-\Delta CT}$ where ΔCT = CT Tubulin – CT gene of interest[443].

Table 2. Primers list

Gene	Primer Forward (5'→3')	Primer Reverse (5'→3')
Adamts1	GTG CCA GCT TGA ATG GTG TG	ACG TGA CCA TGT AGG CAC TG
Ang2	TTA GCA CAA AGG ATT CGG ACA AT	TTT TGT GGG TAG TAC TGT CCA TTC A
β-Tubulin	TCA CTG TGC CTG AAC TTA CC	GGA ACA TAG CCG TAA ACT GC
CaIM3	GCT TTG AGA CTC TCC ACC CC	CCT TGC CCT CAA CTC TAG GC
Casp8 v.1	AAC ATT CGG AGG CAT TTC TGT C	AGA AGA GCT GTA ACC TGT GGC
Cd31	ACG AGA GCC ACA GAG ACG GTG T	CGG GAC ATG GAC GAC CTC CCA
Cd34	GAG CCC TAC AGG AGA AAG GC	ACT GTG AGG AGA GCA CAA AGG
Cre	CGT ACT GAC GGT GGG AGA AT	CCC GGC AAA ACA GGT AGT TA
Dvl3 v.x5	TGG ATG TGA TGT GAT CAG GGC	GGT TAG GGG CTG TAG CAT GG
Emp1 v.1	CGC AAA TGC ATC TGT AGG GC	GAG CTG GAA CAC GAA GAC CA
Fgfr1	CGT AGG CCT GTA GCT CCC TA	TGA ACT TCA CCG TCT TGG CA
Flt3L v.1	GCT TCT GGA GGA CGT CAA CA	TCC CGA TAC AGG GCT TCA GA
Gjα1	TAC CCA ACA GCA GCA GAC TTT	GCC AAA GTG GTG GAA CTC CT
Hgf v.4	ACC CTG GTG TTT CAC AAG CA	TCT ACA CGT CGG GGT AGC A
Icam-1	GAC GCA GAG GAC CTT AAC AG	GAC GCC GCT CAG AAG AAC

Id2	GGA CTC GCA TCC CAC TAT CG	GAT GCC TGC AAG GAC AGG AT
Igfbp3	GTG ACC CGG ACA TCT GGA AG	AGT AGA TCA GGC CAC TTG CG
Jagged1	AGA AGT CAG AGT TCA GAG GCG TCC	AGT AGA AGG CTG TCA CCA AGC AAC
Klhl20	TGG ACA GCT TAT GGC AGT GG	GCC GAC GGT AAT TCA TCC CT
Mcp1	CAG GTC CCT GTC ATG CTT CT	GTG GGG CGT TAA CTG CAT CT
Notch2	GTT GAT CCC CGT CAG TGT GT	CAG GAG GCT GAA GTC GGT TT
Notch3	GGC TTT GAG GGC ACT TTG TG	CTC ACA GCG TAT GCC CGT AT
Opn v.4	CTG GCA GCT CAG AGG AGA AG	ATT CTG TGG CGC AAG GAG AT
Pkcα	GGA ATG AGT CCT TCA CGT TCA AA	TTA GCT CTG AGA CAC CAA AGG
Pkp4 v.x3	CTC CGC CTG AGC TGG AAA G	CAG TGG AGA CAG CTT CCT GG
Plcγ1	CCT GAG GGC AAA AAC AAC CG	CTC CTG TGA GTC AGC TGC AA
Pten	GCA GGA TAC GCG CTT GGG	CAG CGG CTC AAC TCT CAA AC
Rictor ex.4-5	TGC GAT ATT GGC CAT AGT GA	ACC CGG CTG CTC TTA CTT CT
SerpinE1	CCG ATG GGC TCG AGT ATG AC	TTC TCA AAG GGT GCA GCG AT
Sm22α	GCG GCC TTT AAA CCC CTC ACC C	GAG GCA GAG AAG GCT TGG TCG T
sVegfr1	CTC CTC TGT CCA CCC AGG TA	CTG CAC TTT TGC CGT CAG TC
Thbs1 v.x1	CAT GCC ATG GCC AAC AAA CA	TTG CAC TCA CAG CGG TAC AT
Tsc1 v.1	TGG TAC CAC TGC AGG TGG AAA AG	TGC ACA CAG TCA TCT TGG GG
tVegfr1	GTG TCT ATA GGT GCC GAG CC	GTT CCT TGC ACG GTG AGG TA
Vcam-1	GGC TGC GAG TCA CCA TTG	GCA CAG GTA AGA GTG TTC ATT C
VE-Cad	GCT GAC CAG CCT CCA ACG GG	TGC TCT CAA GTG AAA CCG GGC T
Vegfa	TTC GTC CAA CTT CTG GGC TC	CGA GCT AGC ACT TCT CCC AG
Vegfr2	GGA AGG CCC ATT GAG TCC AA	GTT GGT GAG GAT GAC CGT GT

8.13. Protein extraction and immunoblotting

To extract proteins, cells were washed twice with ice cold PBS and then collected by scraping (BD Falcon, #353089) in cold RIPA buffer constituted by bidistilled H_2O, 50 mM TrisHCl (Fluka, #93363), 150 mM NaCl (Fluka, #71378), 1 mM EDTA (Sigma, #E-5134), 1% Triton® X-100 (Fluka, #93418), 0.1% SDS (MERCK, #1.13760.0100) , 0.25% Sodium Deoxycholate (Sigma, # D6750) and containing a complete mini protease inhibitor (Roche, #11836153001) and a phosphatase inhibitor cocktail 2 (Sigma, #P5726) . The cell suspension was then centrifuged for 15 minutes at 14,000 rpm at 4°C and the resulting supernatant was stored in -80°C.

The protein concentration measured by using a BCA protein assay kit (Thermo scientific, #23223). Equal amounts of protein were loaded onto an 8% acrylamide-SDS gel. Separated proteins were transferred to a nitrocellulose membrane (Whatman, #BA85) using a semidry blotting procedure, blocked for 1 hour at room temperature (RT) in 5% BSA (Sigma-Aldrich, #A7906) in Tris buffered saline complemented with 0.1% Tween

(TBST). Membranes were washed once with TBST and incubated overnight at 4°C with one of the primary antibodies listed in the Table 3.

The next day, the membrane was washed three times in TBST and incubated with a secondary antibody goat anti rabbit HRP 1:5,000 (Cell Signaling, #7074) or anti mouse HRP 1:50,000 (Cell Signaling, #7076) for 1 hour at room temperature. After another wash step, a chemiluminescent substrate that is used for the detection of HRP (Thermo Scientific, #34080) was applied to the membrane, and then the membrane was incubated for 1 minute. The signal was detected with a CL-XPosure film (Thermo Scientific 34088), and the resulting bands were quantified by using ImageJ (Wayne Rasband, NIH, MD, USA).

Table 3. Antibodies list

mouse anti β-ACTIN	Sigma #A-5441	1:10000
rabbit anti AKT	Cell Signaling #9272	1:1000
rabbit anti CRE Recombinase	Cell Signaling #7803	1:1000
rabbit anti MAPK	Cell Signaling #9102	1:1000
rabbit anti Phospho-AKT (Ser^{473})	Cell Signaling #9271	1:1000
rabbit anti Phospho-AKT (Thr^{308})	Cell Signaling #9275	1:1000
rabbit anti Phospho-PKCα (Ser^{657})	Santa Cruz Biotechnology #sc-12356	1:1000
rabbit anti Phospho-MAPK (Thr^{202}/Tyr^{204})	Cell Signaling #9101	1:1000
rabbit anti Phospho-S6K1(Thr^{389})	Cell Signaling #9205	1:1000
rabbit anti Phospho-S6 RP ($Ser^{235/236}$)	Cell Signaling #4858	1:1000
rabbit anti PKCα	Cell Signaling #2056S	1:1000
rabbit anti S6K1	Cell Signaling #9202	1:1000
rabbit anti RICTOR	Cell Signaling #2140	1:1000

8.14. Proliferation assay

4500 cells with 100 µl of growth media were seeded in a 96-well plate in 10 replicates. After serum-starvation (1% FCS) for 26 hours, cells were stimulated with 5-25 ng/ml of FGF2 or VEGFA, 10% FCS or 100µg/ml of insulin. After 72 hours, 10 µl of WST-1 solution (Roche Molecular Diagnostics) was added for 2 hours. Absorption was measured (A_{450nm}-A_{690nm}) by using a Spectramax M2 reader (Molecular Devices).

8.15. Migration assay (wound healing)

MAECs were grown to confluence, starved (0.5% FCS) for 24 hours. A straight scratch using a 200 µl sterile tip was applied to the confluent monolayer (Star Lab, #S1120-8810).

The monolayer was stimulated with diluent, FGF2 (25 ng/ml). The migration of the cells was photographed with an inverted microscope (Olympus IX71) at different time points (0, 1, 3, 6 and 9 hours after the stimulation) and measured with the software T-Scratch ® (Tobias Gebäck and Martin Schulz, ETH Zürich, 2008).

8.16. Mouse dorsal skin fold chamber and matrigel sealing

To study the capillary remodeling and angiogenesis in vivo we used the dorsal skin fold chamber as described previously[377] with a novel modification in order to deliver growth factors via matrigel to the tissue. For chamber implantation, two symmetrical titanium frames were mounted on the dorsal skin fold of the animal. One skin layer and the underlying fat were then completely removed in a circular area of 15 mm in diameter, and the remaining layers (consisting of striated skin muscle, subcutaneous tissue and skin) were covered with $NaCl_2$ 0.9% and a glass cover slip incorporated into one of the titanium frames[377]. The animals were allowed to recover for two days. Skin was detached from the underlying muscle and removed in a circular area of 7 mm in diameter from the back of the chamber. Growth-factor reduced matrigel was mixed with FGF2 (1.5 µg/ml) and Heparin (5 IU units) or Heparin alone. The defect on the back of the chamber was sealed with 16 µl of the matrigel mixtures, allowed to polymerize, and covered with a glass cover slip.

8.17. Intravital microscopy

Repetitive intravital microscopic analyses of skin microvasculature were carried out daily over a time period of 7 days. Microscopic images were taken at 8 different areas within the center and the periphery of the wound. After injection of 0.2 ml FITC-labeled dextran (2%; MW 70000, Sigma-Aldrich, Munich, Germany) the microcirculation was visualized by intravital fluorescence microscopy (Leica DM/LM; Leica Microsystems, Wetzlar, Germany). Microscopic images were captured by a CCD television camera (Kappa Messtechnik, Gleichen, Germany) and recorded on video (50Hz; Panasonic AG-7350-SVHS, Tokyo, Japan) for subsequent off-line analysis. Using × 10 (N-Plan ×10/0.25 LD, Leica), ×20 (HCX Apo ×20/0.50W, Leica) objectives blood flow was monitored in capillaries of the superficial and deep dermal plexus of the skin muscle. The epi-illumination setup included a mercury lamp with a blue filter (450–490nm/>520nm excitation/emission wavelength) and a green filter (530–560nm/>580nm).

8.18. Matrigel plug assay

The matrigel plug assay was performed as previously described [446]. In brief, 8-week-old C57BL/6 mice were injected subcutaneously with 0.2 ml of matrigel containing 1.5 μg/ml bFGF with1 μl (5 IU) Heparin. The injected matrigel rapidly formed a single, solid gel plug. After 7 days, mice were euthanized, the skin was pulled back to expose the matrigel plug. The matrigel plug was removed, photographed and fixed in formalin and paraffin embedded. Hemoglobin content was estimated by measuring mean pixel densities from five random 200×200 pixel areas from the magenta channel in CMKY converted images from each plug by the NIH ImageJ program.

The Matrigel plugs were removed and fixed in 4% buffered formalin. After 48 h fixation, the plugs were trimmed, dehydrated in graded alcohol and routinely paraffin wax embedded. Sections (3-5 μm thick) were prepared, mounted on glass slides, de-paraffinized in xylene, rehydrated through graded alcohols and stained with haematoxylin and eosin (HE) for the histological examination. For analysis of immunostainings, sections of one plug were photographed in three different areas (350 ×350 pixels), quantified and averaged. The n number refers to the mean of 3 areas of one plug. E.g. for microvessel invasion n=4/7 refers to 4 groups of 3 averaged areas from control plugs compared to 7 groups of 3 averaged areas from 7 *Rictor* KO plugs. Immunohistology for CD31 antigen was employed to highlight endothelial cells. Anti-CD-31 immunohistochemical staining was performed according to manufacturer's protocol (Lifespan Biosciences). Slides were photographed using a bright-field microscope (Zeiss Axioskop 2, Germany). Immunohistology for the CD68 antigen was employed to highlight cells of the monocyte / macrophage lineage[447]. Briefly, sections were de-paraffinized in xylene (2 × 5 min) and rehydrated in decreasing concentrations of ethanol (2 × 3 min washes in 100% ethanol, followed by 1 × 3 min wash in 96% ethanol). Sections were washed twice with Tris-buffered saline (TBS, 0.1 M Tris–HCl with 0.9% NaCl, pH 7.4) and incubated for 1 h at 37°C with the primary antisera (1:100, ab125212, Clone KP1, Abcam, Cambridge, United Kingdom), after heat pre-treatment in citrate acid (0.01M, pH 9.0) in a 97°C water bath for 20 min. An anti-rabbit IgG DAB detection system was subsequently applied according to the manufacturer's protocols (Discovery OmniMap anti-Rb HRP, Roche, Basel, Switzerland). Sections were then washed 3 × in TBS and 1 × in distilled water and counterstained for 1 min with haematoxylin, followed by rinsing for 5 min in tap water and dehydration in ascending alcohols, clearing in xylene, coverslipping and mounting. Sections of murine immune system organs were used as positive control. All slides were scanned using digital slide scanner NanoZoomer-XR C12000 (Hamamatsu, Japan) and images were taken using NDP.view2 viewing software (Hamamatsu).

8.19. Whole mount cytoskeleton fluorescence staining

Cells seeded in culture slides (Falcon, #354118) were starved overnight and consequently stimulated with 25 ng/ml FGF2, 25 ng/ml VEGFA or full medium for 1, 3 and 6 hours. In brief, MAECs were fixed for 15 minutes with PBS containing 4% PFA and afterwards permeabilized for 5 minutes with PBS containing 0.1% Triton ® X-100 (Fluka, #93418). Subsequently the samples were incubated for one hour at room temperature with Alexa Fluor® 555 Phalloidin (Cell Signaling, #8953) diluted 1:20 in PBS and mounted in medium containing DAPI (Life Technology, #P36935). The following day, images of the stained cytoskeleton were taken using Zeiss micro-scope (SP5; Leica, Wetzlar, Germany).

8.20. Transcriptome analysis

Full confluent MAEC monolayer was starved (0.5% serum) for 24 hours and consequently stimulated with 25 ng/ml of FGF2 or VEGFA for either 3 or 24 hours. The RNA was then collected, purified (RNA extraction chapter) and its integrity was checked on RNA Nano Chips (Agilent Technologies, #5067-1511) with Agilent 2100 Bioanalyzer. Affymetrix work flow was performed by the Functional Genomic Center Zürich. The Chip data were subsequently validated with real-time PCR using the primers listed in Table 2.

8.21. Angiogenic ligands

A confluent MAECs monolayer starved with 0.5% serum for 24 hours was stimulated with 25 ng/ml of FGF2 or VEGFA for 24 hours. After the incubation time, the cell supernatant and the cell lysates were collected. To collect the cell lysates, the cells were scraped in buffer containing 1% Igepal CA-630 (Sigma, #I3021), 20 mM Tris-HCl (pH 8.0), 137 mM NaCl, 10% glycerol, 2 mM EDTA, 10 μg / mL Aprotinin (Sigma, #A6279), 10 μg / mL Leupeptin (Tocris, #1167), and 10 μg / mL Pepstatin (Tocris, #1190). Using the kit Proteome Profiler (R&D Systems, #MVR100), the presence of proteins involved in angiogenesis was detected both in cell lysates and in the cell supernatants on CL-X Posure film (Thermo Scientific, #34090) and quantified with ImageJ software (Wayne Rasband, NIH, MD, USA). The transcription of angiogenesis ligands was also accessed on the RNA level after 1, 3, 6 and 24 hours of stimulation with FGF2 and VEGFA (primers listed in Table 2).

8.22. Nitrites quantification

MAECs were seeded confluent in a 6-well plate and starved in 1 ml of 0.5% FCS medium. The monolayer was then incubated for 20 minutes, 24 and 48 hours with different stimuli:

FGF2 (25 ng/ml), VEGFA (25 ng/ml), full medium, ACh (10 µM) or TNFα (10 ng/ml). At the end of the incubation period, the supernatant was collected and the particles removed after spinning. 100 µl of supernatant were put in duplicates in a 96-well plate and make react first with 50 µl of 5% Ortho-phosphoric acid 1% sulfanilamide (Sigma, #S9251-100G) in water then with 50 µl of 0.1% N-(1-Naphthyl)ethylenediamine dihydrochloride (Sigma, #33461-5G) in water. The optical density of each duplicate, corresponding to the amount of nitrites in the supernatant, was measured at the spectrophotometer at 540 nm wave length.

8.23. Soluble VEGFR1 quantification

A starved (0.5% FCS) MAEC monolayer was incubated with 25 ng/ml of FGF2 or VEGFA at 37°C for 24 hours. The supernatant of the cells was collected and the particulates removed by centrifugation. Using then the kit Quantikine ELISA (R&D Systems, #MVR100) the amount of soluble VEGFR1 was detected at the spectrophotometer (TECAN, Infinite #M200PRO).

8.24. Statistical analysis

Statistical tests were performed by GraphPad Prism 5.04 software (San Diego, CA, USA). On a general basis, two-way analysis of variance (ANOVA), followed by a Bonferroni post-test comparing all pairings was calculated whereby a P value of less than 0.05 was considered as statistically significant. For the comparison of two groups, the unpaired t-test was used.

9. REFERENCES

1. Monahan-Earley R, Dvorak AM and Aird WC. Evolutionary origins of the blood vascular system and endothelium. *J Thromb Haemost*. 2013;11:46-66.
2. Circulatory system in anellidae, http://www2.estrellamountain.edu/faculty/farabee/BIOBK/closedcirc.jpg. (Access Date 1st October 2015). 2015.
3. Circulatory system in vertebrata, http://animalrespriation.weebly.com/summary.html. (Access Date 1st October 2015).
4. Aird WC. Phenotypic heterogeneity of the endothelium: II. Representative vascular beds. *Circ Res*. 2007;100:174-90.
5. Wagenseil JE and Mecham RP. Vascular Extracellular Matrix and Arterial Mechanics. *Physiological reviews*. 2009;89:957-989.
6. Artery, https://classconnection.s3.amazonaws.com/660/flashcards/2365660/png/untitled1361990992835.png. (Access Date 1st October 2015). 2015.
7. Armulik A, Abramsson A and Betsholtz C. Endothelial/pericyte interactions. *Circ Res*. 2005;97:512-23.
8. Aird WC. Phenotypic heterogeneity of the endothelium: I. Structure, function, and mechanisms. *Circ Res*. 2007;100:158-73.
9. Bennett HS, Luft JH and Hampton JC. Morphological classifications of vertebrate blood capillaries. *The American journal of physiology*. 1959;196:381-90.
10. Satchell SC and Braet F. Glomerular endothelial cell fenestrations: an integral component of the glomerular filtration barrier. *American journal of physiology Renal physiology*. 2009;296:F947-56.
11. Braet F and Wisse E. Structural and functional aspects of liver sinusoidal endothelial cell fenestrae: a review. *Comp Hepatol*. 2002;1:1.
12. Stefan W. Hock ZF, Michael Buchfelder, Ilker Y. Eyüpoglu and Nic E. Savaskan. Brain Tumor–Induced Angiogenesis: Approaches and Bioassays. 2013.
13. Capillary, https://en.wikipedia.org/wiki/File:2104_Three_Major_Capillary_Types.jpg, (Access Date 1st October 2015).
14. Degroot CJM, Chao VA, Roberts JM and Taylor RN. Human Endothelial-Cell Morphology and Autacoid Expression. *Am J Physiol-Heart C*. 1995;268:H1613-H1620.
15. Kibria G, Heath D, Smith P and Biggar R. Pulmonary endothelial pavement patterns. *Thorax*. 1980;35:186-91.
16. Petzelbauer P, Bender JR, Wilson J and Pober JS. Heterogeneity of dermal microvascular endothelial cell antigen expression and cytokine responsiveness in situ and in cell culture. *J Immunol*. 1993;151:5062-72.
17. Chi JT, Chang HY, Haraldsen G, Jahnsen FL, Troyanskaya OG, Chang DS, Wang Z, Rockson SG, van de Rijn M, Botstein D and Brown PO. Endothelial cell diversity revealed by global expression profiling. *Proc Natl Acad Sci U S A*. 2003;100:10623-8.
18. Chen J, Braet F, Brodsky S, Weinstein T, Romanov V, Noiri E and Goligorsky MS. VEGF-induced mobilization of caveolae and increase in permeability of endothelial cells. *Am J Physiol Cell Physiol*. 2002;282:C1053-63.
19. Middleton J, Patterson AM, Gardner L, Schmutz C and Ashton BA. Leukocyte extravasation: chemokine transport and presentation by the endothelium. *Blood*. 2002;100:3853-60.
20. Chang CC, Chang TY, Yu CH and Tsai ML. Induction of VE-cadherin in rat placental trophoblasts by VEGF through a NO-dependent pathway. *Placenta*. 2005;26:234-41.

21. Dejana E. Endothelial cell-cell junctions: happy together. *Nature reviews Molecular cell biology*. 2004;5:261-70.

22. Wallez Y and Huber P. Endothelial adherens and tight junctions in vascular homeostasis, inflammation and angiogenesis. *Biochimica et biophysica acta*. 2008;1778:794-809.

23. Gavard J and Gutkind JS. VEGF controls endothelial-cell permeability by promoting the beta-arrestin-dependent endocytosis of VE-cadherin. *Nat Cell Biol*. 2006;8:1223-34.

24. Angelini DJ, Hyun SW, Grigoryev DN, Garg P, Gong P, Singh IS, Passaniti A, Hasday JD and Goldblum SE. TNF-alpha increases tyrosine phosphorylation of vascular endothelial cadherin and opens the paracellular pathway through fyn activation in human lung endothelia. *Am J Physiol-Lung C*. 2006;291:L1232-L1245.

25. Eilken HM and Adams RH. Dynamics of endothelial cell behavior in sprouting angiogenesis. *Curr Opin Cell Biol*. 2010;22:617-25.

26. Newman PJ. The biology of PECAM-1. *J Clin Invest*. 1997;99:3-8.

27. Pearson JD. Endothelial cell function and thrombosis. *Baillieres Best Pract Res Clin Haematol*. 1999;12:329-41.

28. Pearson JD. Endothelial cell function and thrombosis. *Baillieres Clin Haematol*. 1994;7:441-52.

29. Hughes S and Chan-Ling T. Characterization of smooth muscle cell and pericyte differentiation in the rat retina in vivo. *Invest Ophthalmol Vis Sci*. 2004;45:2795-806.

30. Li L, Miano JM, Cserjesi P and Olson EN. SM22 alpha, a marker of adult smooth muscle, is expressed in multiple myogenic lineages during embryogenesis. *Circ Res*. 1996;78:188-95.

31. Rensen SS, Doevendans PA and van Eys GJ. Regulation and characteristics of vascular smooth muscle cell phenotypic diversity. *Netherlands heart journal : monthly journal of the Netherlands Society of Cardiology and the Netherlands Heart Foundation*. 2007;15:100-8.

32. Owens GK, Kumar MS and Wamhoff BR. Molecular regulation of vascular smooth muscle cell differentiation in development and disease. *Physiological reviews*. 2004;84:767-801.

33. Hao H, Gabbiani G and Bochaton-Piallat ML. Arterial smooth muscle cell heterogeneity: implications for atherosclerosis and restenosis development. *Arterioscler Thromb Vasc Biol*. 2003;23:1510-20.

34. Li S, Fan YS, Chow LH, Van Den Diepstraten C, van Der Veer E, Sims SM and Pickering JG. Innate diversity of adult human arterial smooth muscle cells: cloning of distinct subtypes from the internal thoracic artery. *Circ Res*. 2001;89:517-25.

35. Gerhardt H and Betsholtz C. Endothelial-pericyte interactions in angiogenesis. *Cell Tissue Res*. 2003;314:15-23.

36. Bergers G and Song S. The role of pericytes in blood-vessel formation and maintenance. *Neuro-oncology*. 2005;7:452-64.

37. Hammes HP, Lin J, Renner O, Shani M, Lundqvist A, Betsholtz C, Brownlee M and Deutsch U. Pericytes and the pathogenesis of diabetic retinopathy. *Diabetes*. 2002;51:3107-12.

38. Rucker HK, Wynder HJ and Thomas WE. Cellular mechanisms of CNS pericytes. *Brain research bulletin*. 2000;51:363-9.

39. Yurchenco PD. Basement membranes: cell scaffoldings and signaling platforms. *Cold Spring Harbor perspectives in biology*. 2011;3.

40. LeBleu VS, Macdonald B and Kalluri R. Structure and function of basement membranes. *Experimental biology and medicine*. 2007;232:1121-9.

41. Unemori EN, Bouhana KS and Werb Z. Vectorial secretion of extracellular matrix proteins, matrix-degrading proteinases, and tissue inhibitor of metalloproteinases by endothelial cells. *J Biol Chem*. 1990;265:445-51.

42. Rundhaug JE. Matrix metalloproteinases, angiogenesis, and cancer - Commentary re: A. C. Lockhart et al., reduction of wound angiogenesis in patients treated with BMS-275291, a broad spectrum

matrix metalloproteinase inhibitor. Clin. Cancer Res., 9: 00-00, 2003. *Clinical Cancer Research*. 2003;9:551-554.

43. Kubota Y, Kleinman HK, Martin GR and Lawley TJ. Role of laminin and basement membrane in the morphological differentiation of human endothelial cells into capillary-like structures. *J Cell Biol*. 1988;107:1589-98.

44. Dejana E, Languino LR, Polentarutti N, Balconi G, Ryckewaert JJ, Larrieu MJ, Donati MB, Mantovani A and Marguerie G. Interaction between fibrinogen and cultured endothelial cells. Induction of migration and specific binding. *J Clin Invest*. 1985;75:11-8.

45. Form DM, Pratt BM and Madri JA. Endothelial cell proliferation during angiogenesis. In vitro modulation by basement membrane components. *Lab Invest*. 1986;55:521-30.

46. Languino LR, Gehlsen KR, Wayner E, Carter WG, Engvall E and Ruoslahti E. Endothelial cells use alpha 2 beta 1 integrin as a laminin receptor. *J Cell Biol*. 1989;109:2455-62.

47. Calderwood DA, Shattil SJ and Ginsberg MH. Integrins and actin filaments: reciprocal regulation of cell adhesion and signaling. *J Biol Chem*. 2000;275:22607-10.

48. Senger DR, Perruzzi CA, Streit M, Koteliansky VE, de Fougerolles AR and Detmar M. The alpha(1)beta(1) and alpha(2)beta(1) integrins provide critical support for vascular endothelial growth factor signaling, endothelial cell migration, and tumor angiogenesis. *Am J Pathol*. 2002;160:195-204.

49. Ellertsdottir E, Lenard A, Blum Y, Krudewig A, Herwig L, Affolter M and Belting HG. Vascular morphogenesis in the zebrafish embryo. *Dev Biol*. 2010;341:56-65.

50. Isogai S, Horiguchi M and Weinstein BM. The vascular anatomy of the developing zebrafish: An atlas of embryonic and early larval development. *Dev Biol*. 2001;230:278-301.

51. Thompson MA, Ransom DG, Pratt SJ, MacLennan H, Kieran MW, Detrich HW, 3rd, Vail B, Huber TL, Paw B, Brownlie AJ, Oates AC, Fritz A, Gates MA, Amores A, Bahary N, Talbot WS, Her H, Beier DR, Postlethwait JH and Zon LI. The cloche and spadetail genes differentially affect hematopoiesis and vasculogenesis. *Dev Biol*. 1998;197:248-69.

52. Jin SW, Beis D, Mitchell T, Chen JN and Stainier DY. Cellular and molecular analyses of vascular tube and lumen formation in zebrafish. *Development*. 2005;132:5199-209.

53. Swift MR and Weinstein BM. Arterial-Venous Specification During Development. *Circulation research*. 2009;104:576-588.

54. Lawson ND and Weinstein BM. Arteries and veins: Making a difference with zebrafish. *Nat Rev Genet*. 2002;3:674-682.

55. Tang HS, Feng YJ and Yao LQ. Angiogenesis, vasculogenesis, and vasculogenic mimicry in ovarian cancer. *Int J Gynecol Cancer*. 2009;19:605-10.

56. Takahashi T, Kalka C, Masuda H, Chen D, Silver M, Kearney M, Magner M, Isner JM and Asahara T. Ischemia- and cytokine-induced mobilization of bone marrow-derived endothelial progenitor cells for neovascularization. *Nat Med*. 1999;5:434-8.

57. Laschke MW, Giebels C and Menger MD. Vasculogenesis: a new piece of the endometriosis puzzle. *Human reproduction update*. 2011;17:628-36.

58. Ribatti D and Crivellato E. "Sprouting angiogenesis", a reappraisal. *Dev Biol*. 2012;372:157-165.

59. Makanya AN, Hlushchuk R and Djonov VG. Intussusceptive angiogenesis and its role in vascular morphogenesis, patterning, and remodeling. *Angiogenesis*. 2009;12:113-123.

60. Mor F, Quintana FJ and Cohen IR. Angiogenesis-inflammation cross-talk: vascular endothelial growth factor is secreted by activated T cells and induces Th1 polarization. *J Immunol*. 2004;172:4618-23.

61. Kasama T, Shiozawa F, Kobayashi K, Yajima N, Hanyuda M, Takeuchi HT, Mori Y, Negishi M, Ide H and Adachi M. Vascular endothelial growth factor expression by activated synovial leukocytes in rheumatoid arthritis: critical involvement of the interaction with synovial fibroblasts. *Arthritis Rheum*. 2001;44:2512-24.

62. Morales-Ruiz M, Fulton D, Sowa G, Languino LR, Fujio Y, Walsh K and Sessa WC. Vascular endothelial growth factor-stimulated actin reorganization and migration of endothelial cells is regulated via the serine/threonine kinase Akt. *Circ Res*. 2000;86:892-6.

63. Benjamin LE, Hemo I and Keshet E. A plasticity window for blood vessel remodelling is defined by pericyte coverage of the preformed endothelial network and is regulated by PDGF-B and VEGF. *Development*. 1998;125:1591-1598.

64. Abulafia O and Sherer DM. Angiogenesis of the ovary. *Am J Obstet Gynecol*. 2000;182:240-6.

65. Knighton DR, Silver IA and Hunt TK. Regulation of wound-healing angiogenesis-effect of oxygen gradients and inspired oxygen concentration. *Surgery*. 1981;90:262-70.

66. Folkman J. Tumor angiogenesis: therapeutic implications. *N Engl J Med*. 1971;285:1182-6.

67. Taylor PC and Sivakumar B. Hypoxia and angiogenesis in rheumatoid arthritis. *Current opinion in rheumatology*. 2005;17:293-8.

68. Moulton KS. Angiogenesis in atherosclerosis: gathering evidence beyond speculation. *Current opinion in lipidology*. 2006;17:548-55.

69. Heidenreich R, Rocken M and Ghoreschi K. Angiogenesis drives psoriasis pathogenesis. *Int J Exp Pathol*. 2009;90:232-48.

70. Crawford TN, Alfaro DV, 3rd, Kerrison JB and Jablon EP. Diabetic retinopathy and angiogenesis. *Current diabetes reviews*. 2009;5:8-13.

71. Das A and McGuire PG. Retinal and choroidal angiogenesis: pathophysiology and strategies for inhibition. *Progress in retinal and eye research*. 2003;22:721-48.

72. Hanahan D and Folkman J. Patterns and emerging mechanisms of the angiogenic switch during tumorigenesis. *Cell*. 1996;86:353-64.

73. Liang D, Chang JR, Chin AJ, Smith A, Kelly C, Weinberg ES and Ge RW. The role of vascular endothelial growth factor (VEGF) in vasculogenesis, angiogenesis, and hematopoiesis in zebrafish development. *Mechanisms of development*. 2001;108:29-43.

74. Shing Y, Folkman J, Sullivan R, Butterfield C, Murray J and Klagsbrun M. Heparin affinity: purification of a tumor-derived capillary endothelial cell growth factor. *Science*. 1984;223:1296-9.

75. Battegay EJ, Rupp J, Iruela-Arispe L, Sage EH and Pech M. PDGF-BB modulates endothelial proliferation and angiogenesis in vitro via PDGF beta-receptors. *J Cell Biol*. 1994;125:917-28.

76. Bussolino F, Di Renzo MF, Ziche M, Bocchietto E, Olivero M, Naldini L, Gaudino G, Tamagnone L, Coffer A and Comoglio PM. Hepatocyte growth factor is a potent angiogenic factor which stimulates endothelial cell motility and growth. *J Cell Biol*. 1992;119:629-41.

77. van Meeteren LA, Goumans MJ and ten Dijke P. TGF-beta receptor signaling pathways in angiogenesis; emerging targets for anti-angiogenesis therapy. *Curr Pharm Biotechnol*. 2011;12:2108-20.

78. Fukumura D, Gohongi T, Kadambi A, Izumi Y, Ang J, Yun CO, Buerk DG, Huang PL and Jain RK. Predominant role of endothelial nitric oxide synthase in vascular endothelial growth factor-induced angiogenesis and vascular permeability. *Proc Natl Acad Sci U S A*. 2001;98:2604-9.

79. Liao D and Johnson RS. Hypoxia: a key regulator of angiogenesis in cancer. *Cancer Metastasis Rev*. 2007;26:281-90.

80. Grimm C and Willmann G. Hypoxia in the eye: a two-sided coin. *High altitude medicine & biology*. 2012;13:169-75.

81. Good DJ, Polverini PJ, Rastinejad F, Lebeau MM, Lemons RS, Frazier WA and Bouck NP. A Tumor Suppressor-Dependent Inhibitor of Angiogenesis Is Immunologically and Functionally Indistinguishable from a Fragment of Thrombospondin. *Proceedings of the National Academy of Sciences of the United States of America*. 1990;87:6624-6628.

82. Neufeld G, Sabag AD, Rabinovicz N and Kessler O. Semaphorins in Angiogenesis and Tumor Progression. *Cold Spring Harbor perspectives in medicine*. 2012;2.

83. Hippenstiel S, Krull M, Ikemann A, Risau W, Clauss M and Suttorp N. VEGF induces hyperpermeability by a direct action on endothelial cells. *The American journal of physiology*. 1998;274:L678-84.

84. Namiki A, Brogi E, Kearney M, Kim EA, Wu T, Couffinhal T, Varticovski L and Isner JM. Hypoxia induces vascular endothelial growth factor in cultured human endothelial cells. *J Biol Chem*. 1995;270:31189-95.

85. Sunderkotter C, Steinbrink K, Goebeler M, Bhardwaj R and Sorg C. Macrophages and angiogenesis. *J Leukoc Biol*. 1994;55:410-22.

86. Senger DR, Galli SJ, Dvorak AM, Perruzzi CA, Harvey VS and Dvorak HF. Tumor cells secrete a vascular permeability factor that promotes accumulation of ascites fluid. *Science*. 1983;219:983-5.

87. Stone J, Itin A, Alon T, Pe'er J, Gnessin H, Chan-Ling T and Keshet E. Development of retinal vasculature is mediated by hypoxia-induced vascular endothelial growth factor (VEGF) expression by neuroglia. *J Neurosci*. 1995;15:4738-47.

88. Schiera G, Proia P, Alberti C, Mineo M, Savettieri G and Di Liegro I. Neurons produce FGF2 and VEGF and secrete them at least in part by shedding extracellular vesicles. *Journal of cellular and molecular medicine*. 2007;11:1384-94.

89. Ferrara N, Winer J and Burton T. Aortic smooth muscle cells express and secrete vascular endothelial growth factor. *Growth factors*. 1991;5:141-8.

90. Gerhardt H, Golding M, Fruttiger M, Ruhrberg C, Lundkvist A, Abramsson A, Jeltsch M, Mitchell C, Alitalo K, Shima D and Betsholtz C. VEGF guides angiogenic sprouting utilizing endothelial tip cell filopodia. *J Cell Biol*. 2003;161:1163-77.

91. Cai J, Jiang WG, Ahmed A and Boulton M. Vascular endothelial growth factor-induced endothelial cell proliferation is regulated by interaction between VEGFR-2, SH-PTP1 and eNOS. *Microvasc Res*. 2006;71:20-31.

92. Gerber HP, McMurtrey A, Kowalski J, Yan M, Keyt BA, Dixit V and Ferrara N. Vascular endothelial growth factor regulates endothelial cell survival through the phosphatidylinositol 3'-kinase/Akt signal transduction pathway. Requirement for Flk-1/KDR activation. *J Biol Chem*. 1998;273:30336-43.

93. Shamloo A and Heilshorn SC. Matrix density mediates polarization and lumen formation of endothelial sprouts in VEGF gradients. *Lab Chip*. 2010;10:3061-3068.

94. Zeng GF, Taylor SM, McColm JR, Kappas NC, Kearney JB, Williams LH, Hartnett ME and Bautch VL. Orientation of endothelial cell division is regulated by VEGF signaling during blood vessel formation. *Blood*. 2007;109:1345-1352.

95. Kim I, Moon SO, Kim SH, Kim HJ, Koh YS and Koh GY. Vascular endothelial growth factor expression of intercellular adhesion molecule 1 (ICAM-1), vascular cell adhesion molecule 1 (VCAM-1), and E-selectin through nuclear factor-kappa B activation in endothelial cells. *J Biol Chem*. 2001;276:7614-20.

96. Melder RJ, Koenig GC, Witwer BP, Safabakhsh N, Munn LL and Jain RK. During angiogenesis, vascular endothelial growth factor and basic fibroblast growth factor regulate natural killer cell adhesion to tumor endothelium. *Nat Med*. 1996;2:992-7.

97. Seghezzi G, Patel S, Ren CJ, Gualandris A, Pintucci G, Robbins ES, Shapiro RL, Galloway AC, Rifkin DB and Mignatti P. Fibroblast growth factor-2 (FGF-2) induces vascular endothelial growth factor (VEGF) expression in the endothelial cells of forming capillaries: an autocrine mechanism contributing to angiogenesis. *J Cell Biol*. 1998;141:1659-73.

98. Shima DT, Kuroki M, Deutsch U, Ng YS, Adamis AP and DAmore PA. The mouse gene for vascular endothelial growth factor - Genomic structure, definition of the transcriptional unit, and characterization of transcriptional and post-transcriptional regulatory sequences. *Journal of Biological Chemistry*. 1996;271:3877-3883.

99. Park JE, Keller GA and Ferrara N. Vascular Endothelial Growth-Factor (Vegf) Isoforms - Differential Deposition into the Subepithelial Extracellular-Matrix and Bioactivity of Extracellular Matrix-Bound Vegf. *Mol Biol Cell*. 1993;4:1317-1326.

100. Gitay-Goren H, Halaban R and Neufeld G. Human melanoma cells but not normal melanocytes express vascular endothelial growth factor receptors. *Biochem Biophys Res Commun*. 1993;190:702-8.

101. Barleon B, Sozzani S, Zhou D, Weich HA, Mantovani A and Marme D. Migration of human monocytes in response to vascular endothelial growth factor (VEGF) is mediated via the VEGF receptor flt-1. *Blood*. 1996;87:3336-43.

102. Hao TF and Rockwell P. Signaling through the vascular endothelial growth factor receptor VEGFR-2 protects hippocampal neurons from mitochondrial dysfunction and oxidative stress. *Free Radical Bio Med*. 2013;63:421-431.

103. Katoh O, Tauchi H, Kawaishi K, Kimura A and Satow Y. Expression of the Vascular Endothelial Growth-Factor (Vegf) Receptor Gene, Kdr, in Hematopoietic-Cells and Inhibitory Effect of Vegf on Apoptotic Cell-Death Caused by Ionizing-Radiation. *Cancer research*. 1995;55:5687-5692.

104. Charnock-Jones DS, Sharkey AM, Boocock CA, Ahmed A, Plevin R, Ferrara N and Smith SK. Vascular endothelial growth factor receptor localization and activation in human trophoblast and choriocarcinoma cells. *Biol Reprod*. 1994;51:524-30.

105. Rahimi N. VEGFR-1 and VEGFR-2: two non-identical twins with a unique physiognomy. *Front Biosci*. 2006;11:818-29.

106. Doanes AM, Hegland DD, Sethi R, Kovesdi I, Bruder JT and Finkel T. VEGF stimulates MAPK through a pathway that is unique for receptor tyrosine kinases. *Biochem Biophys Res Commun*. 1999;255:545-8.

107. Hood JD, Meininger CJ, Ziche M and Granger HJ. VEGF upregulates ecNOS message, protein, and NO production in human endothelial cells. *The American journal of physiology*. 1998;274:H1054-8.

108. Bruns AF, Herbert SP, Odell AF, Jopling HM, Hooper NM, Zachary IC, Walker JH and Ponnambalam S. Ligand-stimulated VEGFR2 signaling is regulated by co-ordinated trafficking and proteolysis. *Traffic*. 2010;11:161-74.

109. Lorquet S, Berndt S, Blacher S, Gengoux E, Peulen O, Maquoi E, Noel A, Foidart JM, Munaut C and Pequeux C. Soluble forms of VEGF receptor-1 and -2 promote vascular maturation via mural cell recruitment. *Faseb Journal*. 2010;24:3782-3795.

110. Fischer C, Mazzone M, Jonckx B and Carmeliet P. FLT1 and its ligands VEGFB and PlGF: drug targets for anti-angiogenic therapy? *Nature Reviews Cancer*. 2008;8:942-956.

111. Jussila L and Alitalo K. Vascular growth factors and lymphangiogenesis. *Physiological reviews*. 2002;82:673-700.

112. Koch S, Tugues S, Li XJ, Gualandi L and Claesson-Welsh L. Signal transduction by vascular endothelial growth factor receptors. *Biochemical Journal*. 2011;437:169-183.

113. Flamme I and Risau W. Induction of vasculogenesis and hematopoiesis in vitro. *Development*. 1992;116:435-9.

114. Pepper MS, Ferrara N, Orci L and Montesano R. Potent synergism between vascular endothelial growth factor and basic fibroblast growth factor in the induction of angiogenesis in vitro. *Biochem Biophys Res Commun*. 1992;189:824-31.

115. Larsson H, Klint P, Landgren E and Claesson-Welsh L. Fibroblast growth factor receptor-1-mediated endothelial cell proliferation is dependent on the Src homology (SH) 2/SH3 domain-containing adaptor protein Crk. *J Biol Chem*. 1999;274:25726-34.

116. Pintucci G, Moscatelli D, Saponara F, Biernacki PR, Baumann FG, Bizekis C, Galloway AC, Basilico C and Mignatti P. Lack of ERK activation and cell migration in FGF-2-deficient endothelial cells. *FASEB J*. 2002;16:598-600.

117. Laird M, Woad KJ, Hunter MG, Mann GE and Robinson RS. Fibroblast growth factor 2 induces the precocious development of endothelial cell networks in bovine luteinising follicular cells. *Reprod Fertil Dev*. 2013;25:372-86.

118. Mignatti P, Morimoto T and Rifkin DB. Basic fibroblast growth factor, a protein devoid of secretory signal sequence, is released by cells via a pathway independent of the endoplasmic reticulum-Golgi complex. *Journal of cellular physiology*. 1992;151:81-93.

119. Vlodavsky I, Bar-Shavit R, Ishai-Michaeli R, Bashkin P and Fuks Z. Extracellular sequestration and release of fibroblast growth factor: a regulatory mechanism? *Trends in biochemical sciences*. 1991;16:268-71.

120. Mundhenke C, Meyer K, Drew S and Friedl A. Heparan sulfate proteoglycans as regulators of fibroblast growth factor-2 receptor binding in breast carcinomas. *American Journal of Pathology*. 2002;160:185-194.

121. Haugsten EM, Wiedlocha A, Olsnes S and Wesche J. Roles of Fibroblast Growth Factor Receptors in Carcinogenesis. *Mol Cancer Res*. 2010;8:1439-1452.

122. Cross MJ, Hodgkin MN, Roberts S, Landgren E, Wakelam MJ and Claesson-Welsh L. Tyrosine 766 in the fibroblast growth factor receptor-1 is required for FGF-stimulation of phospholipase C, phospholipase D, phospholipase A(2), phosphoinositide 3-kinase and cytoskeletal reorganisation in porcine aortic endothelial cells. *J Cell Sci*. 2000;113 (Pt 4):643-51.

123. Shi YH, Bingle L, Gong LH, Wang YX, Corke KP and Fang WG. Basic FGF augments hypoxia induced HIF-1-alpha expression and VEGF release in T47D breast cancer cells. *Pathology*. 2007;39:396-400.

124. Liu W, Parikh AA, Stoeltzing O, Fan F, McCarty MF, Wey J, Hicklin DJ and Ellis LM. Upregulation of neuropilin-1 by basic fibroblast growth factor enhances vascular smooth muscle cell migration in response to VEGF. *Cytokine*. 2005;32:206-12.

125. Tomanek RJ, Sandra A, Zheng W, Brock T, Bjercke RJ and Holifield JS. Vascular endothelial growth factor and basic fibroblast growth factor differentially modulate early postnatal coronary angiogenesis. *Circ Res*. 2001;88:1135-41.

126. Rosen EM, Zitnik RJ, Elias JA, Bhargava MM, Wines J and Goldberg ID. The interaction of HGF-SF with other cytokines in tumor invasion and angiogenesis. *EXS*. 1993;65:301-10.

127. Morishita R, Nakamura S, Nakamura Y, Aoki M, Moriguchi A, Kida I, Yo Y, Matsumoto K, Nakamura T, Higaki J and Ogihara T. Potential role of an endothelium-specific growth factor, hepatocyte growth factor, on endothelial damage in diabetes. *Diabetes*. 1997;46:138-42.

128. Nakamura Y, Morishita R, Higaki J, Kida I, Aoki M, Moriguchi A, Yamada K, Hayashi S, Yo Y, Matsumoto K and et al. Expression of local hepatocyte growth factor system in vascular tissues. *Biochem Biophys Res Commun*. 1995;215:483-8.

129. Rubin JS, Chan AM, Bottaro DP, Burgess WH, Taylor WG, Cech AC, Hirschfield DW, Wong J, Miki T, Finch PW and et al. A broad-spectrum human lung fibroblast-derived mitogen is a variant of hepatocyte growth factor. *Proc Natl Acad Sci U S A*. 1991;88:415-9.

130. Ohmichi H, Koshimizu U, Matsumoto K and Nakamura T. Hepatocyte growth factor (HGF) acts as a mesenchyme-derived morphogenic factor during fetal lung development. *Development*. 1998;125:1315-24.

131. Walker N, Kahamba T, Woudberg N, Goetsch K and Niesler C. Dose-dependent modulation of myogenesis by HGF: implications for c-Met expression and downstream signalling pathways. *Growth factors*. 2015:1-13.

132. Li JF, Duan HF, Wu CT, Zhang DJ, Deng Y, Yin HL, Han B, Gong HC, Wang HW and Wang YL. HGF accelerates wound healing by promoting the dedifferentiation of epidermal cells through beta1-integrin/ILK pathway. *BioMed research international*. 2013;2013:470418.

133. Rosen EM, Lamszus K, Laterra J, Polverini PJ, Rubin JS and Goldberg ID. HGF/SF in angiogenesis. *Ciba Foundation symposium*. 1997;212:215-26; discussion 227-9.

134. Naldini L, Vigna E, Narsimhan RP, Gaudino G, Zarnegar R, Michalopoulos GK and Comoglio PM. Hepatocyte growth factor (HGF) stimulates the tyrosine kinase activity of the receptor encoded by the proto-oncogene c-MET. *Oncogene*. 1991;6:501-4.

135. Cai W, Rook SL, Jiang ZY, Takahara N and Aiello LP. Mechanisms of hepatocyte growth factor-induced retinal endothelial cell migration and growth. *Invest Ophthalmol Vis Sci*. 2000;41:1885-93.

136. Nakagami H, Morishita R, Yamamoto K, Taniyama Y, Aoki M, Yamasaki K, Matsumoto K, Nakamura T, Kaneda Y and Ogihara T. Hepatocyte growth factor prevents endothelial cell death through inhibition of bax translocation from cytosol to mitochondrial membrane. *Diabetes*. 2002;51:2604-2611.

137. Sulpice E, Ding S, Muscatelli-Groux B, Berge M, Han ZC, Plouet J, Tobelem G and Merkulova-Rainon T. Cross-talk between the VEGF-A and HGF signalling pathways in endothelial cells. *Biology of the cell / under the auspices of the European Cell Biology Organization*. 2009;101:525-39.

138. Usatyuk PV, Fu PF, Mohan V, Epshtein Y, Jacobson JR, Gomez-Cambronero J, Wary KK, Bindokas V, Dudek SM, Salgia R, Garcia JGN and Natarajan V. Role of c-Met/Phosphatidylinositol 3-Kinase (PI3k)/Akt Signaling in Hepatocyte Growth Factor (HGF)- mediated Lamellipodia Formation, Reactive Oxygen Species (ROS) Generation, and Motility of Lung Endothelial Cells. *Journal of Biological Chemistry*. 2014;289:13476-13491.

139. Snyder GK and Sheafor BA. Red blood cells: Centerpiece in the evolution of the vertebrate circulatory system. *Am Zool*. 1999;39:189-198.

140. Caprara C, Thiersch M, Lange C, Joly S, Samardzija M and Grimm C. HIF1A is essential for the development of the intermediate plexus of the retinal vasculature. *Invest Ophthalmol Vis Sci*. 2011;52:2109-17.

141. Meininger CJ, Schelling ME and Granger HJ. Adenosine and hypoxia stimulate proliferation and migration of endothelial cells. *The American journal of physiology*. 1988;255:H554-62.

142. Phillips PG, Birnby LM and Narendran A. Hypoxia induces capillary network formation in cultured bovine pulmonary microvessel endothelial cells. *The American journal of physiology*. 1995;268:L789-800.

143. Tucci M, Hammerman SI, Furfaro S, Saukonnen JJ, Conca TJ and Farber HW. Distinct effect of hypoxia on endothelial cell proliferation and cycling. *The American journal of physiology*. 1997;272:C1700-8.

144. Tang N, Wang L, Esko J, Giordano FJ, Huang Y, Gerber HP, Ferrara N and Johnson RS. Loss of HIF-1alpha in endothelial cells disrupts a hypoxia-driven VEGF autocrine loop necessary for tumorigenesis. *Cancer Cell*. 2004;6:485-95.

145. Semenza GL. Hypoxia-inducible factor 1 (HIF-1) pathway. *Science's STKE : signal transduction knowledge environment*. 2007;2007:cm8.

146. Rahimi N. The ubiquitin-proteasome system meets angiogenesis. *Mol Cancer Ther*. 2012;11:538-48.

147. Semenza GL. Regulation of erythropoietin production. New insights into molecular mechanisms of oxygen homeostasis. *Hematology/oncology clinics of North America*. 1994;8:863-84.

148. Oh H, Takagi H, Suzuma K, Otani A, Matsumura M and Honda Y. Hypoxia and vascular endothelial growth factor selectively up-regulate angiopoietin-2 in bovine microvascular endothelial cells. *J Biol Chem*. 1999;274:15732-9.

149. Kourembanas S, Hannan RL and Faller DV. Oxygen tension regulates the expression of the platelet-derived growth factor-B chain gene in human endothelial cells. *J Clin Invest*. 1990;86:670-4.

150. Ben-Yosef Y, Lahat N, Shapiro S, Bitterman H and Miller A. Regulation of endothelial matrix metalloproteinase-2 by hypoxia/reoxygenation. *Circ Res*. 2002;90:784-91.

151. Ulyatt C, Walker J and Ponnambalam S. Hypoxia differentially regulates VEGFR1 and VEGFR2 levels and alters intracellular signaling and cell migration in endothelial cells. *Biochem Biophys Res Commun*. 2011;404:774-9.

152. Ikeda T, Sun L, Tsuruoka N, Ishigaki Y, Yoshitomi Y, Yoshitake Y and Yonekura H. Hypoxia down-regulates sFlt-1 (sVEGFR-1) expression in human microvascular endothelial cells by a mechanism involving mRNA alternative processing. *The Biochemical journal*. 2011;436:399-407.

153. Palmer LA, Semenza GL, Stoler MH and Johns RA. Hypoxia induces type II NOS gene expression in pulmonary artery endothelial cells via HIF-1. *The American journal of physiology*. 1998;274:L212-9.

154. Waltenberger J, Mayr U, Pentz S and Hombach V. Functional upregulation of the vascular endothelial growth factor receptor KDR by hypoxia. *Circulation*. 1996;94:1647-54.

155. Levy NS, Chung S, Furneaux H and Levy AP. Hypoxic stabilization of vascular endothelial growth factor mRNA by the RNA-binding protein HuR. *J Biol Chem*. 1998;273:6417-23.

156. Stuehr DJ, Kwon NS, Gross SS, Thiel BA, Levi R and Nathan CF. Synthesis of nitrogen oxides from L-arginine by macrophage cytosol: requirement for inducible and constitutive components. *Biochem Biophys Res Commun*. 1989;161:420-6.

157. Palmer RM, Ferrige AG and Moncada S. Nitric oxide release accounts for the biological activity of endothelium-derived relaxing factor. *Nature*. 1987;327:524-6.

158. Marletta MA, Yoon PS, Iyengar R, Leaf CD and Wishnok JS. Macrophage oxidation of L-arginine to nitrite and nitrate: nitric oxide is an intermediate. *Biochemistry*. 1988;27:8706-11.

159. Aymerich MS, Bengoechea-Alonso MT, Lopez-Zabalza MJ, Santiago E and Lopez-Moratalla N. Inducible nitric oxide synthase (iNOS) expression in human monocytes triggered by beta-endorphin through an increase in cAMP. *Biochem Biophys Res Commun*. 1998;245:717-21.

160. Tsukahara Y, Morisaki T, Kojima M, Uchiyama A and Tanaka M. iNOS expression by activated neutrophils from patients with sepsis. *ANZ journal of surgery*. 2001;71:15-20.

161. Bredt DS and Snyder SH. Isolation of nitric oxide synthetase, a calmodulin-requiring enzyme. *Proc Natl Acad Sci U S A*. 1990;87:682-5.

162. Knowles RG, Palacios M, Palmer RM and Moncada S. Formation of nitric oxide from L-arginine in the central nervous system: a transduction mechanism for stimulation of the soluble guanylate cyclase. *Proc Natl Acad Sci U S A*. 1989;86:5159-62.

163. Leone AM, Palmer RM, Knowles RG, Francis PL, Ashton DS and Moncada S. Constitutive and inducible nitric oxide synthases incorporate molecular oxygen into both nitric oxide and citrulline. *J Biol Chem*. 1991;266:23790-5.

164. Nakane M, Schmidt HH, Pollock JS, Forstermann U and Murad F. Cloned human brain nitric oxide synthase is highly expressed in skeletal muscle. *FEBS letters*. 1993;316:175-80.

165. Bellefontaine N, Hanchate NK, Parkash J, Campagne C, de Seranno S, Clasadonte J, d'Anglemont de Tassigny X and Prevot V. Nitric oxide as key mediator of neuron-to-neuron and endothelia-to-glia communication involved in the neuroendocrine control of reproduction. *Neuroendocrinology*. 2011;93:74-89.

166. Green SJ, Scheller LF, Marletta MA, Seguin MC, Klotz FW, Slayter M, Nelson BJ and Nacy CA. Nitric oxide: cytokine-regulation of nitric oxide in host resistance to intracellular pathogens. *Immunology letters*. 1994;43:87-94.

167. Lowenstein CJ and Padalko E. iNOS (NOS2) at a glance. *J Cell Sci*. 2004;117:2865-7.

168. Sessa WC, Barber CM and Lynch KR. Mutation of N-myristoylation site converts endothelial cell nitric oxide synthase from a membrane to a cytosolic protein. *Circ Res*. 1993;72:921-4.

169. Furchgott RF and Zawadzki JV. The obligatory role of endothelial cells in the relaxation of arterial smooth muscle by acetylcholine. *Nature*. 1980;288:373-6.

170. Palmer RM, Ashton DS and Moncada S. Vascular endothelial cells synthesize nitric oxide from L-arginine. *Nature*. 1988;333:664-6.

171. Lee PC, Salyapongse AN, Bragdon GA, Shears LL, 2nd, Watkins SC, Edington HD and Billiar TR. Impaired wound healing and angiogenesis in eNOS-deficient mice. *The American journal of physiology*. 1999;277:H1600-8.

172. Murohara T, Witzenbichler B, Spyridopoulos I, Asahara T, Ding B, Sullivan A, Losordo DW and Isner JM. Role of endothelial nitric oxide synthase in endothelial cell migration. *Arterioscler Thromb Vasc Biol*. 1999;19:1156-61.

173. Ziche M, Parenti A, Ledda F, Dell'Era P, Granger HJ, Maggi CA and Presta M. Nitric oxide promotes proliferation and plasminogen activator production by coronary venular endothelium through endogenous bFGF. *Circ Res*. 1997;80:845-52.

174. Dimmeler S and Zeiher AM. Nitric oxide-an endothelial cell survival factor. *Cell death and differentiation*. 1999;6:964-8.

175. Dimmeler S, Hermann C, Galle J and Zeiher AM. Upregulation of superoxide dismutase and nitric oxide synthase mediates the apoptosis-suppressive effects of shear stress on endothelial cells. *Arterioscl Throm Vas*. 1999;19:656-664.

176. Morbidelli L, Chang CH, Douglas JG, Granger HJ, Ledda F and Ziche M. Nitric oxide mediates mitogenic effect of VEGF on coronary venular endothelium. *The American journal of physiology*. 1996;270:H411-5.

177. Kroll J and Waltenberger J. VEGF-A induces expression of eNOS and iNOS in endothelial cells via VEGF receptor-2 (KDR). *Biochem Biophys Res Commun*. 1998;252:743-6.

178. Mata-Greenwood E, Liao WX, Zheng J and Chen DB. Differential activation of multiple signalling pathways dictates eNOS upregulation by FGF2 but not VEGF in placental artery endothelial cells. *Placenta*. 2008;29:708-17.

179. Mcquillan LP, Leung GK, Marsden PA, Kostyk SK and Kourembanas S. Hypoxia Inhibits Expression of Enos Via Transcriptional and Posttranscriptional Mechanisms. *Am J Physiol-Heart C*. 1994;267:H1921-H1927.

180. Fish JE, Yan MS, Matouk CC, St Bernard R, Ho JJD, Gavryushova A, Srivastava D and Marsden PA. Hypoxic repression of endothelial nitric-oxide synthase transcription is coupled with eviction of promoter histones. (vol 285, pg 810, 2010). *Journal of Biological Chemistry*. 2010;285:11754-11754.

181. Min J, Jin YM, Moon JS, Sung MS, Jo SA and Jo I. Hypoxia-induced endothelial NO synthase gene transcriptional activation is mediated through the tax-responsive element in endothelial cells. *Hypertension*. 2006;47:1189-1196.

182. Dulak J, Jozkowicz A, Dembinska-Kiec A, Guevara I, Zdzienicka A, Zmudzinska-Grochot D, Florek I, Wojtowicz A, Szuba A and Cooke JP. Nitric oxide induces the synthesis of vascular endothelial growth factor by rat vascular smooth muscle cells. *Arterioscler Thromb Vasc Biol*. 2000;20:659-66.

183. Napoli C, de Nigris F, Williams-Ignarro S, Pignalosa O, Sica V and Ignarro LJ. Nitric oxide and atherosclerosis: an update. *Nitric oxide : biology and chemistry / official journal of the Nitric Oxide Society*. 2006;15:265-79.

184. Hermann M, Flammer A and Luscher TF. Nitric oxide in hypertension. *Journal of clinical hypertension*. 2006;8:17-29.

185. Barrachina MD, Panes J and Esplugues JV. Role of nitric oxide in gastrointestinal inflammatory and ulcerative diseases: Perspective for drugs development. *Curr Pharm Design*. 2001;7:31-48.

186. Yan GJ, You B, Chen SP, Liao JK and Sun JX. Tumor necrosis factor-alpha downregulates endothelial nitric oxide synthase mRNA stability via translation elongation factor 1-alpha 1. *Circulation research*. 2008;103:591-597.

187. Anderson HDI, Rahmutula D and Gardner DG. Tumor necrosis factor-alpha inhibits endothelial nitric-oxide synthase gene promoter activity in bovine aortic endothelial cells. *Journal of Biological Chemistry*. 2004;279:963-969.

188. Kuruvilla L and Kartha CC. Treatment with TNF-alpha or bacterial lipopolysaccharide attenuates endocardial endothelial cell-mediated stimulation of cardiac fibroblasts. *J Biomed Sci*. 2009;16.

189. Radomski MW, Palmer RMJ and Moncada S. Modulation of Platelet-Aggregation by an L-Arginine Nitric-Oxide Pathway. *Trends in Pharmacological Sciences*. 1991;12:87-88.

190. Bir SC, Xiong Y, Kevil CG and Luo JC. Emerging role of PKA/eNOS pathway in therapeutic angiogenesis for ischaemic tissue diseases. *Cardiovascular Research*. 2012;95:7-18.

191. Lawler JW, Slayter HS and Coligan JE. Isolation and characterization of a high molecular weight glycoprotein from human blood platelets. *J Biol Chem*. 1978;253:8609-16.

192. Mosher DF, Doyle MJ and Jaffe EA. Synthesis and secretion of thrombospondin by cultured human endothelial cells. *J Cell Biol*. 1982;93:343-8.

193. Iruela-Arispe ML, Bornstein P and Sage H. Thrombospondin exerts an antiangiogenic effect on cord formation by endothelial cells in vitro. *Proc Natl Acad Sci U S A*. 1991;88:5026-30.

194. Taraboletti G, Roberts D, Liotta LA and Giavazzi R. Platelet thrombospondin modulates endothelial cell adhesion, motility, and growth: a potential angiogenesis regulatory factor. *J Cell Biol*. 1990;111:765-72.

195. Dawson DW, Pearce SF, Zhong R, Silverstein RL, Frazier WA and Bouck NP. CD36 mediates the In vitro inhibitory effects of thrombospondin-1 on endothelial cells. *J Cell Biol*. 1997;138:707-17.

196. Jimenez B, Volpert OV, Crawford SE, Febbraio M, Silverstein RL and Bouck N. Signals leading to apoptosis-dependent inhibition of neovascularization by thrombospondin-1. *Nat Med*. 2000;6:41-8.

197. Guo N, Krutzsch HC, Inman JK and Roberts DD. Thrombospondin 1 and type I repeat peptides of thrombospondin 1 specifically induce apoptosis of endothelial cells. *Cancer Res*. 1997;57:1735-42.

198. Rodriguez-Manzaneque JC, Lane TF, Ortega MA, Hynes RO, Lawler J and Iruela-Arispe ML. Thrombospondin-1 suppresses spontaneous tumor growth and inhibits activation of matrix metalloproteinase-9 and mobilization of vascular endothelial growth factor. *Proceedings of the National Academy of Sciences of the United States of America* . 2001;98:12485-12490.

199. Gupta K, Gupta P, Wild R, Ramakrishnan S and Hebbel RP. Binding and displacement of vascular endothelial growth factor (VEGF) by thrombospondin: effect on human microvascular endothelial cell proliferation and angiogenesis. *Angiogenesis*. 1999;3:147-58.

200. Margosio B, Marchetti D, Vergani V, Giavazzi R, Rusnati M, Presta M and Taraboletti G. Thrombospondin 1 as a scavenger for matrix-associated fibroblast growth factor 2. *Blood*. 2003;102:4399-406.

201. Lamszus K, Joseph A, Jin L, Yao Y, Chowdhury S, Fuchs A, Polverini PJ, Goldberg ID and Rosen EM. Scatter factor binds to thrombospondin and other extracellular matrix components. *Am J Pathol*. 1996;149:805-19.

202. Isenberg JS, Ridnour LA, Dimitry J, Frazier WA, Wink DA and Roberts DD. CD47 is necessary for inhibition of nitric oxide-stimulated vascular cell responses by thrombospondin-1. *J Biol Chem*. 2006;281:26069-80.

203. Zhang X and Lawler J. Thrombospondin-based antiangiogenic therapy. *Microvasc Res*. 2007;74:90-9.

204. Ebbinghaus S, Hussain M, Tannir N, Gordon M, Desai AA, Knight RA, Humerickhouse RA, Qian J, Gordon GB and Figlin R. Phase 2 study of ABT-510 in patients with previously untreated advanced renal cell carcinoma. *Clin Cancer Res*. 2007;13:6689-95.

205. Chappell JC, Taylor SM, Ferrara N and Bautch VL. Local guidance of emerging vessel sprouts requires soluble Flt-1. *Dev Cell*. 2009;17:377-86.

206. Suchting S, Freitas C, le Noble F, Benedito R, Breant C, Duarte A and Eichmann A. The Notch ligand Delta-like 4 negatively regulates endothelial tip cell formation and vessel branching. *Proc Natl Acad Sci U S A*. 2007;104:3225-30.

207. Siekmann AF and Lawson ND. Notch signalling limits angiogenic cell behaviour in developing zebrafish arteries. *Nature*. 2007;445:781-784.

208. Hellstrom M, Phng LK, Hofmann JJ, Wallgard E, Coultas L, Lindblom P, Alva J, Nilsson AK, Karlsson L, Gaiano N, Yoon K, Rossant J, Iruela-Arispe ML, Kalen M, Gerhardt H and Betsholtz C. Dll4 signalling through Notch1 regulates formation of tip cells during angiogenesis. *Nature*. 2007;445:776-80.

209. Taylor KL, Henderson AM and Hughes CC. Notch activation during endothelial cell network formation in vitro targets the basic HLH transcription factor HESR-1 and downregulates VEGFR-2/KDR expression. *Microvasc Res*. 2002;64:372-83.

210. Harrington LS, Sainson RC, Williams CK, Taylor JM, Shi W, Li JL and Harris AL. Regulation of multiple angiogenic pathways by Dll4 and Notch in human umbilical vein endothelial cells. *Microvasc Res*. 2008;75:144-54.

211. Benedito R, Roca C, Sorensen I, Adams S, Gossler A, Fruttiger M and Adams RH. The Notch Ligands Dll4 and Jagged1 Have Opposing Effects on Angiogenesis. *Cell*. 2009;137:1124-1135.

212. Dimmeler S, Haendeler J, Rippmann V, Nehls M and Zeiher AM. Shear stress inhibits apoptosis of human endothelial cells. *FEBS letters*. 1996;399:71-4.

213. Blanco R and Gerhardt H. VEGF and Notch in tip and stalk cell selection. *Cold Spring Harb Perspect Med*. 2013;3:a006569.

214. Kamei M, Saunders WB, Bayless KJ, Dye L, Davis GE and Weinstein BM. Endothelial tubes assemble from intracellular vacuoles in vivo. *Nature*. 2006;442:453-6.

215. Davis GE and Camarillo CW. An alpha 2 beta 1 integrin-dependent pinocytic mechanism involving intracellular vacuole formation and coalescence regulates capillary lumen and tube formation in three-dimensional collagen matrix. *Experimental Cell Research*. 1996;224:39-51.

216. Strilic B, Kucera T, Eglinger J, Hughes MR, McNagny KM, Tsukita S, Dejana E, Ferrara N and Lammert E. The molecular basis of vascular lumen formation in the developing mouse aorta. *Dev Cell*. 2009;17:505-15.

217. Strilic B, Eglinger J, Krieg M, Zeeb M, Axnick J, Babal P, Muller DJ and Lammert E. Electrostatic Cell-Surface Repulsion Initiates Lumen Formation in Developing Blood Vessels. *Current Biology*. 2010;20:2003-2009.

218. Tung JJ, Tattersall IW and Kitajewski J. Tips, stalks, tubes: notch-mediated cell fate determination and mechanisms of tubulogenesis during angiogenesis. *Cold Spring Harb Perspect Med*. 2012;2:a006601.

219. Bjarnegard M, Enge M, Norlin J, Gustafsdottir S, Fredriksson S, Abramsson A, Takemoto M, Gustafsson E, Fassler R and Betsholtz C. Endothelium-specific ablation of PDGFB leads to pericyte loss and glomerular, cardiac and placental abnormalities. *Development*. 2004;131:1847-57.

220. Hellstrom M, Kalen M, Lindahl P, Abramsson A and Betsholtz C. Role of PDGF-B and PDGFR-beta in recruitment of vascular smooth muscle cells and pericytes during embryonic blood vessel formation in the mouse. *Development*. 1999;126:3047-3055.

221. Dumont DJ, Yamaguchi TP, Conlon RA, Rossant J and Breitman ML. tek, a novel tyrosine kinase gene located on mouse chromosome 4, is expressed in endothelial cells and their presumptive precursors. *Oncogene*. 1992;7:1471-80.

222. Adamcic U, Yurkiewich A and Coomber BL. Differential Expression of Tie2 Receptor and VEGFR2 by Endothelial Clones Derived from Isolated Bovine Mononuclear Cells. *PloS one*. 2012;7.

223. Patel AS, Smith A, Nucera S, Biziato D, Saha P, Attia RQ, Humphries J, Mattock K, Grover SP, Lyons OT, Guidotti LG, Siow R, Ivetic A, Egginton S, Waltham M, Naldini L, De Palma M and Modarai B. TIE2-expressing monocytes/macrophages regulate revascularization of the ischemic limb. *EMBO Mol Med*. 2013;5:858-69.

224. Iwama A, Hamaguchi I, Hashiyama M, Murayama Y, Yasunaga K and Suda T. Molecular cloning and characterization of mouse TIE and TEK receptor tyrosine kinase genes and their expression in hematopoietic stem cells. *Biochem Biophys Res Commun*. 1993;195:301-9.

225. Li JJ, Huang YQ, Basch R and Karpatkin S. Thrombin induces the release of angiopoietin-1 from platelets. *Thromb Haemost*. 2001;85:204-6.

226. Sundberg C, Kowanetz M, Brown LF, Detmar M and Dvorak HF. Stable expression of angiopoietin-1 and other markers by cultured pericytes: phenotypic similarities to a subpopulation of cells in maturing vessels during later stages of angiogenesis in vivo. *Lab Invest*. 2002;82:387-401.

227. Ju R, Zhuang ZW, Zhang JS, Lanahan AA, Kyriakides T, Sessa WC and Simons M. Angiopoietin-2 Secretion by Endothelial Cell Exosomes REGULATION BY THE PHOSPHATIDYLINOSITOL 3-KINASE (PI3K)/Akt/ENDOTHELIAL NITRIC OXIDE SYNTHASE (eNOS) AND SYNDECAN-4/SYNTENIN PATHWAYS. *Journal of Biological Chemistry*. 2014;289:510-519.

228. Maisonpierre PC, Suri C, Jones PF, Bartunkova S, Wiegand S, Radziejewski C, Compton D, McClain J, Aldrich TH, Papadopoulos N, Daly TJ, Davis S, Sato TN and Yancopoulos GD. Angiopoietin-2, a natural antagonist for Tie2 that disrupts in vivo angiogenesis. *Science*. 1997;277:55-60.

229. Davis S, Aldrich TH, Jones PF, Acheson A, Compton DL, Jain V, Ryan TE, Bruno J, Radziejewski C, Maisonpierre PC and Yancopoulos GD. Isolation of Angiopoietin-1, a ligand for the TIE2 receptor, by secretion-trap expression cloning. *Cell*. 1996;87:1161-1169.

230. Wakui S, Yokoo K, Muto T, Suzuki Y, Takahashi H, Furusato M, Hano H, Endou H and Kanai Y. Localization of Ang-1, -2, Tie-2, and VEGF expression at endothelial-pericyte interdigitation in rat angiogenesis. *Lab Invest*. 2006;86:1172-84.

231. Hammes HP, Lin JH, Wagner P, Feng Y, vom Hagen F, Krzizok T, Renner O, Breier G, Brownlee M and Deutsch U. Angiopoietin-2 causes pericyte dropout in the normal retina - Evidence for involvement in diabetic retinopathy. *Diabetes*. 2004;53:1104-1110.

232. Pichiule P, Chavez JC and LaManna JC. Hypoxic regulation of angiopoietin-2 expression in endothelial cells. *J Biol Chem*. 2004;279:12171-80.

233. Kim I, Kim JH, Ryu YS, Liu M and Koh GY. Tumor necrosis factor-alpha upregulates angiopoietin-2 in human umbilical vein endothelial cells. *Biochem Biophys Res Commun*. 2000;269:361-5.

234. Lobov IB, Brooks PC and Lang RA. Angiopoietin-2 displays VEGF-dependent modulation of capillary structure and endothelial cell survival in vivo. *Proc Natl Acad Sci U S A*. 2002;99:11205-10.

235. Hanahan D. Signaling vascular morphogenesis and maintenance. *Science*. 1997;277:48-50.

236. Burri PH and Tarek MR. A novel mechanism of capillary growth in the rat pulmonary microcirculation. *The Anatomical record*. 1990;228:35-45.

237. Caduff JH, Fischer LC and Burri PH. Scanning electron microscope study of the developing microvasculature in the postnatal rat lung. *The Anatomical record*. 1986;216:154-64.

238. Burri PH, Hlushchuk R and Djonov V. Intussusceptive angiogenesis: its emergence, its characteristics, and its significance. *Dev Dyn*. 2004;231:474-88.

239. Djonov V, Schmid M, Tschanz SA and Burri PH. Intussusceptive angiogenesis - Its role in embryonic vascular network formation. *Circulation research*. 2000;86:286-292.

240. Adams RH and Alitalo K. Molecular regulation of angiogenesis and lymphangiogenesis. *Nature reviews Molecular cell biology*. 2007;8:464-78.

241. Crabb JW, Miyagi M, Gu X, Shadrach K, West KA, Sakaguchi H, Kamei M, Hasan A, Yan L, Rayborn ME, Salomon RG and Hollyfield JG. Drusen proteome analysis: an approach to the etiology of age-related macular degeneration. *Proc Natl Acad Sci U S A*. 2002;99:14682-7.

242. Johnson LV, Ozaki S, Staples MK, Erickson PA and Anderson DH. A potential role for immune complex pathogenesis in drusen formation. *Exp Eye Res*. 2000;70:441-9.

243. Nowak JZ. Age-related macular degeneration (AMD): pathogenesis and therapy. *Pharmacol Rep*. 2006;58:353-63.

244. Killingsworth MC, Sarks JP and Sarks SH. Macrophages related to Bruch's membrane in age-related macular degeneration. *Eye (Lond)*. 1990;4 (Pt 4):613-21.

245. Kijlstra A, La Heij E and Hendrikse F. Immunological factors in the pathogenesis and treatment of age-related macular degeneration. *Ocul Immunol Inflamm*. 2005;13:3-11.

246. McInnes IB and Schett G. The pathogenesis of rheumatoid arthritis. *N Engl J Med*. 2011;365:2205-19.

247. Paleolog EM. Angiogenesis in rheumatoid arthritis. *Arthritis Res*. 2002;4 Suppl 3:S81-90.

248. Brennan FM, Chantry D, Jackson A, Maini R and Feldmann M. Inhibitory effect of TNF alpha antibodies on synovial cell interleukin-1 production in rheumatoid arthritis. *Lancet*. 1989;2:244-7.

249. Hitchon C, Wong K, Ma G, Reed J, Lyttle D and El-Gabalawy H. Hypoxia-induced production of stromal cell-derived factor 1 (CXCL12) and vascular endothelial growth factor by synovial fibroblasts. *Arthritis Rheum*. 2002;46:2587-97.

250. Giatromanolaki A, Sivridis E, Maltezos E, Athanassou N, Papazoglou D, Gatter KC, Harris AL and Koukourakis MI. Upregulated hypoxia inducible factor-1alpha and -2alpha pathway in rheumatoid arthritis and osteoarthritis. *Arthritis Res Ther*. 2003;5:R193-201.

251. Angiogenesis in rheumatoid arthritis, http://www.goodhealth.jp/en/research/antiangiogenesis/angiogenesis-in-arthritis.html. (Access Date 1st October 2015).

252. Jang M, Kim SS and Lee J. Cancer cell metabolism: implications for therapeutic targets. *Exp Mol Med*. 2013;45.

253. Daughaday WH and Deuel TF. Tumor secretion of growth factors. *Endocrinol Metab Clin North Am*. 1991;20:539-63.

254. Hendriksen EM, Span PN, Schuuring J, Peters JP, Sweep FC, van der Kogel AJ and Bussink J. Angiogenesis, hypoxia and VEGF expression during tumour growth in a human xenograft tumour model. *Microvasc Res*. 2009;77:96-103.

255. Riabov V, Gudima A, Wang N, Mickley A, Orekhov A and Kzhyshkowska J. Role of tumor associated macrophages in tumor angiogenesis and lymphangiogenesis. *Front Physiol*. 2014;5:75.

256. Lewis CE, De Palma M and Naldini L. Tie2-expressing monocytes and tumor angiogenesis: regulation by hypoxia and angiopoietin-2. *Cancer Res*. 2007;67:8429-32.

257. Goel S, Wong AH and Jain RK. Vascular normalization as a therapeutic strategy for malignant and nonmalignant disease. *Cold Spring Harb Perspect Med*. 2012;2:a006486.

258. Dome B, Hendrix MJ, Paku S, Tovari J and Timar J. Alternative vascularization mechanisms in cancer: Pathology and therapeutic implications. *Am J Pathol*. 2007;170:1-15.

259. Bisht M, Dhasmana DC and Bist SS. Angiogenesis: Future of pharmacological modulation. *Indian J Pharmacol*. 2010;42:2-8.

260. Folkman J. Anti-angiogenesis: new concept for therapy of solid tumors. *Ann Surg*. 1972;175:409-16.

261. Pavco PA, Bouhana KS, Gallegos AM, Agrawal A, Blanchard KS, Grimm SL, Jensen KL, Andrews LE, Wincott FE, Pitot PA, Tressler RJ, Cushman C, Reynolds MA and Parry TJ. Antitumor and antimetastatic activity of ribozymes targeting the messenger RNA of vascular endothelial growth factor receptors. *Clin Cancer Res*. 2000;6:2094-103.

262. Oshika Y, Nakamura M, Tokunaga T, Ohnishi Y, Abe Y, Tsuchida T, Tomii Y, Kijima H, Yamazaki H, Ozeki Y, Tamaoki N and Ueyama Y. Ribozyme approach to downregulate vascular endothelial growth factor (VEGF) 189 expression in non-small cell lung cancer (NSCLC). *Eur J Cancer*. 2000;36:2390-2396.

263. Shih T and Lindley C. Bevacizumab: an angiogenesis inhibitor for the treatment of solid malignancies. *Clin Ther*. 2006;28:1779-802.

264. Fong AH and Lai TY. Long-term effectiveness of ranibizumab for age-related macular degeneration and diabetic macular edema. *Clin Interv Aging*. 2013;8:467-83.

265. Vinores SA. Pegaptanib in the treatment of wet, age-related macular degeneration. *Int J Nanomed*. 2006;1:263-268.

266. Holash J, Davis S, Papadopoulos N, Croll SD, Ho L, Russell M, Boland P, Leidich R, Hylton D, Burova E, Ioffe E, Huang T, Radziejewski C, Bailey K, Fandl JP, Daly T, Wiegand SJ, Yancopoulos GD and Rudge JS. VEGF-Trap: a VEGF blocker with potent antitumor effects. *Proc Natl Acad Sci U S A*. 2002;99:11393-8.

267. Mahasreshti PJ, Navarro JG, Kataram M, Wang MH, Carey D, Siegal GP, Barnes MN, Nettelbeck DM, Alvarez RD, Hemminki A and Curiel DT. Adenovirus-mediated soluble FLT-1 gene therapy for ovarian carcinoma. *Clin Cancer Res*. 2001;7:2057-66.

268. Sweeney P, Karashima T, Kim SJ, Kedar D, Mian B, Huang S, Baker C, Fan Z, Hicklin DJ, Pettaway CA and Dinney CP. Anti-vascular endothelial growth factor receptor 2 antibody reduces tumorigenicity and metastasis in orthotopic prostate cancer xenografts via induction of endothelial cell apoptosis and reduction of endothelial cell matrix metalloproteinase type 9 production. *Clin Cancer Res*. 2002;8:2714-24.

269. Wood JM, Bold G, Buchdunger E, Cozens R, Ferrari S, Frei J, Hofmann F, Mestan J, Mett H, O'Reilly T, Persohn E, Rosel J, Schnell C, Stover D, Theuer A, Towbin H, Wenger F, Woods-Cook K, Menrad A, Siemeister G, Schirner M, Thierauch KH, Schneider MR, Drevs J, Martiny-Baron G and Totzke F. PTK787/ZK 222584, a novel and potent inhibitor of vascular endothelial growth factor receptor tyrosine kinases, impairs vascular endothelial growth factor-induced responses and tumor growth after oral administration. *Cancer Res*. 2000;60:2178-89.

270. Heier JS, Boyer DS, Ciulla TA, Ferrone PJ, Jumper JM, Gentile RC, Kotlovker D, Chung CY, Kim RY and Group FS. Ranibizumab combined with verteporfin photodynamic therapy in neovascular age-related macular degeneration: year 1 results of the FOCUS Study. *Arch Ophthalmol*. 2006;124:1532-42.

271. Dings RP, Loren M, Heun H, McNiel E, Griffioen AW, Mayo KH and Griffin RJ. Scheduling of radiation with angiogenesis inhibitors anginex and Avastin improves therapeutic outcome via vessel normalization. *Clin Cancer Res*. 2007;13:3395-402.

272. Allen E, Walters IB and Hanahan D. Brivanib, a Dual FGF/VEGF Inhibitor, Is Active Both First and Second Line against Mouse Pancreatic Neuroendocrine Tumors Developing Adaptive/Evasive Resistance to VEGF Inhibition. *Clinical Cancer Research*. 2011;17:5299-5310.

273. Alessi P, Leali D, Camozzi M, Cantelmo A, Albini A and Presta M. Anti-FGF2 approaches as a strategy to compensate resistance to anti-VEGF therapy: long-pentraxin 3 as a novel antiangiogenic FGF2-antagonist. *Eur Cytokine Netw*. 2009;20:225-234.

274. Lieu C, Heymach J, Overman M, Tran H and Kopetz S. Beyond VEGF: Inhibition of the Fibroblast Growth Factor Pathway and Antiangiogenesis. *Clinical Cancer Research*. 2011;17:6130-6139.

275. Toomey DP, Murphy JF and Conlon KC. Cox-2, Vegf and Tumour Angiogenesis. *Surg-J R Coll Surg E*. 2009;7:174-180.

276. Noel A, Jost M, Lambert V, Lecomte J and Rakic JM. Anti-angiogenic therapy of exudative age-related macular degeneration: current progress and emerging concepts. *Trends in Molecular Medicine*. 2007;13:345-352.

277. Vezina C, Kudelski A and Sehgal SN. Rapamycin (AY-22,989), a new antifungal antibiotic. I. Taxonomy of the producing streptomycete and isolation of the active principle. *The Journal of antibiotics*. 1975;28:721-6.

278. Heitman J, Movva NR and Hall MN. Targets for cell cycle arrest by the immunosuppressant rapamycin in yeast. *Science*. 1991;253:905-9.

279. Brown EJ, Albers MW, Shin TB, Ichikawa K, Keith CT, Lane WS and Schreiber SL. A mammalian protein targeted by G1-arresting rapamycin-receptor complex. *Nature*. 1994;369:756-8.

280. Sabatini DM, Erdjument-Bromage H, Lui M, Tempst P and Snyder SH. RAFT1: a mammalian protein that binds to FKBP12 in a rapamycin-dependent fashion and is homologous to yeast TORs. *Cell*. 1994;78:35-43.

281. Laplante M and Sabatini DM. mTOR signaling at a glance. *J Cell Sci*. 2009;122:3589-94.

282. Laplante M and Sabatini DM. mTOR signaling in growth control and disease. *Cell*. 2012;149:274-93.

283. Watanabe R, Wei L and Huang J. mTOR signaling, function, novel inhibitors, and therapeutic targets. *J Nucl Med*. 2011;52:497-500.

284. Kim DH, Sarbassov DD, Ali SM, King JE, Latek RR, Erdjument-Bromage H, Tempst P and Sabatini DM. mTOR interacts with raptor to form a nutrient-sensitive complex that signals to the cell growth machinery. *Cell*. 2002;110:163-75.

285. Chiu MI, Katz H and Berlin V. Rapt1, a Mammalian Homolog of Yeast Tor, Interacts with the Fkbp12 Rapamycin Complex. *Proceedings of the National Academy of Sciences of the United States of America*. 1994;91:12574-12578.

286. Yip CK, Murata K, Walz T, Sabatini DM and Kang SA. Structure of the Human mTOR Complex I and Its Implications for Rapamycin Inhibition. *Molecular Cell*. 2010;38:768-774.

287. Gwinn DM, Shackelford DB, Egan DF, Mihaylova MM, Mery A, Vasquez DS, Turk BE and Shaw RJ. AMPK phosphorylation of raptor mediates a metabolic checkpoint. *Mol Cell*. 2008;30:214-26.

288. Noda T and Ohsumi Y. Tor, a phosphatidylinositol kinase homologue, controls autophagy in yeast. *J Biol Chem*. 1998;273:3963-6.

289. Ravikumar B, Vacher C, Berger Z, Davies JE, Luo S, Oroz LG, Scaravilli F, Easton DF, Duden R, O'Kane CJ and Rubinsztein DC. Inhibition of mTOR induces autophagy and reduces toxicity of polyglutamine expansions in fly and mouse models of Huntington disease. *Nat Genet*. 2004;36:585-95.

290. Malla R, Wang Y, Chan WK, Tiwari AK and Faridi JS. Genetic ablation of PRAS40 improves glucose homeostasis via linking the AKT and mTOR pathways. *Biochemical pharmacology*. 2015;96:65-75.

291. Houde VP, Brule S, Festuccia WT, Blanchard PG, Bellmann K, Deshaies Y and Marette A. Chronic Rapamycin Treatment Causes Glucose Intolerance and Hyperlipidemia by Upregulating Hepatic Gluconeogenesis and Impairing Lipid Deposition in Adipose Tissue. *Diabetes*. 2010;59:1338-1348.

292. Polak P, Cybulski N, Feige JN, Auwerx J, Ruegg MA and Hall MN. Adipose-specific knockout of raptor results in lean mice with enhanced mitochondrial respiration. *Cell Metab*. 2008;8:399-410.

293. Yoon MS, Zhang CB, Sun YT, Schoenherr CJ and Chen J. Mechanistic target of rapamycin controls homeostasis of adipogenesis. *J Lipid Res*. 2013;54:2166-2173.

294. Huang J and Manning BD. The TSC1-TSC2 complex: a molecular switchboard controlling cell growth. *The Biochemical journal*. 2008;412:179-90.

295. Mendoza MC, Er EE and Blenis J. The Ras-ERK and PI3K-mTOR pathways: cross-talk and compensation. *Trends in biochemical sciences*. 2011;36:320-8.

296. Lee DF, Kuo HP, Chen CT, Hsu JM, Chou CK, Wei Y, Sun HL, Li LY, Ping B, Huang WC, He X, Hung JY, Lai CC, Ding Q, Su JL, Yang JY, Sahin AA, Hortobagyi GN, Tsai FJ, Tsai CH and Hung MC. IKK beta suppression of TSC1 links inflammation and tumor angiogenesis via the mTOR pathway. *Cell*. 2007;130:440-55.

297. Mihaylova MM and Shaw RJ. The AMPK signalling pathway coordinates cell growth, autophagy and metabolism. *Nat Cell Biol*. 2011;13:1016-23.

298. Katiyar S, Liu E, Knutzen CA, Lang ES, Lombardo CR, Sankar S, Toth JI, Petroski MD, Ronai Z and Chiang GG. REDD1, an inhibitor of mTOR signalling, is regulated by the CUL4A-DDB1 ubiquitin ligase. *Embo Rep*. 2009;10:866-872.

299. Wullschleger S, Loewith R and Hall MN. TOR signaling in growth and metabolism. *Cell*. 2006;124:471-84.

300. Holz MK, Ballif BA, Gygi SP and Blenis J. mTOR and S6K1 mediate assembly of the translation preinitiation complex through dynamic protein interchange and ordered phosphorylation events. *Cell*. 2005;123:569-80.

301. Meyuhas O and Dreazen A. Ribosomal protein S6 kinase from TOP mRNAs to cell size. *Prog Mol Biol Transl Sci*. 2009;90:109-53.

302. Saitoh M, Pullen N, Brennan P, Cantrell D, Dennis PB and Thomas G. Regulation of an activated S6 kinase 1 variant reveals a novel mammalian target of rapamycin phosphorylation site. *J Biol Chem*. 2002;277:20104-12.

303. Pullen N, Dennis PB, Andjelkovic M, Dufner A, Kozma SC, Hemmings BA and Thomas G. Phosphorylation and activation of p70s6k by PDK1. *Science*. 1998;279:707-10.

304. Harrington LS, Findlay GM and Lamb RF. Restraining PI3K: mTOR signalling goes back to the membrane. *Trends in biochemical sciences*. 2005;30:35-42.

305. Harrington LS, Findlay GM, Gray A, Tolkacheva T, Wigfield S, Rebholz H, Barnett J, Leslie NR, Cheng S, Shepherd PR, Gout I, Downes CP and Lamb RF. The TSC1-2 tumor suppressor controls insulin-PI3K signaling via regulation of IRS proteins. *J Cell Biol*. 2004;166:213-23.

306. Shah OJ, Wang Z and Hunter T. Inappropriate activation of the TSC/Rheb/mTOR/S6K cassette induces IRS1/2 depletion, insulin resistance, and cell survival deficiencies. *Current biology : CB*. 2004;14:1650-6.

307. Raught B and Gingras AC. eIF4E activity is regulated at multiple levels. *Int J Biochem Cell Biol*. 1999;31:43-57.

308. Sarbassov DD, Ali SM, Kim DH, Guertin DA, Latek RR, Erdjument-Bromage H, Tempst P and Sabatini DM. Rictor, a novel binding partner of mTOR, defines a rapamycin-insensitive and raptor-independent pathway that regulates the cytoskeleton. *Current biology : CB*. 2004;14:1296-302.

309. Sarbassov DD, Ali SM, Sengupta S, Sheen JH, Hsu PP, Bagley AF, Markhard AL and Sabatini DM. Prolonged rapamycin treatment inhibits mTORC2 assembly and Akt/PKB. *Mol Cell*. 2006;22:159-68.

310. Shiota C, Woo JT, Lindner J, Shelton KD and Magnuson MA. Multiallelic disruption of the rictor gene in mice reveals that mTOR complex 2 is essential for fetal growth and viability. *Dev Cell*. 2006;11:583-9.

311. Gan X, Wang J, Su B and Wu D. Evidence for direct activation of mTORC2 kinase activity by phosphatidylinositol 3,4,5-trisphosphate. *J Biol Chem*. 2011;286:10998-1002.

312. Jacinto E, Loewith R, Schmidt A, Lin S, Ruegg MA, Hall A and Hall MN. Mammalian TOR complex 2 controls the actin cytoskeleton and is rapamycin insensitive. *Nat Cell Biol*. 2004;6:1122-8.

313. Masri J, Bernath A, Martin J, Jo OD, Vartanian R, Funk A and Gera J. mTORC2 activity is elevated in gliomas and promotes growth and cell motility via overexpression of rictor. *Cancer Res*. 2007;67:11712-20.

314. Garcia-Martinez JM and Alessi DR. mTOR complex 2 (mTORC2) controls hydrophobic motif phosphorylation and activation of serum- and glucocorticoid-induced protein kinase 1 (SGK1). *Biochemical Journal*. 2008;416:375-385.

315. Lawlor MA and Alessi DR. PKB/Akt: a key mediator of cell proliferation, survival and insulin responses? *J Cell Sci*. 2001;114:2903-10.

316. Somanath PR, Razorenova OV, Chen J and Byzova TV. Akt1 in endothelial cell and angiogenesis. *Cell Cycle*. 2006;5:512-8.

317. Song G, Ouyang G and Bao S. The activation of Akt/PKB signaling pathway and cell survival. *Journal of cellular and molecular medicine*. 2005;9:59-71.

318. Xue GD and Hemmings BA. PKB/Akt-Dependent Regulation of Cell Motility. *Jnci-J Natl Cancer I*. 2013;105:393-404.

319. Mazure NM, Chen EY, Laderoute KR and Giaccia AJ. Induction of vascular endothelial growth factor by hypoxia is modulated by a phosphatidylinositol 3-kinase/Akt signaling pathway in Ha-ras-transformed cells through a hypoxia inducible factor-1 transcriptional element. *Blood*. 1997;90:3322-31.

320. Jiang BH and Liu LZ. AKT signaling in regulating angiogenesis. *Curr Cancer Drug Targets*. 2008;8:19-26.

321. Karar J and Maity A. PI3K/AKT/mTOR Pathway in Angiogenesis. *Front Mol Neurosci*. 2011;4:51.

322. Yi T, Cho SG, Yi Z, Pang X, Rodriguez M, Wang Y, Sethi G, Aggarwal BB and Liu M. Thymoquinone inhibits tumor angiogenesis and tumor growth through suppressing AKT and extracellular signal-regulated kinase signaling pathways. *Mol Cancer Ther*. 2008;7:1789-96.

323. Chen J, Somanath PR, Razorenova O, Chen WS, Hay N, Bornstein P and Byzova TV. Akt1 regulates pathological angiogenesis, vascular maturation and permeability in vivo. *Nat Med*. 2005;11:1188-96.

324. Inoki K, Li Y, Zhu T, Wu J and Guan KL. TSC2 is phosphorylated and inhibited by Akt and suppresses mTOR signalling. *Nat Cell Biol*. 2002;4:648-57.

325. Fulton D, Gratton JP, McCabe TJ, Fontana J, Fujio Y, Walsh K, Franke TF, Papapetropoulos A and Sessa WC. Regulation of endothelium-derived nitric oxide production by the protein kinase Akt. *Nature*. 1999;399:597-601.

326. Rokutanda S, Fujita T, Kanatani N, Yoshida CA, Komori H, Liu WG, Mizuno A and Komori T. Akt regulates skeletal development through GSK3, mTOR, and FoxOs. *Dev Biol*. 2009;328:78-93.

327. Cross DA, Alessi DR, Cohen P, Andjelkovich M and Hemmings BA. Inhibition of glycogen synthase kinase-3 by insulin mediated by protein kinase B. *Nature*. 1995;378:785-9.

328. Guertin DA, Stevens DM, Thoreen CC, Burds AA, Kalaany NY, Moffat J, Brown M, Fitzgerald KJ and Sabatini DM. Ablation in mice of the mTORC components raptor, rictor, or mLST8 reveals that mTORC2 is required for signaling to Akt-FOXO and PKCalpha, but not S6K1. *Dev Cell*. 2006;11:859-71.

329. Jacinto E, Facchinetti V, Liu D, Soto N, Wei S, Jung SY, Huang Q, Qin J and Su B. SIN1/MIP1 maintains rictor-mTOR complex integrity and regulates Akt phosphorylation and substrate specificity. *Cell*. 2006;127:125-37.

330. Alessi DR, Andjelkovic M, Caudwell B, Cron P, Morrice N, Cohen P and Hemmings BA. Mechanism of activation of protein kinase B by insulin and IGF-1. *The EMBO journal*. 1996;15:6541-51.

331. Williams MR, Arthur JS, Balendran A, van der Kaay J, Poli V, Cohen P and Alessi DR. The role of 3-phosphoinositide-dependent protein kinase 1 in activating AGC kinases defined in embryonic stem cells. *Current biology : CB*. 2000;10:439-48.

332. Newton AC. Regulation of the ABC kinases by phosphorylation: protein kinase C as a paradigm. *The Biochemical journal*. 2003;370:361-71.

333. Ikenoue T, Inoki K, Yang Q, Zhou X and Guan KL. Essential function of TORC2 in PKC and Akt turn motif phosphorylation, maturation and signalling. *The EMBO journal*. 2008;27:1919-31.

334. Facchinetti V, Ouyang W, Wei H, Soto N, Lazorchak A, Gould C, Lowry C, Newton AC, Mao Y, Miao RQ, Sessa WC, Qin J, Zhang P, Su B and Jacinto E. The mammalian target of rapamycin complex 2 controls folding and stability of Akt and protein kinase C. *The EMBO journal*. 2008;27:1932-43.

335. Sarbassov DD, Guertin DA, Ali SM and Sabatini DM. Phosphorylation and regulation of Akt/PKB by the rictor-mTOR complex. *Science*. 2005;307:1098-101.

336. Partovian C and Simons M. Regulation of protein kinase B/Akt activity and Ser473 phosphorylation by protein kinase Calpha in endothelial cells. *Cell Signal*. 2004;16:951-7.

337. Xie X, Zhang D, Zhao B, Lu MK, You M, Condorelli G, Wang CY and Guan KL. IkappaB kinase epsilon and TANK-binding kinase 1 activate AKT by direct phosphorylation. *Proc Natl Acad Sci U S A*. 2011;108:6474-9.

338. Ou YH, Torres M, Ram R, Formstecher E, Roland C, Cheng T, Brekken R, Wurz R, Tasker A, Polverino T, Tan SL and White MA. TBK1 directly engages Akt/PKB survival signaling to support oncogenic transformation. *Mol Cell*. 2011;41:458-70.

339. Mahajan K, Coppola D, Challa S, Fang B, Chen YA, Zhu W, Lopez AS, Koomen J, Engelman RW, Rivera C, Muraoka-Cook RS, Cheng JQ, Schonbrunn E, Sebti SM, Earp HS and Mahajan NP. Ack1 mediated AKT/PKB tyrosine 176 phosphorylation regulates its activation. *PloS one*. 2010;5:e9646.

340. Oh WJ, Wu CC, Kim SJ, Facchinetti V, Julien LA, Finlan M, Roux PP, Su B and Jacinto E. mTORC2 can associate with ribosomes to promote cotranslational phosphorylation and stability of nascent Akt polypeptide. *The EMBO journal*. 2010;29:3939-51.

341. Lang F, Bohmer C, Palmada M, Seebohm G, Strutz-Seebohm N and Vallon V. (Patho)physiological significance of the serum- and glucocorticoid-inducible kinase isoforms. *Physiological reviews*. 2006;86:1151-78.

342. Buse P, Tran SH, Luther E, Phu PT, Aponte GW and Firestone GL. Cell cycle and hormonal control of nuclear-cytoplasmic localization of the serum- and glucocorticoid-inducible protein kinase, Sgk, in mammary tumor cells. A novel convergence point of anti-proliferative and proliferative cell signaling pathways. *J Biol Chem*. 1999;274:7253-63.

343. Zhang L, Cui R, Cheng X and Du J. Antiapoptotic effect of serum and glucocorticoid-inducible protein kinase is mediated by novel mechanism activating I{kappa}B kinase. *Cancer Res*. 2005;65:457-64.

344. Lang F and Stournaras C. Serum and glucocorticoid inducible kinase, metabolic syndrome, inflammation, and tumor growth. *Hormones (Athens)*. 2013;12:160-71.

345. Yang M, Zheng J, Miao Y, Wang Y, Cui W, Guo J, Qiu S, Han Y, Jia L, Li H, Cheng J and Du J. Serum-glucocorticoid regulated kinase 1 regulates alternatively activated macrophage polarization contributing to angiotensin II-induced inflammation and cardiac fibrosis. *Arterioscler Thromb Vasc Biol*. 2012;32:1675-86.

346. Lang F and Shumilina E. Regulation of ion channels by the serum- and glucocorticoid-inducible kinase SGK1. *FASEB J*. 2013;27:3-12.

347. Kobayashi T and Cohen P. Activation of serum- and glucocorticoid-regulated protein kinase by agonists that activate phosphatidylinositide 3-kinase is mediated by 3-phosphoinositide-dependent protein kinase-1 (PDK1) and PDK2. *The Biochemical journal*. 1999;339 (Pt 2):319-28.

348. Nakashima S. Protein kinase C alpha (PKC alpha): regulation and biological function. *J Biochem*. 2002;132:669-75.

349. Sun XG and Rotenberg SA. Overexpression of protein kinase Calpha in MCF-10A human breast cells engenders dramatic alterations in morphology, proliferation, and motility. *Cell Growth Differ*. 1999;10:343-52.

350. Hryciw DH, Pollock CA and Poronnik P. PKC-alpha-mediated remodeling of the actin cytoskeleton is involved in constitutive albumin uptake by proximal tubule cells. *American journal of physiology Renal physiology*. 2005;288:F1227-35.

351. Sandoval R, Malik AB, Minshall RD, Kouklis P, Ellis CA and Tiruppathi C. Ca(2+) signalling and PKCalpha activate increased endothelial permeability by disassembly of VE-cadherin junctions. *The Journal of physiology*. 2001;533:433-45.

352. Harrington EO, Loffler J, Nelson PR, Kent KC, Simons M and Ware JA. Enhancement of migration by protein kinase Calpha and inhibition of proliferation and cell cycle progression by protein kinase Cdelta in capillary endothelial cells. *J Biol Chem*. 1997;272:7390-7.

353. Wang A, Nomura M, Patan S and Ware JA. Inhibition of protein kinase Calpha prevents endothelial cell migration and vascular tube formation in vitro and myocardial neovascularization in vivo. *Circ Res*. 2002;90:609-16.

354. Partovian C, Zhuang Z, Moodie K, Lin M, Ouchi N, Sessa WC, Walsh K and Simons M. PKCalpha activates eNOS and increases arterial blood flow in vivo. *Circ Res*. 2005;97:482-7.

355. Micol V, Sanchez-Pinera P, Villalain J, de Godos A and Gomez-Fernandez JC. Correlation between protein kinase C alpha activity and membrane phase behavior. *Biophys J*. 1999;76:916-927.

356. Dutil EM, Toker A and Newton AC. Regulation of conventional protein kinase C isozymes by phosphoinositide-dependent kinase 1 (PDK-1). *Current biology : CB*. 1998;8:1366-75.

357. Sarbassov DD, Ali SM and Sabatini DM. Growing roles for the mTOR pathway. *Curr Opin Cell Biol*. 2005;17:596-603.

358. Garlich JR, De P, Dey N, Su JD, Peng X, Miller A, Murali R, Lu Y, Mills GB, Kundra V, Shu HK, Peng Q and Durden DL. A vascular targeted pan phosphoinositide 3-kinase inhibitor prodrug, SF1126, with antitumor and antiangiogenic activity. *Cancer Res*. 2008;68:206-15.

359. Pore N, Gupta AK, Cerniglia GJ and Maity A. HIV protease inhibitors decrease VEGF/HIF-1alpha expression and angiogenesis in glioblastoma cells. *Neoplasia*. 2006;8:889-95.

360. Lane HA, Wood JM, McSheehy PM, Allegrini PR, Boulay A, Brueggen J, Littlewood-Evans A, Maira SM, Martiny-Baron G, Schnell CR, Sini P and O'Reilly T. mTOR inhibitor RAD001 (everolimus) has antiangiogenic/vascular properties distinct from a VEGFR tyrosine kinase inhibitor. *Clin Cancer Res*. 2009;15:1612-22.

361. Guba M, von Breitenbuch P, Steinbauer M, Koehl G, Flegel S, Hornung M, Bruns CJ, Zuelke C, Farkas S, Anthuber M, Jauch KW and Geissler EK. Rapamycin inhibits primary and metastatic tumor growth by antiangiogenesis: involvement of vascular endothelial growth factor. *Nat Med*. 2002;8:128-35.

362. Fokas E, Im JH, Hill S, Yameen S, Stratford M, Beech J, Hackl W, Maira SM, Bernhard EJ, McKenna WG and Muschel RJ. Dual inhibition of the PI3K/mTOR pathway increases tumor radiosensitivity by normalizing tumor vasculature. *Cancer Res*. 2012;72:239-48.

363. Falcon BL, Barr S, Gokhale PC, Chou J, Fogarty J, Depeille P, Miglarese M, Epstein DM and McDonald DM. Reduced VEGF production, angiogenesis, and vascular regrowth contribute to the antitumor properties of dual mTORC1/mTORC2 inhibitors. *Cancer Res*. 2011;71:1573-83.

364. Humar R, Kiefer FN, Berns H, Resink TJ and Battegay EJ. Hypoxia enhances vascular cell proliferation and angiogenesis in vitro via rapamycin (mTOR)-dependent signaling. *FASEB J*. 2002;16:771-80.

365. Li W, Petrimpol M, Molle KD, Hall MN, Battegay EJ and Humar R. Hypoxia-induced endothelial proliferation requires both mTORC1 and mTORC2. *Circ Res*. 2007;100:79-87.

366. Alva JA, Zovein AC, Monvoisin A, Murphy T, Salazar A, Harvey NL, Carmeliet P and Iruela-Arispe ML. VE-Cadherin-Cre-recombinase transgenic mouse: a tool for lineage analysis and gene deletion in endothelial cells. *Dev Dyn*. 2006;235:759-67.

367. Zovein AC, Turlo KA, Ponec RM, Lynch MR, Chen KC, Hofmann JJ, Cox TC, Gasson JC and Iruela-Arispe ML. Vascular remodeling of the vitelline artery initiates extravascular emergence of hematopoietic clusters. *Blood*. 2010;116:3435-44.

368. Klagsbrun M and D'Amore PA. Angiogenesis: Biology and Pathology. *Cold Spring Harbor perspectives in medicine*. 2012:522.

369. Monvoisin A, Alva JA, Hofmann JJ, Zovein AC, Lane TF and Iruela-Arispe ML. VE-cadherin-CreERT2 transgenic mouse: a model for inducible recombination in the endothelium. *Dev Dyn*. 2006;235:3413-22.

370. Gollner H, Dani C, Phillips B, Philipsen S and Suske G. Impaired ossification in mice lacking the transcription factor Sp3. *Mech Dev*. 2001;106:77-83.

371. Arnaoutova I and Kleinman HK. In vitro angiogenesis: endothelial cell tube formation on gelled basement membrane extract. *Nat Protoc*. 2010;5:628-35.

372. Wang S, Amato KR, Song W, Youngblood V, Lee K, Boothby M, Brantley-Sieders DM and Chen J. Regulation of Endothelial Cell Proliferation and Vascular Assembly through Distinct mTORC2 Signaling Pathways. *Mol Cell Biol*. 2015;35:1299-313.

373. Hiraoka D, Okumura E and Kishimoto T. Turn motif phosphorylation negatively regulates activation loop phosphorylation in Akt. *Oncogene*. 2011;30:4487-97.

374. Cross MJ and Claesson-Welsh L. FGF and VEGF function in angiogenesis: signalling pathways, biological responses and therapeutic inhibition. *Trends Pharmacol Sci*. 2001;22:201-7.

375. Presta M, Dell'Era P, Mitola S, Moroni E, Ronca R and Rusnati M. Fibroblast growth factor/fibroblast growth factor receptor system in angiogenesis. *Cytokine Growth Factor Rev*. 2005;16:159-78.

376. De Smet F, Segura I, De Bock K, Hohensinner PJ and Carmeliet P. Mechanisms of vessel branching: filopodia on endothelial tip cells lead the way. *Arterioscler Thromb Vasc Biol*. 2009;29:639-49.

377. Lindenblatt N, Calcagni M, Contaldo C, Menger MD, Giovanoli P and Vollmar B. A new model for studying the revascularization of skin grafts in vivo: the role of angiogenesis. *Plast Reconstr Surg*. 2008;122:1669-80.

378. Calcagni M, Althaus MK, Knapik AD, Hegland N, Contaldo C, Giovanoli P and Lindenblatt N. In vivo visualization of the origination of skin graft vasculature in a wild-type/GFP crossover model. *Microvasc Res*. 2011;82:237-45.

379. de Paula EV, Flores-Nascimento MC, Arruda VR, Garcia RA, Ramos CD, Guillaumon AT and Annichino-Bizzacchi JM. Dual gene transfer of fibroblast growth factor-2 and platelet derived growth factor-BB using plasmid deoxyribonucleic acid promotes effective angiogenesis and arteriogenesis in a rodent model of hindlimb ischemia. *Transl Res*. 2009;153:232-9.

380. Goel S, Duda DG, Xu L, Munn LL, Boucher Y, Fukumura D and Jain RK. Normalization of the vasculature for treatment of cancer and other diseases. *Physiol Rev*. 2011;91:1071-121.

381. Sounni NE, Dehne K, van Kempen L, Egeblad M, Affara NI, Cuevas I, Wiesen J, Junankar S, Korets L, Lee J, Shen J, Morrison CJ, Overall CM, Krane SM, Werb Z, Boudreau N and Coussens LM. Stromal regulation of vessel stability by MMP14 and TGFbeta. *Dis Model Mech*. 2010;3:317-32.

382. Claffey KP, Abrams K, Shih SC, Brown LF, Mullen A and Keough M. Fibroblast growth factor 2 activation of stromal cell vascular endothelial growth factor expression and angiogenesis. *Lab Invest*. 2001;81:61-75.

383. Szade A, Grochot-Przeczek A, Florczyk U, Jozkowicz A and Dulak J. Cellular and molecular mechanisms of inflammation-induced angiogenesis. *IUBMB Life*. 2015;67:145-59.

384. Vestweber D. VE-cadherin: the major endothelial adhesion molecule controlling cellular junctions and blood vessel formation. *Arterioscler Thromb Vasc Biol*. 2008;28:223-32.

385. Schnurch H and Risau W. Expression of tie-2, a member of a novel family of receptor tyrosine kinases, in the endothelial cell lineage. *Development*. 1993;119:957-68.

386. Ordonez NG. Immunohistochemical endothelial markers: a review. *Advances in anatomic pathology*. 2012;19:281-95.

387. Lacorre DA, Baekkevold ES, Garrido I, Brandtzaeg P, Haraldsen G, Amalric F and Girard JP. Plasticity of endothelial cells: rapid dedifferentiation of freshly isolated high endothelial venule endothelial cells outside the lymphoid tissue microenvironment. *Blood*. 2004;103:4164-72.

388. Aird WC. Endothelial cell heterogeneity. *Cold Spring Harb Perspect Med*. 2012;2:a006429.

389. Xiao Y, Karnati S, Qian G, Nenicu A, Fan W, Tchatalbachev S, Holand A, Hossain H, Guillou F, Luers GH and Baumgart-Vogt E. Cre-mediated stress affects sirtuin expression levels, peroxisome biogenesis and metabolism, antioxidant and proinflammatory signaling pathways. *PloS one*. 2012;7:e41097.

390. Distler JH, Hirth A, Kurowska-Stolarska M, Gay RE, Gay S and Distler O. Angiogenic and angiostatic factors in the molecular control of angiogenesis. *The quarterly journal of nuclear medicine : official publication of the Italian Association of Nuclear Medicine*. 2003;47:149-61.

391. Jakobsson L, Franco CA, Bentley K, Collins RT, Ponsioen B, Aspalter IM, Rosewell I, Busse M, Thurston G, Medvinsky A, Schulte-Merker S and Gerhardt H. Endothelial cells dynamically compete for the tip cell position during angiogenic sprouting. *Nat Cell Biol*. 2010;12:943-53.

392. Wu FT, Stefanini MO, Mac Gabhann F, Kontos CD, Annex BH and Popel AS. A systems biology perspective on sVEGFR1: its biological function, pathogenic role and therapeutic use. *Journal of cellular and molecular medicine*. 2010;14:528-52.

393. Tonnesen MG, Feng X and Clark RA. Angiogenesis in wound healing. *The journal of investigative dermatology Symposium proceedings / the Society for Investigative Dermatology, Inc [and] European Society for Dermatological Research*. 2000;5:40-6.

394. Fraser HM and Lunn SF. Angiogenesis and its control in the female reproductive system. *British medical bulletin*. 2000;56:787-97.

395. Angelo LS and Kurzrock R. Vascular endothelial growth factor and its relationship to inflammatory mediators. *Clin Cancer Res*. 2007;13:2825-30.

396. Carmeliet P. Angiogenesis in health and disease. *Nat Med*. 2003;9:653-60.

397. Deshmane SL, Kremlev S, Amini S and Sawaya BE. Monocyte chemoattractant protein-1 (MCP-1): an overview. *Journal of interferon & cytokine research : the official journal of the International Society for Interferon and Cytokine Research*. 2009;29:313-26.

398. Sprague AH and Khalil RA. Inflammatory cytokines in vascular dysfunction and vascular disease. *Biochemical pharmacology*. 2009;78:539-52.

399. Bogatcheva NV and Verin AD. The role of cytoskeleton in the regulation of vascular endothelial barrier function. *Microvasc Res*. 2008;76:202-7.

400. Ausprunk DH and Folkman J. Migration and proliferation of endothelial cells in preformed and newly formed blood vessels during tumor angiogenesis. *Microvasc Res*. 1977;14:53-65.

401. Holinstat M, Mehta D, Kozasa T, Minshall RD and Malik AB. Protein kinase Calpha-induced p115RhoGEF phosphorylation signals endothelial cytoskeletal rearrangement. *J Biol Chem*. 2003;278:28793-8.

402. Ma Y, Zhang P, Wang F, Yang J, Yang Z and Qin H. The relationship between early embryo development and tumourigenesis. *Journal of cellular and molecular medicine*. 2010;14:2697-701.

403. Guertin DA, Stevens DM, Saitoh M, Kinkel S, Crosby K, Sheen JH, Mullholland DJ, Magnuson MA, Wu H and Sabatini DM. mTOR complex 2 is required for the development of prostate cancer induced by Pten loss in mice. *Cancer Cell*. 2009;15:148-59.

404. Hietakangas V and Cohen SM. Re-evaluating AKT regulation: role of TOR complex 2 in tissue growth. *Genes & development*. 2007;21:632-7.

405. Munoz-Chapuli R, Quesada AR and Angel Medina M. Angiogenesis and signal transduction in endothelial cells. *Cell Mol Life Sci*. 2004;61:2224-43.

406. Ziyad S and Iruela-Arispe ML. Molecular mechanisms of tumor angiogenesis. *Genes Cancer*. 2011;2:1085-96.

407. Florkiewicz RZ, Majack RA, Buechler RD and Florkiewicz E. Quantitative export of FGF-2 occurs through an alternative, energy-dependent, non-ER/Golgi pathway. *J Cell Physiol*. 1995;162:388-99.

408. Ittman M and Mansukhani A. Expression of fibroblast growth factors (FGFs) and FGF receptors in human prostate. *J Urol*. 1997;157:351-6.

409. Davol PA and Frackelton AR, Jr. Targeting human prostatic carcinoma through basic fibroblast growth factor receptors in an animal model: characterizing and circumventing mechanisms of tumor resistance. *Prostate*. 1999;40:178-91.

410. Berger W, Setinek U, Mohr T, Kindas-Mugge I, Vetterlein M, Dekan G, Eckersberger F, Caldas C and Micksche M. Evidence for a role of FGF-2 and FGF receptors in the proliferation of non-small cell lung cancer cells. *Int J Cancer*. 1999;83:415-23.

411. Sumitomo S, Okamoto Y, Mizutani G, Kudeken W, Mori M and Takai Y. Immunohistochemical study of fibroblast growth factor-2 (FGF-2) and fibroblast growth factor receptor (FGF-R) in experimental squamous cell carcinoma of rat submandibular gland. *Oral Oncol*. 1999;35:98-104.

412. Tamiya S, Ueki T and Tsuneyoshi M. Expressions of basic fibroblast growth factor and fibroblast growth factor receptor mRNA in soft tissue tumors by in situ hybridization. *Mod Pathol*. 1998;11:533-6.

413. Ueki T, Koji T, Tamiya S, Nakane PK and Tsuneyoshi M. Expression of basic fibroblast growth factor and fibroblast growth factor receptor in advanced gastric carcinoma. *J Pathol*. 1995;177:353-61.

414. Xerri L, Battyani Z, Grob JJ, Parc P, Hassoun J, Bonerandi JJ and Birnbaum D. Expression of FGF1 and FGFR1 in human melanoma tissues. *Melanoma Res*. 1996;6:223-30.

415. Ornitz DM and Itoh N. Fibroblast growth factors. *Genome Biol*. 2001;2:REVIEWS3005.

416. Ornitz DM and Marie PJ. FGF signaling pathways in endochondral and intramembranous bone development and human genetic disease. *Genes Dev*. 2002;16:1446-65.

417. Sullivan R and Klagsbrun M. Purification of cartilage-derived growth factor by heparin affinity chromatography. *J Biol Chem*. 1985;260:2399-403.

418. Hurley MM, Tetradis S, Huang YF, Hock J, Kream BE, Raisz LG and Sabbieti MG. Parathyroid hormone regulates the expression of fibroblast growth factor-2 mRNA and fibroblast growth factor receptor mRNA in osteoblastic cells. *J Bone Miner Res*. 1999;14:776-83.

419. Moore R, Ferretti P, Copp A and Thorogood P. Blocking endogenous FGF-2 activity prevents cranial osteogenesis. *Dev Biol*. 2002;243:99-114.

420. Maffucci T, Piccolo E, Cumashi A, Iezzi M, Riley AM, Saiardi A, Godage HY, Rossi C, Broggini M, Iacobelli S, Potter BVL, Innocenti P and Falasca M. Inhibition of the phosphatidylinositol 3-kinase/Akt pathway by inositol pentakisphosphate results in antiangiogenic and antitumor effects. *Cancer research*. 2005;65:8339-8349.

421. Martin TA, Parr C, Davies G, Watkins G, Lane J, Matsumoto K, Nakamura T, Mansel RE and Jiang WG. Growth and angiogenesis of human breast cancer in a nude mouse tumour model is reduced by NK4, a HGF/SF antagonist. *Carcinogenesis*. 2003;24:1317-23.

422. Shen BQ, Lee DY, Gerber HP, Keyt BA, Ferrara N and Zioncheck TF. Homologous up-regulation of KDR/Flk-1 receptor expression by vascular endothelial growth factor in vitro. *Journal of Biological Chemistry*. 1998;273:29979-29985.

423. Herve MA, Meduri G, Petit FG, Domet TS, Lazennec G, Mourah S and Perrot-Applanat M. Regulation of the vascular endothelial growth factor (VEGF) receptor Flk-1/KDR by estradiol through VEGF in uterus. *J Endocrinol*. 2006;188:91-9.

424. Wang DF, Donner DB and Warren RS. Homeostatic modulation of cell surface KDR and Flt1 expression and expression of the vascular endothelial cell growth factor (VEGF) receptor mRNAs by VEGF. *Journal of Biological Chemistry*. 2000;275:15905-15911.

425. Murakami M, Nguyen LT, Hatanaka K, Schachterle W, Chen PY, Zhuang ZW, Black BL and Simons M. FGF-dependent regulation of VEGF receptor 2 expression in mice. *J Clin Invest*. 2011;121:2668-78.

426. Hegen A, Koidl S, Weindel K, Marme D, Augustin HG and Fiedler U. Expression of angiopoietin-2 in endothelial cells is controlled by positive and negative regulatory promoter elements. *Arterioscl Throm Vas*. 2004;24:1803-1809.

427. Fujii T and Kuwano H. Regulation of the expression balance of angiopoietin-1 and angiopoietin-2 by Shh and FGF-2. *In Vitro Cell Dev-An*. 2010;46:487-491.

428. Weber KSC, Nelson PJ, Grone HJ and Weber C. Expression of CCR2 by endothelial cells - Implications for MCP-1 mediated wound injury repair and in vivo inflammatory activation of endothelium. *Arterioscl Throm Vas*. 1999;19:2085-2093.

429. Bhattacharya I, Dragert K, Albert V, Contassot E, Damjanovic M, Hagiwara A, Zimmerli L, Humar R, Hall MN, Battegay EJ and Haas E. Rictor in perivascular adipose tissue controls vascular function by regulating inflammatory molecule expression. *Arterioscler Thromb Vasc Biol*. 2013;33:2105-11.

430. Lamouille S, Connolly E, Smyth JW, Akhurst RJ and Derynck R. TGF-beta-induced activation of mTOR complex 2 drives epithelial-mesenchymal transition and cell invasion. *J Cell Sci*. 2012;125:1259-73.

431. Serrano I, McDonald PC, Lock FE and Dedhar S. Role of the integrin-linked kinase (ILK)/Rictor complex in TGFbeta-1-induced epithelial-mesenchymal transition (EMT). *Oncogene*. 2013;32:50-60.

432. McDonald PC, Oloumi A, Mills J, Dobreva I, Maidan M, Gray V, Wederell ED, Bally MB, Foster LJ and Dedhar S. Rictor and integrin-linked kinase interact and regulate Akt phosphorylation and cancer cell survival. *Cancer Res*. 2008;68:1618-24.

433. Medici D, Shore EM, Lounev VY, Kaplan FS, Kalluri R and Olsen BR. Conversion of vascular endothelial cells into multipotent stem-like cells. *Nat Med*. 2010;16:1400-6.

434. Welch-Reardon KM, Wu N and Hughes CC. A role for partial endothelial-mesenchymal transitions in angiogenesis? *Arterioscler Thromb Vasc Biol*. 2015;35:303-8.

435. Medici D and Olsen BR. The role of endothelial-mesenchymal transition in heterotopic ossification. *J Bone Miner Res*. 2012;27:1619-22.

436. Medici D and Kalluri R. Endothelial-mesenchymal transition and its contribution to the emergence of stem cell phenotype. *Semin Cancer Biol*. 2012;22:379-84.

437. Carmeliet P and Jain RK. Angiogenesis in cancer and other diseases. *Nature*. 2000;407:249-57.

438. Bergom C, Paddock C, Gao CJ, Holyst T, Newman DK and Newman PJ. An alternatively spliced isoform of PECAM-1 is expressed at high levels in human and murine tissues, and suggests a novel role for the C-terminus of PECAM-1 in cytoprotective signaling. *Journal of Cell Science*. 2008;121:1235-1242.

439. Bentzinger CF, Romanino K, Cloetta D, Lin S, Mascarenhas JB, Oliveri F, Xia J, Casanova E, Costa CF, Brink M, Zorzato F, Hall MN and Ruegg MA. Skeletal muscle-specific ablation of raptor, but not of rictor, causes metabolic changes and results in muscle dystrophy. *Cell Metab*. 2008;8:411-24.

440. Vieira JM, Schwarz Q and Ruhrberg C. Selective requirements for NRP1 ligands during neurovascular patterning. *Development*. 2007;134:1833-43.

441. Nagy A, Gertsenstein M, Vintersten K and Behringer R. Staining Whole Mouse Embryos for {beta}-Galactosidase (lacZ) Activity. *CSH protocols*. 2007;2007:pdb prot4725.

442. Mihic-Probst D, Ikenberg K, Tinguely M, Schraml P, Behnke S, Seifert B, Civenni G, Sommer L, Moch H and Dummer R. Tumor cell plasticity and angiogenesis in human melanomas. *PLoS One*. 2012;7:e33571.

443. Schmittgen TD, Lee EJ, Jiang J, Sarkar A, Yang L, Elton TS and Chen C. Real-time PCR quantification of precursor and mature microRNA. *Methods*. 2008;44:31-8.

444. Peier M, Walpen T, Christofori G, Battegay E and Humar R. Sprouty2 expression controls endothelial monolayer integrity and quiescence. *Angiogenesis*. 2013;16:455-68.

445. Walpen T, Peier M, Haas E, Kalus I, Schwaller J, Battegay E and Humar R. Loss of pim1 imposes a hyperadhesive phenotype on endothelial cells. *Cellular physiology and biochemistry : international journal of experimental cellular physiology, biochemistry, and pharmacology*. 2012;30:1083-96.

446. Akhtar N, Dickerson EB and Auerbach R. The sponge/Matrigel angiogenesis assay. *Angiogenesis*. 2002;5:75-80.

447. Rehg JE, Bush D and Ward JM. The utility of immunohistochemistry for the identification of hematopoietic and lymphoid cells in normal tissues and interpretation of proliferative and inflammatory lesions of mice and rats. *Toxicol Pathol*. 2012;40:345-74.

448. Brognara E, Fabbri E, Aimi F, Manicardi A, Bianchi N, Finotti A, Breveglieri G, Borgatti M, Corradini R, Marchelli R and Gambari R. Peptide nucleic acids targeting miR-221 modulate p27Kip1 expression in breast cancer MDA-MB-231 cells. *Int J Oncol*. 2012;41:2119-27.

10. ABBREVIATIONS

AArch = Aortic Arch
ACh = Acetylcholine
ADAMTS1 = A Disintegrin And Metalloproteinase with Thrombospondin Motifs 1
adipo = Adipocytes
AJ = Adherens Junctions
AKT = Protein kinase B
AMPK = AMP-activated protein Kinase
ANG = Angiopoietin
A-loop = Activation Loop
BSA = Albumin from Bovine Serum
C53BL/6 = C53 Black 6
CalM3 = Calmodulin 3
cAMP = Cyclic Adenosine Monophosphate
CASP8 v.1 = Caspase-8 (variant 1)
CD = Cluster of Differentiation
CD31 = see PECAM1
CD34 = Hematopoietic Progenitor Cell Antigen
cDNA = Complementary DNA
cm = Centimeter
COX = Cyclooxygenase
Ctrl = Control
DA = Dorsal Aorta
DAG = Diacyl-glycerol
DLAV = Dorsal Longitudinal Anastomotic Vessel
DLL4 = Delta Like Ligand 4
DMEM = Dulbecco's Minimal Essential Medium
DNA = Deoxyribonucleic Acid
Dvl3 v.x5 = Segment polarity protein Dishevelled homolog DVL-3 (variant X5)
EC = Endothelial Cell
ECGS = Endothelial Cell Growth Supplement
EDTA = Ethylenediaminetetraacetic Acid
eIFs = Eukaryotic Initiation Factors
Emp1 = Epithelial Membrane Protein 1

eNOS = Endothelial NOS
Eph = Ephrin
EPO = Erythropoietin
FCS = Fetal Calf Serum
FGF = Fibroblast Growth Factor
FGFR = FGF2 Receptor
Flt3L = FMS-Like Tyrosine kinase 3 Ligand
FoxOs = Forkhead box protein O
GF = Growth Factor
GFP = Green Fluorescent Protein
Gjα1 = Gap Junction Alpha-1 protein
GSK3 = Glycogen Synthase Kinase 3
HCl = Hydrochloric Acid
HGF = Hepatocyte Growth Factor
HGF v4 = Hepatocyte Growth Factor (variant 4)
HIF = Hypoxia Inducible Factor
HM = Hydrophobic Motif
Hsp = Heat Shock Protein
HSPGs = Heparan Sulfates Proteoglycans
ICAM-1 = Intercellular Adhesion Molecule 1
ID2 = DNA-binding protein inhibitor
IGF = Insulin- like Growth Factor
IGFBP3 = Insulin-like Growth Factor-Binding Protein 3
IL = Interleukin
iNOS = Inducible NOS
IP3 = Inositol 1,4,5-Trisphosphate
ISV = Intersegmental Vessel
Jag1 = Jagged1
Klhl20 = Kelch-like protein 20
KO = Knock Out
MAEC = Mouse Aortic Endothelial Cell
MAPK = Mitogen-Activated Protein Kinase
MCP1 = Monocyte Chemotactic Protein 1
mM = Millimolar
MMPs = Matrix Metalloproteases
mTOR = Mammalian Target Of Rapamycin

mTORC = Mammalian Target Of Rapamycin Complex

NaCl = Sodium Chloride

NADP ($^{+}$/H) = Nicotinamide Adenine Dinucleotide Phosphate

NaPyr = Sodium Pyruvate

NEAA = Non Essential Amino Acid

NG2 = Neuron Glial 2

nm = Nanometer

nM =Nanomolar

nNOS = Neuronal NOS

NO = Nitric Oxide

NOS = Nitric Oxide Synthase

Notch = Neurogenic locus notch homolog protein

Nrp-1 = Neuropilin-1

NSAID = Non-Steroidal Anti-Inflammatory Drug

OD = Optical Density

OPN v.4 = Osteopontin (variant 4)

PCR = Polymerase Chain Reaction

PBS = Phosphate Buffer Solution

PDGF = Platelet Derived Growth Factor

PDK1 = Pyruvate Dehydrogenase lipoamide Kinase isozyme 1

PDT = Photodynamic Therapy

PECAM-1 = Platelet Endothelial Cell Adhesion Molecule 1

PenStrep = Penicillin Streptomycin

PFA = Paraformaldehyde

PHD = Prolyl Hydroxylase

PlGF = Placental Growth Factor

PIP_3 = Phosphatidylinositol (3,4,5)-trisphosphate

PI3K = Phosphoinositide 3-kinase

PKCα = Protein Kinase C Alpha

Pkp4 = Plakophilin-4

PLCγ = Phosphoinositide Phospholipase Cγ

PMA = Phorbol-12-myristat-13-acetat

Pten = Phosphatase and tensin homolog

PVC = Posterior Cardinal Vein

RA = Rheumatoid Arthritis

RNA = Ribonucleic Acid

RPE = Retinal Pigment Epithelium
RPM = Revolutions Per Minute
qRT-PCR = Quantitative Real Time PCR
SDS = Sodium Dodecyl Sulfate
Ser = Serine
SF = Scatter Factor, see also HGF
SGK1 = Serum and Glucocorticoid-regulated Kinase 1
SMA = Smooth Muscle Actin
SMC = Smooth Muscle Cell
S6K1 = Ribosomal protein S6 kinase beta-1
sVEGFR1 = Soluble Vascular Endothelial Growth Factor 1
TAM = Tumor Associated Macrophage
TBST = Tris Buffer Solution 0.1% Tween
TEM = Tie2- Expressing Monocytes
TF = Tissue Factor
TGF = Transforming Growth Factor
Thbs1 = Thrombospondin 1
Thr = Threonine
TIE1 = Tyrosine kinase with immunoglobulin-like and EGF-like domains 1
TIE2 = Angiopoietin-1 receptor
TJ = Tight Junctions
TM = Turn Motif
TNFα = Tumor Necrosis Factor Alpha
Tris = tris(hydroxymethyl)aminomethane
TSC (1/2) = Tuberous Sclerosis Complex (1 or 2)
TSPs = Thrombospondins
tVEGFR1 = Total Vascular Endothelial Growth Factor Receptor 1
Tyr = Tyrosine
vBM = Vascular Basement Membrane
VCAM-1 = Vascular Cell Adhesion Molecule 1
VE-Cad = Vascular Endothelial Cadherin
VEGFA = Vascular Endothelial Growth Factor A
VEGFR1 = Vascular Endothelial Growth Factor Receptor 1
VEGFR2 = Vascular Endothelial Growth Factor Receptor 2
VEGFR3 = Vascular Endothelial Growth Factor Receptor 3
VHL = von Hippel-Lindau protein

VPF = Vascular Permeability Factor, see also VEGF

vSMCs = Vascular Smooth Muscle Cells

vWF = von Willebrand Factor

wARMD = Wet Age- Related Macular Degeneration

11. AKNOWLEDGEMENTS

In this page reserved for the acknowledgements, I would like to thank Prof. Edouard Battegay for giving me the opportunity to develop the PhD thesis in his laboratory and Dr. Rok Humar for driving me during these years in which I learned a lot about science, biology and ethics.

A particular thank goes to Ms. Ana Perez, the lab-technician whose work for the project was irreplaceable. I would like to thank Dr. Indranil Bhattacharya and Dr. Elvira Haas for the precious suggestions given me during the development of the project and for their genuine support during this long period. Thanks also to Dr. Christian Schaer for helping in analyzing the results of the transcriptomic array.

To the members of my thesis committee, Prof. Gerhard Christofori, Prof. Max Gassmann and, in particular, Prof. Christian Grimm I would like to address sincere thanks for supporting me during this period, trying to help me in growing as scientist.

Last but not the least: I would like to thank all the people who stayed beside me during this difficult and long period. I am not going to mention their names, but I will take the time to thank personally all the members of my family, my friends and the people scientists and not who simply walked with me during this time of my life and decided to share with me the good and the bad moments.

12. *CURRICULUM VITAE*

CONTACT INFORMATION	
Name (first, last)	Fabio, Aimi
Address	Research Unit of Internal Medicine Department, Wagistrasse 12, 8952 Zürich Schlieren, Switzerland
Phone	+41 (0) 44 55 63230
Email	fabio.aimi@usz.ch

PERSONAL INFORMATION	
Date of birth	March 31st, 1985
Place of birth	Parma, Italy
Nationality	Italian

PROFESSIONAL EXPERIENCE	
05.2011 – 11.2015	Ph.D. Thesis (Title: "*The Role of Endothelial RICTOR (mTORC2)in Angiogenesis in Vivo and in Vitro*" (UNDER DISCUSSION)) University Hospital Zürich (USZ), Switzerland Laboratory of Prof. Dr. Med. Edouard Battegay
07.2009 – 07.2010	M.Sc. Thesis (Title: "*Synthesis of anti-miR PNAs (Peptide Nucleic Acid) and their use in the regulation of the gene expression"*) University of Parma (UNIPR) and University of Ferrara (UNIFE), Italy Laboratory of Prof. Roberto Corradini and Laboratory of Prof. Roberto Gambari
09.2007 – 02.2008	B.Sc. Thesis (Title: "*Cloning, expression and purification of the fusion protein Nus-VA48"*) University of Parma (UNIPR), Italy Laboratory of Prof. Angelo Bolchi

EDUCATION	
05.2011 – 11.2015	(TO BE DISCUSSED) Ph.D. in Molecular Biology University of Zürich (UZH) – University Hospital of Zürich (USZ)
10.2007 – 07.2010	Graduation: Master in Molecular Biology University of Parma (UNIPR), Italy *Mark: 110/110 with honors*
10.2004 – 02.2008	Graduation: Bachelor in Biology University of Parma (UNIPR), Italy *Mark: 107/11*
09.1999 –07.2004	Degree: Scientific High School Diploma High School G. Marconi, Parma, Italy *Mark: 89/100*

LANGUAGE SKILLS	
Italian	Mother language
English	Advanced (C2)
German	Intermediate (B1)
Spanish	Basic (A2)

COMPUTER SKILLS	
Office programs	Excel, Word, Power Point
Operative systems	Windows, Linux and MacOS
Graphic programs	Adobe Acrobat, Adobe Photoshop, Adobe Illustrator
Scientific programs	ImageJ, EndNote, GraphPad Prism, RasMol, Pymol, GeneDoc, Blast, TreeView

TECHNICAL SKILLS	
In vivo	Murine animal model: injections, tumor and retina vascularization
In vitro	Cell culture: Mouse Aortic Endothelial Cells (MAECs), Tumor cells (B16 melanoma, MCF7, MDA-MB-231), Prokaryotes (*Escherichia coli*)
Molecular	Real Time PCR, Immunoblotting, Fluorescence and Confocal Microscopy, Biostation, Immunohistochemistry, Immunofluorescence, Gel electrophoresis, HPLC, FACS, Mass Spectrometry, Solid Phase Peptide Synthesis
Teaching	Master Students supervised during the process of thesis writing

ADDITIONAL COURSES	
SS 2013	Mouse Pathophysiology
AS 2012	Model Organisms in Developmental Biology
AS 2012	Clinical Cancer Research
SS 2012	Flow Cytometry
AS 2011	Supervising Students
AS 2011	LTK Module 1 (habilitation for animal experimentation)

PRESENTATIONS	
April 09th, 2015	14th Day of Clinical Research, University Hospital Zürich, Switzerland (oral)
January 13th-18th, 2015	Keystone Symposia on Molecular and Cell Biology: PI3-Kinase Signaling Pathway in Disease, Vancouver, Canada (poster)
August 24th, 2012	8th ZIHP Symposium, Zürich, Switzerland (oral)

PUBBLICATIONS

Fabio Aimi, Stavroula Georgiopoulou, Ina Kalus, Fabienne Lehner, Alica Hegglin, Përparim Limani, Vinicius Gomez de Lima, Markus Rüegg, Michael N. Hall, Nicole Lindenblatt, Elvira Haas, Edouard J. Battegay, Rok Humar. "*Endothelial mTORC2 is crucial for midgestational development and sustained and extensive FGF2-induced neovascularization in the adult*" (IN PRESS)

Brognara E, Fabbri E, Aimi F, Manicardi A, Bianchi N, Finotti A, Breveglieri G, Borgatti M, Corradini R, Marchelli R and Gambari R. Peptide nucleic acids targeting miR-221 modulate p27Kip1 expression in breast cancer MDA-MB-231 cells. Int J Oncol. 2012;41:2119-27. [448]

AWARDS

August 24th, 2012 Best Presentation, 8th ZIHP symposium, Zürich, Switzerland